University Of Alberta

Temporal and Spatial Characterization of Uterine and Oviductal Environment in the Pig

By

J. Alex Pasternak

A thesis submitted to the Faculty of Graduate Studies and Research in Partial fulfillment of the requirements for the degree of

Doctor of Philosophy

In

Animal Science

Department of Agricultural, Food and Nutritional Science

Fall 2012

Edmonton, Alberta

"*Science is more than a body of knowledge, it's a way of thinking. A way of skeptically interrogating the universe with a fine understanding of human fallibility.*"

Carl Sagan (1934-1996)

Abstract

Early embryonic development is a dynamic period that requires precise and timely interaction between the developing embryo and the maternal environment. A series of studies were carried out in order to identify the vital components of this environment and to understand their temporal and spatial changes during the period of cleavage stage development of the porcine embryo. This environment was characterized in animals following precise timing of ovulation using transcutaneous real time ovarian ultrasonography. Analysis of the glycosaminoglycan hyaluronic acid (HA) in this environment suggests a role for HA in fertilization and blastocyst development. In addition, analysis of the associated HA synthase (HAS) genes suggests a common regulatory mechanism at play in the oviduct and uterus for HAS 1 and 2, but not HAS3. Evaluation of the histotrophic proteome identified 269 unique proteins, ten of which were shown to significantly decrease and six significantly increased in abundance between the germinal vesicle and blastocyst stages. Fourteen proteins were identified by mass spectrometry revealing proteins such as CLU and CA2 in the histotroph at the germinal vesicle stage and members of the GST family at the blastocyst stage. These proteins likely play a role in maintaining a suitable environment for sperm and embryos respectively. Analysis of the associated transcripts suggests the majority of these changes are the results of either post-transcriptional regulation or changes in importation from another source. Additionally, microarray analysis of the temporal and spatial changes in the uterine transcriptome showed a decreasing spatial variation at the blastocyst stage. Gene ontology enrichment revealed an up-regulation of genes associated with signal transduction combined with a down-regulation in response to stimulus suggesting maternal-embryonic communication plays an important role in regulating the uterine environment. Finally, a novel bioinformatic program was developed to allow for the visualization of potential protein-protein interactions in paired sets of transcriptomic data; applied to transcriptomic data from the embryo and uterus this program identified multiple potential signaling pathways. In conclusion, these studies demonstrate the complexity of the uterine and oviductal environments and suggest the early embryo plays a role in modulating it.

Acknowledgements

I would first and foremost like to thank my supervisor, Dr. Michael Dyck, for his invaluable guidance, advice and candor. Your seemingly endless patience and support for my scientific tangents has nurtured in me a strong desire to become a well-rounded scientist and teacher, I could not have asked for a better mentor and role model. I would also like to thank Dr. Walter Dixon, Dr. George Foxcroft and Dr. Richard Uwiera for their additional mentoring and advice which was instrumental to the completion of this work.

I owe a great debt too all the members of the SRDP and SRTC both past and present who have made this research possible. I would specifically like to thank Joan Turchinski and Rose O'Donohue, without your help I would at best have accomplished nothing and at worst lit myself ablaze. I would also like to thank Jenny Patterson for her indispensable help with all aspects of this work, your positive attitude and friendship made my sleepless nights at the swine unit bearable. Also to Dr. Francois Paradis and Dr. Susan Novak; our conversations on all facets of science over the past five years have taught me more than I could ever imagine, you are dear friends and I look forward to many years of future collaboration.

I would like to thank Coral Kent-Dennis for her substantial support while I wrote this thesis; you are a fantastic friend and partner. Finely I thank my family, and in particular my parents John and Barb Pasternak. The environment, in which I was nurtured, instilled an endless curiosity and the highest regard for evidence over blind faith. In this way you have directly contributed to any past, present or future successes in both science and life.

I would acknowledge the countless scientific giants both past and present in this field and others, whose work has not only laid the foundation for my studies, but has inspired me to look further into the fascinating world that surrounds us.

Table of Contents

List of Tables

List of Figures

List of Symbols, Nomenclature, or Abbreviations

2cell	Two Cell Stage Of Embryonic Development
2D	Two Dimensional
4cell	Four Cell Stage Of Embryonic Development
AI	Artificial Insemination
AIJ	Ampullary-Isthmic Junction
AMP	Ampulla
ATP	Adenosine-5'-triphosphate
BIND	Biomolecular Interaction Network Database
BioGrid	Biological General Repository for Interaction Datasets
BLAST	Basic Logical Alignment Search Tool
Blast	Blastocyst Stage of Embryonic Development
BLASTn	Basic Logical Alignment Search Tool for Nucleotides
BLASTp	Basic Logical Alignment Search Tool for Proteins
BLAT	BLAST Like Alignment Tool
BSA	Bovine Serum Albumen
BSE	Bovine Spongiform Encephalophy
BUT	Caudal, Cervical or Bottom 1/3 of the Uterus
CETA	Canadian Embryo Transfer Association
DNA	Deoxyribonucleic acid
DNMT	DNA Methyl Transferase
DNMT1	DNA Methyl Transferase 1
DNMT3a	DNA Methyl Transferase 3 a
DNMT3b	DNA Methyl Transferase 3 b
DNMTo	DNA Methyl Transferase Ω
EC	Embryo Culture
EGF	Epidermal Growth Factor
Elisa	Enzyme-Linked Immunosorbent Assay
Emor	8-16 cell or Early Morula Stage of Embryonic Development
EPIA	Extracellular Protein Interaction Analyser
ES	Electro Spray
ET	Embryo Transfer
FCS	Fetal Calf Serum
FITC	Fluorescein Isothiocyanate
FSH	Follicle Stimulating Hormone
Gene	NCBI Gene Database
GFP	Green Fluorescent Protein
GLM	General Linear Model
GLUT	Glucose Transporter Family

GLUT1	Official Symbol for the Gene: Glucose Transporter Type 1
GLUT2	Official Symbol for the Gene: Glucose Transporter Type 2
GLUT3	Official Symbol for the Gene: Glucose Transporter Type 3
GLUT4	Official Symbol for the Gene: Glucose Transporter Type 4
GnRH	Gonadotropin Releasing Hormone
GO	Gene Ontology
GV	Germinal Vesicle Stage of Development
HAS	Hyaluronic Acid Synthase Family
hCG	Human Chorionic Gonadotropin
HDACi	Histone Deacetylase Inhibitors
HPRD	Human Protein Reference Database
ICM	Inner Cellular Mass
IGF1	Insulin Like Growth Factor 1
IGF2	Insulin Like Growth Factor 2
IGF2r	Insulin Like Growth Factor 2 Receptor
INFT	Interferon Tau
IST	Isthmus
IVD	In vitro Development
IVF	In vitro Fertilization
IVM	In vitro Maturation
IVP	In vitro Production
KEGG	Kyoto Encyclopedia of Genes and Genomes
MII	Metaphase Two
ml	Millilitre
Mor	Morula Stage of Embryo Development
MS	Mass Spectrometry
MUT	Middle 1/3 of the Uterus
MZT	Major Zygotic Transition
NCBI	National Center for Biotechnology Information
ng	Nanogram
NSET	Non-Surgical Embryo Transfer
OVGP1	Oviductal Glycoprotein 1
P4	Progesterone
PAGE	Poly Acrylamide Gel Electrophoresis
PBS	Phosphate Buffered Saline
PGF2a	Prostaglandin F2α
PCR	Polymerase Chain Reaction
PED	Official Symbol for the Gene: Preimplantation Embryo Development
pg	Picogram
PGF2α	Prostaglandin F2α
PI3K	Official Symbol for the Gene: Phosphatidylinositol-4,5-bisphosphate 3-kinase
pLH	Porcine Lutienizing Hormone

PMSG	Pregnant Mare Serum Gonadotropin
PVA	Polyvinylalcohol
PVP	Polyvinylpyrrolidone
RefSeq	NCBI Reference Sequence Database
RENBP	Renin Binding Protein
RNA	Ribonucleic Acid
RNAi	RNA Interference
RP-LC	Reverse Phase-Liquid Chromatography
RT-PCR	Reverse Transcription-Polymerase Chain Reaction
SA	Serum Albumen
SAS	Statistical Analysis System
SDS	Sodium Dodecyl Sulfate
SEM	Standard Error of the Mean
SSH	Selective Subtractive Hybridization
STRING	Search Tool for the Retrieval of Interacting Genes/Proteins
TUT	Cranial, Oviductal or Top 1/3 of the Uterus
V	Volts
v/v	Volume/Volume
VEGF	Vascular Epidermal Growth Factor
Vhr	Volt-hours
w/v	Weight/Volume
ZGA	Zygotic Genome Activation
ZP3	Zonal Protein 3
Δ	Delta
µg	Microgram
µl	Microliter

Chapter 1: General Introduction

Embryonic development requires the coordination of a series of complex events which transform the single cell zygote into a fetus. Each stage in this developmental process requires not only specific conditions, but also nutrients and precursors necessary to drive its metabolic system. In mammals, this process takes place in the maternal reproductive tract which must not only provide all the necessary developmental components, but also protect the developing embryo from the maternal immune system. In addition, it is well established that perturbations in the maternal environment during any stage of development can have long term detrimental effects on the offspring through the processes of epigenetics (Barker and Martyn 1992).

Prior to implantation, the mammalian embryo must survive unattached in the local environment or histotroph provided by the maternal reproductive tract. Previous experiments conducted across a range of different animal species have demonstrated embryonic requirements for hormones (Strunker *et al.* 2011), amino acids (Swain *et al.* 2002), proteins (Buhi *et al.* 1990), carbohydrates (Flood and Wiebold 1988), glycosaminoglycans (Leese and Barton 1984) and lipids (Pratt 1980). Which of these components play a key role in embryo development and how tightly regulated they are within the female reproductive tract, is as yet not well understood. Given past research in this area and our current understanding of embryogenesis, our hypothesis is that the maternal environment is dynamic and changes in response to the evolving requirements of the early developing porcine embryo. Furthermore, based on the increasing requirements (Dobrinsky *et al.* 1996) and sensitivity of developing embryos in culture (Rijnders and Jansen 1998) and the increased embryonic mortality observed *in vivo* (Perry and Rowlands 1962), we propose that the maternal environment will become increasingly regulated as embryonic development progresses.

Substantial value exists in understanding the components required for healthy embryonic development during the early cleavage stages of development, as it is during this period that all embryo based assisted reproductive technologies (ART) are applied. As the dairy industry has shown, such technologies can substantially increase the rate of genetic improvement in livestock. In addition, embryo based ART create the opportunity to transport female genetics in a disease free manner (Singh *et al.* 1982; Singh and Thomas 1987), a substantial issue in the current swine industry. However, in many ways these technologies have seen minimal success and poor industry application in swine relative to other agricultural species (Hazeleger and Kemp 1994; Ducro-Steverink *et al.* 2004). A better understanding of the physiologically appropriate environment in which a porcine embryo develops could help make these technologies more successful, opening the doors to their application in industry.

One of the single most important factors determining profitability in the swine industry currently is the number of live pigs born per sow per year. Genetic selection has driven ovulation rates in the modern sow to substantially higher levels than previously observed (Foxcroft *et al.* 2006; Foxcroft *et al.* 2007; Novak *et al.* 2012). Unfortunately, the number of pigs born alive per litter has not increased at the same rate, making prenatal mortality a significant target for potential improvement. A substantial portion of this loss is known to occur during embryonic development (Novak *et al.* 2012); however some controversy exists regarding the specific time point at which the embryos become compromised (Perry and Rowlands 1962; Polge 1982; van der Lende and Schoenmaker 1990). Additional value can therefore be obtained from understanding the key factors involved in embryo survival and how these factors are regulated for optimal development.

The following chapter of this thesis will serve as a comprehensive review of the existing literature in the field of early embryonic development focused on

two areas. First, it will review the current understanding of the complex events that take place from fertilization to the development of the blastocyst stage embryo. Secondly, it will review the current understanding of maternal environment during this period of development in regards to both the necessary components and their regulation. As a whole, the review will seek to highlight the known effects that perturbations to this environment have on development, as well as the potential of the resulting offspring.

The subsequent chapters will describe a series of experiments designed to characterize the environment of the sow's reproductive tract and identify the factors associated with healthy embryonic development. It has previously been shown that transferring embryos into an abnormal location (Stein-Stefani and Holtz 1987; Wallenhorst and Holtz 1999), or at an inappropriate time (Pope *et al.* 1986; Wilde *et al.* 1988), can have detrimental effects on embryonic survival. Based on this information we hypothesise that key factors involved in the survival and development of the embryo will increase and decrease in abundance in a manner temporally and spatially consistent with the location of the embryo. As such, the subsequent chapters of this thesis will assess the reproductive tract environment in relation to the associated stages of embryonic development, in both physiologically appropriate and inappropriate locations. In addition, given that much of this environment is thought to be regulated by pregnancy associated hormones, such as progesterone, these experiments will use preovulatory stages as a physiological benchmark to which comparisons will be made.

Due to a combination of embryonic plasticity and the lack of a clear definition for a healthy embryo, it is difficult to define the ideal or normal environment for embryo development. In swine, a positive effect of delayed breeding on embryo survival in primiparous sows has been well established (Clowes *et al.* 1994; Patterson *et al.* 2008; Oliver *et al.* 2011). While a portion of

this effect is likely due to the recovery from a catabolic state of the sow during follicular development in late lactation (Zak *et al.* 1997a; Zak *et al.* 1997b; Almeida *et al.* 2001), it is not possible to rule out an effect of delayed breeding on the uterine and oviductal environments. It has previously been shown that delayed breeding in swine affects progesterone levels (Clowes *et al.* 1994), and that these levels regulate the uterine and oviductal environments. To account for these possible negative effects seen in primiparous sows bred at the first post-weaning estrus, the experiments described in the subsequent chapters were designed to evaluate the uterine environment in primiparous sows bred at the second post weaning estrus.

The third chapter of this thesis focuses on the characterization of the unique glycosaminoglycan, hyaluronic acid, within the healthy reproductive tract of the sow. Hyaluronic acid when used at an appropriate level has previously been shown to improve embryo development *in vitro* (Miyano *et al.* 1994; Furnus *et al.* 1998; Kano *et al.* 1998). Furthermore, its addition to human embryo transfer media has been shown to increase pregnancy rates (Simon *et al.* 2003; Correa-Pérez 2004). Although this molecule has been partially characterized in the pig (Tienthai *et al.* 2000; Tienthai *et al.* 2003a; Tienthai *et al.* 2003b), its biology is exceedingly complex and it is known to create different and often opposite effects depending on its size, concentration and localization (Stern *et al.* 2006). As such, chapter 3 will describe an experiment designed to not only characterize hyaluronic acid but also hyaluronic acid associated transcripts and proteins.

Many of the chemical components of the uterine histotroph have been previously described in swine (Iritani *et al.* 1974). However, while proteomic profiles of uterine fluid have been determined in other species (MacLaughlin *et al.* 1986) and at later time points in the pig (Kayser *et al.* 2006), the specific protein constituents present during cleavage stage development in the pig

remain unknown. Chapter 4 will describe the quantitative changes in the histotrophic proteome of the sow's uterus during early embryonic development. Based on the hypothesis that proteins vital to embryo and sperm survival will increase in abundance during time points when these gametes are present in specific locations in the female reproductive tract, the proteome of the reproductive tract at the onset of standing estrus, corresponding to the germinal vesicle stage of oocyte development, will be compared to that at the blastocyst stage of embryonic development.

With the application of high throughput molecular methodologies such as microarray analysis and the continued development of large databases of biological information, it becomes possible to assess reproductive events from the perspective of systems biology. Much of this approach centers on understanding the communication between separate physiological entities such as the embryo and uterus. Existing bioinformatics tools are ill-equipped to efficiently utilize the available information to compare two sets of data in this manner. Chapter 5 will discuss the development of a novel bioinformatics tool specifically designed to assess the potential protein-protein interactions identified by two sets of transcriptomic data.

It is well understood that the conditions in the reproductive tract are modulated within the pregnant female by hormonal signals such as estrogen and progesterone (Buhi *et al.* 1992; McMaster *et al.* 1992; Novak *et al.* 2003). However, recent work has revealed that this environment is also altered by the presence of an embryo during the early cleavage stages of development (Bauersachs *et al.* 2003; Georgiou *et al.* 2005; Georgiou *et al.* 2007). Chapter 6 of this thesis evaluates changes in the uterine transcriptome at time points corresponding to the preovulatory oocyte germinal vesicle stage and the embryonic blastocyst stage of the reproductive cycle. In addition, this chapter

attempts to apply the tools described in the previous chapter to identify potential factors in the maternal-embryonic cross-talk.

The final chapter of this thesis will present the unifying conclusions drawn from the existing literature and experimental data presented. In addition, it will present specific questions raised by the results obtained and potential future studies necessary to better understand the impact of the maternal environment on early embryo development, and how it is temporally and spatially regulated in the pig.

References

Almeida, F.R., Mao, J., Novak, S., Cosgrove, J.R., and Foxcroft, G.R. (2001) Effects of different patterns of feed restriction and insulin treatment during the luteal phase on reproductive, metabolic, and endocrine parameters in cyclic gilts. J Anim Sci 79(1), 200-212

Barker, D.J., and Martyn, C.N. (1992) The maternal and fetal origins of cardiovascular disease. J Epidemiol Community Health 46(1), 8-11

Bauersachs, S., Blum, H., Mallok, S., Wenigerkind, H., Rief, S., Prelle, K., and Wolf, E. (2003) Regulation of Ipsilateral and Contralateral Bovine Oviduct Epithelial Cell Function in the Postovulation Period: A Transcriptomics Approach. Biol Reprod 68(4), 1170-1177

Buhi, W.C., Alvarez, I.M., Sudhipong, V., and Dones-Smith, M.M. (1990) Identification and characterization of de novo-synthesized porcine oviductal secretory proteins. Biol Reprod 43(6), 929-938

Buhi, W.C., Ashworth, C.J., Bazer, F.W., and Alvarez, I.M. (1992) In vitro synthesis of oviductal secretory proteins by estrogen-treated ovariectomized gilts. J Exp Zool 262(4), 426-435

Clowes, E.J., Aherne, F.X., and Foxcroft, G.R. (1994) Effect of delayed breeding on the endocrinology and fecundity of sows. J. Anim Sci. 72(2), 283-291

Correa-Pérez, J.R. (2004) Embryo transfer medium--hyaluronic acid in place of albumin? Fertil Steril 81(4), 1157-1157

Dobrinsky, J.R., Johnson, L.A., and Rath, D. (1996) Development of a culture medium (BECM-3) for porcine embryos: effects of bovine serum albumin and fetal bovine serum on embryo development. Biol Reprod 55(5), 1069-1074

Ducro-Steverink, D.W.B., Peters, C.G.W., Maters, C.C., Hazeleger, W., and Merks, J.W.M. (2004) Reproduction results and offspring performance after non-surgical embryo transfer in pigs. Theriogenology 62(3-4), 522-531

Flood, M.R., and Wiebold, J.L. (1988) Glucose metabolism by preimplantation pig embryos. J Reprod Fertil 84(1), 7-12

Foxcroft, G.R., Dixon, W.T., Novak, S., Putman, C.T., Town, S.C., and Vinsky, M.D.A. (2006) The biological basis for prenatal programming of postnatal performance in pigs. J Anim Sci 84(13 suppl), E105-E112

Foxcroft, G.R., Vinsky, M.D., Paradis, F., Tse, W.Y., Town, S.C., Putman, C.T., Dyck, M.K., and Dixon, W.T. (2007) Macroenvironment effects on oocytes and embryos in swine. Theriogenology 68(Supplement 1), S30-S39

Furnus, C.C., de Matos, D.G., and Martinez, A.G. (1998) Effect of hyaluronic acid on development of in vitro produced bovine embryos. Theriogenology 49(8), 1489-1499

Georgiou, A.S., Snijders, A.P.L., Sostaric, E., Aflatoonian, R., Vazquez, J.L., Vazquez, J.M., Roca, J., Martinez, E.A., Wright, P.C., and Fazeli, A. (2007) Modulation of The Oviductal Environment by Gametes. J Proteome Res 6(12), 4656-4666

Georgiou, A.S., Sostaric, E., Wong, C.H., Snijders, A.P.L., Wright, P.C., Moore, H.D., and Fazeli, A. (2005) Gametes Alter the Oviductal Secretory Proteome. Mol Cell Proteomics 4(11), 1785-1796

Hazeleger, W., and Kemp, B. (1994) Farrowing Rate and Litter Size after Transcervical Embryo Transfer in Sows. Reprod Domestic Anim 29(6), 481-487

Iritani, A., Sato, E., and Nishikawa, Y. (1974) Secretion Rates and Chemical Composition of Oviduct and Uterine Fluids in Sows. J Anim Sci 39(3), 582-588

Kano, K., Miyano, T., and Kato, S. (1998) Effects of glycosaminoglycans on the development of in vitro-matured and -fertilized porcine oocytes to the blastocyst stage in vitro. Biol Reprod 58(5), 1226-1232

Kayser, J.-P.R., Kim, J.G., Cerny, R.L., and Vallet, J.L. (2006) Global characterization of porcine intrauterine proteins during early pregnancy. Reproduction 131(2), 379-388

Leese, H.J., and Barton, A.M. (1984) Pyruvate and glucose uptake by mouse ova and preimplantation embryos. J Reprod Fertil 72(1), 9-13

MacLaughlin, D.T., Santoro, N.F., Bauer, H.H., Lawrence, D., and Richardson, G.S. (1986) Two-dimensional gel electrophoresis of endometrial protein in human uterine fluids: qualitative and quantitative analysis. Biol Reprod 34(3), 579-585

McMaster, M.T., Teng, C.T., Dey, S.K., and Andrews, G.K. (1992) Lactoferrin in the mouse uterus: analyses of the preimplantation period and regulation by ovarian steroids. Mol Endocrinol 6(1), 101-111

Miyano, T., Hiro-oka, R.E., Kano, K., Miyake, M., Kusunoki, H., and Kato, S. (1994) Effects of hyaluronic acid on the development of 1- and 2-cell porcine embryos to the blastocyst stage in vitro. Theriogenology 41(6), 1299-1305

Novak, S., Almeida, F.R.C.L., Cosgrove, J.R., Dixon, W.T., and Foxcroft, G.R. (2003) Effect of pre- and postmating nutritional manipulation on plasma progesterone, blastocyst development, and the oviductal environment during early pregnancy in gilts. J Anim Sci 81(3), 772-783

Novak, S., Paradis, F., Patterson, J.L., Pasternak, J.A., Oxtoby, K., Moore, H.S., Hahn, M., Dyck, M.K., Dixon, W.T., and Foxcroft, G.R. (2012) Temporal candidate gene expression in the sow placenta and embryo during early gestation and effect of maternal Progenos supplementation on embryonic and placental development. Reprod Fertil Dev 24(4), 550-558

Oliver, G., Novak, S., Patterson, J.L., Pasternak, J.A., Paradis, F., Norrby, M., Oxtoby, K., Dyck, M.K., Dixon, W.T., and Foxcroft, G.R. (2011) Restricted feed intake in lactating primiparous sows. II. Effects on subsequent litter sex ratio and embryonic gene expression. Reprod Fertil Dev 23(7), 899-911

Patterson, J., Wellen, A., Hahn, M., Pasternak, A., Lowe, J., DeHaas, S., Kraus, D., Williams, N., and Foxcroft, G. (2008) Responses to delayed estrus after weaning in sows using oral progestagen treatment. J Anim Sci 86(8), 1996-2004

Perry, J.S., and Rowlands, I.W. (1962) Early Pregnancy in the Pig. J Reprod Fertil 4(2), 175-188

Polge, C. (Ed.) (1982) 'Embryo Transplantation and Preservation.' Control of Pig Reproduction (Butterworths: London)

Pope, W.F., Lawyer, M.S., Nara, B.S., and First, N.L. (1986) Effect of asynchronous superinduction on embryo survival and range of blastocyst development in swine. Biol Reprod 35(1), 133-137

Pratt, H.P.M. (1980) Phospholipid synthesis in the preimplantation mouse embryo. J Reprod Fertil 58(1), 237-248

Rijnders, P.M., and Jansen, C.A. (1998) The predictive value of day 3 embryo morphology regarding blastocyst formation, pregnancy and implantation rate after day 5 transfer following in-vitro fertilization or intracytoplasmic sperm injection. Human Reproduction 13(10), 2869-2873

Simon, A., Safran, A., Revel, A., Aizenman, E., Reubinoff, B., Porat-Katz, A., Lewin, A., and Laufer, N. (2003) Hyaluronic acid can successfully replace albumin as the sole macromolecule in a human embryo transfer medium. Fertil Steril 79(6), 1434-1438

Singh, E.L., Eaglesome, M.D., Thomas, F.C., Papp-Vid, G., and Hare, W.C. (1982) Embryo transfer as a means of controlling the transmission of viral infections. I. The in vitro exposure of preimplantation bovine embryos to akabane, bluetongue and bovine viral diarrhea viruses. Theriogenology 17(4), 437-444

Singh, E.L., and Thomas, F.C. (1987) Embryo transfer as a means of controlling the transmission of viral infections. IX. The in vitro exposure of zona pellucida-intact porcine embryos to swine vesicular disease virus. Theriogenology 27(3), 443-449

Stein-Stefani, J., and Holtz, W. (1987) Surgical and endoscopic transfer of porcine embryos to different uterine sites. Theriogenology 27(1), 278

Stern, R., Asari, A.A., and Sugahara, K.N. (2006) Hyaluronan fragments: an information-rich system. Eur J Cell Biol 85(8), 699-715

Strunker, T., Goodwin, N., Brenker, C., Kashikar, N.D., Weyand, I., Seifert, R., and Kaupp, U.B. (2011) The CatSper channel mediates progesterone-induced Ca2+ influx in human sperm. Nature 471(7338), 382-386

Swain, J., Bormann, C., Clark, S., Walters, E., Wheeler, M., and Krisher, R. (2002) Use of energy substrates by various stage preimplantation pig embryos produced in vivo and in vitro. Reproduction 123(2), 253-260

Tienthai, P., Kimura, N., Heldin, P., Sato, E., and Rodriguez-Martinez, H. (2003a) Expression of hyaluronan synthase-3 in porcine oviducal epithelium during oestrus. Reprod Fertil Dev 15(1-2), 99-105

Tienthai, P., Kjellen, L., Pertoft, H., Suzuki, K., and Rodriguez-Martinez, H. (2000) Localization and quantitation of hyaluronan and sulfated glycosaminoglycans in the tissues and intraluminal fluid of the pig oviduct. Reprod Fertil Dev 12(3-4), 173-182

Tienthai, P., Yokoo, M., Kimura, N., Heldin, P., Sato, E., and Rodriguez-Martinez, H. (2003b) Immunohistochemical localization and expression of the hyaluronan receptor CD44 in the epithelium of the pig oviduct during oestrus. Reprod. 125(1), 119-132

van der Lende, T., and Schoenmaker, G.J.W. (1990) The relationship between ovulation rate and litter size before and after Day 35 of pregnancy in gilts and sows: An analysis of published data. Liv. Prod. Sci 26(3), 217-229

Wallenhorst, S., and Holtz, W. (1999) Transfer of pig embryos to different uterine sites. J Anim Sci 77(9), 2327-2329Wilde, M.H., Xie, S., Day, M.L., and Pope, W.F. (1988) Survival of small and large littermate blastocysts in swine after synchronous and asynchronous transfer procedures. Theriogenology 30(6), 1069-1074

Zak, L.J., Cosgrove, J.R., Aherne, F.X., and Foxcroft, G.R. (1997a) Pattern of feed intake and associated metabolic and endocrine changes differentially affect postweaning fertility in primiparous lactating sows. J Anim Sci 75(1), 208-216

Zak, L.J., Xu, X., Hardin, R.T., and Foxcroft, G.R. (1997b) Impact of different patterns of feed intake during lactation in the primiparous sow on follicular development and oocyte maturation. J Reprod Fertil 110(1), 99-106

Chapter 2: Literature Review

Introduction

Prenatal development is typically defined as the period between fertilization of the oocyte and parturition. Development is characterized by substantial external and internal morphological changes to the conceptus (Evans and Sack 1973), as well as epigenetic and molecular modifications. As a result of this complexity, the process by which a single cell zygote can develop into a functional organism, and later a healthy adult, must be subdivided in physiologically meaningful sections. This was initially done in livestock species using a separation into three segments, that of the ovum, embryo and fetus; using implantation and the formation of major tissues and organs as the two division points (Hanly 1961). In livestock species, this system of classification has since been modified to include the embryonic, placental and fetal stages, with the transition to the fetal stage marked by the appearance of all major anatomical structures (Symonds *et al.* 2007).

Based on either definition, the period of embryonic development is of particular interest, as it is during this time that the initial differentiation and development of an organism occurs. Physiologically this is also the period when numerous key events such as maternal recognition of pregnancy, implantation, and neural tube formation must occur (Dyck and Ruvinsky 2011). In livestock species this is made increasingly complicated, as implantation occurs not shortly after hatching from the zona pellucida, as it does in humans, but much later after expansion to a filamentous state. The embryo must therefore survive unattached in the uterine luminal fluid or histotroph (Mullen *et al.* 2012), while gastrulation and elongation of the trophectoderm (TE) occur. For these reasons, the original separation of embryonic development into pre and post implantation stages is

particularly fitting for the study of reproduction in agriculturally important species. This review will therefore concentrate on the physiological mechanisms associated with the preimplantation period, paying particular attention to the role of the embryonic environment from initial cell division to the hatching of the blastocyst from the zona pellucida.

While from a simplistic view the preimplantation development of eutherian mammals is similar, substantial differences have begun to emerge between what is known in common model organisms such as mice and large animal species (Papaioannou and Ebert 1988). For this reason the following review will also focus primarily on the current accumulation of physiological information regarding preimplantation development in the pig. This information will be supplemented with information gleaned from other species to fill in fundamental gaps in knowledge and provide physiological contrast where substantial differences occur. Furthermore, as swine production represents an integral part of the agricultural system at both a Canadian and global level, this review will attempt to ground these physiological concepts in technologies applicable to swine production and management.

Dynamics of Embryo Development

The degree of complexity and sensitivity of embryonic development, specifically in the early stages, can be seen in the distribution of prenatal loss. In humans, prenatal losses are staggering; with estimates based on mathematical modeling suggesting 78% of fertilized embryos are lost prior to the detection of pregnancy (Roberts and Lowe 1975). The majority of pre-detection loss is assumed to be the result of deterioration due to abnormalities at the very early embryonic stage. In humans the full embryonic stage is, in its most modern sense, defined as the eight week period following the first mitotic division (Findlay *et al.* 2007). While this amounts to only the first 20% of prenatal development, it is estimated that between 25 and 30% of detectable pregnancies, based on the detection of human chorionic gonadotropin (hCG), are

lost during this stage (Vitzthum *et al.* 2006). When compared to pregnancy loss during the fetal period, which has been estimated at just two percent (Goldstein 1994), it is clear that the period of embryonic development is by far the most challenging and perilous portion of the prenatal period. If this period is further subdivided based on the appearance of anatomical embryonic landmarks, the largest losses occur prior to the development of the yolk sack and decrease rapidly to the point where almost no loss occurs beyond 10mm in size (Goldstein 1994).

A similar trend is observed in dairy cattle where, despite fertilization rates in excess of 95%, pregnancy rates remain at just 40%, with the majority of this loss suggested to occur between days 8 and 17 post-insemination (Diskin and Morris 2008). Other estimates of embryonic loss suggest that the most significant portion (40%) occurs during the first 7 days following insemination (Ryan *et al.* 1993). This latter estimate coincides with the development at very early cleavage and immediately post-hatching stages of development. Embryonic mortality at this very early stage appears to be an indirect result of high maternal milk production and, as such, is likely mediated through the effects of catabolism on either oocyte maturation or the post-fertilization uterine environment.

Prenatal mortality in swine and other polytocous species is more difficult to quantify, as partial loss of the litter does not necessarily result in a failed pregnancy and a return to cyclicity. In swine, if greater than two viable conseptuses are present in each uterine horn, maternal recognition at day 11-12 can be successful and the pregnancy will proceed (Polge *et al.* 1966; Dziuk 1985; Senger 1999). Therefore, prenatal mortality in poly-ovulatory species is almost always measured via terminal hysterectomy and the subsequent comparison of conseptuses to a count of corpora lutea (CL) which indicates the ovulation rate. This methodology functions based on two assumptions, that every ovulation results in a single fertilized oocyte and that experimental recovery of

conseptuses is complete. Both these assumptions are generally valid in swine as the fertilization rate is above 95 % (Perry and Rowlands 1962), twinning occurs in less than 0.2% of ovulations (Grapes *et al.* 2001) and flushing of even very early embryos using the methodology described by Polge (1982) yields between 95 and 100% recovery (Polge 1982).

A broad application of this methodology, simply looking at litter size and ovulation rate, shows substantial prenatal loss in the modern swine industry. Average litter size in 2011 was 12 and 11.83 born alive per sow per litter in Canada (PigCHAMP 2011a) and the Unites States (PigCHAMP 2011b), respectively. However, a recent study of contemporary sows carried out by our research group at the University of Alberta showed average ovulation rates to be over 25 (Novak *et al.* 2012), creating a total estimation of prenatal loss of approximately 52% in modern genetic lines. It was initially considered that embryonic loss was by far the most significant portion of prenatal mortality, with the number of viable embryos dropping by as much as 30% by day 30 of gestation (Pope *et al.* 1986). However, ovulation rates in swine have increased drastically in modern commercial lines when compared to those of the recent past, which appears to have had an effect on the timing of prenatal loss. Early embryonic loss is still the most significant, estimated at roughly 40% by day 21-30 of gestation (Novak *et al.* 2012). While this loss appears to plateau up to day 50 of gestations (Novak *et al.* 2012), it increases slightly thereafter as a result of uterine crowding, with the most significant fetal losses seen in later parity sows (Town *et al.* 2005). It is however important to note that while prenatal losses between day 20-30 average to 40%, there are animals in which survival at this stage appears to be 100%, as well as others where it is substantially lower as well. This would suggest that individual variation at the maternal level may significantly alter embryonic survival rates. Furthermore, it should be stated that the presence of an embryo within the day 20-30 uterus does not in any way guarantee that it is either of good quality or that it will develop in the same way

as its cohorts. In addition, it has previously been shown that the distribution of embryonic mortality can be altered by the previous nutritional state of the mother with selective loss of female embryos (Vinsky et al. 2006).

There is some controversy regarding how early embryonic loss occurs in swine. A study by Perry and Rowlands (1962) assessed embryo status from 48 hours to 40 days after the onset of estrus. Between the 6^{th} and 9^{th} day following onset of estrus they identified 22% of embryos as degenerating, which increased to only 34.8% by day 25-40. In addition, they found substantial variation in the embryos flushed prior to day 6 and identified many of them as having atypical cell numbers (3,5,6,7 etc.) for cleavage stage embryos (Figure 2.1). These results are contrary to those of Polge (1982), who found only 1% of embryos collected up to nine days following onset of estrus showed "obvious signs of degeneration". Although this report makes no mention of the proportion of embryos with atypical cell numbers, it suggests results of both studies should be viewed with some reservations given the variability seen by Perry and Rowlands and the superficial examination of embryos in their own study. However, a third experiment dealing with embryos flushed from the reproductive tracts in which ovulation rates were high (40.3±21.4), showed that with high recovery and fertilization rates only 47% of embryos were suitable for transfer, with the rest showing delayed development or signs of degeneration (Stein-Stefani and Holtz 1987). It should also be noted that the accumulation of lipids in the porcine cleavage stage embryo darkens their appearance (Sturmey and Leese 2003) making differentiation between normal development and fragmentation or degeneration difficult. A more recently published study by Vinsky *et al.* (2007) evaluated embryo recovery at day 5.5 and 7 (Ovulation set as Day 1) and showed that recovery rates fell between 40 and 100%. While this study did recover a small number of embryos a stages ranging from 1-32 cells, the authors note that a positive correlation exists between the number of blastocysts and the recovery rate (Vinsky *et al.* 2007). While this correlation is likely an artifact of the

variability in flushing effectiveness as a result of both viability and developmental stage it is clear that at least a portion of embryo mortality in some pregnancies occurs during cleavage stages of embryonic development.

The localization of prenatal mortality primarily into the embryonic stages, with particular issues seen during the preimplantation period, demonstrates the sensitivity of this important biological process. In order to further understand the dynamic, physiological processes at play during this period it is necessary to examine the key cellular, structural, metabolic and molecular mechanisms involved in both gamete and preimplantation embryo development.

Gametes, Fertilization and Cleavage

Embryonic development begins with the fertilization of the oocyte by a single spermatozoon, which will immediately initiate a complex series of events starting with the first embryonic cleavage. However, the process of reproduction starts long before fertilization or cleavage with the development and preparation of both maternal and paternal gametes. Like the embryo each gamete is a specialized cell which relies heavily on the support of its immediate environment for survival, maintenance and development. The quality and viability of each gamete has a direct effect on the developmental potential of the embryo.

The oocyte in particular contributes not only the maternal genetic component but also cytoplasmic macromolecules, organelles and maternal RNA to the zygote. As such the potential for embryonic development, during the early stages in particular, is directly influenced by follicular development and oocyte maturation (Hunter 2000). The population of oocytes in the ovary is established early in gestation of the developing female when the primordial germ cells migrate from the yolk sack to the gonadal ridge, and then begin mitotic proliferation. In the pig, meiosis begins around day 40 of gestation and continues until shortly after birth by which time all oocytes are brought to nuclear arrest at the germinal vesicle stage (Hunter 2000). Each oocyte is initially surrounded by a single layer of squamous pre-granulosa cells forming what is

termed a primordial follicle. At approximately 70 days of gestation the follicles have started to advance to the primary stage (Christenson *et al.* 1985), identified by the transition of the pre-granulosa cells to a cuboidal state. Secondary follicles, defined by the proliferation of the granulosa cells to form more than one layer, are identified in the ovary around the time of birth and will increase in number up to around 90 days following parturition (Christenson *et al.* 1985). These secondary follicles will go on to develop a fluid filled antrum and subsequently large tertiary follicles with substantial populations of granulosa and theca cells which further support oocyte development.

Follicular recruitment, selection, dominance and ovulation in swine and in other mammals are under the control of the hypothamic-pituitary-gonadal axis (Ireland 1987). While aspects of recruitment and selection will occur in pre pubertal animals, the remaining stages of oocyte development require puberty and the full activation of this regulatory mechanism. Tonic levels of gonadotropin releasing hormone (GnRH) released by the hypothalamus stimulate pituitary production of both follicle stimulating hormone (FSH) and luteinizing hormone (LH), which in turn promote follicular development and hormonal production. The production of estrogen by the follicle will result from the combined action of LH on the theca cells to produce androgens and LH and FSH on the granulosa cells to convert this androgen pool into estrogen (Leung and Armstrong 1980). Ovarian estrogen subsequently feeds back on the hypothalamus and the pituitary to control LH secretion (Christenson *et al.* 1985).

While the hypothalamic pituitary axis is a key regulator of follicular development, recent findings from our own laboratory have shown a more localized regulation arises from the cross-talk between the oocyte, granulosa and theca cells (Paradis 2009). These localized mechanisms likely respond to the modulation of gonadotropins to produce the maternal components in the oocyte necessary for embryonic development. This localized regulation appears to be

central in providing the oocyte with developmental competence following fertilization. The current understanding of this complex cross-talk in relation to developmental competence has been reviewed in depth by Zuccotti *et al.* (2011). When bovine oocytes are matured *in vitro* and this localized cross-talk is disrupted, subsequent development *in vivo* is negatively affected relative to *in vivo* matured control oocytes (Leibfried-Rutledge *et al.* 1987). In the pig, Mattioli *et al.* (1989) reported 61% development of embryos recovered at day 4 following the transfer of cleaved zygotes produced from *in vitro* matured oocytes. However, recovery in this experiment was only 79% of embryos transferred. Based on the experiences of our lab, the non-recovered embryos are likely to have degenerated, leaving the developmental potential at just 48% of those transferred into recipient gilts. While this particular experiment contained no *in vivo* matured experimental control, the level of development is substantially lower than that observed in flushing of *in vivo* produced embryos (eg. Vinsky *et al.* 2007). Therefore, the maturation of porcine oocytes and/or 48 hours of embryo culture have a substantial impact on developmental competence. Experiments examining the effect of the maturation media formulation on subsequent *in vitro* fertilization and development in the pig, demonstrate a substantial effect on blastocyst development and cell number (Wang *et al.* 1997). Taken together, these results clearly demonstrate that the developmental competence of the oocyte and embryo are linked and are directly affected by the conditions of oocyte maturation.

Unlike the oocyte, sperm contribute little beyond the paternal genetic material to the zygote. Even the sperm's mitochondria contributed to the zygote at the time of fertilization are directly targeted for destruction by the maternal ubiquitin system (Sutovsky *et al.* 2004). In addition, while the initial population of spermatogonia are established during early gestation from primordial germ cells, this pool of stem cells is constantly renewed (Brinster and Zimmermann 1994). Rather than halting meiosis at the germinal vesicle (GV) stage as in oocytes,

sperm develop as the result of continuous mitotic and meiotic divisions throughout the life of the male. In the pig, development from an A1 spermatogonial stem cell to a mature spermatozoon occurs in just 39 days (Senger 1999). However the constant renewal and short developmental timespan of the sperm relative to the oocyte does not make it immune to the environmental effects discussed later.

Following mating or insemination, the sperm must survive and overcome a series of barriers presented by the female reproductive tract in order to reach and fertilize the oocyte. The first of these barriers is the maternal immune system. There is, as of yet, no consensus regarding the primary source of the immune response in pigs following mating. A study by Rozeboom *et al.* (1999) showed that the number of polymorphonuclear neutrophilic granulocytes in the uterine lumen was significantly greater when gilts were inseminated with sperm suspended in PBS than with PBS alone (Rozeboom *et al.* 1999). Other studies in swine have shown that natural mating with vasectomized boars also results in leukocyte infiltration and cytokine response (Bischof *et al.* 1994; O'Leary *et al.* 2006). This later implication of seminal plasma in initiating the immune response is also in agreement with studies conducted in mice (Robertson *et al.* 1996).

Regardless of whether it is seminal plasma or sperm which are involved in this response, it is clear that semen is involved in altering the condition or state of the female reproductive tract. Seminal constituents in the pig have been shown to have a substantial effect on the transcriptome of the uterine endometrium with a particular effect on genes associated with immune function (Taylor *et al.* 2009). The effect of semen on the female however, appears to extend beyond the uterine endometrium. Seminal plasma, which contains substantial quantities of estrogen, has been shown to shorten the interval between onset of estrus and ovulation by as much as 14 hours (Waberski 1997). This effect could be mediated either directly on the ovary via transport though

the sub-ovarian counter-current-system or through feedback on the hypothamic-pituitary-axis. Interestingly, the effect of estrogen infusion alone had a significantly diminished effect relative to seminal plasma, suggesting there may be other communicative factors at play. Experiments in lamas, have also demonstrated the existence of a pro-ovulatory factor in seminal plasma, and have shown an effect on ovulation and CL formation even when this factor is injected intramuscularly (Adams *et al.* 2005). Recently, a 13,221 kDa protein was identified in the seminal plasma of both lamas and bulls which shows similarity to β nerve growth factor (β-NGF) at both a sequence and functional level and is able to induce ovulation (Ratto *et al.* 2012). Furthermore these authors suggest β-NGF plays a direct endocrine role on the female hypothalamo-pituitary-gonadal axis. Uterine infusion of seminal plasma in gilts has also been shown to increase plasma progesterone levels with the most significant source of this effect observed in granulosa cell cultures (O'Leary *et al.* 2006). Furthermore, this increase in progesterone in response to seminal plasma appears to last up to nine days following treatment (O'Leary *et al.* 2006). Given that progesterone plays a substantial role in modulating the uterine environment (reviewed later), it is not surprising that such treatment has been previously associated with increased embryonic survival (O'Leary *et al.* 2004). This apparent semen-uterine-ovarian communication axis is of particular interest in the pig given the standard practice of AI with heavily extended semen doses.

A second barrier to fertilization which the sperm must overcome is the combination of the cumulus cells and zona pellucida. Penetration through these barriers is accomplished by a combination of mechanical pressure and chemical digestion. Once in close proximity to the cumulus-oocyte complex the sperm will become hyper-activated. This change in motility pattern is brought on by an influx of calcium through the CatSper family of Ca2+ ion channels on the sperm membrane (Qi *et al.* 2007). More significantly, this effect is mediated by the action of cumulus produced progesterone directly on the CatSper protein in the

sperm membrane (Strunker *et al.* 2011). This system is of particular interest, as sperm are considered to be transcriptionally and translationally silent and CatSper is a membrane bound protein, making it the first known instance of non-genomic signaling for progesterone. Once through the cumulus cell layer, sperm proteins will bind the zonal protein ZP3 and the acrosome reaction will be initiated (Berger *et al.* 1989). Proteins released during the acrosome reaction will hydrolyze the surrounding zona pellucida, which, combined with hyperactivity, allow the sperm to penetrate the oocyte. Subsequently, the equatorial region of the sperm membrane fuses with that of the oocyte and cortical granules are released which modify the zona pellucida to prevent binding and penetration of additional sperm (Miller *et al.* 1992). The modification of the zona pellucida is referred to as the zona block and is necessary in preventing polyspermy, which will result in developmental failure.

The complex series of events that result in sperm penetration and the hardening of the zona pellucida, are heavily affected by the environment of the oocyte either during maturation or prior to fertilization. *In vitro* fertilization of (*in vivo* matured) pig oocytes has been shown to result in a failure (Cran and Cheng 1986) or reduction (Kim *et al.* 1996) in the ability to disperse the contents of the cortical granules necessary to produce the zona block. Modifications to the formulation of *in vitro* fertilization media have been shown to affect the proportion of *in vitro* matured oocytes that experienced a cortical reaction, as well as the incidence of polyspermy (Coy *et al.* 2002). Furthermore, the exposure of porcine oocytes to oviductal fluid prior to fertilization resulted in a hardening of the zona pellucida, an increased rate of normal cortical exocytosis and higher incidence of monospermy. The effect of oviductal fluid on the structure of the zona pellucida has been further confirmed by 2D SDS PAGE, which showed ovulated oocytes collected from the oviduct have three additional, relatively high molecular weight proteins not found in the oocyte prior to oviductal exposure (Hedrick *et al.* 1987). These results show that the

interaction between the sperm and oocyte is mediated in some unknown manner by the environment of the reproductive tract, which is in turn affected by the presence of both sperm and seminal plasma. Furthermore, experiments using *in vivo* matured bovine oocytes fertilized either *in vivo* or *in vitro* and then developed *in vitro* show that the the use of in vitro fertilization alone causes a reduction in both cleavage rates and blastocyst yields (Rizos *et al.* 2002). It is therefore clear that the conditions in which fertilization occurs are vital, not only to the process of fertilization itself, but also to the developmental potential of the embryos produced.

Following penetration of the oocyte by sperm, an early developmental program is initiated that will continue until maternal activation of the zygotic genome (Moor and Gandolfi 1987). Initially this involves the final stages of oocyte meiosis concluding with the expulsion of the second polar body (Figure 2.2). At the same time, the morphology of the sperm head will change and its DNA will be de-condensed. Together these events result in the formation of one small and one large pronucleus of maternal and paternal origin, respectively. The female pronucleus is then brought toward the male pronucleus by the centrosome inherited from the body of the sperm and the two merge in the process of syngamy to produce a diploid embryo (Palermo *et al.* 1997).

Following syngamy the embryo will begin a series of symmetrical cell divisions within the zona pellucida (Figure 2.2). The volume of individual blastomeres is reduced by roughly 50% per cell cycle, while the total size and volume of the embryo will remain unchanged up to and including development of the blastocoel (Hamilton and Laing 1946). The initial cleavages of mammalian embryos are under the control of maternal transcripts present in the oocyte and furthermore, in mice, are affected by maternal genotype (Shire and Whitten 1980) and in particular the specific alleles of the PED gene (Brownell and Warner 1988). However, cleavage interval does appear to be affected by the formulation

of culture media (Devreker and Hardy 1997). It has been shown using *in vitro* produced bovine embryos that those which cleave along a timeline similar to that of their *in vivo* counterparts are more likely to develop into high quality morulae and blastocysts, as well as hatch from the zona pellucida (van Soom *et al.* 1997; Lonergan *et al.* 1999).

Genome Activation

Unlike other organisms which rely on maternal RNA to regulate much of embryonic development, mammalian zygotes degrade these RNAs shortly after fertilization (Oestrup *et al.* 2009). To compensate for this, activation of the full diploid genome, referred to as zygotic genome activation (ZGA), occurs early during the cleavage stages. This combination of degradation and activation is referred to as the maternal-to-zygotic transition or MZT, and it ensures the availability of mRNA and proteins necessary for the development process to continue.

The first stage of MZT involves the removal of maternal mRNA contributed to the zygote through the cytoplasm of the oocyte. In the mouse the maternal contribution of mRNA present at the MII stage is between 35 and 38 % of all known protein coding genes (Wang *et al.* 2004). However, by the late 2-cell stage, 90% of these poly[A] transcripts will be removed (Schultz 1993). A portion of these transcripts are present much earlier and survive for a prolonged period prior to elimination, suggesting removal involves a substantial change in stability (Tadros and Lipshitz 2009). Degradation of maternal RNA appears to take place by two separate mechanisms. The first mechanism is initiated upon fertilization and is maternally derived, as it occurs in spite of transcriptional inhibition. In the mouse this form of degradation accounts for 60% removal of maternal transcripts and corresponds to transcripts which are otherwise unexpressed in the early embryo (Alizadeh *et al.* 2005). A secondary mechanism of degradation appears to involve zygotic transcription and is absent when embryos are treated with alpha-amanitin. This latter mechanism has been

demonstrated in the pig and has been shown to affect at least one gene transcript (CDC25c) with known involvement in cell cycle control (Anderson *et al.* 2001). Although not directly demonstrated in mammals, the later transcriptionally dependant de-adenylation and degradation is thought to be mediated by zygotically derived micro RNA, which accumulates during the MZT (Minami *et al.* 2007).

Coinciding with the loss of maternal RNA is the generation of new transcripts from the full diploid genome. Studies measuring incorporation of radiolabeled uridine into RNA (Tománek *et al.* 1989) and methionine into protein (Jarrell *et al.* 1991) show zygotic genome activation (ZGA) in the porcine embryo starts at the 4-cell stage. Similar methods applied to mice, humans and cattle suggest their ZGA occurs at the two, four and eight cell stages, respectively, for these species (Kopecny 1989). Though zygotic genome activation (ZGA) was initially thought to occur in a single step, it is now understood that at least two distinct waves: a minor and major activation of transcriptional activity occur during cleavage (Tadros and Lipshitz 2009). Based on a large scale microarray experiment covering seven stages of embryonic development it has been proposed that in the mouse, minor activation occurs at the one-cell stage and major activation at the two-cell stage (Hamatani *et al.* 2004). It is important to note that minor activation, as identified by microarray analysis, occurs prior to the detection of transcription based on tritiated uridine. It is therefore, reasonable to assume that the 4-cell stage transcription identified thus far in the pig represents the major activation rather than the minor activation. While similar microarray experiments are currently underway for cattle and swine within our research group, no clear identification of the minor genome activation has been made in these species.

Interestingly, the stage of development in which murine, bovine and porcine embryos achieve major ZGA coincides precisely with the point of development in which these embryos experience what is termed the ``*in vitro*

block`` (Telford *et al.* 1990). Though the mechanism through which it occurs is not well understood, the *in vitro* block is the cell cycle in which the majority of embryos cease development. Through the manipulation of culture conditions it has become possible to develop some embryos of each species past this point, however the cost to embryo health or quality of this adaptive stress is unknown. Curiously, murine embryos produced by outbred strains are more likely to experience the *in vitro* block than those of inbred lines. Taking advantage of this oddity, Goddard and Pratt (1983) conducted a series of reciprocal crosses between an outbreed line (CFLP) known to experience the 2-cell block and an inbred laboratory F1 line (C57BL/10ScSn/Ola x CBA/Ca/Ola) known to produce embryos that culture well. The embryos collected from female CFLP mice had greater than 90% blocked at the (2-cell) stage regardless of parental line or fertilization method. The converse is true of embryos collected from the female F1 line of which over 90% developed past the 2-cell stage. Additional studies using similar strains have shown that the murine 2-cell block can be eliminated through the transfer of small quantities of cytoplasm from no blocking to blocking embryos (Muggleton-Harris *et al.* 1982). Together, these results would clearly suggest that the *in vitro* block is mediated by mechanisms inherent to the maternal cytoplasm. Furthermore, the temporal synchrony in multiple species with the major ZGA, combined with its occurrence in only some media, would suggest a significant interaction between maternal RNA depletion and the embryonic environment.

Compaction

Following the transition from maternal to embryonic genome, the next major event in embryonic development is the morphological rearrangement of the blastomeres known as compaction. This represents the first stage in the formation of the blastocyst, which will consist of two sections: an outer layer, the trophectoderm (TE) comprised of cuboidal or irregularly polygonal cells, and a closely associated inner cell mass (ICM) (Hamilton and Laing 1946). The process

of compaction has been studied overwhelmingly in mouse embryos through a series of elegant experiments conducted by Ziomek and Johnson (1980). The morphological changes associated with compaction occur in mouse embryos starting at the 8-cell stage and continuing through the cleavage of 8- to 16-cells (Bloom and McConnell 1990). The process can be split into four segments, one involving the reorganization of intracellular components and the remaining three are associated with intercellular reorganization (Pratt *et al.* 1982), the end result of which is the establishment of both a spatial and structural bias in blastomeric cell fate within the cleavage stage embryo.

Immediately following division of the 4-cell embryo to form an 8-cell embryo each blastomere appears to have no appreciable polarization. However, after this cleavage, an intracellular reorganization of the blastomeres begins, which will produce cellular polarity with a radial symmetry. Over the course of the 6-7 hours following the 3rd cell division, each of the eight blastomeres achieves polarization defined by surface binding of fluorescein isothiocyanate (FITC) labeled CON A (Ziomek and Johnson 1980). This polarization appears to occur as the result of surface adhesion with other blastomeres or any other structure, including cell debris or culture plates, and the axis of polarization is perpendicular to that of the adhesion (Ziomek and Johnson 1980). Surface adhesion is not, however, strictly required for polarization and, if absent, polarization appears to occur based on the location of a peripherally located nucleus (Houliston *et al.* 1989). The final result of this first stage of compaction involving intracellular reorganization is a radial symmetry with the ligand binding portion of each blastomere facing outward and the microvilli pole facing inward.

Following polarization of the blastomeres in the 8-cell embryos, the 4th embryonic cell division will begin. During this division, 82% of the blastomeres will divide in such a manner that the ligand binding pole and the pole of microvilli will be distributed to only one of the daughter cells (Johnson and Ziomek 1981).

This division will therefore, generate two cell populations each equally totipotent, but one made up of larger polarized cells and the other made up of smaller apolar cells (Ziomek and Johnson 1982). The two populations typically sort themselves into a core of six smaller apolar cells surrounded by ten larger polarized blastomeres. The asymmetry in number is caused by the minority of cells which divide, such that the polarity is contiguous at the midbody generating a pair of large polarized cells (Johnson and Ziomek 1981).

In an experiment involving the reconstruction of 16 blastomere aggregates based on the structure of an equivalent embryo described above, Ziomek and Johnson (1982) were able to further show that both cell type and position at this stage are key regulators of cell fate. The experiment involved placing a single FITC labeled cell of either a small apolar or large polar phenotype into the central core or external layer of the aggregates and observing the presence of the florescent label in the TE or ICM which developed. When each cell type was positioned in its "normal" position, large outer cells became TE and inner smaller cells became the inner cellular mass (ICM), with some exceptions associated with "leakage" out of position (Ziomek and Johnson 1982). In contrast, when labeled cells were positioned abnormally, the large cells still developed predominantly to TE, with only a small proportion developing between the two structures, while the small apolar cells placed outside the central core were able to produce either lineage or a combination of the two more evenly. This latter result would suggest that although the two cell populations remain totipotent, the small apolar cells are less differentiated than their larger polar counterparts.

An important step in compaction is the formation of cell adhesions between the blastomeres. The physical distinctiveness of each cell is lost during compaction as zonal adherins form between each blastomere. A precursor to more developed junctions, these zonal adherins are formed between actin

bound, transmembrane cadherin proteins (Watson and Barcroft 2001). Murine embryos homozygous for a null mutation in E-cadherin initially compact, but fail to develop further and eventually lose cell adhesion (Larue *et al.* 1994). The initial adhesion is thought to be mediated by maternally derived cadherin, though it appears that embryonic transcription of this gene is required to maintain these bonds. The bonds between opposing cadherins are calcium dependant and it has been shown that compaction and subsequent TE formation requires at least a minimum concentration of calcium (>0.02mM) in order to progress (Ducibella and Anderson 1979). This requirement indicates that even these initial stages of morphological change are environmentally dependent.

In addition to zonal adherins, communicative intercellular junctions, known as gap junctions, also form. These junctions functionally couple the cytoplasmic pools of adjacent blastomeres, allowing the exchange of ions and low molecular weight molecules (Caveney 1985). In murine embryos, gap junctions are initially present at the early 8-cell stage but only between sister blastomeres (McLachlin and Kidder 1986). The gap junctions will be further developed through gastrulation such that all cells in the morula will be coupled to one another (Lo and Gilula 1979). Similar to the zonal adherins, the gap junctions initially develop between sister blastomeres in spite of transcriptional and translational repression, but further development to join the remaining blastomeres requires embryonic transcription (McLachlin and Kidder 1986).

In the pig, compaction has not been studied as comprehensively. An analysis of *in vivo* derived porcine embryos by Papaioannou and Ebert (1988) would suggest morphological changes start to occur in blastomeres during the 4^{th} cleavage stage. It has been further observed that the actin structure begins to change after the 4-cell stage (Albertini *et al.* 1987). Taken together, these results indicate that compaction of porcine embryos occurs at a similar stage of embryonic development as that of the mouse. In fact, it is at the 8-16 cell stage

that the morula takes on a more spherical appearance with a smoother surface (Oestrup *et al.* 2009), which are both morphological indicators of compaction.

Experiments involving the exposure of early cleavage stage embryos to protein synthesis inhibitors suggest the mechanism by which compaction is initiated is post transcriptional and utilizes proteins generated as early as the 2- to 4-cell stages (Levy *et al.* 1986). Furthermore, it has been shown that compaction is linked to specific changes in protein phosphorylation, suggesting phosphate metabolism pathways are key to this developmental step (Bloom and McConnell 1990). Protein phosphorylation is also associated with the interaction of receptor ligand pairs which might suggest extra embryonic signals play a role along with cell contact in regulating this process.

Blastocoel formation

Following compaction two groups of blastomeres exist that have not fully differentiated from one another. Through the subsequent blastulation, the outer layer of large polarized cells will differentiate to form the TE, while the inner apolar cells will form the ICM. Ionic and dye coupling experiments show that during blastocoel formation the embryo will maintain gap junctions both within and between these two cell types. Despite this, fundamental differences will develop in their degree of differentiation, the manner in which they join together and their rate of cell proliferation.

During blastulation the TE results from the formation of tight junctions between this outer cell layer effectively sealing the blastocoel cavity (Oestrup *et al.* 2009). These tight junctions, also known as zonal occludens, are extracellular structures resulting from numerous proteins, including cingulin occludin and claudin, which are directly linked to the cytoskeleton (Watson and Barcroft 2001). While formation of zonal occludens does not strictly require the zonal adherins established during compaction, they will appear in a disordered and distorted manner without them (Riethmacher *et al.* 1995).

The tight junctions that form play two distinct roles which allow the TE to begin acting as a specialized epithelium. First, they create a tight barrier that allows accumulation of fluid within the developing blastocoel cavity. This structure requires time to form and in the mouse embryo is not fully complete until after cavitation has been initiated (McLaren and Smith 1977), at which point it becomes capable of true partitioning between the internal and external environment. The second role of the tight junction is to separate the basal and apical sides of the epithelial structure. The fluid accumulation required for cavitation is brought into the blastocoel cavity through the creation of an ionic gradient followed by transport of water across the TE. This separation of apical and blastolateral membranes allows the localization of the necessary ion transporters and aquaporines to specific sides of the epithelial layer. For example, it has been shown that aquaporin 3 and 8 are localized to the blastolateral membrane of the murine TE, while aquaporin 9 localizes to the apical membrane (Barcroft *et al.* 2003). Similar localization has been seen in the isoforms of the sodium potassium ATPase transporter, with the alpha 1 subunit localized to the blastolateral membrane and the alpha 3 subunit localized to the apical membrane (Betts *et al.* 1998).

In contrast to the differentiation of the outer polar cells into the epithelial structure of the TE, the inner apolar cells remain relatively undifferentiated, as they transition into the ICM. It is not until later, during hatching, that the ICM will differentiate into a ventral hypoblast and dorsal epiblast (Oestrup *et al.* 2009). The ICM will remain unpolarized and though it will produce some of the ion transport and aquaporins used by the TE, they will not localize to any portion of the cellular membranes (Betts *et al.* 1998; Barcroft *et al.* 2003)

The major activity in the ICM during blastulation is cell proliferation. In the porcine embryo, the ratio of cells in the ICM relative to the TE increases to the expanded blastocyst stage and then only starts to decrease following hatching (Papaioannou and Ebert 1988) when massive expansion of the TE

begins. In the murine embryo during blastulation, a similar increase in ICM cell proliferation is observed (Copp 1978). However, if the polar TE (immediately adjacent to the ICM) is analysed separately from the mural regions it appears to proliferate at a rate equivalent to the ICM (Copp 1978). This would suggest that ICM is producing and responding to a paracrine factor that encourages cell proliferation that also affects the TE cells in close proximity. Interestingly, bovine embryos which form a blastocoel later in development appear to have fewer total cells and an increased probability of having a low ICM/TE ratio (van Soom *et al.* 1997). This would indicate that the ability of the ICM to undergo accelerated proliferation is either time sensitive or susceptible to embryonic stressors which retard blastocyst formation.

When porcine embryos are restricted to the oviduct via ligature at the uterotubular junction they fail to develop past the morula stage and undergo fragmentation and resorption (Murray *et al.* 1971). However, when restricted to the ampullary region of the oviduct, the embryos are able to cavitate and differentiate into ICM and TE, albeit at a much slower rate than embryos maintained in the uterus (Pope and Day 1972). This result is similar to that of *in vitro* cultured porcine embryos which are able to form a blastula but do so slowly and with fewer cells (Papaioannou and Ebert 1988). In sheep, the ampullary segment of the oviduct produces nearly twice the fluid volume of the isthmus, but the fluid composition with regards to the ionic and carbohydrate portions remain the same (Restall and Wales 1968). Taken together, this would suggest that an environmental component other than the previously mentioned calcium is required for proper formation of the blastocoel, and pre-hatch development.

Embryonic Metabolism

During the development from an oocyte to the blastocyst stage the mouse embryo will increase its DNA content over 18 fold from 23.8 to 439 pg (Olds *et al.* 1973). In addition, it will produce large quantities of ribosomal RNA (Pikó 1970) and increase its total RNA content by over 0.8 ng (Olds *et al.* 1973).

Furthermore, if cytoplasmic volume and blastomeres are considered to be constant and spherical, geometric calculations suggest total surface area increases 1.26 fold with each cell cycle creating a continual requirement for phospholipids. The rapid cellular and morphological change which occurs in the embryo requires not only the production of energy, but also access to fundamental macromolecules necessary for the construction of additional biomass such as nucleic acids, amino acids and lipids. For this reason, preimplantation embryonic metabolism is inherently altered from that of somatic cells (Krisher and Prather 2012). To maintain such a metabolism, the developing embryo requires substantial quantities of metabolic substrates provided either from the oocyte or the maternal environment.

Thomson and Brinster (1996) conducted a histological examination of mouse oocytes and embryos for glycogen and found that its concentration was highest between the 2-cell and morula stages, with no differences detected between *in vivo* and *in vitro* embryos. Embryonic glycogen content in the blastocyst was shown to disappear almost entirely from the TE while only minimal content, detected by staining, was observed in the ICM (Thomson and Brinster 1966). Most importantly, they found that while the oocyte and zygote did stain positively for glycogen, the quantities were substantially less than at later stages. This confirmed that glycogen of maternal origin is not a primary source of energy for the cleavage stage embryo. An additional study on the protein content of mouse embryos found that there was a significant decrease in total protein from the 1-cell to morula stages. However, this reduction amounted to only 7 ng, of which almost half was recovered by the blastocyst stage (Brinster 1967). Subsequent experiments were able to show that protein content fluctuated a number of times throughout development, while free amino acid content remained relatively constant until after hatching, with the exception of a dip at the 2-cell stage (Sellens *et al.* 1981). The concentration of adenosine `triphosphate (ATP) in mouse embryos has been shown to drop by roughly half

from the oocyte to the early blastocyst stage, and then half again by the late blastocyst stage (Quinn and Wales 1971). However, the quantity of ATP in the embryo was found to range between just 0.82 pmol in the oocyte to 0.25 pmol in the late blastocyst, a difference likely too minor to support development in a meaningful way. These results demonstrate that the oocyte does not contain many of the standard metabolic substrates or energy sources. In addition, the fluctuations observed in amino acid, glycogen and other macromolecules further demonstrate just how dynamic the early embryonic need for macromolecules is.

One additional group of metabolic substrates present in the oocyte which is of particular interest in the pig is fatty acids. The pig oocyte contains substantially more lipids than that of sheep or cattle, with a larger proportion consisting of polyunsaturated fatty acids (McEvoy *et al.* 2000). There is, however, a degree of controversy regarding the fate of the lipids contained in the oocyte. Chemical analysis of the triglyceride content in the porcine oocyte and embryo found a decrease of about 13 ng during maturation, whereas during embryonic development triglyceride content was found to remain constant (Sturmey and Leese 2003). In contrast, a study evaluating the cytoplasmic volume of total lipid in the developing pig embryo using stereology found it remains constant only as far as the blastocyst stage, whereupon the volume drops substantially (Romek *et al.* 2009). While this later study fails to account for any change in lipid density, it does measure total fatty acid content rather than only that stored as triglyceride. Total fatty acid stores in the pig oocyte are only about 61% triglyceride, when corrected for phospholipid content (McEvoy *et al.* 2000), which may account for the difference between the two studies. However, even if the results of Romek *et al.* (2009) are taken as a more accurate measure of the embryonic consumption of lipids, it accounts only for a portion of metabolic activity initiated after the formation of the blastocoel.

In a recent review, Krisher and Prather (2012) proposed that embryonic metabolism functions in a manner similar to that of the Warburg effect observed

in other proliferative cells, such as those observed in cancer. Central to this theory, when applied to embryos, is that while glucose metabolism is directed toward the generation of macromolecule precursors, the energy requirements of the embryo are met through beta oxidation of fatty acids (Krisher and Prather 2012). This is based on published observations in both the mouse and pig embryo conducted *in vitro* under extreme culture conditions. The rate limiting step in the beta oxidation of fatty acids is mediated by the enzyme carnitine palmitoyl transferase one, encoded by the gene Cpt1B. In the *in vivo* produced murine embryo, this gene is only found to be expressed at the blastocyst stage (Dunning *et al.* 2010), confirming that under natural conditions fatty acids only play a role after blastocyst formation. However, when beta oxidation is inhibited through exposure of murine embryos to Etomoxir during the first cell division with no other energy source available, significant differences are observed in development as early as the 48 cell stage (Dunning *et al.* 2010). This demonstrates that the Cpt1B enzyme must be inherited through the cytoplasm of the oocyte and allows beta oxidation when no other substrate is present. Similar results have been reported for the pig embryo when cultured with oxaloacetate in the place of glucose. Development is inhibited by the addition of palmoxirate, an inhibitor of triglyceride metabolism (Sturmey and Leese 2008). This is not surprising given oxaloacetate acts only as a primer for the Krebs cycle and cannot be used to generate ATP on its own. Beta oxidation of fatty acids for the production of energy requires oxygen to create carbon dioxide as a terminal electron receptor. The pig embryo does demonstrate ample consumption of oxygen under normal culture conditions, with a significant peak at the early blastocyst stage (Sturmey and Leese 2003). However, Sturmey and Leese (2003) observed that when embryos were cultured in the presence of amino acids and glucose, the quantity of embryonic lipid remains absolutely stable. This led them to conclude that the proposed use of endogenous lipid by the embryo was not compelling.

If the oocyte does not contain the necessary starting material for metabolic production of energy and macromolecules, it is likely that these are derived from the surrounding environment. Carbohydrates or other hydrophilic metabolic substrates, such as amino acids or pyruvate, could be easily provided to the embryo through the uterine and oviductal histotroph. In order to acquire metabolic substrates and precursors from the surrounding environment, the embryo is likely to employ both passive and active transport mechanisms. This is in fact true in a number of instances. For example, methyl tritiated choline uptake by the 2-cell embryo appears to be passive, while the uptake by morulae and blastocysts involves active transport (Pratt 1980). Similarly, the complex uptake kinetics of tritiated methionine and leucine have been used to demonstrate that a while a single uptake system is active early on, two distinct systems are later active (Borland and Tasca 1974). What's more, the uptake of amino acids during embryonic development is initially Na+-independent, but then becomes completely Na+-dependant at the blastocyst stage (Borland and Tasca 1974).

When amino acids are added to mouse embryo culture media, they display few of the signs of metabolic perturbations common to other media formulations and cultured embryos maintain a normal level of viability after transfer (Lane and Gardner 1998). The murine embryo also takes up a consistent amount of pyruvate, with small spikes in uptake identified at the 2-cell and 8- to 16-cell stages (Leese and Barton 1984). Pyruvate can be converted to oxaloacetate, which allows for the priming of the citric acid cycle. Sturmey and Leese (2003) calculated that 95% of energy is derived from oxidative phosphorylation, which lends credence to the Warburg hypothesis of Krisher and Prather (2012). However, given the observation that embryonic lipid content changes only after blastocyst formation, we propose that it is likely exogenous amino acids, perhaps in concert with exogenous choline, that supports energy production in the embryo. This modification to the hypothesis does not,

however, affect the proposed role of glucose metabolism for the production of biomolecules. In the rabbit embryo, increased use of oxidative phosphorylation coincides with a drop in cytoplasmic concentration of amino acids from 31.6 mM in the morula to 4.13 mM in the blastocyst (Miller and Schultz 1987). This decrease occurs despite a substantial increase in the concentration of amino acids in the rabbit's uterine histotroph, suggesting that the cellular concentration is reduced by metabolic consumption.

The embryonic uptake of glucose, much like choline and amino acids, is initially low but shows a major increase after the 8- to 16-cell stage (Leese and Barton 1984). Glucose uptake in the mouse embryo appears to be independent of Na2+ concentration and is therefore not likely ion pump dependant at least up until the 8-cell stage (Powers and Tupper 1977). The GLUT or Solute carrier 2 (Slc2a) family is a large group of proteins which function in a Na2+-independent glucose transport pathway. In the mouse, embryonic expression of GLUT1 (Slc2a1) has been identified at all stages of development, while transcription of GLUT3 (Slc2a3) and GLUT4 (Slc2a4) has not been detected (Hogan *et al.* 1991). Interestingly, the expression of GLUT2 (Slc2a2) is only detected after the 8-cell stage (Hogan *et al.* 1991), which corresponds well with the previously mentioned increase in glucose uptake by the murine embryo.

In the pig embryo, metabolism of glucose tends to increase steadily to the 8-cell stage and then significantly increases to the blastocyst-late blastocyst stage (Flood and Wiebold 1988; Sturmey and Leese 2003). The relative amount of glucose consumed by the embryo has been shown to be significantly higher at every progressive stage of development, with a peak difference at the blastocyst stage of almost 10-fold (Swain *et al.* 2002). While this pattern of glucose usage is similar to that of the mouse, the rapid transition to glucose utilization appears to occur earlier. In addition, the relative consumption of glucose, based on the uptake of tritiated glucose, increases by 300-fold between the 2-cell and blastocyst stage in the pig. In contrast it increases by only 10 fold in the mouse

(Flood and Wiebold 1988). The substantial change in porcine embryo metabolism during this period relative to the mouse would suggest that the embryonic requirements of large animals may shift more rapidly and substantially than that of rodent models. This difference comes despite the fact that the relative size of cleavage stage embryos is consistent across almost all mammals.

The glucose taken up by the porcine embryo at later stages appears to be used primarily via the glycolytic pathway (Flood and Wiebold 1988) consistent with the Warburg effect described by Krisher and Prather (2012). However, studies with Carbon 14 labelled glucose show that consumption of glucose by the Kreb cycle does increase throughout early development for *in vivo* derived porcine embryos (Flood and Wiebold 1988; Swain *et al.* 2002). Using the relative metabolism of tritiated glucose versus that of carbon one and six labeled glucose, Flood and Wiebold (1988) calculated that prior to the increase in glucose uptake; the embryo primarily uses this substrate via the pentose phosphate pathway. A similar result was found in murine and bovine embryos which showed reduced pentose phosphate pathway activity as development progressed (O'Fallon and Wright 1986; Javed and Wright Jr 1991). This particular pathway utilizes glucose-6-phosphate as a starting material and results in the production of precursors to the synthesis of nucleotides, fatty acids and some amino acids.

Remarkably a study published in 2005 by Kimura *et al.* was able to demonstrate that the addition of glucose above 1 mM to bovine embryo culture media at the 8-cell stage, not only decreased blastocyst formation but significantly altered sex ratio in favor of male blastocysts. However, when these researchers added fructose to culture media in concentrations as high as 5.6 mM, no reduction in blastocyst formation or alteration in sex ratio was observed (Kimura *et al.* 2005). Given that the first step in the metabolism of fructose is the transition to fructose-6-phosphate it is likely not eligible for use in the pentose phosphate pathway. Prior studies have demonstrated that male and female

bovine embryos exhibit substantially different metabolism of glucose, which may explain these results. Tiffin *et al.* (1991) showed that while total metabolism of glucose by male embryos was twice that of female embryos, pentose phosphate pathway usage was reduced 4-fold. This difference may be related to the fact that a rate limiting enzyme in the pentose phosphate pathway is glucose-6-phosphate dehydrogenase (G6PD) (Zimmer 2001) whose gene is located on the X chromosome in swine, cattle, rodents and humans (NCBI-Gene). In mammalian embryos, the first evidence of transcriptional inactivation through histone modification (heterochromatization) of the second X chromosome in females is not detected until blastocyst stage (Lyon 1972). Prior to heterochromatization the expression from the second copy of G6PD appears to result in a preferential use of the pentose phosphate pathway by female embryos in the presence of high levels of glucose. In fact, when Kimura *et al.* (2005) treated bovine embryos with inhibitors of G6PD there was no observable effect on blastocyst development of sex ratio even at glucose concentrations as high as 4mM. This difference in the ability of male and female embryos to respond to abnormal conditions further demonstrates just how specific and complicated their requirements are. More importantly, these results show that while the glucose may be used by the pentose phosphate pathway early on, it becomes detrimental in later stages of development.

If use of the pentose phosphate pathway becomes detrimental to embryonic development, then it is likely that biomass production switches to glycolysis via the Warburg effect as mentioned earlier. In the Warburg effect, glucose is metabolised via anaerobic glycolysis to produce lactate, resulting in a buildup of ribose, acetyl-CoA and other metabolic intermediates, which can be subsequently converted to nucleotides, fatty acids and non-essential amino acids, respectively (Vander Heiden *et al.* 2009). One apparent sign of the Warburg effect in action is the production of lactate through anaerobic glycolysis, even in the presence of oxygen. As Krisher and Prather (2012) point

out in their discussion of a role for the Warburg effect in embryonic metabolism, the embryonic accumulation of lactate, which has traditionally been attributed to the embryonic adaptation to abnormal culture conditions, may in fact be a result of normal embryonic metabolism. Another characteristic of the Warburg effect proposed by Vander Heiden *et al.* (2009), is its inherent link with the phosphoinositide 3-kinase (PI3K) signaling mechanism. Both vascular epithelial growth factor (VEGF) and Insulin signaling pathways are known to involve the PI3K mechanism. Interestingly, VEGF, insulin and other related growth factors are considered to play an active role in embryo development and maternal-embryonic communication (Hardy and Spanos 2002). It is therefore, possible that the abnormal metabolism often observed during *in vitro* development may be a result of failure to activate these signaling mechanisms.

Interestingly, Flood and Wiebold (1988) reported that when the whole embryonic metabolism of glucose is analysed on a per blastomere basis, the highest level of glucose metabolism occurs just prior to the morula stage and decreases at the early blastocyst and blastocyst stages. The authors suggest that this peak at the morula stage could be due to increased metabolic requirements during compaction of the embryo. However, the peak oxygen consumption of porcine embryos does not occur during compaction, but later during the early blastocyst stage (Sturmey and Leese 2003). As compaction involves the first separation of blastomeres into two distinct populations, it is possible that the reduction in calculated glucose metabolism is the result of lower glucose metabolism of only one blastomere population in the blastocyst. Swain *et al.* (2002) showed glutamate consumption of *in vivo* produced embryos also began to rise during this period, suggesting amino acids may be a potential alternate source of energy. If this is in fact occurring, it would mean that the requirements for the ICM and TE may diverge at compaction. The embryonic environment would therefore be required to support the growth of both cell lines, substantially increasing the need for a complex milieu.

One thing that is clear from the studies thus far is that the metabolism of early embryos is substantially altered from that of other cell types. In addition, it is clear that *in vitro* produced/manipulated embryos are substantially altered by the abnormal and often simplistic culture conditions. Direct comparisons of *in vitro* and *in vivo* produced embryos show that beyond the absolute effect on the metabolic pathways of each, there is substantial modification to the ratios of one pathway to another, as well as the relative preference for energy substrates (Swain *et al.* 2002). The metabolic plasticity of the embryo observed in abnormal conditions does however appear to have a substantial effect on subsequent development and viability. This plasticity in early embryonic metabolism likely results in the buildup of detrimental pools of substrates and waste products that will produce substantial stress. Furthermore, because these metabolic pathways are also responsible for the creation of biological building blocks, modulation in their relative use is likely to create shortfalls of specific molecules involved in the continuation of the developmental program.

Epigenetics

Epigenetics is a burgeoning field and currently an extremely fashionable term in science, and as such requires a careful definition prior to further discussion. The term was initially coined by Waddington in 1957 (Waddington 1957) to describe the manner in which genes produced phenotypes. However, it was later repurposed to refer to meiotically and/or mitotically heritable changes in gene function that are not a direct result of changes in the DNA sequence. In reproductive physiology both of these definitions are applicable, as the mechanisms of epigenetics appear to be involved in reprograming/differentiation, as well as adaptation to environmental conditions in both an immediate and trans-generational manner. Recently, a unifying definition of epigenetics has been proposed which is ideally suited to the study of reproduction and reads as follows: “the structural adaptation of chromosomal regions so as to register, signal or perpetuate altered activity states” (Bird 2007).

The following section will utilize this definition, focusing heavily on the "structural" aspect known to be mediated by DNA methylation and chromatin modification.

Methylation

In addition to the four standard DNA nucleobases of guanine, cytosine, adenine and thymine, there exists a fifth base, 5-methyl-cytosine identified as naturally occurring in 1925 (Johnson and Coghill 1925). This base is a chemically modified version of cytosine with a methyl group attached to the fifth carbon of the pyrimidine ring and is the key molecule in DNA methylation. The 5-methyl cytosine arises almost exclusively at sites where the cytosine is directly paired with a guanidine residue (Razin and Cedar 1991), creating a two base pair sequence with obvious dyad symmetry. There are at least three known mammalian proteins capable of methylating cytosines in DNA, including DNMT1, DNMT3a and DNMT3b. The DNA methylation state is maintained through semiconservative replication, primarily though the action of DNMT1, which has a strong affinity for CpG's in a hemi-methylated state. While the C-terminal domain of DNMT1 is capable of both *de novo* and maintenance methylation, an N-terminal domain in the same protein appears to limit the *de novo* capacity of the C-terminal domain under normal conditions (Bestor 1992). DNMT3a and DNMT3b on the other hand are primarily *de novo* methylases, and are involved in establishing new CpG methylation states.

Structurally, the addition of a methyl group to the fifth carbon of a cytosine locally modifies the major groove in the DNA helix and thereby effects the way DNA binding domains on proteins can interact with that portion of the sequence (Jones and Takai 2001). As a result of its effect on the structure of DNA, hypermethylation of genes was initially associated with transcriptional suppression and hypomethylation associated with transcriptional activity (Razin and Cedar 1991). However, the effect of DNA methylation appears to depend on where methylation occurs relative to gene structure, because when Keshet *et al.*

artificially methylated the APRT gene in the 5' region they noted reduced expression, whereas methylation in the 3' region had no effect. It has, therefore, been proposed that promoter methylation acts though a variety of mechanisms as a sort of "molecular lock" that directly affects gene expression (Siegfried and Cedar 1997).

Nuclear reprogramming of the DNA obtained from the fully differentiated gametes must occur in a newly formed zygote in order to produce the totipotency necessary for development. A portion of this reprogramming involves the removal and subsequent re-establishment of a major portion of the DNA methylation present in the genome. Methylation dynamics in the early embryo are however complex and vary between maternal and paternally derived DNA (Figure 2.3). Shortly after fertilization the paternal DNA is actively demethylated in a process which is intricately linked with pronuclear formation and in the mouse is complete within four hours of fertilization (Santos *et al.* 2002b). The mechanism by which active demethylation occurs is somewhat controversial. In a 2010 review, Wu and Zhang present the evidence for five previously proposed mechanisms of active demethylation, and discuss evidence that none of them are responsible for male pronuclear demethylation. They do however review additional data from their own lab which had identified elongator complex protein 3 (ELP3) through RNA interference (RNAi) and live cell methylation imaging, as a necessary component of the process, and they present a potential stepwise chemical reaction resulting in the conversion of 5-methyl cytosine to cytosine (Wu and Zhang 2010). This conversionary process does not conform with the images presented by Santos *et al.* (2002) which appear to show an increased cytoplasmic staining when polyspermic oocytes are demethylated. This increased staining of the cytoplasm would suggest that the 5-methyl cytosine is removed from the DNA intact and ends up in the cytoplasm rather than being converted.

On the other hand, the female pronucleus is passively demethylated, a process whereby methylation is lost through the repeated process of DNA replication. Each CpG remains in a hemi-methylated state as a result of DNA replication, and following three cell cycles methylation is reduced to $1/4^{th}$ of its initial level. Initially, this process was thought to be due to exclusion of DNMT1 from the embryonic nucleus up to the 8-cell stage (Dean *et al.* 2003a). This was based on a relatively primitive staining of DNA methyltransferases and confocal imaging, which showed the methyltransferases to be localized to the peripheral cytoplasm (Carlson *et al.* 1992). However, subsequent studies that selectively stained oocyte and somatic specific variants of DNMT1 (DNMTo and DNMTs respectively) have shown that only DNMTo is excluded up to the 8-cell stage, while low concentrations of DNMTs are detected in the nucleus at all stages of cleavage (Kurihara *et al.* 2008). Taken together, it is clear that while the DNA of the zygote does lose the majority of its methylation, the specific mechanisms that produce this effect are yet to be fully understood.

Following global demethylation of both maternal and paternal genomes a rapid wave of remethylation is initiated. In the mouse this remethylation process begins at the blastocyst stage (Santos *et al.* 2002b). It is likely accomplished by the known *de novo* methyltransferases DNMT3a and DNMT3b. However, DNMT1o expression has also been localized to the nucleus at the 8-cell stage (Kurihara *et al.* 2008), suggesting it may also play a role earlier in development. Interestingly, *de novo* methylation does not occur evenly throughout the embryo. Staining for 5-methly cytosine in mouse blastocysts shows substantially higher intensity in the ICM than the TE cells (Dean *et al.* 2003b), further indicating a role for methylation in the process of differentiation.

To complicate the process further, it is well known that not all methylation in the maternal or paternal genome is lost during early cleavage. Bisulphite sequencing of preimplantation mouse embryos at different stage shows that intracisternal A particle elements (also known as endogenous

retrovirus-like elements) are able to escape demethylation (Lane *et al.* 2003). In addition, it has been shown that, like some retroviral elements, the differentially methylated regions associated with some imprinted genes such as IGF2 and IGF2r are maintained on either the maternal or paternal DNA throughout the preimplantation period (Brandeis *et al.* 1993). These regions must in some way be resistant to both the passive and active demethylation observed in the remainder of the genome. Furthermore, they represent a mechanism by which epigenetic information can be passed trans-generationally.

What is particularly interesting about these imprinted genes is that their maintenance in the embryo is susceptible to culture conditions. Doherty *et al.* (2000) showed that when murine embryos were cultured in Whitten's medium both expression and methylation of the paternal H19 gene became unstable at the blastocyst stage. In contrast, when the embryos were cultured in KSOM media, with added amino acids, the paternal gene remained normally methylated and its expression was suppressed. In a similar experiment conducted by Khosla *et al.* (2001), mouse embryos were cultured in M16 media with or without the addition of fetal calf serum (FCS), and their developmental potential as well as their epigenetic status monitored following embryo transfer (ET). At day 14 of gestation, only 33% of the transferred embryos exposed to FCS were identified as viable fetuses versus 79 and 60% in the ET control and no FCS groups, respectively (Khosla *et al.* 2001). In addition, the fetal weights were substantially reduced following exposure to FCS in culture. Subsequent analysis showed abnormal transcription and methylation of H19, IGF2, GRB10 and GRB7 in response to FCS treatment (Khosla *et al.* 2001). Subsequent studies focusing on the effect of FCS on postnatal development were able to identify significant alterations to the offspring's anxiety, implicit memories and neuromotor development (Fernandez-Gonzalez *et al.* 2004).

Experiments by Waterland and Jirtle (2003) involving the agouti gene in mice have demonstrated that DNA methylation of this transposable element can

be manipulated through modulation of maternal nutrition. Supplementation of the diet with methyl donors such as folic acid, vitamin B12, choline, and betaine resulted in increased methylation of the agouti allele (Waterland and Jirtle 2003). Given that the mechanisms of demethylation, and imprint maintenance in the early embryo are yet unknown, it is difficult to speculate on how the addition of amino acids or FCS could create the substantial epigenetic effect described above. It is possible that the stress of culture has a direct impact on the methylation mechanisms. However, it is also possible that modulation of the metabolic pathways create a situation whereby the necessary substrates are not available to the methylation machinery.

The methylation dynamics of the early embryo are not universal among mammals. In sheep, there is no apparent difference in the degree of methylation between maternal and paternal pronuclei, as well only a small reduction in signal intensity of the fluorescent label to the 8-cell stage was observed, which the authors believe to be an artifact of their image analysis methodology (Beaujean *et al.* 2004). In the pig, there is no consensus on the methylation dynamics in the cleavage stage embryo. Fulka *et al.* (2006) assessed the methylation levels for *in vivo* produced oocytes, zygotes and different cleavage stage embryos, and identified no decrease in methylation from the 2-cell to blastocyst stages of development. The study did however identify active demethylation of the paternal pronuclei and showed no decrease in active demethylation with polyspermy (Fulka *et al.* 2006). In contrast, Deshmukh *et al.* (2011) failed to identify active demethylation in the male pronuclei, but did observe passive demethylation through the early cleavages stages for *in vivo* produced pig embryos. The lack of active demethylation in the paternal pronuclei observed in the latter study is in agreement with the results of Jeong *et al.* (2007), where they used targeted bisulphite sequencing to confirm initial observations made via fluorescent labeling of 5-methyl cytosine (Jeong *et al.* 2007). While the pattern of global DNA methylation dynamics in the pig is not

fully understood, it is clear that *in vitro* culture has an effect on this process, as described in the mouse. Bonk *et al.* (2008) showed that 18.5% of the genomic regions tested showed significant differences in methylation pattern between *in vivo* and *in vitro* produced blastocysts. Perhaps more surprising, the methylation pattern of *in vitro* produced blastocysts diverged more from their *in vivo* produced counterparts than from parthenogenetic and nuclear transfer generated blastocysts (Bonk *et al.* 2008).

Chromatin

The second major structural modification of DNA associated with epigenetics is chromatin modification. The nucleosome is the primary repeating unit in the structure of DNA and is comprised of 146 base pairs structured around a proteinaceous octamer containing the subunits H2A, H2B, H3 and H4 (Fischle *et al.* 2003). The amino acid residues of each histone can be post-translationally modified in a number of ways, each of which uniquely alters the inherent structure of the nucleosome and mediates accessibility of transcription factors and binding proteins to the DNA sequence. Specific amino acid residues on the amino terminal tails of each histone may be modified including, lysine, threonine, serine and arginine. The residues are known to be chemically modified through acetylation, methylation, phosphorlyation and ubiquitination; and the effect of each modification at any given residue is dependent on other modifications. While not all of these modifications are known to occur at each of the susceptible residues, the sheer number of combinations and permutations is enormous, and thus the full range of cause and effect relationships is not yet fully understood.

Chromatin modification, like demethylation occurs rapidly in paternal DNA and is associated with formation of the male pronucleus. The density of DNA in sperm is increased by the use of protamine in the place of histones. However, upon entering the oocyte these protamines are replaced with histones. During the histone-protamine exchange, chromatin in the murine male

pronucleus shows elevated H4 hyper-acetylation relative to the female pronucleus, which is typically associated with transcriptional activity, (Adenot *et al.* 1997). It has been suggested that rapid demethylation occurs in the male, but not the female pronucleus, because the histone-protamine exchange triggers the demethylation reaction (Santos *et al.* 2002a). Shortly thereafter the female pronucleus will also stain brightly for hyper-acetlyated H4 histones and by the first cell division the zygotic chromosomes will show a distinct banding pattern (Adenot *et al.* 1997) which will likely aid in maternal demethylation. This is coincident with the peak expression of GCN5, a histone acetlytransferase, identified in the MII stage bovine oocyte (McGraw *et al.* 2003). Similar phosphorlyation of serine 1 in Histone 4 and 2A in maternal and paternal DNA has been observed, while other histone modifications such as the methylation of lysine 4 and 9 on histone 3 have only been identified in the female pronucleus (Sarmento *et al.* 2004).

Interestingly, not all of the histone modifications made to chromatin in the cleavage stage embryo are stable. Through a careful examination of fluorescent labeling of DNA and specific modifications at varying points in the cell cycle, Sarmento *et al.* (2004) were able to show that some chromatin modifications were not maintained during metaphase. This group included hyper-acetylation of histone H4 as well as methylation of arginine 17 and 3 on histone 3 and 4, respectively (Sarmento *et al.* 2004). In contrast, histone 3 lysine 9 methylation [Me(Lys9)H3], histone H3 lysine 4 methylation [Me(Lys4)H3] and histone H4/H2A serine 1 phosphorylation [Ph(Ser1)H4/H2A], were present at all points throughout the cell cycle in the cleavage stage embryo. Despite the lack of maintenance in chromatin state through cell division, it is clear that modifications of this type play a role in early embryonic development. Using a novel carrier chromatin immune precipitation procedure O'Neill *et al.* (2006) examined ICM and TE cells isolated by immuno surgery and manual dissection, respectively. This method demonstrated that the histone modifications in the

promoter regions of DNA from the two cell types were substantially different at the blastocyst stage (O'Neill *et al.* 2006). The differences that arise between the two cell types are likely to play a role in differentiation and the regulation of transcription.

Unlike methylation, aberrant histone modification resulting from embryo culture is not well-studied. This is likely due to the extremely small quantities of DNA in a cleavage stage embryo relative to the requirements for chromatin immuno precipitation (ChIP) techniques. Immuno-fluorescent staining of three histone modifications (AcH4, MeH3K9 and PhH3S10) in murine embryos produced either *in vivo* or *in vitro*, showed no significant differences in their global intensity levels up to the blastocyst stage (Huang *et al.* 2007). However, when Li *et al.* (2005) conducted an analysis on specific genomic regions associated with imprinted loci, such as the IGF2/H19 gene complexes, they noted an *in vitro* fertilization (IVF) induced increase in lysine 9 methylation and lysine 4 methylation of histone 3 in the maternal and paternal chromatin, respectively. This modification was associated with aberrant H19 expression and a paternal methylation pattern in the maternal imprinting control region associated with the gene (Li *et al.* 2005). This latter result makes it clear that despite a lack of chromatin modification to the global level of many modifications, there are specific effects on imprinted loci as a result of culture.

Perhaps more interesting, is the interaction between DNA methylation state and chromatin modifications. When cells expressing GFP under the control of hyper-methylated promoters are treated with histone deacetylase inhibitors (HDACi), promoter chromatin remained in an “open” state and GFP expression, as well as expression of other genes, was restored (Raynal *et al.* 2012). These changes to expression came despite the maintenance of the promoter’s methylation state and were only maintained temporarily (< two weeks) after treatment. This suggests that methylation acts to preserve the long term memory transcriptional repression, an effect which is mediated through

chromatin state (Raynal *et al.* 2012). Based on this information, it is possible that the chromatin structure need not be modified directly, but will be affected by the aberrant methylation that results from embryo culture.

The Environment of the Reproductive Tract

All the previously described morphological, metabolic, genetic and epigenetic changes associated with mammalian embryonic development create substantial requirements for the embryo's local environment. We have thus far seen in each of the processes described; how environmental conditions, particularly those of embryo culture, can result in aberrant or failed development. Under *in vivo* conditions, early embryonic development occurs in the oviductal and uterine histotroph which, in theory, meets the very specific embryonic requirements for each stage of development. However, the normal conditions under which early embryonic development occurs are largely unknown, beyond the most basic components. This lack of understanding is due to the fact that, as with the embryo's requirements, the components of the oviductal and uterine environment are constantly shifting under the control of numerous hormones and paracrine factors. What's more, the structure and environmental conditions of the oviduct and uterus vary substantially, as do the mechanisms by which they are controlled.

Unlike mice and primate embryos, which implant shortly after hatching of the blastocyst, the embryos of agricultural species implant much later in embryonic development. The prolonged pre-implantation period in cattle and swine increases their reliance on the uterine histotroph for nutrients, ions and dissolved gasses. While a great deal of information exists on the embryonic requirements, histotroph composition and maternal embryonic interactions during the latter portion of preimplantation development, much less is known about the period prior to hatching of the blastocyst. This period is particularly

difficult to study, because both the embryo and the volume of histotroph are substantially smaller than in the period immediately prior to implantation.

Oviduct

Structurally the oviduct can be broken down into three functionally and histologically different layers termed the mucous membrane, muscular coat and the adventitial serous coat (Ham 1950). The oviduct can be further subdivided into two distinct segments, the ampulla which begins at the ostium and continues to a point of constriction referred to as the ampulary-isthmic junction (AIJ), and the isthmus which continues from this point to the opening into the uterine horn. The majority of the oviductal histotroph is produced by the mucous membrane which lines the interior surface of the oviduct. Structurally, the mucous membrane consists of a ciliated columnar epithelium supported by an aglandular submucosa. However, due to the complex fimbrial projections of the sub-mucosal layer, the relative abundance of the secreting epithelial layer is substantially higher in the ampullary portion of the oviduct compared to the isthmus, as can be seen in Figure 2.3. This corresponds to a significantly higher rate of de novo protein synthesis in the ampulla relative to the isthmus in the pig (Buhi *et al.* 1989). This substantial increase in surface area may increase the ability of the ampulla to support embryonic development as will be discussed later.

The production of oviductal fluid is localized around the time of ovulation. In one study, where the oviducts of swine were surgically catheterized, fluid production during estrus was on average only 1.18 ml/day, dropping to just 0.69ml per day following estrus in some animals and stopping entirely in others (Wiseman *et al.* 1992). Another experiment involving surgical catheterization of the oviducts found that the volume was much higher, starting at 8.44 ml/day just 24 hrs after ovulation and falling to 4.64 ml/day by 96 hrs (Archibong *et al.* 1989). This latter result is similar to that of Iritani *et al.* (1974) who, also using catheterization, found oviductal fluid production to be 5.1

ml/day during estrus and 2.1 ml/day in diestrus. It is however unclear as to whether these values represent a physiologically normal state, as the process of surgical catheterization is likely to have resulted in inflammation and accumulation of fluid. In addition, the constant removal of oviductal fluid is likely to remove any end-product feedback on the oviduct and result in further secretion.

Given the close association of the infundibulum with the porcine ovary, it is logical to assume the follicular fluid released during ovulation is another source of oviductal histotroph components. Hansen *et al.* (1991) carried out an experiment where follicular and oviductal fluids were collected from gilts following pregnant mare serum gonadotropin (eCG) and hCG induced follicular development and ovulation. These fluids were collected at 38 hours (pre-ovulation), 42 hours (during ovulation) and 46 hours (post-ovulation) after hCG treatment, and progesterone (P4) concentrations in the fluids determined by radioimmunoassay. In this publication, Hansen *et al.* (1991) state that the porcine oviduct contains approximately 200 µl of fluid, and that this fluid is composed of 0.51 and 0.04 % of the available follicular fluid at 42 and 46 hours, respectively. However, working on the assumptions that the only additional source of P4 in the oviduct following ovulation originates from the follicle, and that fluid volume of the oviduct is unchanged by ovulation; the % contribution of follicular fluid to oviductal fluid ($\%_{tran}$) can be calculated using the following equation:

$$\%_{tran} = \frac{V_o\ (C_{of} - C_{oi})}{C_f\ x\ V_o}$$

Where V_o: Oviductal volume, C_{of}: P4 concentration in the oviduct after ovulation, C_{oi}: P4 concentration in the oviduct before ovulation, C_f: P4 concentration in the follicle

Using the values reported by Hansen *et al.* (1991), transmission percentage of 0.112 and 0.074 for mid- and post-ovulation can be calculated respectively. Regardless of the method of calculation it is clear that the contribution of follicular fluid to the oviductal environment is minimal.

A review by Leese *et al.* (2001) suggests that while the production of oviductal fluid is linked to the blood flow to the oviduct, the role of the epithelium should not be ignored (Leese *et al.* 2001). Tandem evaluation of oviductal fluid and serum of rabbits led Feigelson and Key (1972) to conclude that while some proteins are selectively transferred into the oviductal lumen from the blood, others are generated locally in the mucous membrane (Feigelson and Kya 1972). Explant culture of pig oviducts conducted by Buhi *et al.* (1989) show the highest rate of *de novo* protein production was during the first two days of the estrous cycle, followed by a steep decline. One dimensional analysis of the proteins showed no difference in the total secreted protein, detecting bands consistent with serum proteins such as albumin, transferrin and immunoglobulin. Radiolabeled leucine was, however, incorporated into three bands observed on the blots, revealing the presence of *de novo* synthesized oviductal secretory proteins present during estrus and later lost during diestrus (Buhi *et al.* 1989). Further study of the two low molecular weight bands by Buhi *et al.* (1990) using 2D SDS PAGE, found that each was comprised of two separate proteins. Of these four, it was shown that three were produced exclusively in the ampulla and only during fertilization and early embryo development (Buhi *et al.* 1990). These results in the pig further suggest that *de novo* proteins are produced in specific tissues and only during the period where the oocyte, sperm and embryo will be found in these areas. The unique timing of their expression to the peri-ovulatory period suggests that their synthesis or secretion is hormonally regulated and in all likelihood by estrogen.

Beyond the protein content of the oviductal fluid, the concentration of a number of other chemical components has been measured in different species. In the rabbit, the oviductal amino acid profile is heavily skewed toward glycine, with moderate quantities of glutamine, alanine, serine and threonine, and only minor quantities of the other fifteen amino acids (Miller and Schultz 1987). A similar profile has been reported in the cow, with glycine representing the

overwhelming portion of oviductal amino acids at just over 14000 µM, followed by glutamate, alanine and cysteine (Elhassan *et al.* 2001). Porcine oviductal fluid also contains substantial amounts of both the insulin like growth factors (IGF1 and IGF2), which peak in concentration during the peri-ovulatory period. However, oviductal concentrations were found to be as much as five-fold lower than plasma samples from the same animal (Wiseman *et al.* 1992).

During the peri-ovulatory period and early luteal phase the porcine oviduct contains receptors for both estrogen and progesterone (Stanchev *et al.* 1985). In addition, the oviduct is functionally responsive to both of these steroids as well as LH, which together appear responsible for maintaining its relaxed state following ovulation (Gawronska *et al.* 2000). In a study by Wollenhaupt *et al.* (2001), involving ovariectomy and estrogen replacement, this steroid was identified as a key regulator of the increased expression of epidermal growth factor (EGF) receptor in the oviduct (Wollenhaupt *et al.* 2001). Furthermore, estrogen has been found to be a key factor in the up regulation of oviductal progesterone receptors prior to ovulation (Wollenhaupt *et al.* 2001).

In a study by Pharazyn *et al.* (1991) in the pig, it was shown that progesterone concentrations increase quickly after ovulation and are detectable in the veins draining all segments of the reproductive tract by day 1 of gestation. However, when progesterone concentrations were analysed in different blood pools, it was found that progesterone was highly concentrated in the ovarian and oviductal blood at all measured stages (Pharazyn *et al.* 1991). Of particular interest in this study was a single animal examined on day 2 following standing estrus that had only formed corpora lutea (CL) on one ovary. In this particular animal, progesterone in the oviductal veins ipsilateral to the CL-bearing ovary were several fold higher than in the contralateral veins which more closely resembled concentrations in the peripheral circulation (Pharazyn *et al.* 1991). This latter chance finding suggests a localized link between the ovarian and oviductal blood supply, capable of allowing progesterone signaling prior to

substantial increases in peripheral blood concentration. Progesterone receptor expression peaks during the early luteal phase in the cow along with estrogen receptor alpha (Ulbrich *et al.* 2003). Initial work in the pig concluded that the concentrations of IGF1 and pOSP in the oviductal fluid changed in response to a shift in estrogen and progesterone ratio (Novak et al. 2002). However, a subsequent study by Novak et al. (2003) found no effect of nutritional restriction during lactation on pOSP or IGF1, but did note an increase in oviductal histotrophic protein and a significant shift in the estrogen to progesterone ratio, suggesting these factors are not in fact linked. As such, it is unclear what role progesterone plays in the modulation of the oviductal environment in the peri-ovulatory period.

Uterus

Similar to the structure of the oviduct, the uterus is also comprised of three layers including the endometrium, myometrium and serosa (Ham 1950). Of these, the inner-most endometrium and its associated glands are responsible for the generation of the uterine histotroph. Unlike ruminants, where the inner surface of the uterus is marked by the presence of caruncles, the surface of the uterus in the pig is characterized by small uterine folds such that it appears relatively smooth at a macroscopic level (See Figure 2.4). However, unlike the oviductal epithelium, the endometrium is substantially more complex and includes the openings of deep coiled uterine glands which penetrate into the sub-mucosal layer (Perry and Crombie 1982), substantially increasing the secretory capacity of this tissue. These glands are established shortly after birth and are vital to the creation of a normal uterine environment for the embryo. Estradiol-17b valerate has been used to disrupt the estrogen sensitive development of the uterine endometrium in the pig, and as a result subsequent embryonic survival at day 45 of gestation was decreased by 22% (Bartol *et al.* 1993). Subsequent studies showed this treatment reduced the responsiveness of uterine secretions to embryonic estrogen from 130% in normal animals to

36% in those with disrupted uterine development (Tarleton *et al.* 2003). These results demonstrate the key role that the glandular structures of the endometrium play in creating a normal uterine histotroph expression and embryonic development

The production of uterine fluid is temporally similar to that previously discussed in the oviduct. Measures of uterine fluid in the pig using surgical catheterization showed that production during estrus averaged 6.9 ml/day and drops to 2.9 ml/day during diestrus. A study by Knight *et al.* (1973) quantified protein flushed from the uteri of gilts on day 4 of the estrous cycle following treatment with progesterone, estrogen or a combination of the two. The results show that while progesterone can independently increase total protein quantity, estrogen cannot. However, in conjunction progesterone and estrogen result in substantial secretions, suggesting the two hormones work in concert to regulate at least the protein component of uterine histotroph production (Knight *et al.* 1973). Blood flow to the uterus is at its minimal level while progesterone is high during the luteal phase (Ford and Stice 1985). This would suggest that the bulk of the components in the uterine histotroph that are regulated by progesterone are likely generated locally rather than imported from the serum.

Unlike the oviduct, which responds to pre-ovulatory oviductal estrogen by up regulating progesterone receptors, the uterus does the opposite (Wollenhaupt *et al.* 2001). In addition, the expression of the EGF receptor in the uterine endometrium occurs without an ovarian signal and is in fact disrupted by exogenous estrogens (Wollenhaupt *et al.* 2001). From a simplistic standpoint, these results are not surprising given the directionality of the sub-ovarian counter current system that moves hormones from the uterine horn to the ovary and not the other way around. Beyond this, it is clear that the uterine environment responds to different signaling mechanisms than the oviduct.

Unfortunately, most assessments made of the uterine histotroph in any species have been made later in the pre-implantation period, during elongation

and maternal recognition. As well, many of these studies analyse only a limited number of poorly defined time points, so a true measure of the dynamic nature of histotroph composition remains elusive. The most complete study of the chemical composition of the uterine histotroph was conducted by Iritani *et al.* (1974), who analysed its composition during estrus and diestrus. This study found that uterine fluid contains significantly more dry matter and protein than the oviductal fluid. In addition, significantly higher concentrations of lipid were observed in the uterus during estrus, along with increased glycerophosphorylcholine diesterase (GPCD) activity (Iritani *et al.* 1974). The observation of high lipid content along with enzymatic activity associated with extracellular separation of choline from phospholipids creates the potential for substantial free choline; however, no direct measurement of choline has been made. The amino acid content and complexity of the uterine histotroph in the pig increases from estrus to diestrus, with glycine representing the largest proportion at any time. This overwhelming predominance of glycine is also reported in the rabbit (Miller and Schultz 1987) and cow (Elhassan *et al.* 2001). In the pig, the complexity of the amino acid pool in the uterus is far greater than the oviduct (Iritani *et al.* 1974), a trend also observed in cattle.

The best studied component of the uterine histotroph in swine, is the so called “purple protein” or uteroferrin. It was originally reported by Chen *et al.* (1973) as a strongly basic, purple coloured protein comprising as much as 15% of the protein in the uterine fluid at day 15 of gestation (Chen *et al.* 1973). The protein is 32 kDa in size and contains a single atom of iron (Schlosnagle *et al.* 1974). Other proteins which play a role in supporting late embryonic and subsequent fetal development have also been well studied. For example, retinol binding protein has also been identified in the uterine fluid of the pig during this period, and has also been shown to be regulated by progesterone (Adams *et al.* 1981). These proteins have not, however, been shown to play a role in the early

support of the cleavage stage embryo development, and if such proteins do exist they remain uncharacterized.

Maternal Embryonic Communication

It is well understood that communication between the eutherian embryo and it maternal environment must occur in order for successful pregnancy and development to proceed. Early communication between the two entities is necessary from an embryonic standpoint in order to halt maternal cyclicity, provide access to maternal nutrients, and modulate the maternal immune system; and from a maternal standpoint, to avoid embryonic exploitation and assess the potential fitness of the conceptus (Roberts *et al.* 2008). Molecules involved in this two-way communication are of particular interest from a scientific, as well as practical and economic stand point. Scientifically, these communicative links allow a more holistic understanding of reproductive processes in which embryonic and maternal physiology are viewed as two sides of a complex system, rather than separate processes. By studying reproductive physiology through such a framework, we are better able to understand concepts related to fetal/embryonic origins of disease, phenotypic plasticity and infertility. From a practical standpoint, molecules involved in this crosstalk are candidates for early pregnancy detection, markers of *in vitro* embryo health, or potential culture media additives to improve embryo based assisted reproductive technologies.

To date, only a select group of signals have been identified related to the localized crosstalk between the embryo and the uterine lumen (Wolf *et al.* 2003), with the majority of scientific focus on periods around the time of implantation. Identification of earlier embryo-uterine communicative pathways between the time of fertilization and hatching of the blastocyst is not well developed, owing primarily to the small size of the early embryo relative to the oviductal and endometrial lumen, as well as the embryos rapidly changing requirements. Even at a molecular level, the quantities of RNA and protein within the embryo are at

the lower limit of the functional threshold of modern technologies. Furthermore, functional bioassays typically involve the use of *in vitro* embryo development which is poorly established in a number of species, and often requires the addition of complex or undefined biological fractions and produces embryos of questionable quality.

The canonical example of early maternal-embryonic communication is pregnancy recognition, which must transpire in higher mammals where gestation is longer than the natural luteal phase. While in humans and primates, pregnancy recognition is mediated through the endocrine action of hCG (Auletta and Kelm 1994), the mechanism in most agricultural species is a more localized paracrine system. In ruminants, pregnancy recognition is initiated by embryonic production of interferon tau (INFT), while in swine it is mediated by conceptus produced estrogen. In the pig, maternal recognition of pregnancy does not begin until day 11 of gestation (M.K. Dyck and Ruvinsky 2011, Geisert *et al.* 1982). In response to estrogen, the uterine endometrium redirects PGF2α into the lumen of the reproductive tract, effectively isolating it from the sub-ovarian counter current system and preventing luteolysis (Bazer and Thatcher 1977). Conceptus produced estrogen was also thought to be responsible for modulating the secretions of the uterine glands (Senger 1999, Geisert *et al.* 1982)), however it was later shown that this process is independent of the conceptus and likely regulated by maternal progesterone (Vallet *et al.* 1998). Regardless, maternal recognition starting at day 11 was initially thought to be the first instance of embryonic communication and manipulation of maternal physiology (Geisert *et al.* 1982).

Earlier signals were detected by Nieder *et al.* (1987) using culture of mouse embryos in radio labeled methionine and 2D SDS PAGE. This study identified only one protein produced by the early day 4 (1000hrs) embryo and 22 more proteins which appeared in embryos by late day 5 (1600hrs). These

proteins were detected in media with just 30-100 embryos, suggesting more proteins may be produced at physiologically relevant levels, but well below the sensitivity of 2D SDS PAGE. The same study also reported on the intracellular and secreted proteins of pregnant and non-pregnant uterine horns following reactivation of lactationally delayed pregnancies. These results clearly showed that production of both intracellular and secreted proteins in the pregnant uterine horns is substantially higher 24 hrs after administration of estradiol and progesterone. The difference between the gravid and non-gravid uterine horns must be attributed to the presence of the conceptus, which would suggest a pre-implantation signaling mechanism.

More recently, through the application of high throughput and high sensitivity molecular methodologies to well-designed animal experiments, it is becoming increasingly apparent that maternal-embryonic cross talk not only starts significantly earlier in development, but is far more complicated than previously thought. One such study was performed in a murine model by Lee *et al.* (2002) in which 1-cell embryos and oocytes were transferred into contralateral oviducts. Oviductal tissue samples were collected 48hrs later and subjected to suppressive subtractive hybridization (SSH) using RNA from the embryo containing oviduct used as the "tester" and RNA from the oocyte containing oviduct used as "driver". Reverse dot-blot hybridization of putative clones yielded 97 positive sequence fragments which mapped to 79 and 11 known and novel sequences, respectively, of which only six had been previously annotated (Lee *et al.* 2002). The most significant of these factors was identified as thymosin beta 4 (TMSB4X), which the authors linked to transition of the ciliated cells of the oviduct into secretory cells and a number of known secretory pathways in other tissues including surfactants, chloride and insulin (Lee *et al.* 2002).

A subsequent study by Bauersachs *et al.* (2003) comparing ipsilateral and contralateral oviductal epithelium (relative to ovulation) in the cow, also employed SSH. This study identified 35 differentially expressed transcripts which fell into the functional classifications of cell surface, cell-cell interaction, immune related and signal transduction (Bauersachs *et al.* 2003). Unfortunately, the source of these transcriptomic changes was confounded by the experimental design. The authors noted that differences could arise either from communication between the cumulus-oocyte complex and the oviductal epithelium, or as a result of signals originating in the ipsilateral ovary. As previously mentioned, an experiment examining progesterone concentration in the oviductal veins in swine showed a multi-fold increase in an oviduct ipsilateral to the corpora lutea present on only one ovary (Pharazyn *et al.* 1991). However a pair of experiments, similar to that of Bauersachs *et al.* (2003), were conducted by Georgliou *et al.* (2005 and 2007) on the oviductal transcriptome and proteome of the pig in response to the presence of both oocytes and spermatozoa. The first study identified 20 differentially expressed proteins in response to the introduction of sperm and 5 in response to denuded oocytes in *ex vivo* oviducts (Georgiou *et al.* 2005). The second experiment, conducted *in vivo,* identified 19 proteins modulated by sperm and 3 modulated by the oocyte (Georgiou *et al.* 2007). In addition, the transcripts for oviductal glycoprotein 1 (OVGP1), renin binding protein (RENBP) and compliment C3 were also shown to be up-regulated by the presence of sperm, with the latter two also up-regulated by the presence of the oocyte (Georgiou *et al.* 2007). Unlike the previously described study in cattle those conducted by Georgiou *et al.* in swine show minimal effect of the oocyte but do indicate a substantial oviductal recognition of sperm. This difference can perhaps be attributed to a better model, in which ovulation occurs on both ovaries producing results less confounded by progesterone variation between the sides of the reproductive tract.

A recent study carried out by Alminana *et al.* (2012), used a porcine model to demonstrate a significant influence of the blastocyst on the transcriptome of the uterine endometrium. Laparoscopic oviductal inseminations with viable sperm in one ampulla and BTS diluent in the contralateral ampulla, allowed uterine and oviductal mucosal epithelial samples of pregnant and non-pregnant control tracts to be collected from each experimental animal (Alminana *et al.* 2012). Using the Affymetrics porcine gene expression array the authors were able to identify 210 differentially expressed genes, of which the vast majority (208) were down-regulated in the presence of a blastocyst (Alminana *et al.* 2012). This confirmed the hypothesis that the embryo can elicit a localized response in the uterine horn. Bioinformatics analysis of the differentially expressed gene list for enriched KEGG pathways identified the immune system as one of three primary pathways affected. When these data were computationally modeled, it suggested that uterine effects may in fact be a result of pre-emptive signaling between the oviduct and embryo (Alminana *et al.* 2012).

Asynchrony

While uterine crowding likely plays a significant role in porcine fetal survival and growth it appears that early embryonic loss in pigs is more closely associated with an inappropriate interaction of embryonic factors with the uterine environment than a limitation in uterine space (Polge 1982). In fact, it has been proposed that substantial embryonic loss occurs when the uterine environment becomes asynchronous with the needs of the developing embryo (Pope 1988). As discussed previously, the preimplantation embryo is reliant on the constituents within the uterine histotroph or on the surface of the endometrium for survival and this period is substantially longer in agricultural species than in higher primates.

While it has been recently shown that the embryo participates in a degree of communication with the maternal system, even during the early

cleavage stages of development (Lee *et al.* 2002; Alminana *et al.* 2012), it is not entirely clear how much the embryo can effectively modulate this environment to its needs. As well, it is not yet clear how rapidly the needs of the preimplantation embryo change, or the degree of variance between its requirements and environment that is required to produce permanent developmental consequences. To better understand this issue it is necessary to separate the effects based on the physiological source. To that end we propose three distinct mechanisms resulting in maternal embryonic asynchrony in the pig based on variation in time, variation in space and variation among embryos within a litter.

Temporal Asynchrony

When the timing of preimplantation embryonic development and cytological changes to the uterine epithelium are compared, the close relationship between embryonic and uterine environment becomes clear (Stroband and Van der Lende 1990). In an experiment described by Polge (1982), embryo transfer was used to assess the effect of temporal asynchrony on pregnancy rates and embryonic survival. In this experiment, embryos were transferred into recipients that were either synchronous with the donor or one and two days asynchronous in each direction. Pregnancy rate in synchronous or retarded recipients was above 70% and highest in recipients who were two days behind the gestational stage of the embryo donors. When transfers were made into gestationally advanced recipients, pregnancy rates were drastically reduced with just a one day difference and virtually absent in recipients 2 days advanced relative to the donors (Polge 1982). In addition, embryonic survival at day 30 was reduced to below 40% in the single pregnancy achieved with a two day advanced donor (Polge 1982). These results were substantiated by Pope *et al.* (1986) who were able to show that the effect of temporal asynchrony was greater when embryos were placed into gestationally advanced stage uteri compared to embryos placed in retarded uteri (Pope *et al.* 1986). It should be

noted that synchrony and asynchrony were established in both these studies based on onset of standing estrus, which ultrasound studies have shown correlates poorly with actual time of ovulation (Degenstein *et al.* 2008) and conception, and may have increased the error in matching donor and recipient pairs. However, taken together the results of these studies suggest that the embryo is capable of either advancing the uterine environment to its needs or slowing its own development, allowing the environment of the temporally retarded uterus to "catch up" naturally. The converse does not appear to be true, as a comparatively "younger" embryo is not able to retard an advanced environment or otherwise compensate with an increased developmental rate.

This interpretation is in agreement with results from an experiment conducted by Wilde *et al.* (1988) which took advantage of the natural variation in developmental rate within litters to show the effect of temporal asynchrony. Embryos from a single donor were divided into large and small subsets based on the variation in embryonic diameter and transferred into apposing uterine horns which were separated by a ligature. When the transfer was conducted in temporally synchronous recipients, significantly fewer small embryos survived to day 12.5 (Wilde *et al.* 1988). However, when embryos were transferred to recipients one day behind the donors, equivalent embryonic survival between the two groups was observed (Wilde *et al.* 1988). These results further suggest that if survival in the earlier stage uterus is the result of embryonic modulation, as opposed to delayed development, this modulation must be a localized effect mediated by paracrine versus endocrine signaling.

The ability of the embryo to either survive in a temporally asynchronous uterine environment or otherwise modulate it, appears to increase with time. Newcomb and Rowson (1975) transferred cattle embryos between 2 and 7 days post onset of estrus to recipients who were either 1 day ahead or behind the gestation stage of the embryonic donor(s). While no pregnancies were produced

in asynchronous transfers at 2 days, the number achieved increased rapidly between day 3 and 6 (Newcomb and Rowson 1975). In addition, the mean conception rate in recipients 1 day behind donors was noted to be higher than those of advanced recipients. This skew toward higher survival rates with developmentally advanced embryos relative to the recipient is consistent with prior studies from the same lab. Although not specifically reported, data from the earlier study looking at pregnancy rate with recipients temporally asynchronous up to three days relative to the donor, shows an increasing gap between advanced vs. delayed embryos as the degree of asynchrony increases (Rowson *et al.* 1972).

The results of these experiments with temporal asynchrony in swine and cattle, do not agree with a similar experiment conducted by Moore and Shelton (1964) using sheep. They reported a strong quadratic relationship between the degree of temporal synchrony of donor and recipient with both pregnancy rate and litter size. In addition, they showed a strong linear relationship between age at transfer and pregnancy rate and litter size. However, there does not appear to be a skew in the data that would suggest asynchrony in one direction is more or less severe that the other (Moore and Shelton 1964).

Spatial Asynchrony

The anatomical structure of female reproductive tract can in its simplest form be considered a series of interconnected tubes, each with distinct features. The features of each portion have developed to serve multiple roles including sperm and embryo transport, as well as support of the conceptus throughout the highly variable stages of development. However, the relative size and structure of each segment is better suited to supporting specific stages of conceptus development over others. It is therefore apparent that a close synchrony between the age or stage of an embryo and its location within the length of the

reproductive tract is vital to maintain optimal early embryonic survival (Moore and Shelton 1964).

In order to understand the relative effect of position within the reproductive tract, it is necessary to recognise the movements of embryos relative to their stage of development. In the pig 1-cell, 2-cell and 4-cell embryos can be found in the oviduct up to about 40 hours after ovulation (Polge 1982). At the 4-cell stage, the embryos begin to migrate toward the uterus and for a short time some embryos are present in both the oviduct and uterus. This movement is under the control of ovarian progesterone (Day and Polge 1968) and can be inhibited for up to 21 day by exogenous estrogen (Dziuk 1985). Following this transit, and for as long as five to six days after estrus, the embryos remain in the upper portion of the uterus within close proximity of the utero-tubular junction (Polge 1982). During this period, the embryo will continue cell division, develop a blastocoel and expand before hatching from the zona pellucida. After day 6 the embryos begin to migrate toward the body of the uterus, by day 9 they can be found in the contralateral uterine horn, and continue to migrate until approximately day 12 (Dziuk 1985). In comparison to other species, the transit of porcine embryos to the uterus occurs relatively early. Table 2.1 shows the time and stage of oviductal-uterine transit for six different species relative to the rate of cleavage. From the table it is clear that while the timing of cell cycle progression in the early embryo is quite conserved, the timing of transit is not. Furthermore, Table 2.1 also demonstrates that in the pig, transition into the uterus occurs substantially earlier than it does in other species.

Embryo transfer experiments, which are typically conducted with embryos prior to the hatching of the blastocyst (before day 6 in the pig) have demonstrated susceptibility of different species to spatial asynchrony. In cattle, 0 and 11% of uterine transfers in synchronized animals at day 2 and 3, respectively, (following onset of standing estrus) were found to produce a viable pregnancy, while nearly 70% were successful at day 4 (Newcomb and Rowson

1975). Similar results have been reported in the transfer of sheep embryos, with higher pregnancy rates and larger litter size when embryos were transferred to the oviduct between 48 and 84 hrs (after the onset of standing estrus). Given that the oviductal-uterine transition occurs between 96-110 hrs and 77-96 hrs in cattle and sheep respectively, these results demonstrate that embryonic development and survival is diminished when a conceptus is forced into a spatially asynchronous uterus.

It has been shown that collection of 2-cell embryos from the oviduct and transfer into the uterus of a temporally synchronous recipient, does not reduce embryonic survival or pregnancy rate in swine (Polge 1982). This is, however, unsurprising given a study by Perry and Rowlands (1962) who found 4-cell embryos to be located in either the uterus or split between the uterus and the oviduct (Perry and Rowlands 1962). This would suggest that the 4-cell stage is when transition between the oviduct and the upper portion of the uterus occurs and that the environment between the two is likely comparable. As previously mentioned, if embryos are maintained in the isthmus of the pig too long they will either fail to develop past the morula stage (Murray *et al.* 1971) or develop abnormally if constrained to the ampulla (Pope and Day 1972). This would suggest that, in the pig, the oviductal and uterine environments are equivalent early on, but later diverge as the embryonic requirements of the uterine endometrium become more complex.

The reproductive tract varies greatly in eutherian species. From a simplistic standpoint, much of the variation stems from the relative proportions of the uterine horn and the uterine body. In the simplex uterus, present in human and primate females, the oviduct joins directly to the uterine body creating a single uterine cavity and likely a single uterine environment. The artiodactyl (pig and cow) and perissodactyl (horse) species all possess what is termed a bicornuate uterus, defined as having both uterine horns and a uterine body. The relative proportion of these two segments is a direct result of the

degree of fusion between the left and right paramesonephric ducts in the developing embryo and varies substantially (Senger 1999). For the agricultural species, maximum fusion occurs in the horse, followed by the cow. Finally, a minimal amount of fusion is found in the pig in what is termed a highly developed bicornuate uterus. The porcine uterus, while considered bicornuate, has many of the features of the bipartite uterus found in carnivores, which is characterized by having two separate uteri which join only at the attachment to the cervix. Figure 2.6 shows the uterus of the pig in relation to that of the cow, with the relative sections clearly marked.

Under normal conditions in swine, only the tip of each uterine horn is occupied by embryos prior to hatching from the zona pellucida. Yet, this situation can be altered through specific placement of embryos during transfer. A series of such studies have been conducted by the laboratory of W. Holtz, wherein porcine embryos were surgically placed out of their natural developmental environments, and the subsequent effects on pregnancy rate and embryonic survival observed. In the first study, morula and blastocysts were placed either into the distal ampulla, tip of the uterine horn or the middle of the uterine horn. Transfers to the distal ampulla produced just over 50% pregnancy rate and had less that 6 normal conceptuses at day 30 (Stein-Stefani and Holtz 1987). In contrast, transfers to either the tip or middle of the uterine horn produced equivalent pregnancy rates (79 vs. 80%) and normal day 30 conceptuses (10 vs 10.4) (Stein-Stefani and Holtz 1987). The second study pushed embryos further from their biological norm by placing embryos into the middle of the uterine horn, the caudal quarter or into the uterine body. Pregnancy rate between the middle and caudal portion of the uterine horn were comparable at 88% and 81% respectively, but dropped to just 12% when embryos were placed in the uterine body (Wallenhorst and Holtz 1999). Interestingly, when litter size was assessed at day 28-30, significantly fewer conceptuses were found in animals where embryos were placed in the caudal

quarter of the horn (Wallenhorst and Holtz 1999). In fact, when all recipients are taken into account, embryo survival dropped from 41% in the middle horn and 29% in the caudal portion to just 3% in the uterine body (Wallenhorst and Holtz 1999). Taken together these results suggest that, while the environment of at least the upper half of the uterus is conducive to blastocyst stage embryo development and survival, the uterine environment becomes increasingly less synchronous to embryonic requirements further away from the tip.

Wallenhorst and Holtz (1999) note that the pregnancy rate achieved using transfer to the uterine body is equivalent to that achieved through non-surgical embryo transfer. However, when transcervical embryo transfer was conducted by Hazeleger and Kemp (1994) average pregnancy rates were just 33%. Interestingly, when embryonic stage is taken into consideration with non-surgical embryo transfers, pregnancy rates are substantially different. Transfers of later stage blastocysts resulted in a pregnancy rate of 55% while those conducted with early stage blastocysts result in only 10% pregnancy rate (Hazeleger and Kemp 1994). From this information it may be proposed that the effect of spatial asynchrony increases substantially with earlier stage embryos, which are less capable of surviving outside their natural location. This is contradictory to the results from embryo transfer in other species, such as horses, where transfer of morula stage embryos (day 5-6) results in significantly lower embryonic loss when compared to transfer at the blastocyst stage (day 7-8) (Carnevale *et al.* 2000). One must also consider that the reproductive tract of the mare has poorly developed uterine horns and a large uterine body and is, therefore, unlikely to experience the same degree of spatial asynchrony at this stage.

Interestingly, plasma progesterone concentrations in the veins draining the caudal, mid and cranial uterine horns of the pig are constant at days 1, 2 and 4 of gestation, with elevated levels found only in the oviduct (Pharazyn *et al.* 1991). This would suggest that embryonic death due to spatial asynchrony is not

the result of the differences in the uterine environment resulting from progesterone and that another mechanism may be at work. The study of Alminana *et al.* (2012) shows that the embryo has the ability to communicate with a spatially synchronous uterus; however, it is possible that this crosstalk breaks down when embryos are improperly placed. It is also possible that some as yet undescribed anatomical or histological differences exist over the length of the uterine horn and that these differences preclude embryonic survival even if appropriate communication is established. A third possibility is that the early uterine environment is regulated by a mechanism other than ovarian progesterone, which exhibits tempero-spatial variance during cleavage stage embryonic development.

Embryo to Embryo Asynchrony

In monotocous species, the embryo need only maintain synchrony with the maternal tract, while in polytocous species, such as the pig, it is necessary to also maintain synchrony with the other embryos of the litter. Variation between pig embryos appears very early in the cleavage stages and is strongly skewed with a majority of embryos at an advanced stage relative to the remaining embryos, which are widely distributed over lesser developed stages (Pope *et al.* 1990). When blastocysts are assessed at 6 days following the onset of estrus, there is a group comprising roughly 20% of each litter that has significantly lower total protein levels and viability (Wright Jr *et al.* 1983). This is the result of an initial gap in development of just 2-4 hours, which is thought to expand over time as the more developed blastocysts take advantage of the advancing uterine environment and grow more rapidly (Pope *et al.* 1990). The increase in embryonic diversity over time can be seen if expressed as the standard deviation of the number of embryonic nuclei per sow which is significantly correlated to the age of the embryos (Soede *et al.* 1992).

A study by Pope *et al.* (1982), using a unique model of embryo transfer and coat color phenotype, demonstrated the effects of embryo-embryo asynchrony in the pig. Asynchronous embryos, with either a black or white phenotype, were transferred to opposite uterine horns in the same recipient. There was no effect on embryo survival or pregnancy rate at day 11, but at day 60, embryonic survival of the mature embryos was over 60% while that of the less mature group was only 8.2% (Pope *et al.* 1982). Interestingly, an analysis of embryonic migration showed that the surviving less mature embryos traveled significantly further than the mature ones. These results clearly demonstrate that, in a polytocous species, asynchrony between the embryos results in the selective loss of less mature conceptuses.

The effect of embryo-to-embryo variation on reproductive performance in swine can also be seen when comparing the highly prolific Meishan breed of pigs to more common Western breeds. Despite equivalent ovulation rates and uterine size, the Meishan breed has substantially lower prenatal loss both during early embryonic development and after day 30 of gestation, resulting in significant improvements in litter size (Ford 1997). This difference in fertility is often associated with a reduced prenatal growth rate and less uterine crowding (Wilson and Ford 1997). However, when variation in embryo development is compared, the coefficient of variance of conceptus size in the Meishan line is roughly half that of the Large white line between days 8 and 11 of gestation (Bazer *et al.* 1988). This reduced variation early on in development, combined with reduced in utero growth rate, may explain the much larger litter size generally observed in the Meishan breed.

The link between embryo-embryo asynchrony and early embryonic mortality is likely a result of a disruption in communication between this minority population and their uterine environment. Starting at day 10 to 12 of gestation, porcine embryos begin production of estrogens in increasing amounts (Spencer and Bazer 2004, Geisert et al. 1982). Although this signal is considered

to play a primary role in maternal recognition of pregnancy, it also affects endometrial gene expression, uterine receptivity and composition of the uterine histotroph (Johnson *et al.* 2009). The resulting modifications to the uterine environment have a detrimental effect on embryos experiencing a retarded growth curve which likely results in their removal from the population. In addition to the lower embryo-to-embryo variation already discussed, Meishan conceptuses produce less estradiol, which has been directly correlated with a reduced uterine production of important molecules such as IGF2 (Wilson and Ford 1997). It is assumed that the reduced effect on uterine histotroph composition allows more of the embryos to survive beyond day 18 of gestation (Ford 1997).

There is a degree of controversy regarding the source of early embryonic diversity in swine. There is some evidence that this early diversity is the result of the duration of ovulation. Ovulation has been described as a heavily skewed process, with the majority of follicles (70%) ovulating almost synchronously and the remaining (30%) ovulating over a protracted period of time (Pope *et al.* 1990). This was consistent with the population of follicles prior to the LH surge that show a significant skew toward highly developed follicles with a minority that appeared to be developmentally retarded (Xie *et al.* 1990). However, a study by Soede *et al.* (1992) using transrectal ovarian ultrasonography at 30 minute intervals to assess the duration of ovulation, followed by embryo analysis at 100hrs, failed to find a relation between these factors. In the group of animals slaughtered, the range in the duration of estrus was .75 to 3.25 hrs and range of embryonic cell cycles from 1 to 5.5 (Soede *et al.* 1992). While these results may be due to the relatively low ovulation rate (19) and embryo recovery rate (84%) in the study, it is also possible that the effects of variation in ovulation where not apparent at 100 hrs. As well, the previously discussed study by Pope *et al.* (1982) failed to show an effect on survival as far into gestation as day 11, which may suggest that these effects become more apparent with time.

If ovulation is the source of embryonic asynchrony, a yet unanswered question is how such a small variation in the timing of ovulation results in sufficient asynchrony to cause embryonic loss at later stages. The most prolonged ovulation period observed by Soede *et al.* (1992) was just seven hours in length, which is significantly less dramatic than the embryo-to-embryo asynchrony observed in the experiments discussed thus far. One explanation is that the latter pool of oocytes ovulated are less developed which will have a carry-over effect on embryonic development and therefore, survival. However, another possibility is that even a slight lag in development is amplified by the effect of temporal and spatial asynchrony with the environment of the reproductive tract and grows exponentially more severe as embryo development progresses.

Summary

While each stage of prenatal development is important in the generation of healthy offspring, the initial stages are disproportionately vital in that they produce the foundation from which subsequent development is built. The vital nature of these processes can be seen in the distribution of prenatal loss, which is heavily skewed toward the complex and dynamic portion of embryonic development. Pre-implantation embryonic development is a particularly vital period, as it is during this time that reprogramming of the parental genome must occur. It is also during this very early period that embryo based assisted reproductive technologies can be applied and therefore, the success of such technologies relies heavily on our understanding of the biologically normal environment in which this development is carried out.

Substantial work has thus far been carried out on the later portions of pre-implantation embryonic development, focusing on maternal recognition of pregnancy and maternal conceptus crosstalk immediately preceding implantation. Furthermore, numerous experiments utilizing *in vitro* embryo culture systems have provided information on a limited number of candidate

molecules likely to be involved in promoting earlier cleavage stage development. These experiments that apply a “candidate approach” are somewhat limited in light of the complex nature of both the uterine environment and the embryonic-uterine communication. Recent developments in the areas of high throughput proteomics and transcriptomics have allowed work on ever earlier stages of embryonic development and have confirmed the hypothesis that this system is both dynamic and highly complex. Additional characterization of the reproductive tract environment during the very early stages of embryonic development is likely to improve the success of embryo-based assisted reproductive technologies and potentially new candidates in a search for earlier detection of pregnancy.

The following chapters detail a series of experiments designed to better characterize reproductive function, the uterine and oviductal environments and maternal-embryonic communication during the development of the pig embryo to the blastocyst stage.

Tables

Species	Observed Period of Specific cell cleavage stages (hrs Post Ovulation)						Oviductal-Uterine Transit	
	2cell	3-4cell	5-8cell	9-16 cell	Morula	Blast	Time	Stage
Pig	24	48	48-71	71-84	84	96-128	48	4 cell
Cow	40-55	44-65	46-96	71-141	132-144	182-190	96-110	8-16cell
Sheep	38-39	60	85	98	120-140	158	77-96	16cell
Primate	0-24	24-36	36-48	48-72	72-96	120	96	morula
Mouse	24-38	38-50	50-64	60-70	68-80	74-82	72	morula
Rabbit	21-34	30-75	80	-	100-115	115-140	70	Blastocyst

Table 2.1: Embryonic c0leavage rates and oviductal-uterine transit times for different Species. Addapted from Hamilton, W. J., and J. A. Laing. (1946), Polge, C (1982), Perry, J. S., and I. W. Rowlands. (1962) and Senger, P. L. (1999).

Figures

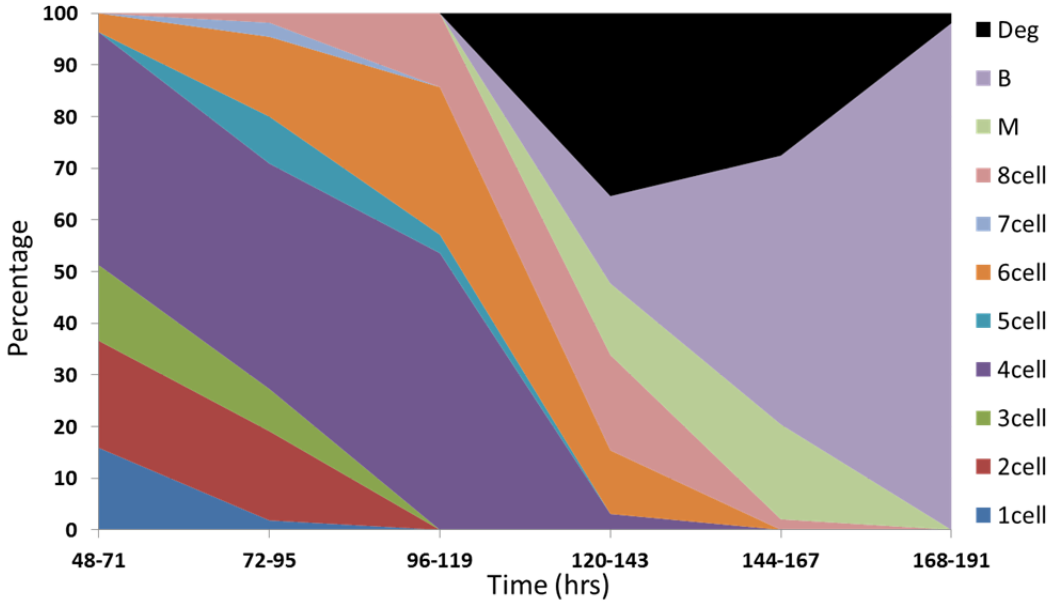

Figure 2.1: Embryo variability within fixed time points following onset of standing estrus in the pig. Adapted from Perry and Rowlands (1962)

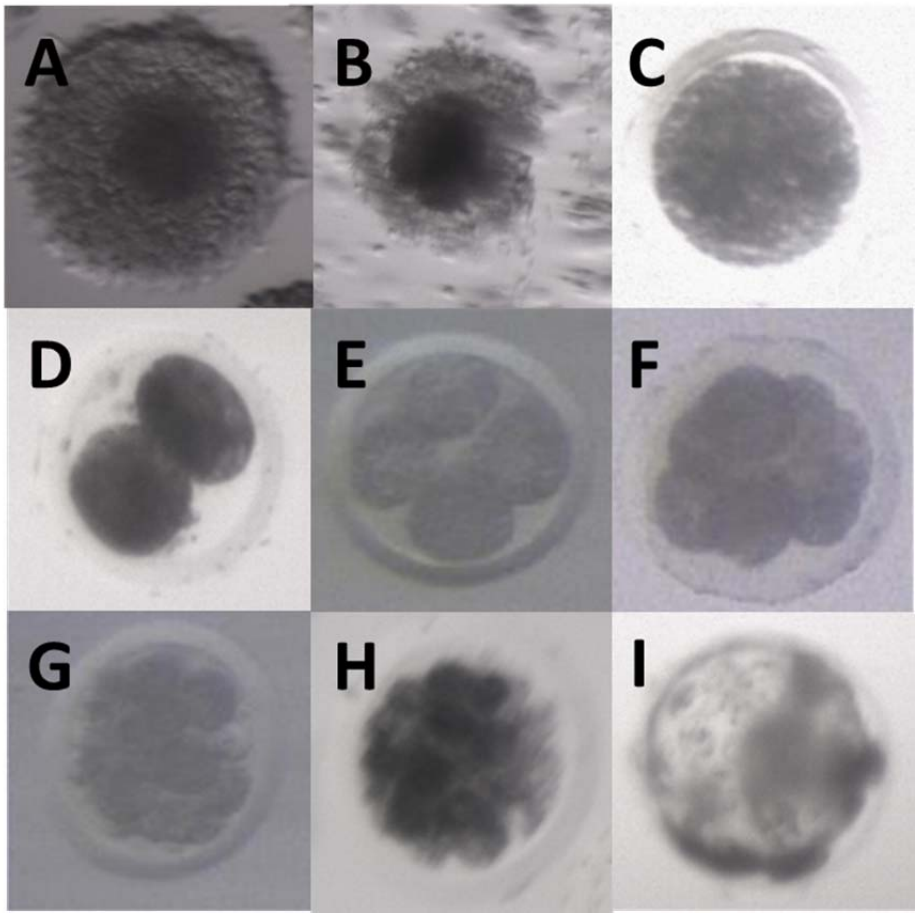

Figure 2.2: Visual appearance of oocytes and cleavage stage embryos at A. germinal vesicle, B. metaphase two, C. zygote, D. 2-cell, E. 4-cell, F. 8-cell, G. early morula, H. late morula and I. Blastocyst stages. Images were produced in-house as part of the research in this Thesis.

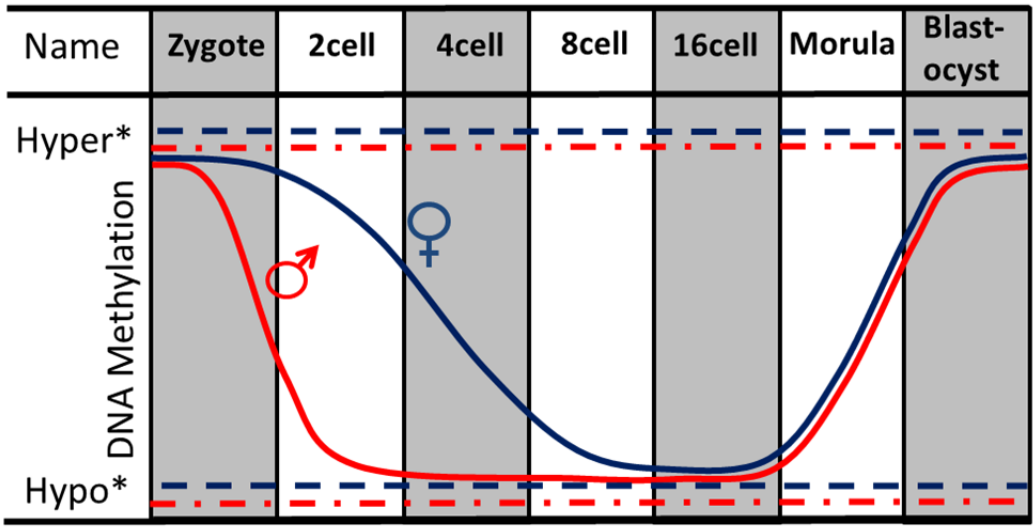

Figure 2.3: Maternal and paternal methylation dynamics of the early embryo. * hypo and hyper methylated imprints (marked as interrupted lines). Adapted from Reik et al 2001.

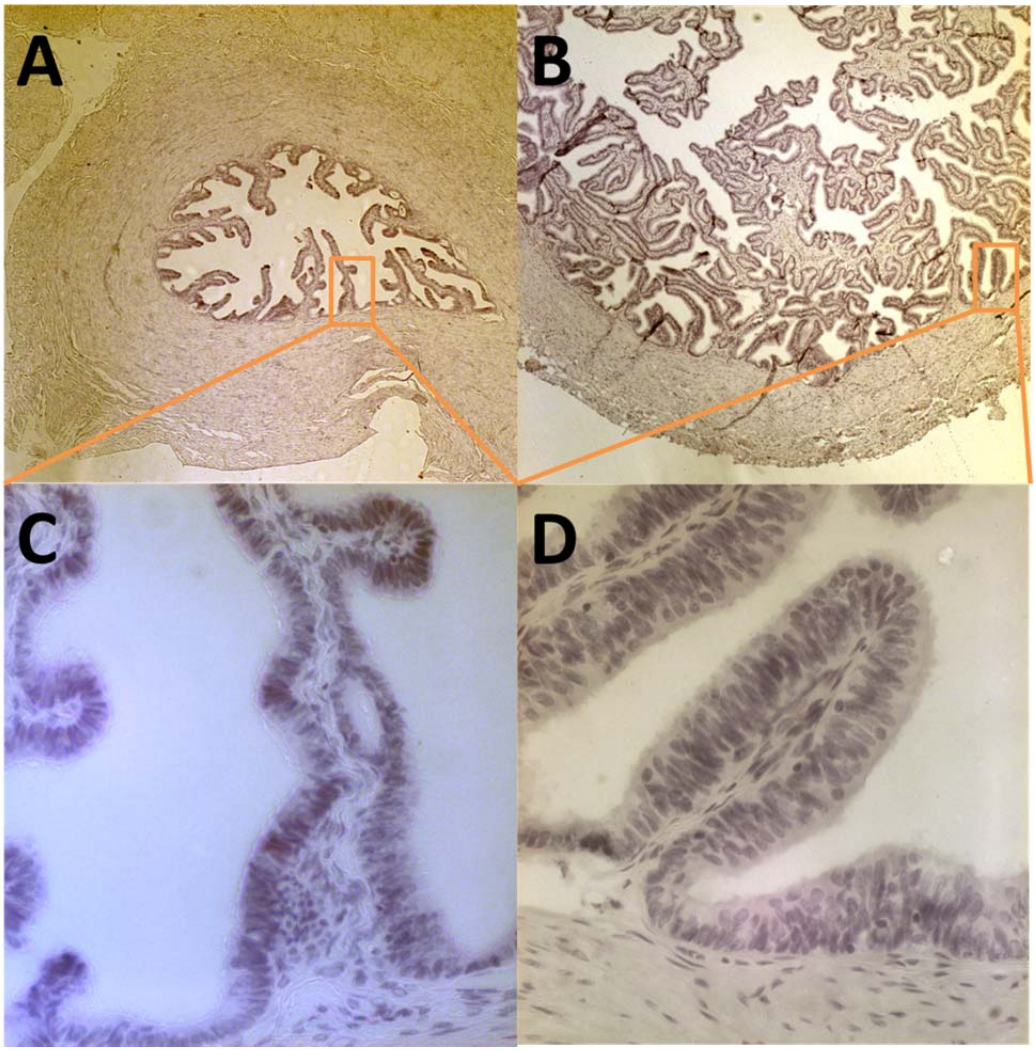

Figure 2.4: Cross sections of the porcine oviductal isthmus and ampulla showing the relative complexity of the luminal fimbrial projections and luminal epithelium. A. isthmus at 10X magnification, B. ampulla at 10X magnification, C. 40X magnification of isthmus fimbreal projection D. 40 X magnification of ampulla fimbreal projection. Images were produced in-house as a part of the research presented in this Thesis.

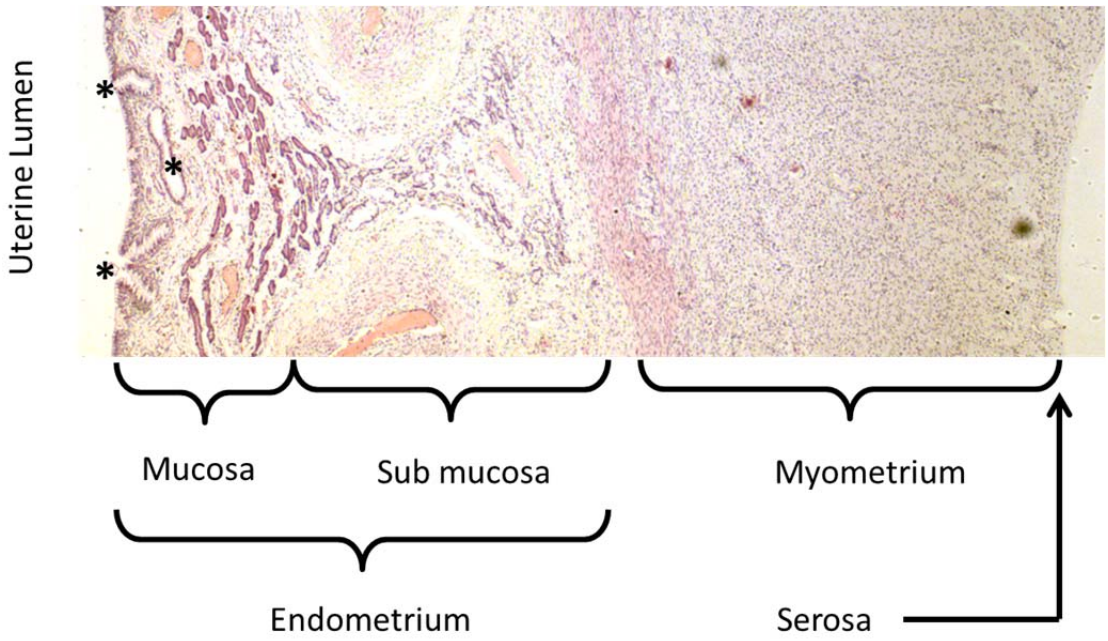

Figure 2.5: Magnification (10 X) of a cross section from the porcine uterine wall, divided into anatomical layers. *marks the uterine glands. Images were produced in-house as a part of the research presented in this Thesis.

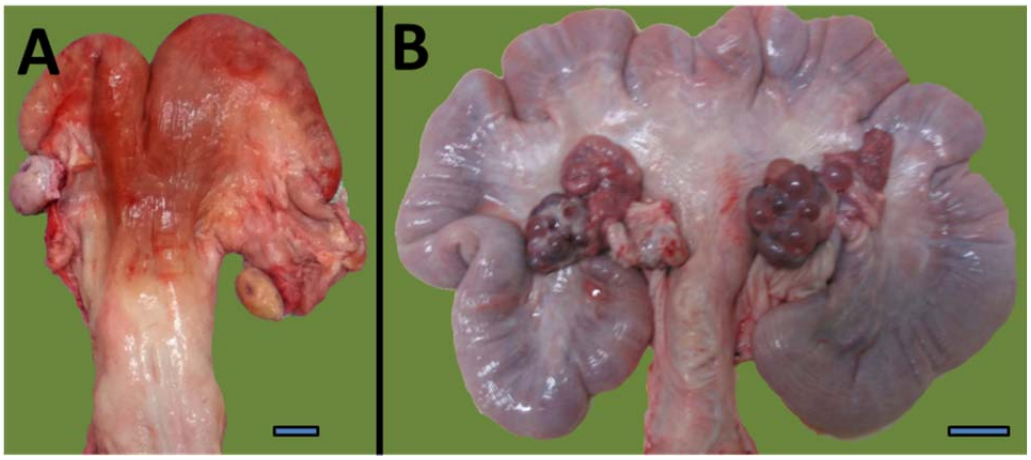

Figure 2.6: Comparison of gross uterine anatomy between: A. bovine and B. porcine reproductive tracts. Images were produced in-house as a part of the research presented in this Thesis.

References

Adams, K.L., Bazer, F.W., and Roberts, R.M. (1981) Progesterone-induced secretion of a retinol-binding protein in the pig uterus. J Reprod Fertil **62**(1), 39-47

Adams, G.P., Ratto, M.H., Huanca, W., and Singh, J. (2005) Ovulation-Inducing Factor in the Seminal Plasma of Alpacas and Llamas. Biol Reprod **73**(3), 452-457

Adenot, P.G., Mercier, Y., Renard, J.P., and Thompson, E.M. (1997) Differential H4 acetylation of paternal and maternal chromatin precedes DNA replication and differential transcriptional activity in pronuclei of 1-cell mouse embryos. Development **124**(22), 4615-4625

Albertini, D.F., Overstrom, E.W., and Ebert, K.M. (1987) Changes in the organization of the actin cytoskeleton during preimplantation development of the pig embryo. Biol Reprod **37**(2), 441-451

Alizadeh, Z., Kageyama, S.-I., and Aoki, F. (2005) Degradation of maternal mRNA in mouse embryos: Selective degradation of specific mRNAs after fertilization. Mol Reprod Dev **72**(3), 281-290

Alminana, C., Heath, P.R., Wilkinson, S., Sanchez-Osorio, J., Cuello, C., Parrilla, I., Gil, M.A., Vazquez, J.L., Vazquez, J.M., Roca, J., Martinez, E.A., and Fazeli, A. (2012) Early developing pig embryos mediate their own environment in the maternal tract. PLoS One **7**(3), e33625

Anderson, J.E., Matteri, R.L., Abeydeera, L.R., Day, B.N., and Prather, R.S. (2001) Degradation of maternal cdc25c during the maternal to zygotic transition is dependent upon embryonic transcription. Mol Reprod Dev **60**(2), 181-188

Archibong, A.E., Petters, R.M., and Johnson, B.H. (1989) Development of porcine embryos from one- and two-cell stages to blastocysts in culture medium supplemented with porcine oviductal fluid. Biol Reprod **41**(6), 1076-1083

Auletta, F.J., and Kelm, L.B. (1994) Mechanisms controlling corpus luteum function in the rhesus monkey (Macaca mulatta): inhibitory action of hCG on luteolysis induced by PGF2 alpha. J Reprod Fertil **102**(1), 215-220

Barcroft, L.C., Offenberg, H., Thomsen, P., and Watson, A.J. (2003) Aquaporin proteins in murine trophectoderm mediate transepithelial water movements during cavitation. Dev Biol **256**(2), 342-354

Bartol, F.F., Wiley, A.A., Spencer, T.E., Vallet, J.L., and Christenson, R.K. (1993) Early uterine development in pigs. J Reprod Fertil Suppl **48**, 99-116

Bauersachs, S., Blum, H., Mallok, S., Wenigerkind, H., Rief, S., Prelle, K., and Wolf, E. (2003) Regulation of Ipsilateral and Contralateral Bovine Oviduct Epithelial Cell Function in the Postovulation Period: A Transcriptomics Approach. Biol Reprod **68**(4), 1170-1177

Bazer, F.W., and Thatcher, W.W. (1977) Theory of maternal recognition of pregnancy in swine based on estrogen controlled endocrine versus exocrine secretion of prostaglandin F2alpha by the uterine endometrium. Prostaglandins **14**(2), 397-400

Bazer, F.W., Thatcher, W.W., Martinat-Botte, F., and Terqui, M. (1988) Conceptus development in large white and prolific Chinese Meishan pigs. J Reprod Fertil **84**(1), 37-42

Beaujean, N., Hartshorne, G., Cavilla, J., Taylor, J., Gardner, J., Wilmut, I., Meehan, R., and Young, L. (2004) Non-conservation of mammalian preimplantation methylation dynamics. Curr Biol **14**(7), R266-267

Berger, T., Turner, K.O., Meizel, S., and Hedrick, J.L. (1989) Zona pellucida-induced acrosome reaction in boar sperm. Biol Reprod **40**(3), 525-530

Bestor, T.H. (1992) Activation of mammalian DNA methyltransferase by cleavage of a Zn binding regulatory domain. EMBO J **11**(7), 2611-2617

Betts, D.H., Barcroft, L.C., and Watson, A.J. (1998) Na/K-ATPase-Mediated86Rb+Uptake and Asymmetrical Trophectoderm Localization of α1 and α3 Na/K-ATPase Isoforms during Bovine Preattachment Development. Dev Biol **197**(1), 77-92

Bird, A. (2007) Perceptions of epigenetics. Nature **447**(7143), 396-398

Bischof, R.J., Lee, C.S., Brandon, M.R., and Meeusen, E. (1994) Inflammatory response in the pig uterus induced by seminal plasma. J Reprod Immunol **26**(2), 131-146

Bloom, T., and McConnell, J. (1990) Changes in protein phosphorylation associated with compaction of the mouse preimplantation embryo. Mol Reprod Dev **26**(3), 199-210

Bonk, A.J., Li, R., Lai, L., Hao, Y., Liu, Z., Samuel, M., Fergason, E.A., Whitworth, K.M., Murphy, C.N., Antoniou, E., and Prather, R.S. (2008) Aberrant DNA methylation in porcine in vitro-, parthenogenetic-, and somatic cell nuclear transfer-produced blastocysts. Mol Reprod Dev **75**(2), 250-264

Borland, R.M., and Tasca, R.J. (1974) Activation of a Na+-dependent amino acid transport system in preimplantation mouse embryos. Dev Biol **36**(1), 169-182

Brandeis, M., Kafri, T., Ariel, M., Chaillet, J.R., McCarrey, J., Razin, A., and Cedar, H. (1993) The ontogeny of allele-specific methylation associated with imprinted genes in the mouse. EMBO J **12**(9), 3669-3677

Brinster, R.L. (1967) Protein Content Of The Mouse Embryo During The First Five Days Of Development. J Reprod Fertil **13**(3), 413-420

Brinster, R.L., and Zimmermann, J.W. (1994) Spermatogenesis following male germ-cell transplantation. PNAS **91**(24), 11298-11302

Brownell, M.S., and Warner, C.M. (1988) Ped gene expression by embryos cultured in vitro. Biol Reprod **39**(4), 806-811

Buhi, W.C., Alvarez, I.M., Sudhipong, V., and Dones-Smith, M.M. (1990) Identification and characterization of de novo-synthesized porcine oviductal secretory proteins. Biol Reprod **43**(6), 929-938

Buhi, W.C., Vallet, J.L., and Bazer, F.W. (1989) De novo synthesis and release of polypeptides from cyclic and early pregnant porcine oviductal tissue in explant culture. J Exp Zool **252**(1), 79-88

Carlson, L.L., Page, A.W., and Bestor, T.H. (1992) Properties and localization of DNA methyltransferase in preimplantation mouse embryos: implications for genomic imprinting. Genes Dev **6**(12B), 2536-2541

Carnevale, E.M., Ramirez, R.J., Squires, E.L., Alvarenga, M.A., Vanderwall, D.K., and McCue, P.M. (2000) Factors affecting pregnancy rates and early embryonic death after equine embryo transfer. Theriogenology **54**(6), 965-979

Caveney, S. (1985) The role of gap junctions in development. Annu Rev Physiol **47**, 319-335

Chen, T.T., Bazer, F.W., Cetorelli, J.J., Pollard, W.E., and Roberts, R.M. (1973) Purification and properties of a progesterone-induced basic glycoprotein from the uterine fluids of pigs. J Biol Chem **248**(24), 8560-8566

Christenson, R.K., Ford, J.J., and Redmer, D.A. (1985) Maturation of ovarian follicles in the prepubertal gilt. J Reprod Fertil Suppl **33**, 21-36

Copp, A.J. (1978) Interaction between inner cell mass and trophectoderm of the mouse blastocyst. JEEM **48**(1), 109-125

Coy, P., Gadea, J., Romar, R., Matas, C., and Garcia, E. (2002) Effect of in vitrofertilization medium on the acrosome reaction, cortical reaction, zona pellucida hardening and in vitro development in pigs. Reproduction **124**(2), 279-288

Cran, D.G., and Cheng, W.T.K. (1986) The cortical reaction in pig oocytes during in vivo and in vitro fertilization. Gamete Res **13**(3), 241-251

Day, B.N., and Polge, C. (1968) Effects Of Progesterone On Fertilization And Egg Transport In The Pig. J Reprod Fertil **17**(1), 227-230

Dean, W., Santos, F., and Reik, W. (2003a) Epigenetic reprogramming in early mammalian development and following somatic nuclear transfer. Sem Cell Dev Biol **14**(1), 93-100

Degenstein, K.L., O'Donoghue, R., Patterson, J.L., Beltranena, E., Ambrose, D.J., Foxcroft, G.R., and Dyck, M.K. (2008) Synchronization of ovulation in cyclic gilts with porcine luteinizing hormone (pLH) and its effects on reproductive function. Theriogenology **70**(7), 1075-1085

Deshmukh, R.S., Ostrup, O., Ostrup, E., Vejlsted, M., Niemann, H., Lucas-Hahn, A., Petersen, B., Li, J., Callesen, H., and Hyttel, P. (2011) DNA methylation in porcine preimplantation embryos developed in vivo and produced by in vitro fertilization, parthenogenetic activation and somatic cell nuclear transfer. Epigenetics **6**(2), 177-187

Devreker, F., and Hardy, K. (1997) Effects of glutamine and taurine on preimplantation development and cleavage of mouse embryos in vitro. Biol Reprod **57**(4), 921-928

Diskin, M.G., and Morris, D.G. (2008) Embryonic and Early Foetal Losses in Cattle and Other Ruminants. Reprod Domestic Anim **43**, 260-267

Ducibella, T., and Anderson, E. (1979) The effects of calcium deficiency on the formation of the zonula occludens and blastocoel in the mouse embryo. Dev Biol **73**(1), 46-58

Dunning, K.R., Cashman, K., Russell, D.L., Thompson, J.G., Norman, R.J., and Robker, R.L. (2010) Beta-Oxidation Is Essential for Mouse Oocyte Developmental Competence and Early Embryo Development. Biol Reprod **83**(6), 909-918

Dziuk, P. (1985) Effect of migration, distribution and spacing of pig embryos on pregnancy and fetal survival. J Reprod Fertil Suppl **33**, 57-63

Elhassan, Y.M., Wu, G., Leanez, A.C., Tasca, R.J., Watson, A.J., and Westhusin, M.E. (2001) Amino acid concentrations in fluids from the bovine oviduct and uterus and in ksom-based culture media. Theriogenology **55**(9), 1907-1918

Evans, H.E., and Sack, W.O. (1973) Prenatal Development of Domestic and Laboratory Mammals: Growth Curves, External Features and Selected References. Anat Histol Embryol **2**(1), 11-45

Feigelson, M., and Kya, E. (1972) Protein Patterns of Rabbit Oviducal Fluid. Biol Reprod **6**(2), 244-252

Fernandez-Gonzalez, R., Moreira, P., Bilbao, A., Jimenez, A., Perez-Crespo, M., Ramirez, M.A., Rodriguez De Fonseca, F., Pintado, B., and Gutierrez-Adan, A. (2004) Long-term effect of in vitro culture of mouse embryos with serum on mRNA expression of imprinting genes, development, and behavior. Proc Natl Acad Sci U S A **101**(16), 5880-5885

Findlay, J.K., Gear, M.L., Illingworth, P.J., Junk, S.M., Kay, G., Mackerras, A.H., Pope, A., Rothenfluh, H.S., and Wilton, L. (2007) Human embryo: a biological definition. Hum Reprod **22**(4), 905-911

Fischle, W., Wang, Y., and Allis, C.D. (2003) Histone and chromatin cross-talk. Curr Opin Cell Biol **15**(2), 172-183

Flood, M.R., and Wiebold, J.L. (1988) Glucose metabolism by preimplantation pig embryos. J Reprod Fertil **84**(1), 7-12

Ford, S.P. (1997) Embryonic and fetal development in different genotypes in pigs. J Reprod Fertil Suppl **52**, 165-176

Ford, S.P., and Stice, S.L. (1985) Effects of the ovary and conceptus on uterine blood flow in the pig. J Reprod Fertil Suppl **33**, 83-90

Fulka, J., Fulka, H., Slavik, T., Okada, K., and Fulka, J., Jr. (2006) DNA methylation pattern in pig in vivo produced embryos. Histochem Cell Biol **126**(2), 213-217

Gawronska, B., Stepien, A., and Ziecik, A.J. (2000) Effect of estradiol and progesterone on oviductal LH-receptors and LH-dependent relaxation of the porcine oviduct. Theriogenology **53**(3), 659-672

Geisert, R.D., Renegar, R.H., Thatcher, W.W., Roberts, R.M., and Bazer, F.W. (1982) Establishment of pregnancy in the pig: I. Interrelationships between preimplantation development of the pig blastocyst and uterine endometrial secretions. Biol Reprod 27(4), 925-939

Georgiou, A.S., Snijders, A.P.L., Sostaric, E., Aflatoonian, R., Vazquez, J.L., Vazquez, J.M., Roca, J., Martinez, E.A., Wright, P.C., and Fazeli, A. (2007) Modulation of The Oviductal Environment by Gametes. J Proteome Res **6**(12), 4656-4666

Georgiou, A.S., Sostaric, E., Wong, C.H., Snijders, A.P.L., Wright, P.C., Moore, H.D., and Fazeli, A. (2005) Gametes Alter the Oviductal Secretory Proteome. Mol Cell Proteomics **4**(11), 1785-1796

Goldstein, S.R. (1994) Embryonic death in early pregnancy: a new look at the first trimester. Obstet Gynecol **84**(2), 294-297

Grapes, L., Malek, M., and Rothschild, M.F. (2001) Identification of monozygous twins and microsatellite mutation rate in pigs from QTL linkage analysis data. J Anim Breed Genet **118**(5), 311-315

Ham, A.W. (1950) 'Histology.' (Pitman Medical Publishing: London)

Hamatani, T., Carter, M.G., Sharov, A.A., and Ko, M.S. (2004) Dynamics of global gene expression changes during mouse preimplantation development. Dev Cell **6**(1), 117-131

Hamilton, W.J., and Laing, J.A. (1946) Development of the egg of the cow up to the stage of blastocyst formation. J Anat **80**(4), 194-204

Hanly, S. (1961) Prenatal mortality in farm animals. J Reprod Fertil **2**, 182-194

Hardy, K., and Spanos, S. (2002) Growth factor expression and function in the human and mouse preimplantation embryo. J Endocrinol **172**(2), 221-236

Hazeleger, W., and Kemp, B. (1994) Farrowing Rate and Litter Size after Transcervical Embryo Transfer in Sows. Reprod Domestic Anim **29**(6), 481-487

Hedrick, J.L., Wardrip, N.J., and Berger, T. (1987) Differences in the macromolecular composition of the zona pellucida isolated from pig oocytes, eggs, and zygotes. J Exp Zool **241**(2), 257-262

Hogan, A., Heyner, S., Charron, M.J., Copeland, N.G., Gilbert, D.J., Jenkins, N.A., Thorens, B., and Schultz, G.A. (1991) Glucose transporter gene expression in early mouse embryos. Development **113**(1), 363-372

Houliston, E., Pickering, S.J., and Maro, B. (1989) Alternative routes for the establishment of surface polarity during compaction of the mouse embryo. Dev Biol **134**(2), 342-350

Huang, J.-C., Lei, Z.-L., Shi, L.-H., Miao, Y.-L., Yang, J.-W., Ouyang, Y.-C., Sun, Q.-Y., and Chen, D.-Y. (2007) Comparison of histone modifications in in vivo and in vitro fertilization mouse embryos. Biochem Biophys Res Commun **354**(1), 77-83

Hunter, M.G. (2000) Oocyte maturation and ovum quality in pigs. Rev Reprod **5**(2), 122-130

Ireland, J.J. (1987) Control of follicular growth and development. J Reprod Fertil Suppl **34**, 39-54

Iritani, A., Sato, E., and Nishikawa, Y. (1974) Secretion Rates and Chemical Composition of Oviduct and Uterine Fluids in Sows. J Anim Sci **39**(3), 582-588

Jarrell, V.L., Day, B.N., and Prather, R.S. (1991) The transition from maternal to zygotic control of development occurs during the 4-cell stage in the domestic pig, Sus scrofa: quantitative and qualitative aspects of protein synthesis. Biol Reprod **44**(1), 62-68

Javed, M.H., and Wright Jr, R.W. (1991) Determination of pentose phosphate and Embden-Meyerhof pathway activities in bovine embryos. Theriogenology **35**(5), 1029-1037

Jeong, Y.S., Yeo, S., Park, J.S., Koo, D.B., Chang, W.K., Lee, K.K., and Kang, Y.K. (2007) DNA methylation state is preserved in the sperm-derived pronucleus of the pig zygote. Int J Dev Biol **51**(8), 707-714

Johnson, G.A., Bazer, F.W., Burghardt, R.C., Spencer, T.E., Wu, G., and Bayless, K.J. (2009) Conceptus-uterus interactions in pigs: endometrial gene expression in response to estrogens and interferons from conceptuses. Soc Reprod Fertil Suppl **66**, 321-332

Johnson, M.H., and Ziomek, C.A. (1981) The foundation of two distinct cell lineages within the mouse morula. Cell **24**(1), 71-80

Johnson, T.B., and Coghill, R.D. (1925) Researches on pyrimidines. C111. The discovery of 5-methyl-cytosine in tuberculinic acid, the nucleic acid of the tubercle bacillus. J Am Chem Soc **47**(11), 2838-2844

Jones, P.A., and Takai, D. (2001) The role of DNA methylation in mammalian epigenetics. Science **293**(5532), 1068-1070

Keshet, I., Yisraeli, J., and Cedar, H. (1985) Effect of regional DNA methylation on gene expression. Proc Natl Acad Sci U S A **82**(9), 2560-2564

Khosla, S., Dean, W., Brown, D., Reik, W., and Feil, R. (2001) Culture of preimplantation mouse embryos affects fetal development and the expression of imprinted genes. Biol Reprod **64**(3), 918-926

Kim, N.-H., Funahashi, H., Abeydeera, L.R., Moon, S.J., Prather, R.S., and Day, B.N. (1996) Effects of oviductal fluid on sperm penetration and cortical granule exocytosis during fertilization of pig oocytes in vitro. J Reprod Fertil **107**(1), 79-86

Kimura, K., Spate, L.D., Green, M.P., and Roberts, R.M. (2005) Effects of D-glucose concentration, D-fructose, and inhibitors of enzymes of the pentose phosphate pathway on the development and sex ratio of bovine blastocysts. Mol Reprod Dev **72**(2), 201-207

Knight, J.W., Bazer, F.W., and Wallace, H.D. (1973) Hormonal Regulation of Porcine Uterine Protein Secretion. J Anim Sci **36**(3), 546-553

Kopecny, V. (1989) High-resolution autoradiographic studies of comparative nucleologenesis and genome reactivation during early embryogenesis in pig, man and cattle. Reprod Nutr Dev **29**(5), 589-600

Krisher, R.L., and Prather, R.S. (2012) A role for the Warburg effect in preimplantation embryo development: metabolic modification to support rapid cell proliferation. Mol Reprod Dev **79**(5), 311-320

Kurihara, Y., Kawamura, Y., Uchijima, Y., Amamo, T., Kobayashi, H., Asano, T., and Kurihara, H. (2008) Maintenance of genomic methylation patterns during preimplantation development requires the somatic form of DNA methyltransferase 1. Dev Biol **313**(1), 335-346

Lane, M., and Gardner, D.K. (1998) Amino acids and vitamins prevent culture-induced metabolic perturbations and associated loss of viability of mouse blastocysts. Hum Reprod **13**(4), 991-997

Lane, N., Dean, W., Erhardt, S., Hajkova, P., Surani, A., Walter, J., and Reik, W. (2003) Resistance of IAPs to methylation reprogramming may provide a mechanism for epigenetic inheritance in the mouse. Genesis **35**(2), 88-93

Larue, L., Ohsugi, M., Hirchenhain, J., and Kemler, R. (1994) E-cadherin null mutant embryos fail to form a trophectoderm epithelium. PNAS **91**(17), 8263-8267

Lee, K.F., Yao, Y.Q., Kwok, K.L., Xu, J.S., and Yeung, W.S. (2002) Early developing embryos affect the gene expression patterns in the mouse oviduct. Biochem Biophys Res Commun **292**(2), 564-570

Leese, H., Tay, J., Reischl, J., and Downing, S. (2001) Formation of Fallopian tubal fluid: role of a neglected epithelium. Reproduction **121**(3), 339-346

Leese, H.J., and Barton, A.M. (1984) Pyruvate and glucose uptake by mouse ova and preimplantation embryos. J Reprod Fertil **72**(1), 9-13

Leibfried-Rutledge, M.L., Critser, E.S., Eyestone, W.H., Northey, D.L., and First, N.L. (1987) Development potential of bovine oocytes matured in vitro or in vivo. Biol Reprod **36**(2), 376-383

Leung, P.C., and Armstrong, D.T. (1980) Interactions of steroids and gonadotropins in the control of steroidogenesis in the ovarian follicle. Annu Rev Physiol **42**, 71-82

Levy, J.B., Johnson, M.H., Goodall, H., and Maro, B. (1986) The timing of compaction: control of a major developmental transition in mouse early embryogenesis. JEEM **95**(1), 213-237

Li, T., Vu, T.H., Ulaner, G.A., Littman, E., Ling, J.-Q., Chen, H.-L., Hu, J.-F., Behr, B., Giudice, L., and Hoffman, A.R. (2005) IVF results in de novo DNA methylation and histone methylation at an Igf2-H19 imprinting epigenetic switch. Mol Hum Reprod **11**(9), 631-640

Lo, C.W., and Gilula, N.B. (1979) Gap junctional communication in the preimplantation mouse embryo. Cell **18**(2), 399-409

Lonergan, P., Khatir, H., Piumi, F., Rieger, D., Humblot, P., and Boland, M.P. (1999) Effect of time interval from insemination to first cleavage on the developmental characteristics, sex ratio and pregnancy rate after transfer of bovine embryos. J Reprod Fertil **117**(1), 159-167

Lyon, M.F. (1972) X-Chromosome Inactivation And Developmental Patterns In Mammals. Biological Reviews **47**(1), 1-35

M.K. Dyck, and Ruvinsky, A. (2011) Developmental Genetics. In 'The Genetics of the Pig, 2nd Edition.' (Eds. M.F. Rothchild and A Ruvinsky) pp. 263-305. (CABI: Oxforshire, UK)

Mattioli, M., Bacci, M.L., Galeati, G., and Seren, E. (1989) Developmental competence of pig oocytes matured and fertilized in vitro. Theriogenology **31**(6), 1201-1207

McEvoy, T., Coull, G., Broadbent, P., Hutchinson, J., and Speake, B. (2000) Fatty acid composition of lipids in immature cattle, pig and sheep oocytes with intact zona pellucida. J Reprod Fertil **118**(1), 163-170

McGraw, S., Robert, C., Massicotte, L., and Sirard, M.-A. (2003) Quantification of Histone Acetyltransferase and Histone Deacetylase Transcripts During Early Bovine Embryo Development. Biol Reprod **68**(2), 383-389

McLachlin, J.R., and Kidder, G.M. (1986) Intercellular junctional coupling in preimplantation mouse embryos: effect of blocking transcription or translation. Dev Biol **117**(1), 146-155

McLaren, A., and Smith, R. (1977) Functional test of tight junctions in the mouse blastocyst. Nature **267**(5609), 351-353

Miller, D.J., Macek, M.B., and Shur, B.D. (1992) Complementarity between sperm surface [beta]-l,4-galactosyl-transferase and egg-coat ZP3 mediates sperm-egg binding. Nature **357**(6379), 589-593

Miller, J.G., and Schultz, G.A. (1987) Amino acid content of preimplantation rabbit embryos and fluids of the reproductive tract. Biol Reprod **36**(1), 125-129

Minami, N., Suzuki, T., and Tsukamoto, S. (2007) Zygotic gene activation and maternal factors in mammals. J Reprod Dev **53**(4), 707-715

Moor, R.M., and Gandolfi, F. (1987) Molecular and cellular changes associated with maturation and early development of sheep eggs. J Reprod Fertil Suppl **34**, 55-69

Moore, N.W., and Shelton, J.N. (1964) Egg Transfer in Sheep. J Reprod Fertil **7**(2), 145-152

Muggleton-Harris, A., Whittingham, D.G., and Wilson, L. (1982) Cytoplasmic control of preimplantation development in vitro in the mouse. Nature **299**(5882), 460-462

Mullen, M.P., Elia, G., Hilliard, M., Parr, M.H., Diskin, M.G., Evans, A.C., and Crowe, M.A. (2012) Proteomic Characterization of Histotroph during the Preimplantation Phase of the Estrous Cycle in Cattle. J Proteome Res **11**(5): 3004-3018

Murray, F.A., Bazer, F.W., Rundel, J.W., Vincent, C.K., Wallace, H.D., and Warnick, A.C. (1971) Developmental Failure Of Swine Embryos Restricted To The Oviducal Environment. J Reprod Fertil **24**(3), 445-448

NCBI-Gene Gene Database. In '.' pp. Gene integrates information from a wide range of species. A record may include nomenclature, Reference Sequences (RefSeqs), maps, pathways, variations, phenotypes, and links to genome-, phenotype-, and locus-specific resources worldwide. (NCBI)

Newcomb, R., and Rowson, L.E.A. (1975) Conception Rate After Uterine Transfer Of Cow Eggs, In Relation To Synchronization Of Oestrus And Age Of Eggs. J Reprod Fertil **43**(3), 539-541

Nieder, G.L., Weitlauf, H.M., and Suda-Hartman, M. (1987) Synthesis and secretion of stage-specific proteins by peri-implantation mouse embryos. Biol Reprod **36**(3), 687-699

Novak, S., Almeida, F.R.C.L., Cosgrove, J.R., Dixon, W.T., and Foxcroft, G.R. (2003) Effect of pre- and postmating nutritional manipulation on plasma progesterone, blastocyst development, and the oviductal environmentduring early pregnancy in gilts. J Anim Sci 81(3), 772-783

Novak, S., Paradis, F., Patterson, J.L., Pasternak, J.A., Oxtoby, K., Moore, H.S., Hahn, M., Dyck, M.K., Dixon, W.T., and Foxcroft, G.R. (2012) Temporal candidate gene expression in the sow placenta and embryo during early gestation and effect of maternal Progenos supplementation on embryonic and placental development. Reprod Fertil Dev **24**(4), 550-558

Novak, S., Treacy, B.K., Almeida, F.R.C.L., Mao, J., Buhi, W.C., Dixon, W.T., and Foxcroft, G.R. (2002) Regulation of IGF-I and porcine oviductal secretory protein (pOSP) secretion into the pig oviduct in the peri-ovulatory period, and effects of previous nutrition. Reprod. Nutr. Dev. **42**(4), 355-372

O'Fallon, J.V., and Wright, R.W. (1986) Quantitative determination of the pentose phosphate pathway in preimplantation mouse embryos. Biol Reprod **34**(1), 58-64

O'Leary, S., Jasper, M.J., Warnes, G.M., Armstrong, D.T., and Robertson, S.A. (2004) Seminal plasma regulates endometrial cytokine expression, leukocyte recruitment and embryo development in the pig. Reproduction **128**(2), 237-247

O'Neill, L.P., VerMilyea, M.D., and Turner, B.M. (2006) Epigenetic characterization of the early embryo with a chromatin immunoprecipitation protocol applicable to small cell populations. Nat Genet **38**(7), 835-841

O'Leary, S., Jasper, M.J., Robertson, S.A., and Armstrong, D.T. (2006) Seminal plasma regulates ovarian progesterone production, leukocyte recruitment and follicular cell responses in the pig. Reproduction **132**(1), 147-158

Oestrup, O., Hall, V., Petkov, S.G., Wolf, X.A., Hyldig, S., and Hyttel, P. (2009) From Zygote to Implantation: Morphological and Molecular Dynamics during Embryo Development in the Pig. Reprod Domestic Anim **44**, 39-49

Olds, P.J., Stern, S., and Biggers, J.D. (1973) Chemical estimates of the RNA and DNA contents of the early mouse embryo. J Exp Zool **186**(1), 39-45

Palermo, G., Colombero, L., and Rosenwaks, Z. (1997) The human sperm centrosome is responsible for normal syngamy and early embryonic development. Rev Reprod **2**(1), 19-27

Papaioannou, V.E., and Ebert, K.M. (1988) The preimplantation pig embryo: cell number and allocation to trophectoderm and inner cell mass of the blastocyst in vivo and in vitro. Development **102**(4), 793-803

Paradis, F. (2009) Intra-follicular growth factors and preovulatory follicle development in the sow. PhD. Thesis, University of Alberta, Edmonton, Alberta

Perry, J.S., and Crombie, P.R. (1982) Ultrastructure of the uterine glands of the pig. J Anat **134**(Pt 2), 339-550

Perry, J.S., and Rowlands, I.W. (1962) Early Pregnancy in the Pig. J Reprod Fertil **4**(2), 175-188

Pharazyn, A., Foxcroft, G.R., and Aherne, F.X. (1991) Temporal relationship between plasma progesterone concentrations in the utero-ovarian and jugular veins during early pregnancy in the pig. Anim Reprod Sci **26**(3–4), 323-332

PigCHAMP (2011a) Canada 2011 year end summary. In 'PigCHAMP Benchmarking.')

PigCHAMP (2011b) USA 2011 year end summary. In 'PigCHAMP Benchmarking. Vol. 2012.')

Pikó, L. (1970) Synthesis of macromolecules in early mouse embryos cultured in vitro: RNA, DNA, and a polysaccharide component. Dev Biol **21**(1–2), 257-279

Polge, C. (Ed.) (1982) 'Embryo Transplantation and Preservation.' Control of Pig Reproduction (Butterworths: London)

Polge, C., Rowson, L.E.A., and Chang, M.C. (1966) The Effect Of Reducing The Number Of Embryos During Early Stages Of Gestation On The Maintenance Of Pregnancy In The Pig. J Reprod Fertil **12**(2), 395-397

Pope, C.E., and Day, B.N. (1972) Development Of Pig Embryos Following Restriction To The Ampullar Portion Of The Oviduct. J Reprod Fertil **31**(1), 135-138

Pope, W.F. (1988) Uterine asynchrony: a cause of embryonic loss. Biol Reprod **39**(5), 999-1003

Pope, W.F., Lawyer, M.S., Nara, B.S., and First, N.L. (1986) Effect of asynchronous superinduction on embryo survival and range of blastocyst development in swine. Biol Reprod **35**(1), 133-137

Pope, W.F., Maurer, R.R., and Stormshak, F. (1982) Survival of porcine embryos after asynchronous transfer (41495). Proc Soc Exp Biol Med **171**(2), 179-183

Pope, W.F., Xie, S., Broermann, D.M., and Nephew, K.P. (1990) Causes and consequences of early embryonic diversity in pigs. J Reprod Fertil Suppl **40**, 251-260

Powers, R.D., and Tupper, J.T. (1977) Developmental changes in membrane transport and permeability in the early mouse embryo. Dev Biol **56**(2), 306-315

Pratt, H.P.M. (1980) Phospholipid synthesis in the preimplantation mouse embryo. J Reprod Fertil **58**(1), 237-248

Pratt, H.P.M., Ziomek, C.A., Reeve, W.J.D., and Johnson, M.H. (1982) Compaction of the mouse embryo: an analysis of its components. JEEM **70**(1), 113-132

Qi, H., Moran, M.M., Navarro, B., Chong, J.A., Krapivinsky, G., Krapivinsky, L., Kirichok, Y., Ramsey, I.S., Quill, T.A., and Clapham, D.E. (2007) All four CatSper ion channel proteins are required for male fertility and sperm cell hyperactivated motility. PNAS **104**(4), 1219-1223

Quinn, P., and Wales, R.G. (1971) Adenosine Triphosphate Content Of Preimplantation Mouse Embryos. J Reprod Fertil **25**(1), 133-135

Ratto, M.H., Leduc, Y.A., Valderrama, X.P., van Straaten, K.E., Delbaere, L.T., Pierson, R.A., and Adams, G.P. (2012) The nerve of ovulation-inducing factor in semen. Proc Natl Acad Sci U S A **109**(37), 15042-15047Raynal, N.J., Si, J., Taby, R.F., Gharibyan, V., Ahmed, S., Jelinek, J., Estecio, M.R., and Issa, J.P. (2012) DNA methylation does not stably lock gene expression but instead serves as a molecular mark for gene silencing memory. Cancer Res **72**(5), 1170-1181

Razin, A., and Cedar, H. (1991) DNA methylation and gene expression. Microbiol Rev **55**(3), 451-458

Restall, B., and Wales, R. (1968) The Fallopian Tube of the Sheep. V. Secretion From the Ampullla and Isthmus. Aust J Biol Sci **21**(3), 491-498

Riethmacher, D., Brinkmann, V., and Birchmeier, C. (1995) A targeted mutation in the mouse E-cadherin gene results in defective preimplantation development. PNAS **92**(3), 855-859

Rizos, D., Ward, F., Duffy, P., Boland, M.P., and Lonergan, P. (2002) Consequences of bovine oocyte maturation, fertilization or early embryo development in vitro versus in vivo: Implications for blastocyst yield and blastocyst quality. Mol Reprod Dev **61**(2), 234-248

Roberts, C.J., and Lowe, C.R. (1975) Where have all the conceptions gone? Lancet **305**(7905), 498-499

Roberts, R.M., Chen, Y., Ezashi, T., and Walker, A.M. (2008) Interferons and the maternal-conceptus dialog in mammals. Semin Cell Dev Biol **19**(2), 170-177

Robertson, S.A., Mau, V.J., Tremellen, K.P., and Seamark, R.F. (1996) Role of high molecular weight seminal vesicle proteins in eliciting the uterine inflammatory response to semen in mice. J Reprod Fertil **107**(2), 265-277

Romek, M., Gajda, B., Krzysztofowicz, E., and Smorąg, Z. (2009) Lipid Content of Non-cultured and Cultured Pig Embryo. Reprod Domestic Anim **44**(1), 24-32

Rowson, L.E.A., Lawson, R.A.S., Moor, R.M., and Baker, A.A. (1972) Egg Transfer In The Cow: Synchronization Requirements. J Reprod Fertil **28**(3), 427-431

Rozeboom, K.J., Troedsson, M.H., Molitor, T.W., and Crabo, B.G. (1999) The effect of spermatozoa and seminal plasma on leukocyte migration into the uterus of gilts. J Anim Sci **77**(8), 2201-2206

Ryan, D.P., Prichard, J.F., Kopel, E., and Godke, R.A. (1993) Comparing early embryo mortality in dairy cows during hot and cool seasons of the year. Theriogenology **39**(3), 719-737

Santos, F., Hendrich, B., Reik, W., and Dean, W. (2002a) Dynamic Reprogramming of DNA Methylation in the Early Mouse Embryo. Dev Biol **241**(1), 172-182

Santos, F., Hendrich, B., Reik, W., and Dean, W. (2002b) Dynamic reprogramming of DNA methylation in the early mouse embryo. Dev Biol **241**(1), 172-182

Sarmento, O.F., Digilio, L.C., Wang, Y., Perlin, J., Herr, J.C., Allis, C.D., and Coonrod, S.A. (2004) Dynamic alterations of specific histone modifications during early murine development. J Cell Sci **117**(19), 4449-4459

Schlosnagle, D.C., Bazer, F.W., Tsibris, J.C.M., and Roberts, R.M. (1974) An Iron-containing Phosphatase Induced by Progesterone in the Uterine Fluids of Pigs. J Biol Chem **249**(23), 7574-7579

Schultz, R.M. (1993) Regulation of zygotic gene activation in the mouse. BioEssays **15**(8), 531-538

Sellens, M.H., Stein, S., and Sherman, M.I. (1981) Protein and free amino acid content in preimplantation mouse embryos and in blastocysts under various culture conditions. J Reprod Fertil **61**(2), 307-315

Senger, P.L. (1999) 'Pathways to pregnancy and parturition.' 1st rev. edn. (Current Conceptions: Pullman, WA) xiii, 281 p.

Shire, J.G.M., and Whitten, W.K. (1980) Genetic Variation in the Timing of First Cleavage in Mice: Effect of Maternal Genotype. Biol Reprod **23**(2), 369-376

Siegfried, Z., and Cedar, H. (1997) DNA methylation: a molecular lock. Curr Biol **7**(5), R305-307

Symonds, M.E., Stephenson, T., Gardner, D.S., and Budge, H. (2006) Long-term effects of nutritional programming of the embryo and fetus: mechanisms and critical windows. Reproduction, Fertility and Development **19**(1), 53-63Soede, N.M., Noordhuizen, J.P.T.M., and Kemp, B. (1992) The duration of ovulation in pigs, studied by transrectal ultrasonography, is not related to early embryonic diversity. Theriogenology **38**(4), 653-666

Spencer, T., and Bazer, F. (2004) Conceptus signals for establishment and maintenance of pregnancy. Reproductive Biology and Endocrinology **2**(1), 49

Stanchev, P., Rodriguez-Martinez, H., Edqvist, L.E., and Eriksson, H. (1985) Oestradiol and progesterone receptors in the pig oviduct during the oestrous cycle. J Steroid Biochem **22**(1), 115-120

Stein-Stefani, J., and Holtz, W. (1987) Surgical and endoscopic transfer of porcine embryos to different uterine sites. Theriogenology **27**(1), 278

Stroband, H.W., and Van der Lende, T. (1990) Embryonic and uterine development during early pregnancy in pigs. J Reprod Fertil Suppl **40**, 261-277

Strunker, T., Goodwin, N., Brenker, C., Kashikar, N.D., Weyand, I., Seifert, R., and Kaupp, U.B. (2011) The CatSper channel mediates progesterone-induced Ca2+ influx in human sperm. Nature **471**(7338), 382-386

Sturmey, R., and Leese, H. (2003) Energy metabolism in pig oocytes and early embryos. Reproduction **126**(2), 197-204

Sturmey, R.G., and Leese, H.J. (2008) Role Of Glucose And Fatty Acid Metabolism In Porcine Early Embryo Development. Reprod Fertil Dev **20**(1), 149-149

Sutovsky, P., Van Leyen, K., McCauley, T., Day, B.N., and Sutovsky, M. (2004) Degradation of paternal mitochondria after fertilization: implications for heteroplasmy, assisted reproductive technologies and mtDNA inheritance. Repro BioMed Online **8**(1), 24-33

Swain, J., Bormann, C., Clark, S., Walters, E., Wheeler, M., and Krisher, R. (2002) Use of energy substrates by various stage preimplantation pig embryos produced in vivo and in vitro. Reproduction **123**(2), 253-260

Tadros, W., and Lipshitz, H.D. (2009) The maternal-to-zygotic transition: a play in two acts. Development **136**(18), 3033-3042

Tarleton, B.J., Braden, T.D., Wiley, A.A., and Bartol, F.F. (2003) Estrogen-Induced Disruption of Neonatal Porcine Uterine Development Alters Adult Uterine Function. Biol Reprod **68**(4), 1387-1393

Taylor, U., Zerbe, H., Seyfert, H.-M., Rath, D., Baulain, U., Langner, K.F.A., and Schuberth, H.-J. (2009) Porcine spermatozoa inhibit post-breeding cytokine induction in uterine epithelial cells in vivo. Anim Reprod Sci **115**(1–4), 279-289

Telford, N.A., Watson, A.J., and Schultz, G.A. (1990) Transition from maternal to embryonic control in early mammalian development: a comparison of several species. Mol Reprod Dev **26**(1), 90-100

Thomson, J.L., and Brinster, R.L. (1966) Glycogen content of preimplantation mouse embryos. Anat Rec **155**(1), 97-102

Tománek, M., Kopečný, V., and Kaňka, J. (1989) Genome reactivaton in developing early pig embryos: an ultrastructural and autoradiographic analysis. Anat Embryol (Berl) **180**(3), 309-316

Town, S.C., Patterson, J.L., Pereira, C.Z., Gourley, G., and Foxcroft, G.R. (2005) Embryonic and fetal development in a commercial dam-line genotype. Anim Reprod Sci **85**(3-4), 301-316

Ulbrich, S.E., Kettler, A., and Einspanier, R. (2003) Expression and localization of estrogen receptor α, estrogen receptor β and progesterone receptor in the bovine oviduct in vivo and in vitro. J Steroid Biochem Mol Biol **84**(2–3), 279-289

Vallet, J.L., Christenson, R.K., Trout, W.E., and Klemcke, H.G. (1998) Conceptus, progesterone, and breed effects on uterine protein secretion in swine. J Anim Sci **76**(10), 2657-2670

Van Soom, A., Ysebaert, M.T., and de Kruif, A. (1997) Relationship between timing of development, morula morphology, and cell allocation to inner cell mass and trophectoderm in in vitro-produced bovine embryos. Mol Reprod Dev **47**(1), 47-56

Vander Heiden, M.G., Cantley, L.C., and Thompson, C.B. (2009) Understanding the Warburg effect: the metabolic requirements of cell proliferation. Science **324**(5930), 1029-1033

Vinsky, M.D., Novak, S., Dixon, W.T., Dyck, M.K., and Foxcroft, G.R. (2006) Nutritional restriction in lactating primiparous sows selectively affects female embryo survival and overall litter development. Reproduction, Fertility and Development **18**(3), 347-355

Vinsky, M.D., Paradis, F., Dixon, W.T., Dyck, M.K., and Foxcroft, G.R. (2007) Ontogeny of metabolic effects on embryonic development in lactating and weaned primiparous sows. Reproduction, Fertility and Development **19**(5), 603-611

Vitzthum, V.J., Spielvogel, H., Thornburg, J., and West, B. (2006) A prospective study of early pregnancy loss in humans. Fertil Steril **86**(2), 373-379

Waberski, D. (1997) Effects of semen components on ovulation and fertilization. J Reprod Fertil Suppl **52**, 105-109

Waddington, C.H. (1957) 'The strategy of the genes. A discussion of some aspects of theoretical biology.' (Allen & Unwin: London) 262

Wallenhorst, S., and Holtz, W. (1999) Transfer of pig embryos to different uterine sites. J Anim Sci **77**(9), 2327-2329

Wang, Q.T., Piotrowska, K., Ciemerych, M.A., Milenkovic, L., Scott, M.P., Davis, R.W., and Zernicka-Goetz, M. (2004) A Genome-Wide Study of Gene Activity Reveals Developmental Signaling Pathways in the Preimplantation Mouse Embryo. Dev Cell **6**(1), 133-144

Wang, W.H., Abeydeera, L.R., Cantley, T.C., and Day, B.N. (1997) Effects of oocyte maturation media on development of pig embryos produced by in vitro fertilization. J Reprod Fertil **111**(1), 101-118

Waterland, R.A., and Jirtle, R.L. (2003) Transposable Elements: Targets for Early Nutritional Effects on Epigenetic Gene Regulation. Mol Cell Biol **23**(15), 5293-5300

Watson, A.J., and Barcroft, L.C. (2001) Regulation of blastocyst formation. Front Biosci **6**, D708-730

Wilde, M.H., Xie, S., Day, M.L., and Pope, W.F. (1988) Survival of small and large littermate blastocysts in swine after synchronous and asynchronous transfer procedures. Theriogenology **30**(6), 1069-1074

Wilson, M.E., and Ford, S.P. (1997) Differences in trophectoderm mitotic rate and P450 17alpha-hydroxylase expression between late preimplantation Meishan and Yorkshire conceptuses. Biol Reprod **56**(2), 380-385

Wiseman, D.L., Henricks, D.M., Eberhardt, D.M., and Bridges, W.C. (1992) Identification and content of insulin-like growth factors in porcine oviductal fluid. Biol Reprod **47**(1), 126-132

Wolf, E., Arnold, G.J., Bauersachs, S., Beier, H.M., Blum, H., Einspanier, R., Frohlich, T., Herrler, A., Hiendleder, S., Kolle, S., Prelle, K., Reichenbach, H.D., Stojkovic, M., Wenigerkind, H., and Sinowatz, F. (2003) Embryo-maternal communication in bovine - strategies for deciphering a complex cross-talk. Reprod Domest Anim **38**(4), 276-289

Wollenhaupt, K., Kettler, A., Br, #252, ssow, K.-P., Schneider, F., Kanitz, W., and Einspanier, R. (2001) Regulation of the expression and bioactivation of the epidermal growth factor receptor system by estradiol in pig oviduct and endometrium. Reprod Fertil Dev **13**(3), 167-176

Wright Jr, R.W., Grammer, J., Bondioli, K., Kuzan, F., and Menino Jr, A. (1983) Protein content and volume of early porcine blastocysts. Anim Reprod Sci **5**(3), 207-212

Wu, S.C., and Zhang, Y. (2010) Active DNA demethylation: many roads lead to Rome. Nat Rev Mol Cell Biol **11**(9), 607-620

Xie, S., Broermann, D.M., Nephew, K.P., Ottobre, J.S., Day, M.L., and Pope, W.F. (1990) Changes in follicular endocrinology during final maturation of porcine oocytes. Domest Anim Endocrinol **7**(1), 75-82

Zimmer, H.-G. (2001) Pentose Phosphate Pathway. In 'eLS.' (John Wiley & Sons, Ltd)

Ziomek, C.A., and Johnson, M.H. (1980) Cell surface interaction induces polarization of mouse 8-cell blastomeres at compaction. Cell **21**(3), 935-942

Ziomek, C.A., and Johnson, M.H. (1982) The roles of phenotype and position in guiding the fate of 16-cell mouse blastomeres. Dev Biol **91**(2), 440-447

Zuccotti, M., Merico, V., Cecconi, S., Redi, C.A., and Garagna, S. (2011) What does it take to make a developmentally competent mammalian egg? Hum Reprod Update **17**(4), 525-540

Chapter 3: Temporal and Spatial Characterization of Hyaluronic Acid and Associated Transcriptional Activity During Early Embryo Development in the Porcine Uterus

Introduction

Fertilization and early embryonic development *in vivo* occurs within the active and dynamic environment of the female reproductive tract which is naturally tailored to the precise requirements of each developmental stage. As embryo based assisted reproductive technologies (ART's) are generally implemented prior to the hatching stage of development, an understanding of the specific components of the oviductal and uterine environments is vital for creating a milieu suitable for embryo development, manipulation, storage or transfer. Current *in vitro* culture systems for porcine embryos suffer from poor success rates, low quality and poor performance post transfer (Kikuchi *et al.* 1999). Furthermore, it has been shown that deviation in cell number and ratio (Machaty *et al.* 1998), as well as global transcriptome expression (Miles *et al.* 2008), are present as early as the blastocyst stage when compared to *in vivo* produced controls, suggesting current *in vitro* conditions are suboptimal. The development of non-surgical embryo transfer (NSET) techniques, which typically place embryos just past the cervix of the sow into the uterine body, have had minimal success when compared to surgical transfer which places embryos in a physiologically appropriate position. This difference is likely due to variance in the environment between the uterine body and the tip of the uterine horn. Currently however, little information exists regarding the key environmental components for embryo development or their temporal and spatial distribution within the porcine reproductive tract.

Additionally, current embryo transfer media utilize serum albumen (SA) which acts as a lubricant, osmotic regulator, energy source, viscosity agent and as a reservoir for hormones, vitamins and metals (Simon *et al.* 2003). In particular, both flushing and transfer media used in agricultural species normally contain SA derived from bovine sources (BSA). Blood derived serum products such as BSA are not only physiologically atypical in the embryo environment, but raise substantial concerns with regards to batch variability (Simon *et al.* 2003). Perhaps more importantly, as the ingredient originates from an animal source, its use in embryo transfer (ET) reduces the potential of this technology to move genetic material in a guaranteed pathogen free manner. The perceived risk of Bovine Spongiform Encephalopathy (BSE) in particular is expected to result in future regulatory intervention against the use of BSA in embryo culture and transfer media (Evans 1999).

The glycoaminoglycan, hyaluronic acid (HA), is a complex macromolecule consisting of repeating dimers of D-glucuronic acid and N-acetyl-D-glucosamine (Laurent and Fraser 1992). Expressed throughout the mammalian body, HA has been implicated in numerous physiological processes including cell proliferation (Itano *et al.* 2002), angiogenesis (Slevin *et al.* 2002) and cell locomotion (Turley *et al.* 1991). The structure and biology of HA is extremely variable, given it can range in size from four saccharides to 20 $x10^4$ Da (Kogan *et al.* 2007) and reside in the cytoplasm, as part of the pericellular coat or extracellular fluid (Weigel *et al.* 1997). Furthermore, its physiological role can vary, with high molecular weight HA acting in an antiangiogenic and immunosuppressive capacity and low molecular weight HA acting in an immune stimulator and angiogenic capacity (Kogan *et al.* 2007). The molecule is produced by a series of three functionally independent synthase proteins aptly named hyaluronic acid synthase (HAS) 1, 2 and 3. Each of these synthase enzymes produces HA in different size ranges, at different rates and favours either the formation of a pericellular coat or free HA (Itano *et al.* 1999). In addition, a number of receptors for HA have been

identified and characterized including CD44, the receptor for hyaluronic acid mediated motility (RHAMM) and hyaluronic acid receptor for endocytosis (HARE), with additional receptors likely yet to be identified (Barnes 2000).

The addition of HA to culture media has been shown to increase blastocyst formation rate in a number of species (Furnus *et al.* 1998; Gardner *et al.* 1999; Stojkovic *et al.* 1999), including swine (Miyano *et al.* 1994; Kano *et al.* 1998; Miyoshi *et al.* 1999). As well, the benefit of HA in embryo transfer media has been demonstrated in both murine (Gardner *et al.* 1999) and human (Simon *et al.* 2003; Friedler *et al.* 2007) transfer systems. Experiments with HA in porcine embryo culture media (Kano *et al.* 1998; Miyoshi *et al.* 1999) demonstrate that an optimal concentration of HA for a single stage embryo culture system exists. These culture systems, however, represent a compromised environment, where in, the optimal concentration of a single molecule is not representative of the typical physiological optimum. Furthermore, experiments examining the role of HA in *in vitro* embryo culture have relied on single sources of the molecule, representing only a limited range of molecular weight of the glycosaminoglycan (GAG). Therefore, little information exists with regards to how these *in vitro* values relate to the *in vivo* concentration of HA, or its true physiological structure or function.

Physiological concentration and composition of a variety of GAG's were measured by Lee and Ax (1984). This study concluded that the bovine oviduct and uterine fluid contained 9mg/100mg and 20mg/100mg protein, respectively (Lee and Ax 1984). Using values for total protein concentration in the bovine reproductive tract obtained from other literature, Kano *et al.* (1998) calculate the total GAG concentration in the oviduct and uterine fluid to be 0.1-0.47 mg/ml and 2.0-3.7 mg/ml, respectively Of which 38 and 15.7% is HA respectively (Lee and Ax 1984), making for a final HA concentration of 0.04-1.83mg/ml and 0.32-0.59mg/ml in the oviduct and uterus respectively. While these values have

in the past been erroneously cited as concentrations in the pig (Kim *et al.* 2005), a review of the literature reveals that no values for HA concentration in the porcine female reproductive tract have been reported for a period relevant to ET. Concentrations of HA have however been measured in the oviduct of the porcine tract immediately pre and post ovulation, and range between 2.2 and 6.7 mg/L (Tienthai *et al.* 2000).

In order to better understand the potential role of HA in porcine ART's it is necessary to first understand its normal physiological function and distribution. While the concentration and composition of uterine and oviductal GAG's have been determined in cattle (Lee and Ax 1984), to our knowledge, this is the first study to 1) establish the biological chemistry of HA during the period of embryo development to the blastocyst stage, 2) determine the degree to which HA influences temporal or spatial variation in the uterine and oviductal lumen and 3) evaluate the potential role for HA in communication between the reproductive tract of the sow and the pre-hatch embryo.

Materials and Methods

Animals

All procedures were conducted in accordance within Canadian Council on Animal Care guidelines and with the approval of the University of Alberta, Animal Care and Use Committee for Livestock (Protocol #2006-11C). A total of 22 primiparous Landrace X Large White sows (Hypor), were allocated from a lactation trial. Sows were ad libitum fed up to and including first post weaning estrus followed by 1.5 times maintenance feeding as calculated based on post estrus body weight and back fat. Starting 18 days after their first post-lactation estrus, animals were heat checked twice daily using fence line contact with mature boars. Following the onset of the second standing estrus animals were subject to ovarian exam by transcutaneous real-time ultrasonography at four hour intervals to determine timing of ovulation. Ovarian images were examined

for the presence of pre-ovulatory follicles and ovulation time reported as the midpoint between last detection of pre-ovulatory follicles and first detection of a corpara hemorrhagica. Based on the timing of ovulation, animals were allocated for euthanasia at times corresponding to two cell (2C), four cell (4C), 8-16 cell, early morula (EMor), Morula (Mor) and Blastocyst (Blast) stages of embryonic development. Animals were excluded from the study if more than one embryonic stage or degenerate embryos was found. Additional animals were allocated for collection at the pre-ovulatory Germinal Vesicle (GV) and Metaphase Two (MII) stages based on onset of standing estrus and the first signs of ovulation (as detected by ultrasound), respectively.

Sample Collection

Following euthanasia on site, the reproductive tracts were removed from the sows through a midline incision and severance of the cervix at the most caudal internal point. Tracts were moved to an adjacent dissection suite where the broad ligament was removed allowing a total length measurement of each uterine horn from the uterine bifurcation to the uterotubular junction. Each horn was then divided by ligature into three equal parts representing the posterior (BUT), Middle (MUT) and Anterior (TUT) section of the uterus. Each section was subsequently flushed with 20ml of warm PBS. In addition each oviduct was flushed in a similar manner using 5ml of warm PBS injected into the isthmus immediately above the uterotubular junction and collected via glass funnel inserted into the ampulla through the infundibulum. Embryos were isolated from each flush, imaged and staged by examination of the morphology by trained individuals using stereomicroscopy before flash freezing in microdroplets. Tissue samples were immediately collected from each uterine section as well as from the uterotubular junction (UTJ), ampulla (AMP), ampullary-ismic junction (AIJ) and isthmus (IST) and flash frozen in liquid nitrogen. All samples were then stored at -80 °C until required for analysis.

Hyaluronic Acid Quantification

Following isolation of embryos, flushes were centrifuged at 5000xg to remove cellular debris and then frozen in 3ml aliquots at -20 °C until analysis. Quantification of HA was performed using the Hyaluronic Acid Duo Kit (R&D systems) as per manufacturer's instructions and with the following additions. Samples were thawed on ice, inverted multiple times and then vortexed for 30 seconds to ensure equal distribution of HA throughout the flushings. Samples were then run in duplicate on high binding surface flat bottomed 96 well plates (Costar) and read at a final optical density of 450nm with wavelength correction at 570nm using a SpectraMax 190 plate reader (Molecular Devices) and values exported to excel for further analysis. Due to the different flushing volumes used for the oviduct and uterine sections, concentrations were converted to absolute quantities through multiplication with flushing volume (5ml for oviduct and 20ml for uterine segments).

Real Time Primer Design

TaqMan (ABI) primer probe sets for transcripts associated with each of the four genes of interest (HAS 1,2,3 and CD44) along with those of 3 potential housekeeping genes (18S, UBC and Cyclophyllin) were designed using Primer Express v3.0 software (ABI), based on sequence data obtained through GenBank or through sequencing (Table 1). Where porcine genomic sequence information was available, primers were designed such that the amplicon would span exon-exon junctions as identified by either Basic Local Alignment Search Tool (BLAST) or Blast Like Alignment Tool (BLAT). When porcine sequence information was unavailable, attempts were made to design primers to span exon-exon junctions conserved in human, mouse and rat. In the case of CD44, for which no information regarding transcript variants was available at the time, primers were designed to span the regions of known human and mouse transcript variance. These primers were used to amplify the region from a pool of porcine oviductal and uterine cDNA and separately in DNA from ocular tissue. The single resulting

band was isolated on a 2% w/v agarose gel using Sybr Safe (ABI), purified and sequenced from both ends using the Big Dye Direct Cycle Sanger Sequencing kit (ABI). Sequence data was collected by capillary electrophoresis using the 3700 DNA Sequencer Analyzer (ABI) and sequence data from each primer aligned such that overlapping sequence was accepted. The resulting sequence information was used to design the CD44 primer probe set to ensure all transcript variants were measured. Primer probe sets were further verified for dimer and hairpin formation using OligoAnalyser v3.1 (IDT) and amplicon specificity verified through genomic blast. Specificity of the primers for the target sequence was also verified using BLAST against the NCBI nt database. The PCR efficiency for each primer probe set was evaluated against a serial dilution of pooled samples, and found to be greater than 95% for all genes. Post-PCR specificity of primers was not assessed in this experiment, as hydrolysis probes require the ordered annealing of primers and probe. The probability of a non-target signal being produced by binding of the primer probe complex to a complimentary sequence by random chance in this experiment is in excess of one over four to the power of sixty or 1.33E+36.

Quantification of Uterine and Oviductal Gene Expression

Tissue samples from each segment of the right oviduct and uterine horn were ground to a fine powder under liquid nitrogen using a mortar and pestle pre-cooled to -80 °C. Total RNA was extracted from a 0.1 g subsample with Trizol reagent (Invitrogen) following the manufacturer's instructions with the following exceptions. Following initial re-suspension of the RNA pellet in 100 µl DEPC-treated water (Ambion), samples were precipitated a second time overnight at -20 °C with the addition of 10 µl 3M sodium acetate and 100 µl absolute ethanol. Following precipitation, samples were centrifuged at 15000g for 10 min, the supernatant was removed and the pellet washed twice with 1 ml of absolute ethanol, before final re-suspension in 100 µl DEPC-treated water. The total RNA in the samples was quantified using the spectrophotometer ND-1000

(NanoDrop), and 10 µg of total RNA was DNase treated using DNA free (Ambion) as per manufactures instructions with the following exceptions. Reaction volume was set at 20 µl including 1 µl rDNase1 and 1 µl RNaseOUT (Invitrogen). Total RNA was then re-quantified and the integrity of 2 µg RNA evaluated on a 1.2% (w/v) denaturing agarose gel containing 10 µl/100ml sybr Safe (Life Technologies). Samples were only used for reverse transcription if two clear bands representing 28s and 18s ribosomal RNA were visible at an equivalent intensity and migration point compared to the majority of samples.

Reverse transcription was carried out on 2 µg of total RNA using the High Capacity cDNA Reverse Transcription Kit (ABI) with RNase inhibitor as per manufacturer's instructions. Samples were then diluted in DEPC-treated water to 10 ng/µl equivalent cDNA for assay in duplicate at 20 ng per reaction. Real time PCR was carried out over 40 cycles using an ABI 7900HT thermocycler (ABI) in 96 well plates using the TaqMan fast universal mastermix (ABI). Reaction volume was 20 µl and contained 0.25 µl target probe and had a primer concentration of 10 mM per primer.

Embryonic Gene expression

Embryo RNA was extracted from pools of five similar stage embryos collected from a single donor animal. Extraction of total RNA was carried out using the PicoPure RNA isolation kit (Arcturus) following manufacturer's instructions. Due to the extremely low quantities of RNA in each pool of embryos, no quantification of embryonic RNA was attempted. The integrity of embryo RNA was assessed on 1 µl of the final elution, using RNA 6000 Pico Bio-Analyser Kit (Agilent) as per manufacturer's instructions. All samples had RNA integrity numbers (RIN) greater than 8.5 and the remaining RNA from each pool was used for reverse transcription using the High Capacity cDNA Reverse Transcription Kit (ABI) with RNase inhibitor as per manufacturer's instructions. The resulting cDNA was subsequently diluted in DEPC-treated water, to 0.125

embryo equivalent cDNA /µl. Real Time PCR was conducted as described above using 2 µl diluted cDNA or 0.25 embryo equivalents per reaction.

Western Blot Analysis of CD44 Protein

Additional tissue samples for the right oviductal AMP and IST and uterine TUT and BUT corresponding to the GV and Blast stages were ground to a fine powder under liquid nitrogen using a mortar and pestle pre-cooled to -80 °C. Total protein was extracted from 50 mg of tissue using a commercial cell extraction buffer (BioSource, Invitrogen) with the addition of P2714 protease inhibitor cocktail (Sigma). Following standard protein extraction procedures, total protein was quantified in the supernatant using BCA protein assay kit (Pierce) as per the manufacturer's protocol. A total of 120 µg of protein from each sample was resolved on a composite SDS PAGE gel consisting of a 5% w/v stacking gel and 8% w/v analytic gel. Protein extracted from pig lymph was used as a positive control (Binns and Pabst 1994) and inter-gel standard. Proteins were transferred to a nitrocellulose membrane at 30 V at 4°C for 16hrs. Membranes were temporarily stained with Ponceau (Life Technologies) and separated into two segments at 50-75 kDa. Each segment was incubated in 5% w/v skim milk in TBS for 2hrs to block non-specific binding. The segments of membrane containing high molecular weight proteins was then incubated for 2hrs in a solution of 0.5% w/v skim milk in TBS with 1:1000 dilution of rabbit anti human CD44 variant 7 polyclonal antibody (abcam: ab78469). The segment containing low molecular weight proteins was incubated for 2hrs in the same base solution only, with a 1:3000 dilution of rabbit anti human βactin polyclonal antibody (abcam: ab8227). Each segment was washed and then incubated in a 0.5% w/v skim milk in TBS solution containing a 1:3000 dilution of goat anti rabbit IgG polyclonal 2° antibody conjugated to horse radish peroxidase (abcam: ab6721) for 1hr. Segments were washed again and incubated in ECL Plus (Pierce) for 4 minutes prior to scanning on a Typhoon 9400 (GE Healthcare). Segmented images from the same gel were combined and cropped to the gel area and

analysed using the Image Quant Software (Amersham Biosciences). Built in rolling ball background correction was used and values normalized against porcine lymph βactin across gels.

Statistical Analysis

All data was checked for distribution normality and homoscedasticity prior to analysis using the Univariate procedure of SAS. Subsequent analysis was carried out using the General Linear Model (GLM) of SAS. Analysis of expression data obtained through Real Time PCR for each gene of interest was carried out on comparative critical threshold values ($\Delta CT=CT_{GOI}-C_{TEC}$) to account for variation in extraction, quantification and reverse transcription. Data normality was verified using the univariate procedure prior to analysis using the GLM of SAS. Fluidic HA quantities, as determined by ELISA, were analysed as the mean concentration of replicates. Uterine Real time Data is presented as $2^{-(\Delta\Delta CT)}$, where ΔΔCT is the difference between the mean sample ΔCT and the highest ΔCT value (lowest expression) for that gene. No suitable housekeeping gene could be identified for embryos between the 2cell and Blast stages Therefore to account for technical variation as well as variation in transcriptional activity a method similar to the residual covariate method used by Vallet *et al.* (2009) and Novak *et al.* (2012) was employed. This residual represents an estimate of the error in each measurement due to non-experimental factors. As this is only an estimate of error in each sample, accuracy improves with additional measurements. Therefore the average residual was calculated and used as a covariate in the GLM model of SAS. Fold changes in expression reported were calculated using the formula $2^{(\Delta CT1-\Delta CT2)}$, in the case of endometrial expression and $2^{(CT1-CT2)}$ in the case of embryonic expression.

Results

Hyaluronic Acid

Raw data from the HA specific ELISA was found to be abnormally distributed for the GV, 2cell, 4cell, Mor, and Blast stages, and required log normalization prior to analysis with the general linear model. A significant tempero-spatial interaction was identified in the log normalized HA ELISA data only when oviductal data were included in the analysis. However, when oviductal and uterine data was analysed separately no such tempero-spatial interaction was detected in the uterine data alone, suggesting the initially detected interaction was an artifact of the variation in tissue type and size between the oviduct and uterus rather than a biologically meaning full interaction. HA when analysed over time in all uterine segments combined, exhibited the most significant decrease from the GV to the 2cell stage ($P<0.001$). Following the 2cell stage, uterine total HA increased significantly ($P<0.001$) to the early Mor stage where it plateaued through to the blastocyst stage (Figure 3.1). Analysis of spatial differences within time points shows the HA in BUT segments to be consistently lower than both MUT and BUT, however no significant differences between uterine segments were identified likely owing to the large variance identified in the BUT samples (Figure 3.2). Separate analysis of oviductal HA content yielded no significant differences over time (Figure 3.3). Comparison of oviductal and total uterine HA content showed, as expected, significantly higher quantities in the uterus than oviduct.

Sequencing of CD44

A single band of approximately 650bp was detected in the pool of porcine oviductal and uterine cDNA. A similar band was identified in porcine ocular cDNA along with an additional band of 350bp (Figure 3.4a). The larger band from each well was extracted and sequenced in both directions. The corresponding sequence alignment against all currently known porcine CD44 transcript variants can be found in Figure 3.4b. The band identified in the pig reproductive tract

corresponds with XM_00003480710 with a single base pair mismatch at 684 on the published sequence. Given no larger sequences were amplified in the ocular cDNA this result does not preclude the existence of longer transcript variants which may not have amplified due to their length. As such, the primer-probe set for CD44 was designed at the 3' end of our segment which lay outside the region of transcript variance identified in the human and mouse at that time.

Oviductal and Uterine Gene Expression

Expression of all target genes was identified in both oviductal and uterine tissues and at all-time points assayed. Data from the oviductal and uterine samples were analysed separately in order to produce less complicated and more biologically relevant output. Data from the UTJ showed high variation and non-normal distribution, likely due to variation in the relative quantities of oviductal and uterine tissue taken during tissue collections. For this reason, as well as the fact that this tissue did not physically correspond to either the uterus or oviduct, gene expression data on the UTJ was removed from all subsequent analysis. Of the three potential housekeeping genes assayed 18s was found to be the most temporally ($P=0.1414$) and spatially ($P=0.8327$) stable. The stability of UBC was higher temporally ($P=0.3628$), however a trend toward spatial instability was identified ($P=0.0793$). In contrast, the analysis of cyclophilin expression was significantly affected by both time and space ($P<0.001$) and also showed a highly significant interaction between the two ($P=0.0008$). All subsequent analysis was therefore conducted using 18s as the sole housekeeping gene.

In both the oviduct and uterus, no significant interaction between time and space was observed therefore it was removed from the model and expression analysed for temporal and spatial effects separately. CD44 showed the highest overall expression in both tissue types, whereas HAS3 was the dominant synthase followed by HAS1 and finally HAS2. The sole spatial expression effects identified in this trial were for HAS2 and CD44 within the

oviduct with no significant effect observed in the uterus (Figure 3.5). For both genes, small but significant increases in expression level (less than 2.25 fold) were found in the IST when compared to the AMP or AIJ (Figure 3.5).

Temporal analysis on the other hand yielded unique profiles for each gene in both the oviductal and uterine samples. The oviductal expression pattern of HAS1 showed an initial increase between the GV and Emor stages of 2.2 fold (P=0.027), dropped 2-fold to the Mor stage and then recovered to near Emor level by the Blastocyst stage (Figure 3.6). Though slightly higher expression was observed, a nearly identical temporal pattern was seen with HAS1 in the uterus (Figure 3.7). The expression of HAS2 did not differ between the oviduct and uterus showing high initial expression at the GV stage and then dropping 4fold by the 2cell stage (P<0.001). Beyond the 2cell stage, expression of HAS2 was relatively stable increasing by 1.6 (P=0.003) and 2 (P<0.001) fold in the oviduct (Figure 3.6) and uterus (Figure 3.7) respectively. The expression pattern of HAS3 was relatively static in the oviduct with the highest expression at the GV stage and lowest at the morula stage (Figure 3.6). In contrast, the expression of HAS3 in the uterus was dynamic, increasing 2 fold between the GV to 4cell stages (P=0.01) and then decreasing 3.9 fold by the blastocyst stage (P<0.001) (Figure 3.7). In comparison, between oviductal and uterine samples expression of HAS3 was similar at the GV and Blastocyst stages; however expression was significantly higher in the uterus during the 2cell, 4cell and EMor stages. Analysis of total synthase expression over time, shows a relatively stable pattern with highest and lowest expression seen at the GV and morula stage, respectively. In the oviduct, expression of CD44 was stable between the GV and Blast stages (Figure 3.6), whereas expression in the uterus showed a gradual 3 fold decrease over the same time period (Figure 3.7). When compared between tissue types, CD44 expression was 5.9 fold higher in the uterus (P<0.001) than in the oviduct but by the Blast stage uterine expression had dropped to a level similar to that of the oviduct.

Embryonic Gene Expression

Of the three presumptive housekeeping genes assessed in this study only two, 18S and Cyclophilin, were found to be expressed in all embryonic stages, however both genes were found to be significantly affected by time ($P<0.001$). The expression pattern was similar ifor both genes, with minimal expression observed at the 4cell to Emor stages (Figure 3.8a). Correlation analysis of the residuals from each gene shows a strong inter relationship ($X^2=0.714$ $P=0.0028$) (Figure 3.8b). In order to account for technical variation in the measure of genes of interest, a modified form of the correction method originally published by Vallet *et al.* (2009) was used and all further results are based on this analysis.

Real time PCR analysis of embryonic transcripts from the 2cell to blastocyst stage identified the expression of HAS 1 and 3 as well as CD44 but failed to reliably amplify HAS2. HAS3 showed the highest embryonic expression followed by HAS1 and CD44, respectively. Expression of HAS1 showed a significant 77 fold decrease between the 2cell and Emor stages followed by a 60 fold increase to the blastocyst stage ($P<0.001$) (Figure 3.9a). Expression of HAS3 was high at the 2 cell stage, then decreased 97 fold ($P<0.001$) by the Emor stage where its expression plateaued at an almost undetectable level similar to the level of HAS1 observed at the Emor stage (Figure 3.9b). Embryonic expression of CD44 however showed no significant variation across embryo stages (Figure 3.9c).

Uterine and Oviductal Quantification of CD44 Protein

Non-specific binding was detected in total oviductal protein by Western blot, generating two additional bands at 25 and 50 kDa. These additional bands were presumed to be the light and heavy chains of porcine IgG. This was confirmed by running samples without a reducing agent, which resulted in a single non-specific band at >150kDa, and these bands were removed from subsequent analysis. Analysis of oviductal βactin showed no significant differences in either space ($P=0.951$) or time ($P=0.3676$) suggesting it is an ideal

control protein. Subsequent analysis of oviductal CD44 protein abundance found no significant effect of either space or time (Figure 3.10). When βactin was analysed in uterine samples, a trend was identified for both time (P=0.088) and space (P=0.053), bringing into question its validity as a housekeeping protein. When analysed in time by space or space by time these trends became significant in the TUT and Blast comparisons, respectively. For the sake of clarity, the data for uncorrected normalized volume (UNV) for CD44 and βactin are presented alongside the corrected normalized ratio (CNR) of CD44 to βactin in Figure 3.11. A significant temporal effect was observed for CD44 which decreases in the uterus between the GV and Blast stages in both UNV (P=0.008) and CNR (P=0.0165) data. It can be seen in Figure 3.10 that the trend observed in βactin only decreases the degree of significance between GV and Blast stages, supporting this as a legitimate result. An analysis of spatial effects, however, showed a significant effect only in the CNR data (P=0.0482) and a trend in the UNV data (P=0.0822). While this result is similar to that observed in the spatial analysis of uterine CD44 gene expression, it is unclear whether this is an artifact of the trend observed in βactin and will therefore be left out of future discussion.

Discussion

HA in the Oviductal and Uterine Environment

The concentration of total HA measured in the oviduct shows no temporal variation throughout the time points measured in this experiment. Interestingly, this stability was maintained over the time point where the oviduct was inhabited by the freshly ovulated cumulus-oocyte-complexes (COCs). The cumulus of the COC is known to exhibit HA synthesis and release as an integral part of the maturation process (Chen *et al.* 1990). Salustri *et al.* (1992) measured the HA synthesis capacity of ovulated cumulus complexes at about 11 ng/ COC. On average 14 COC's at the MII stage were collected from the animals flushed for this experiment. The small peak observed at this stage is therefore less than the quantity that could be attributed to the production of HA by the cumulus

cells. In addition, as follicular fluid is known to contain substantial quantities of HA (Sato *et al.* 1990; Suchanek *et al.* 1994) the apparent stability of oviductal HA content from the GV stage (pre-ovulation) to the blastocyst stage would suggest very little follicular fluid captured by the infundibulum enters the oviduct. This result is consistent with that of Hansen *et al.* (1991) who, through the measurement of hormone concentrations in follicular and oviductal fluid, calculated that the proportion of the oviductal milieu which results from follicular fluid released at ovulation is extremely small (0.04-0.51%) .

In contrast to the oviduct, this experiment shows a particularly dynamic HA profile in the uterus with two distinct peaks on either side of the 2cell stage (24hrs post ovulation). This temporal localization of HA would suggest it plays two distinct roles, one associated with the preovulatory period and another associated with later stage cleavage development. The most significant peak in uterine HA was observed at the GV stage, in samples taken from animals at a time point corresponding with the onset of standing estrus. Under natural conditions sows in standing estrus would be receptive to breeding, so it is likely this peak in HA corresponds with uterine preparation for insemination. Human sperm have been shown to possess the CD44 protein in their plasma membranes (Bains *et al.* 2002), which suggests they are susceptible to HA signalling. A product known as Sperm Select (Pharmacia AB) is an HA containing medium for the preparation of sperm prior to *in vitro* fertilization (IVF). Relative to control media the HA in Sperm Select improves numerous motility parameters in normal and compromised human sperm including total motility and velocity (Huszar *et al.* 1990; Sbracia *et al.* 1997). HA appears to induce improved sperm motility through an increase in intracellular Ca^{2+}, and this effect is abolished by the addition of antibodies against CD44 (Bains *et al.* 2001). In addition, treatment of capacitated sperm with HA has been shown to double the percentages which undergo the acrosome reactions in response to both progesterone and zona pellucida exposure, a response that appears to be mediated by the PH-20

proteins in the sperm plasma membrane (Sabeur *et al.* 1998). While neither CD44 nor PH-20 proteins have been characterized in pig sperm, the presence of a strong peak in HA during standing estrus would suggest HA may play an *in vivo* role in sperm function.

By the 2cell stage, uterine HA content decreased to its most minimal level, dropping from an average of over 600 ng to just 50 ng per uterine segment. Other biological reservoirs of HA in the body also exhibit rapid turnover, with a half-life in skin and joints of approximately twelve hours (Laurent and Fraser 1992). Given such high catabolism of HA in biological systems, Correa-Perez (2004) has questioned whether supplemental HA provided in transfer medium will remain in adequate quantities to effect changes in the post-hatching implantation period. Here we observe how rapidly HA content within the uterus can change at the early stage of embryonic development. This illustrates not only how dynamic the uterine environment is during the cleavage stages of development, but also how temporally specific any *in vivo* application of HA to ART's would have to be.

Following the 2cell stage, uterine HA content begins to rapidly increase to the Emor stage where the rate of increase slows, and once over 250 ng per uterine segment. Uterine histotroph production of 2.9 ml/day during diestrus has been previously reported for swine (Iritani *et al.* 1974). This measurement was made using a surgical catheterization model, which continually removed the histotroph from the lumen to an externally affixed tube. This constant HA elimination likely triggered a homeostatic mechanism which would have replaced the lost fluid. As a result, this value cannot be considered a reliable quantification of the physiological norm. If however, in the absence of any other reported value, the daily production of 2.9 ml is used as a maximum value for uterine histotroph, this would result in a predicted concentration of 259 ng/ml.

A study by Gardner *et al.* (1999) demonstrated the potential benefits of utilizing HA in both the culture and transfer media for mouse embryos. In an initial experiment the effects of HA in culture media were examined against BSA, PVA (polyvinyl alcohol), Dextran and a macromolecule free media. Embryos were collected from equine (eCG) and human (hCG) chorionic gonadotropin induced mice, denuded, washed and subsequently cultured in media containing the different macromolecules for 96 hours. Blastocyst formation rates and cell numbers were similar for concentrations of HA between 0.125-2.0 and 0.125-1.0 mg/ml respectively to BSA supplemented media. However at concentrations greater than 1.0 mg/ml, embryo cell number was significantly decreased and at 2.0 mg/ml blastocyst formation rates were significantly reduced. This result would suggest that optimization of HA concentration in media is required in order to avoid a negative impact on embryo development. As well, embryos cultured in the previously mentioned macromolecules, and combinations thereof, were transferred to recipient females and the resulting implantation and development rates determined. The results of this experiment showed that HA or a combination of HA and BSA resulted in the highest implantation rates. A similar synergistic relationship between HA and BSA was noted for *in vitro* produced porcine embryo in culture by Miyano *et al.* (1994). Finally embryos previously cultured in the absence of macromolecules were transferred in media either with or without 0.5 mg/ml HA as the sole macromolecule, following a five minute incubation period (Gardner *et al.* 1999). The resulting implantation and fetal development rates were significantly higher in transfers incorporating HA. However, as BSA was not included as a control, the observed advantage could be the general result of including a proteinaceous macromolecule rather than the result of HA specifically (Gardner *et al.* 1999).

Based on its physio-chemical nature Friedler *et al.* (2007) hypothesised that HA may improve embryo-endometrial interactions during the early phases of implantation. The physical structure and biological function of HA offers a

number of advantages over BSA as a protein supplement to embryo cultures and transfer media. Firstly, the hydrated gel formed by HA has been shown to promote expansion of extracellular spaces, cell migration, metastasis, and angiogenesis (Comper and Laurent 1978). Secondly, it has been suggested that the interaction between HA and its associated receptors are involved in migration, cell proliferation, maturation, adhesion, protein phosphorylation and development of gametes and uterine environments (Tienthai *et al.* 2003b).

Despite the substantial length of the porcine uterine horns, no spatial variation in uterine HA quantity was detected in this trial. This result suggests that HA is not primarily responsible for the reduction in embryo survival observed by Wallenhorst and Holtz (1999) resulting from embryo transfer into regions further away from the utero-tubal junction. Regardless of whether HA contributes to uterine spatial variation, the temporal increase in HA during formation of the morula and blastocyst would suggest that it still plays a vital role in early embryo development. In addition to the beneficial effects observed in embryo culture systems, HA has also proven to be effective at increasing pregnancy rates when included in transfer media. Murine embryos cultured in the absence of macromolecules and subsequently transferred in media either with or without 0.5 mg/ml HA as the sole macromolecule, had improved implantation and fetal development rates (Gardner *et al.* 1999). In a study published in 2003, Simon *et al.* replaced a synthetic serum substitute (SSS) with HA in human embryo transfer media. Despite slight improvements with HA, the study failed to find a significant difference between SSS and HA with regards to implantation, pregnancy or birth rate. However, when patients with a history of multiple implantation failure (>4) were selected for a similar trial using a commercial HA enriched transfer medium (EmbryoGlue®, Vitrolife USA), there was a statistically significant increase in clinical pregnancy rate when compared to controls (10 vs 35.2%) (Friedler *et al.* 2007). While it is possible the conflicting results of these two experiments are due to differences in control medium, SSS

versus human tubal fluid, the observed effect of sample population should not be disregarded. In fact, the differences encountered between these two studies mirror that of another human ET trial where no significant effect of HA was found in the sample population as a whole, but a beneficial effect of HA became evident when data from a sub-population was analysed. The sub-population represented individuals with past histories of failed ET due to tubal factors (Valojerdi *et al.* 2006).

If spatial variation in uterine HA is absent in the bicornuate uterus of the pig, one would assume that it is likely absent from the simplex uterus found in humans. It therefore remains unclear by what mechanism HA is able to improve embryo transfer outcomes in low fertility patient populations. Fraser *et al.* (1997) points out that the non-ideal osmotic properties and fully ionized carboxyl groups of HA at extracellular pH allow it to produce profound effects in water movement and distribution (Fraser *et al.* 1997). Moreover, Gardner *et al.* (1999) suggested that addition of HA to transfer media may improve diffusion of the media, and thereby embryos, into the viscous endometrial fluid. This assertion is based on the idea that HA supplemented media is itself inherently more viscous than BSA supplemented media (Gardner *et al.* 1999). The previously mentioned study by Valojerdi *et al.* (2006) found a lower pregnancy rate (though not statistically significant) for patients suffering from ovarian, idiopathic and multiple factor ET failure, regardless of transfer media. Citing Gardner *et al.* (1999), the authors suggested that the uterine fluid found in these patients may be too viscous for dispersal, even with the addition of HA. Though not fully understood, a lack of diffusion of the embryos into the endometrial fluid of the recipient could result in the formation of a micro-environment around the embryos that prevented the establishment of maternal embryonic communication. As ET disrupts the natural onset of communication between the embryo and uterus, establishment of the cross-talk would be of critical importance, particularly in low fertility recipients.

Although the flushing methodology employed for this experiment involved the manual stripping of flushing fluid along the uterine segments, it is unclear how much of the HA associated with luminal epithelial pericellular coat was dissolved in the flushes. Anecdotally, our experiences with purified high molecular weight HA, suggest it is poorly soluble in aqueous solutions even at physiological temperature and under continual vortex. Higher molecular weight HA appears to favour the formation of a thick globular gel, which requires protracted amounts of time to dissolve. It is therefore unlikely that the flushing methodology was able to solubilize pericellular coat HA for quantification in the ELISA. HA contained within the extracellular coat, may form a protective barrier against immune cells (Fraser *et al.* 1997), which are moved toward the endometrium and lumen during normal insemination. In addition, once the embryo has shed its zona pellucida, HA in the pericellular coat of the uterine epithelium may play a role in juxtacrine signaling. While the pool of HA contained in the pericellular coat is unlikely to play a key role in cleavage stage development, additional work in this area is required to complete the understanding of HA role during this period.

HA Associated Activity in the Oviduct and Uterus

All four genes of interest (HAS1, HAS2, HAS3 and CD44) were successfully amplified in both uterine and oviductal tissue segments and at each time point assayed. This is consistent with previous research (Tienthai *et al.* 2003b), except in the case of HAS2 which has previously gone undetected in the oviduct (Tienthai *et al.* 2003a). The amplification of HAS2 in reproductive tissues also contradicts the results of Spicer and McDonald (1998) which suggested that in the human, HAS2 expression was largely limited to cardiac and intestinal tissue (Spicer and McDonald 1998). This analysis was, however, conducted using northern blots which are significantly less sensitive than the Real Time PCR used in the present study. The universal expression of all three HAS genes, as well as

the primary receptor CD44, supports a significant role for HA in the physiology of the reproductive tract during early development.

As previously mentioned, the synthesis of HA is carried out by a family of three trans-membrane proteins known as Hyaluronic Acid Synthases, (HAS 1,2 and 3). Each of these synthases contains a domain capable of joining alternating D-glucuronic acid and D-N-acetylglucosamine sugars into a non-branching molecule. It has been suggested that synthesis of HA occurs through continual addition of sugar molecules to the reducing end of the polymer with the opposing end being extruded directly into the extracellular space (Salustri *et al.* 1999). This unique mode of biosynthesis allows for unconstrained spatial growth of the polymer which permits the polymer to reach extraordinary lengths (Weigel *et al.* 1997). The functional nature of the HAS family is important, as it not only allows for release of free HA into the extracellular fluid but also the addition of HA to the pericellular coat.

The three gene products of the HAS family share 51-71 percent sequence homology despite being located on distinct chromosomes (Spicer and McDonald 1998). The partial sequences for porcine HAS 2 shows 74 and 80.4 percent homology with mouse and human sequences and porcine HAS 3 shows greater than 90 percent homology with both mouse and human sequences (Kimura *et al.* 2002). Based on the location of each HAS isozyme on a different chromosome and prolific nature of these genes throughout the vertebrate class, Weigel *et al*. (1997) suggests that the duplication of this gene occurred early in vertebrate evolution. In spite of their common origin, Spicer and McDonald (1998) were able to demonstrate that temporal and spatial expression of HAS isozymes is variable and dependant on cell type, developmental stage and species. Our transcriptomic analysis of the HAS family in oviductal and uterine tissue has identified similar temporal and spatial variation. The only significant spatial variation was identified in the oviduct for HAS2 with higher expression measured

in the IST relative to the AIJ and AMP (Figure 3.5). Compared to the complex projections in the aglandular submucosa of the AMP, the IST is fairly smooth and contains a thicker myometrium layer. Increased expression of HAS2 in RNA isolated from the whole IST is surprising given, the relative surface area of the luminal epithelium and the quantity of myometrial tissue compared to the AMP.

Previous research has shown that the three forms of HAS are not functionally equivalent (Spicer and McDonald 1998; Itano *et al.* 1999). To evaluate functional differences between the three isozymes of HAS, Itano *et al.* (1999) transfected COS and Rat 3Y1 cells with each of the HA synthase genes. Upon transfection, all three HAS cell lines were capable of forming pericellular HA coats and carrying out biosynthesis of HA. This contradicts previous research which showed that while HA1 was able to synthesize HA, it did not form a pericellular coat (Spicer and McDonald 1998). Itano *et al.* (1999) did however report a significantly diminished HA coat for the HAS1 transfectants, and suggest that diminished coat thickness is the result of a higher K_m value for this particular isozyme. However, HAS 1 and 2 together were shown to have significantly higher elongation rates (1256 and 1014 monosacarides/min respectively) when compared to HAS 3 (174 monosacarides/min) (Itano *et al.* 1999). Perhaps most importantly, the molecular mass of HA produced by each isozyme was variable, with HAS 2 producing the largest polymers at 4×10^6 compared to HAS 1 and 3 which fashioned products with a molecular mass of 2.5×10^6 and 2.5×10^5, respectively (Itano *et al.* 1999).

If the temporal expression profiles of HAS genes are examined between the oviduct and uterus (Figure 3.6 and 4.6 A-C), it is clear those of HAS1 and HAS2 follow a near identical pattern. The expression profile of HAS3 on the other hand varies substantially between the two tissue types with a peak expression in the uterus at the 4cell stage while expression in the oviduct remained relatively stable after ovulation. A study by Guo *et al.* (2006) examined

the temporal expression of the HAS family in bovine ocular keratocytes in response to the stimulatory effect of transforming growth factor beta (TGFβ). Real time reverse transcriptase PCR results showed peak expression of HAS 1 and 2 mRNA within four to six hours and falling back to basal levels by seventy two hours. In contrast, HAS 3 showed no response to treatment and remained at basal levels throughout the experiment (Guo *et al.* 2007). Yamada *et al.* (2004) showed a differential HAS transcriptional response to interleukin 1β (IL1β) and epidermal growth factor (EGF) in cells of the human oral mucosa and skin (Yamada *et al.* 2004). Together these results suggest that regulation of HAS is not only variable between isoforms, but also across tissues. Data from the present study appears to show that different systems are regulating each of the HAS genes in the reproductive tract of the sow with the mechanisms controlling HAS1 and HAS2 being universal between the uterus and oviduct, while regulation of HAS3 is more tissue specific.

Based on relative CT values, HAS3 transcript is the most abundant in both the oviduct and uterus, followed by HAS1 and then HAS2. If HAS3 is the most abundantly transcribed synthase in the reproductive tract, the results of Itano *et al.* (1999) would suggest a preference for lower molecular weight HA. One must keep in mind that post transcriptional as well as translational regulation means these PCR results are not directly related to protein abundance or enzymatic activity. The type of relative data generated in this experiment is not able to truly support a cause and effect relationship between any single synthase and HA quantity. However, the GV stage peak in uterine HA coincides with a peak expression of HAS2 in both the oviduct and uterus

Expression of CD44 was found to be temporally stable in the oviduct, but a significant spatial variation was identified, with greater expression in the IST than AMP or AIJ. This spatial variation was also seen in oviductal HAS2, which may suggest that HA plays a role in autocrine signaling in the IST. Such pathways

have been previously suggested in non-reproductive tissues (Ishida *et al.* 1997) and in relation to cancer (Ahrens *et al.* 2001). It should be noted that while Western blot analysis of oviductal CD44 confirmed a lack of temporal variation, it also failed to confirm the spatial variation between oviductal segments. Tienthai *et al.* (2003) showed the presence of CD44 in the porcine oviduct through immunohistochemistry from 8 hours before ovulation to 8 hours following and reported no obvious change. The same study also demonstrated that CD44 expression in the oviduct increased in response to insemination relative to non-inseminated controls (Tienthai *et al.* 2003b). However, in the present study, there was no difference between the GV stage samples (non-inseminated) and the remaining time points including the 2cell stage (24hrs post-insemination).

In the uterus, CD44 expression was highest at the GV stage, and steadily decreased 3-fold at the Blast stage (Figure 3.7). This pattern was also reflected in the protein abundance of CD44 which was significantly reduced between the GV and Blast samples, further validating transcriptomic analysis through real time PCR for CD44 in the uterus. Together the results for CD44 transcript and protein abundance would suggest that hyaluronic acid receptivity in the uterus is decreasing at later stages of cleavage development. However, during this time uterine HA content is increasing, which if not for signaling within the uterus, is likely aimed at the affecting the embryo.

HA Associated Activity in the Embryo

Quantification of any particular mRNA in the embryo, at least during the early stages, is not necessarily the result of transcription. Inheritance of maternal mRNA via the oocyte cytoplasm provides the embryo with transcripts necessary to support the initial embryonic cleavages. In the mouse, maternal mRNA storage in the oocyte is thought to constitute as much as 38% of the known protein coding genes (Wang *et al.* 2004). With such substantial stores of maternal mRNA it is difficult to isolate embryonic transcript abundance due to inheritance from that of expression. The maternal mRNA is thought to be

removed in two waves. The first wave removes transcripts not otherwise expressed in the early embryo and is independent of zygotic genome activation (Alizadeh *et al.* 2005). The second wave appears to require embryonic transcription and removes transcripts which are almost immediately replaced by those of zygotic origin and are necessary for development (Anderson *et al.* 2001).

To allow for ontogenetic analysis of real time PCR data in this trial, real time PCR was run using embryo equivalents. As expected, analysis of previously reported somatic (Paradis *et al.* 2009) and germ cell (Kuijk *et al.* 2007) endogenous control genes failed to yield a suitable reference gene for the embryos collected in this trial. Both control genes which successfully amplified in the embryo show a parabolic expression pattern in which abundance reaches a minimal state at the early morula stage. This particular expression pattern is consistent with the known pattern of maternally inherited transcripts being selectively removed and subsequently replaced through transcription from the embryonic genome. Taking advantage of this temporal pattern, the residuals of 18s and cyclophilin (Figure 3.8B) were used to normalize embryonic real time data. The correlation between the expression profile of 18s and cyclophilin (Figure 3.8A) was highly significant (X^2=0.714 P=0.0028) which further validates the use of their combined residuals to correct for technical variation in the real time PCR measurement.

Of the four genes of interest assayed in the embryo, only one, HAS2, failed to amplify to a level acceptable for reliable quantification (CT<40). Of the two remaining synthases, HAS 3 amplified earliest with CT values ranging from 26 to 35 whereas HAS1 amplified to threshold in the range of 31 to 38 cycles suggesting HAS3 is expressed at a substantially greater level in the embryo. The transcript abundance profile of HAS 3 shows a sharp drop off from the 2 cell stage to the early morula stage at which point it remains low (Figure 3.9B). This

profile is consistent with the initial wave of maternal transcript removal suggested by Alizadeh *et al.* (2005), suggesting that HAS3 is not an important factor in the later stages of embryonic development (Alizadeh *et al.* 2005). The transcript abundance profile of HAS1 on the other hand shows the characteristic decrease in abundance to the early morula stage, but this is followed by a sharp increase to the blastocyst stage. The profile of HAS1 is similar to the second wave of maternal transcript degradation, and it is likely that HAS1 plays a substantial role in subsequent development of the embryo.

In mice the HAS2 knockout (-/-) genotype is embryonically lethal at day 9.5-10 (Camenisch *et al.* 2000) and is therefore only viable using a conditional knockout system (Kobayashi *et al.* 2010). However, homozygous knockouts of either HAS1 (Kobayashi *et al.* 2010) or HAS3 (Bai *et al.* 2005) produce viable offspring. Our results in the pig suggest that HAS1 plays the most significant role in embryo development, while HAS3 likely plays a more important role in oocyte maturation or fertilization. This is consistent with the previous results, which showed HAS3 present in the porcine oocyte while HAS2 is found only in the cumulus cells (Kimura *et al.* 2002). In addition, the HAS2 primer probe set amplified uterine and oviductal transcripts in this experiment, and reliably amplified transcripts in a global library, which included ovarian tissue. As yet there are no known transcript variants published for HAS2 in human, mouse or pig so it is unlikely that an embryo specific variant undetectable by our primer probe set exists. One alternative transcript, a natural antisense RNA to HAS2, known as either HAS2na or HAS2as, has however been identified in the mouse and human (Chao and Spicer 2005). This RNA has two known transcript variants both of which contain complimentary sequences to a portion of the first exon of HAS2, with the remaining portion lying in either the first intron, or the upstream region of the gene in mice and humans respectively. As exon 1 contains only non-coding sequence, and our primer probe set was designed specifically for the coding region, it is not possible for our probe to have detected HAS2as.

Functional analysis of HAS2as conducted by Chao and Spicer (2005) showed that cells transfected with either transcript variant in an inducible vector were able to reduce HAS2 expression by over 80% (Chao and Spicer 2005). Interestingly, a BLAT search of the human HAS2as sequence against build 9.2 of the pig genome identifies a significant match (981bp with 89% similarity) on chromosome 4, partially overlapping the first exon of the porcine HAS2 gene that has been previously sequenced. Given the presence of this similar sequence in the pig, it is possible that HAS2 is being expressed in the early embryo, but its transcript is being otherwise reduced by HAS2as. Additional experiments would be necessary to sequence HAS2as and subsequently measure its abundance in the early embryo to take this hypothesis any further.

The receptor CD44 has been identified in *in vitro* matured porcine cumulus cells (Yokoo *et al.* 2007) and has further been identified in all pre-implantation stage porcine embryos produced through *in vitro* maturation and fertilization (Kim *et al.* 2005). Quantification of CD44 showed an unexpectedly stable profile between the 2cell and Blast stages, with no apparent drop in quantity during the MZT (Figure 3.9C). It should be noted that CT values for CD44 were near the limits of detection by our real time PCR methodology. Currently, there are six known porcine transcript variants of CD44 and the primer probe set used in the present study was designed to target a region common to all of these. Similarly in humans, CD44 has eight known transcript variants, only one of which (CD44tv5, NM_001001392) does not contain the sequence targeted by our primer probe set. The embryonic CD44 profile measured in this trial (Figure 3.9 C) therefore likely represents global CD44 transcript abundance. As such, it is a distinct possibility that in an effort to measure total transcript abundance we failed to assess a shift in variant type within the CD44 population. It is important to note that the binding affinity of CD44 for HA has been shown to vary substantially between at least two variants (Peach *et al.* 1993). As a result the approach described in this study, which focused on total CD44 abundance,

may have missed an important part of HA receptor physiology. CD44 has been previously identified in all stages between the cumulus oocyte complex and the blastocyst using a non-quantitative PCR method (Kim *et al.* 2005). The primers used by Kim *et al.* (2005) also span the currently known region of transcript variance in porcine CD44. However, when the PCR product was run on a gel only a single band was identified, which corresponds in size to only one transcript variant (XM_003480710.1). Therefore, it is unlikely that any important variant shift occurs during development.

The receptor for hyaluronic acid mediated motility (RHAMM) is an additional receptor found in both intercellular and membrane bound domains and has two possible sites for binding HA. Interactions between HA and RHAMM may play a role in the modulation of protein kinases that modulate cellular behaviour (Schoenfelder and Einspanier 2003). Stojkovic *et al.* (2003) suggest that RHAMM may play a role in reorganization of the blastomere during embryonic development. The mRNA specific to the RHAMM protein has been identified in *in vitro* matured bovine COC's and has been shown to vary with time (Schoenfelder and Einspanier 2003). Furthermore, the RHAMM mRNA has been isolated from all zona bound stages of bovine embryos, with levels diminishing from the 2cell to 16 cell stage and then spiking in morula and blastocysts (Stojkovic *et al.* 2003). Immunohistochemistry showed expression of RHAMM in both the trophectoderm and inner cellular mass (ICM) of bovine embryos with the most prevalent staining between 8cell and morula stages. When real time primers were designed for this experiment, insufficient sequence information had been published for porcine RHAMM or chromosome 16 where it resides. Following publication of the full porcine genome a computational prediction of the RHAMM gene sequence was published by Ensemble (ENSSSCG00000017022) and a long (1800+ bp) clone was identified in the ovary and published online later that year (NCBI: AK395606). As of yet, no information exists regarding either transcript or protein abundance of RHAMM in porcine embryos, and

additional work in this area will be required to understand the potential role of HA in maternal embryonic signaling.

Conclusions

The results of this study clearly demonstrate the complex nature of hyaluronic acid physiology within the reproductive tract of the pig up to the blastocyst stage of embryonic development. To our knowledge this is the first study to characterize the HA content of uterine histotroph in the pig at a physiological time point relevant to *in vitro* culture. Even so, the distinct expression patterns of each HAS isoform and, in particular, differences in HAS3 expression between oviductal and uterine tissue, raise questions regarding the regulatory mechanisms at play. Furthermore, two additional segments of reproductive HA physiology remain uncharacterized including the HA content in the pericellular coat of the luminal epithelium as well as an accurate measure of the molecular weight of HA. However, the results of this experiment support a role for HA in both fertilization, and later stage cleavage development. Despite stable expression of CD44 in the embryo, the pattern of expression observed for HAS1 suggests HA plays an important role in embryonic development. Up-regulation in uterine HA coupled with decreased uterine sensitivity suggest that the production is directed toward supporting embryonic development. Finally, the lack of spatial variation observed in uterine HA or HA associated gene expression, suggests HA is not responsible for the suboptimal environment encountered in the caudal segments of the uterine horn.

Tables

Gene	Accession Number	Primer	Sequence (5'-3')/ Assay ID	Amplicon Size	Annealing Temperature
18S	**AY265350**	Forward	GGGTCGGGAGTGGGTAATTT	**60**	**60**
		Reverse	GAGAAACGGCTACCACATCCA		
		Probe	CCT GCT GCC TTC C		
HAS1	**NM_001136212**	Forward	TGGGTGGCCTTCAACGT	**60**	**61**
		Reverse	GATGCAGGACACACAGTGGAA		
		Probe	AGCGGGCTTGTCAGA		
HAS2	**NM_214053**	Forward	TGGGACGAAGTGTGGATTATG	**62**	**58**
		Reverse	TGAGGCAGGGTCAAGCAT		
		Probe	ACAGGTTTGTGATTCAGAC		
HAS3	**NM_001001268**	Forward	GGACTAAGTACACAGCACGCTCTAAA	**63**	**59**
		Reverse	GCCACCGGAGGTACTTGGT		
		Probe	CCTCACAGAGACCC		
CD44	**Sequenced**	Forward	CAACCTCTGGTCCTATACGGAAA		**60**
		Reverse	AAGGGACGCCAGGATGATC		
		Probe	TCAAATTCCAGAATGGC		
Cyclophilin	**AY266299**	Forward	AATGCTGGCCCCAACACA	**56**	**60**
		Reverse	TCAGTCTTGGCAGTGCAAATG		
		Probe	ACGGTTCCCAGTTTT		

Table 3.1: Details of primer probe sets used for real time PCR.

Figures

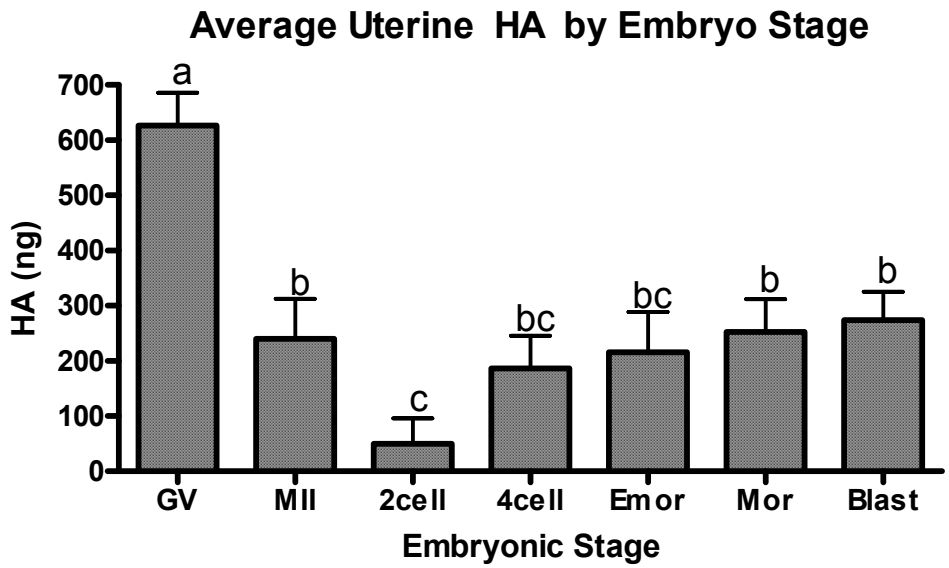

Figure 3.1: Quantification by ELISA of the total uterine HA over time points corresponding to the oocyte stages of GV (n=3x3) and MII (n=2x3) or embryonic stages of 2cell (n=5x3), 4cell (n=3x3), Emor (n=2x3), Mor (n=3x3) and Blast (n=4x3). Reported as un-normalized values with error bars representing standard error of the mean. Different letters represent significant differences ($p<0.05$) identified in log normalized data.

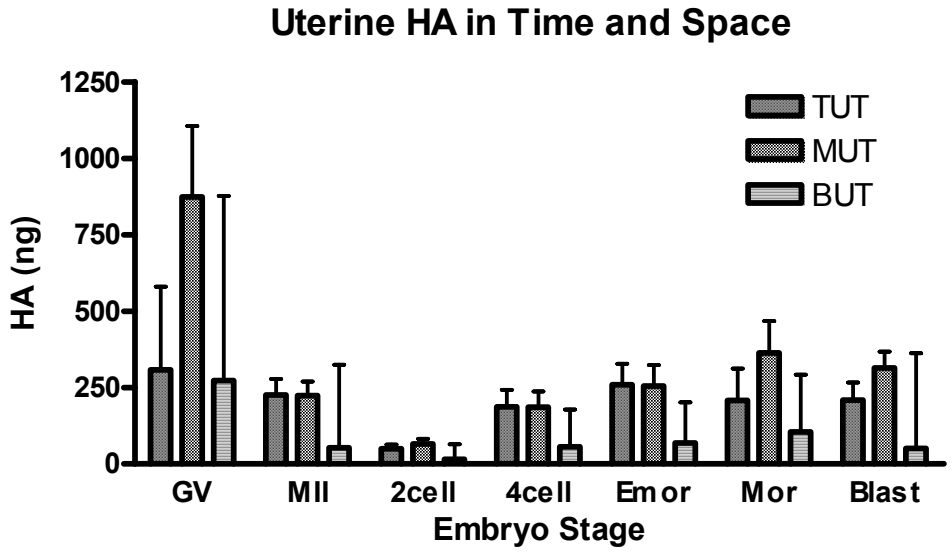

Figure 3.2: Quantification by ELISA of total uterine HA content in each segment analysed within time points corresponding to the oocyte stages of GV (n=3) and MII (n=2) or Embryonic stages of 2cell (n=5), 4cell (n=3), Emor (n=2), Mor (n=3) and Blast (n=4), reported as un-normalized values with error bars representing standard error of the mean. Statistical analysis of log normalized values found no differences between segments within time points.

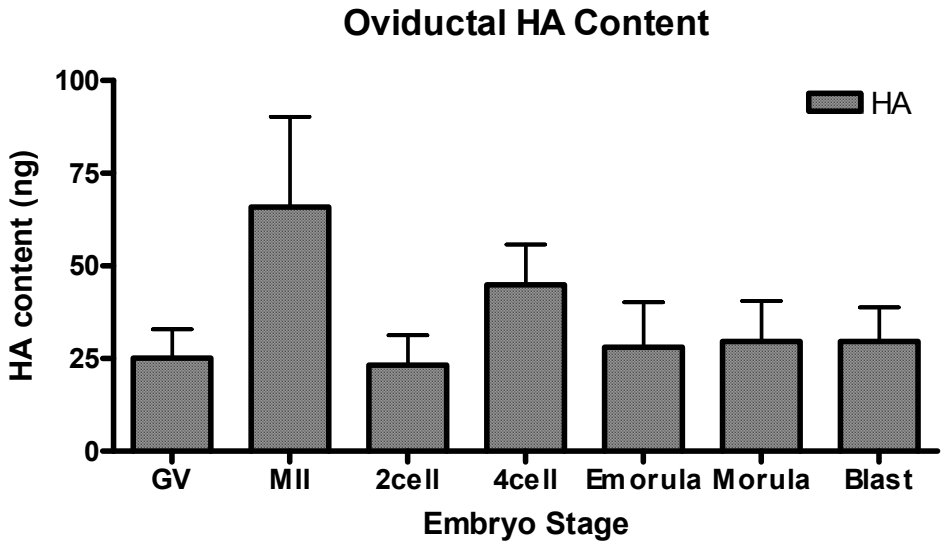

Figure 3.3: Quantification by ELISA of oviductal HA at time points corresponding to the oocyte stages of GV (n=3) and MII (n=2) or Embryonic 2cell (n=5), 4cell (n=3), Emor (n=2), Mor (n=3) and Blast (n=4) stages, reported as un-normalized values with error bars representing standard error of the mean. Statistical analysis of log normalized values found no difference over this time course.

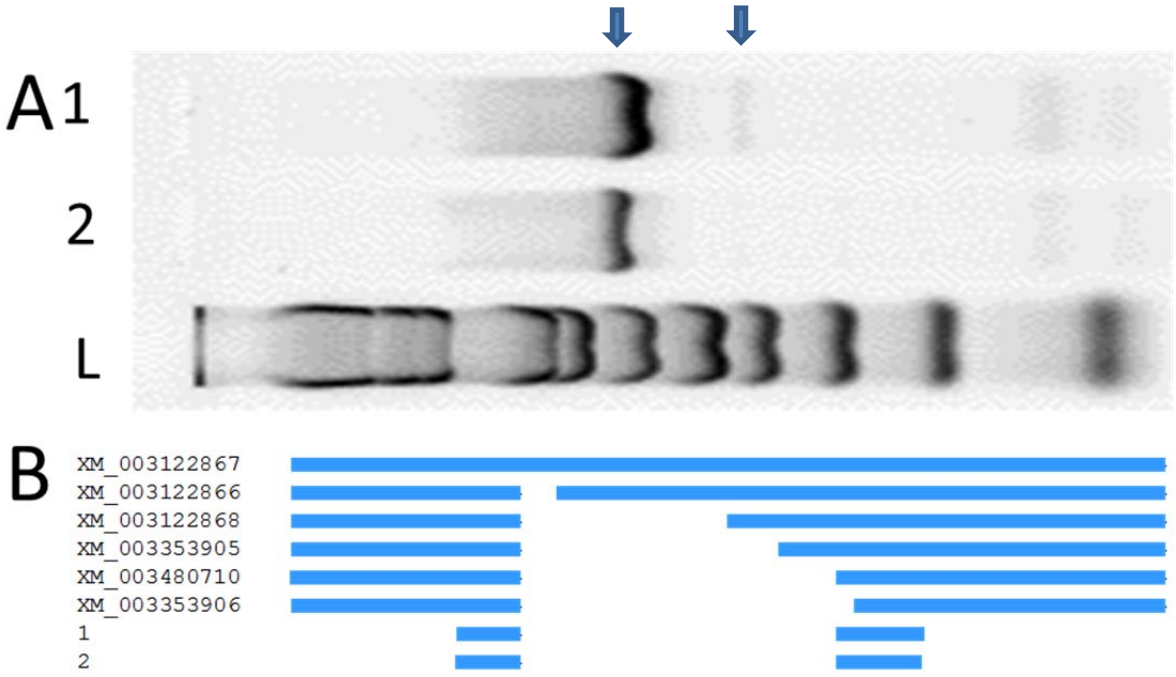

Figure 3.4: CD44 sequencing results. A: 2% w/v agarose gel using Sybr Safe 1: amplified products from Ocular cDNA 2: amplified product of oviductal and uterine cDNA L: 100 bp ladder. B: sequence alignment against all currently known porcine transcript variants of CD44. Sequence 1 and 2 correspond to the major band in the respective lanes of the above gel.

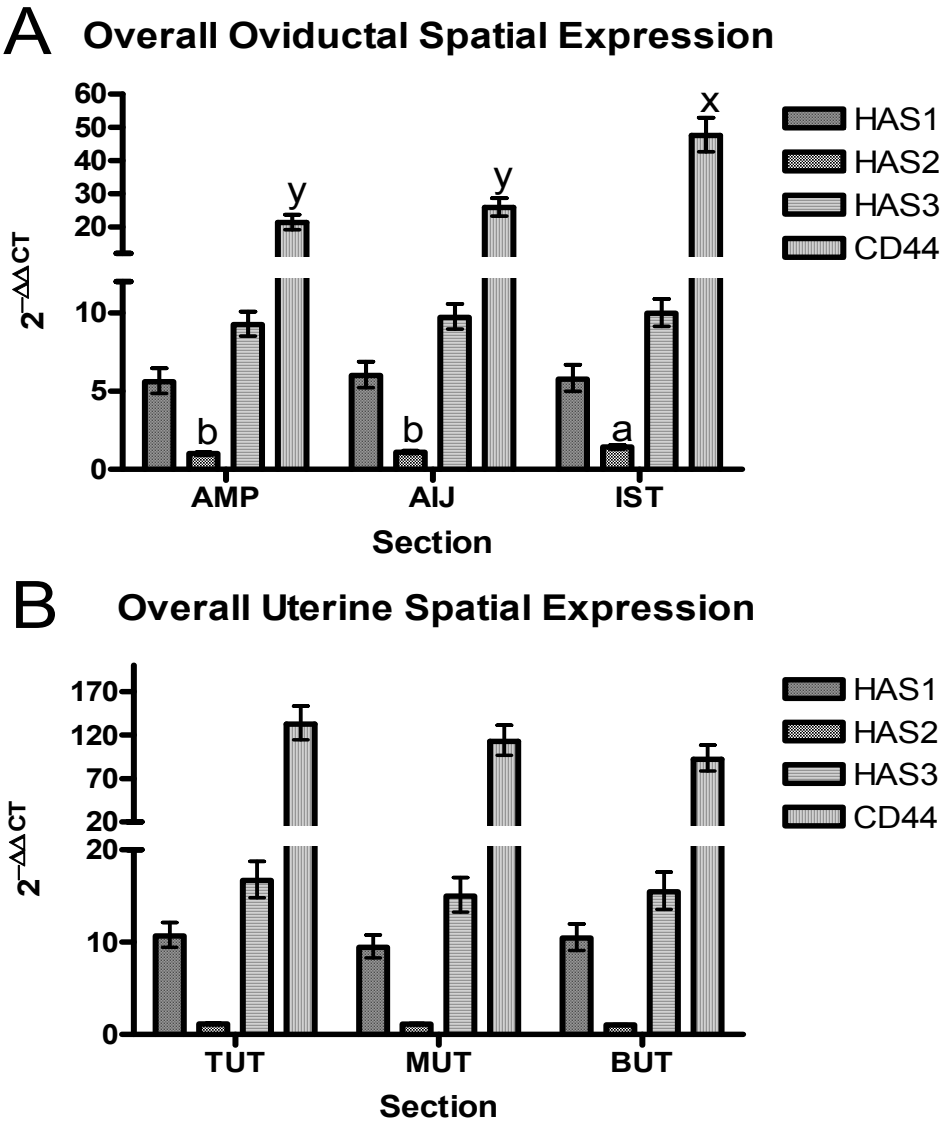

Figure 3.5: Relative expression of HA associated transcripts over the spatial segments of the oviduct and uterus as measured by real time PCR. Groupings correspond to A: the oviductal segments of AMP (n=18), AIJ (n=20) and IST (n=18) B: the uterine thirds, including TUT (n=20), MUT (n=15) and BUT (n=15). Data is expressed in fold changes relative to the point of lowest expression, with different letters representing statistical significance ($P<0.05$) relative to this point. Error bars show exponential corrected standard error of the mean calculated separately for positive and negative error.

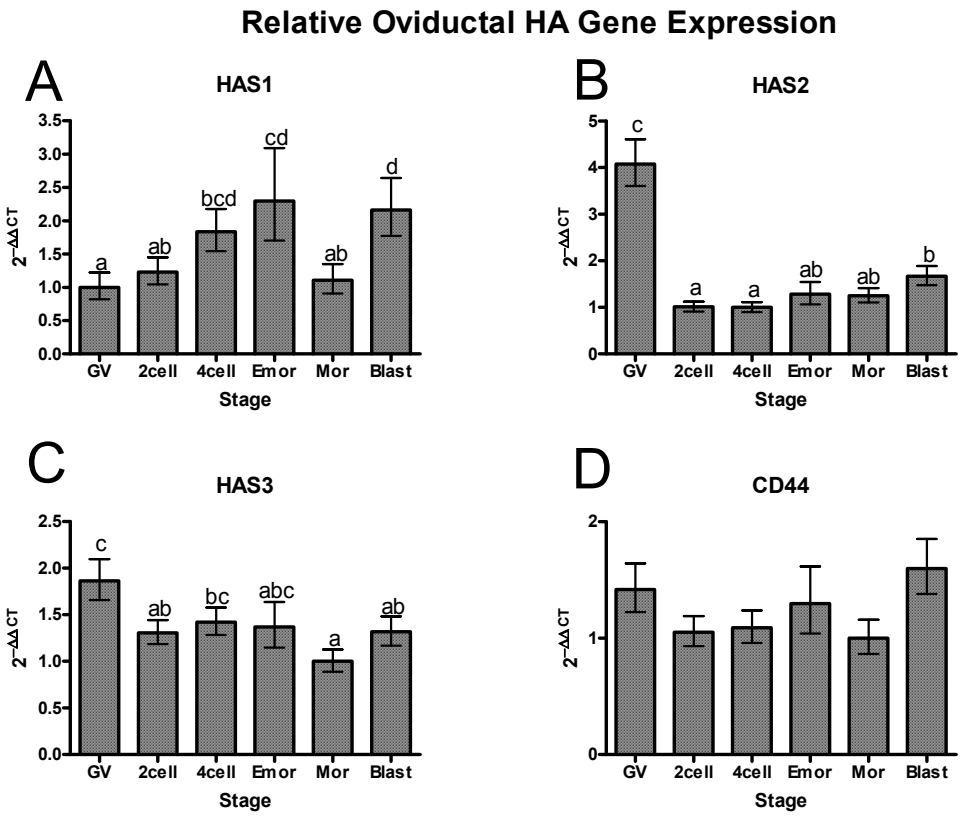

Figure 3.6: Relative expression of HA associated transcripts in the oviduct over time as measured by real time PCR. Groupings correspond to the oocyte GV (n=3) or embryonic 2cell (n=5), 4cell (n=4), Emor (n=2), Mor (n=3) and Blast (n=3) stages found in each animal at the time of slaughter. Data are expressed as in fold changes relative to the point of lowest expression with different letters representing statistical significance ($P<0.05$) relative to this point. Error bars show exponential corrected standard error of the mean calculated separately for positive and negative error.

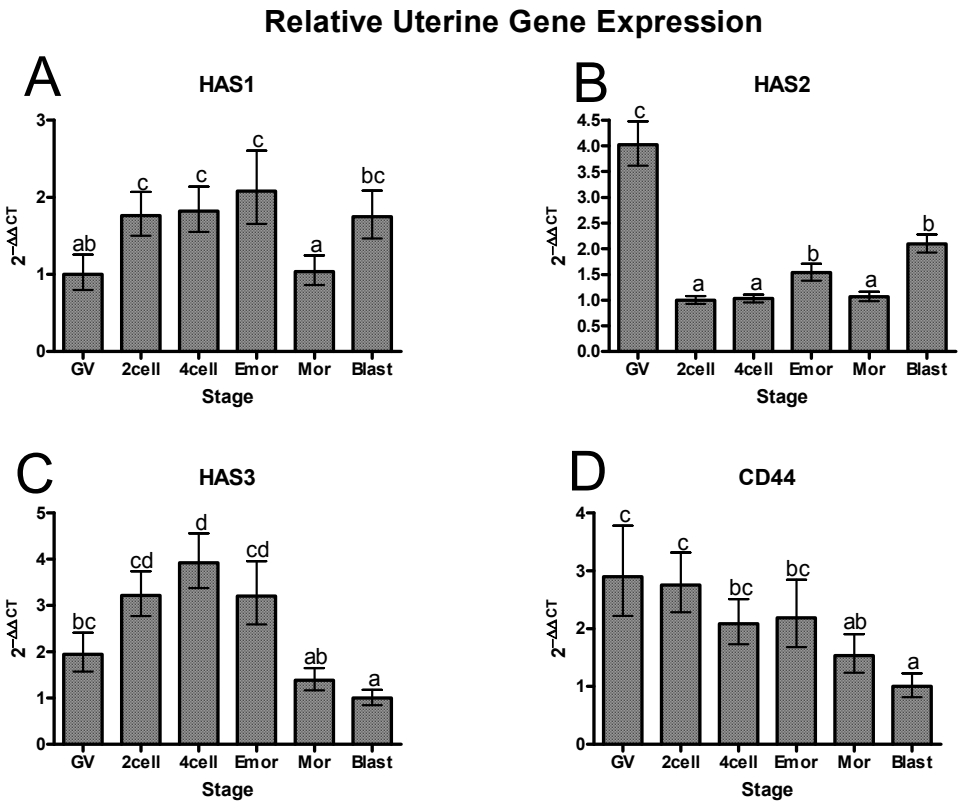

Figure 3.7: Relative expression of HA associated transcripts in the uterus over time as measured by real time PCR. Groupings correspond to the oocyte GV (n=3) or embryonic 2cell (n=5), 4cell (n=4), Emor (n=2), Mor (n=3) and Blast (n=3) stages found in each animal at the time of slaughter. Data are expressed as in fold changes relative to the point of lowest expression with different letters representing statistical significance ($P<0.05$) relative to this point. Error bars show exponential corrected standard error of the mean calculated separately for positive and negative error.

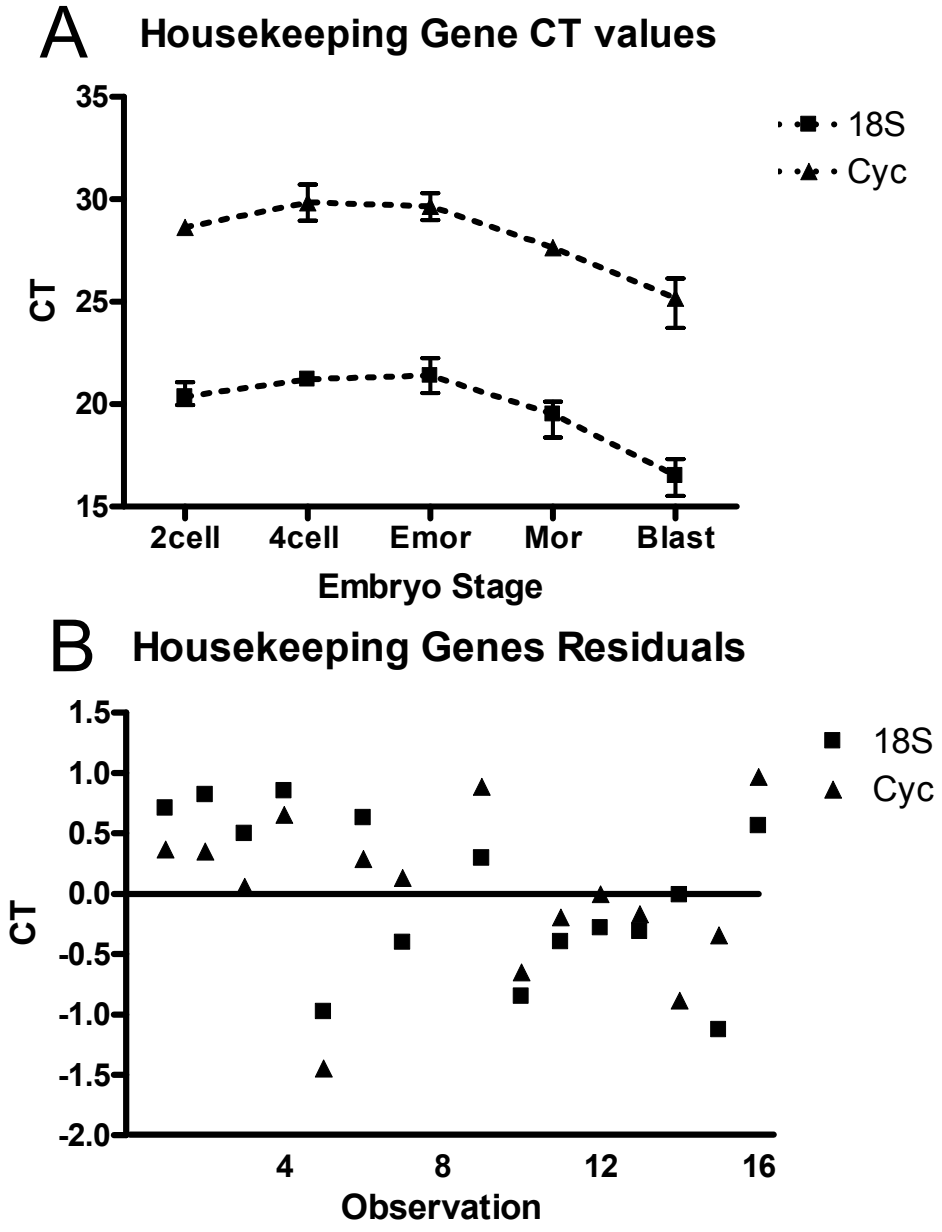

Figure 3.8: Presumptive embryonic housekeeping genes. A: Expression profile of raw CT values produced by real time PCR for embryos classified into 2cell (n=3), 4cell (n=3), Emor (n=2), Mor (n=4) and Blast (n=4) stages. Error bars represent range in CT values observed at each stage. B: distribution of residuals for 18S and Cyclophilin (Cyc), correlation coefficient of residuals between genes is 0.714 (P=0.0028)

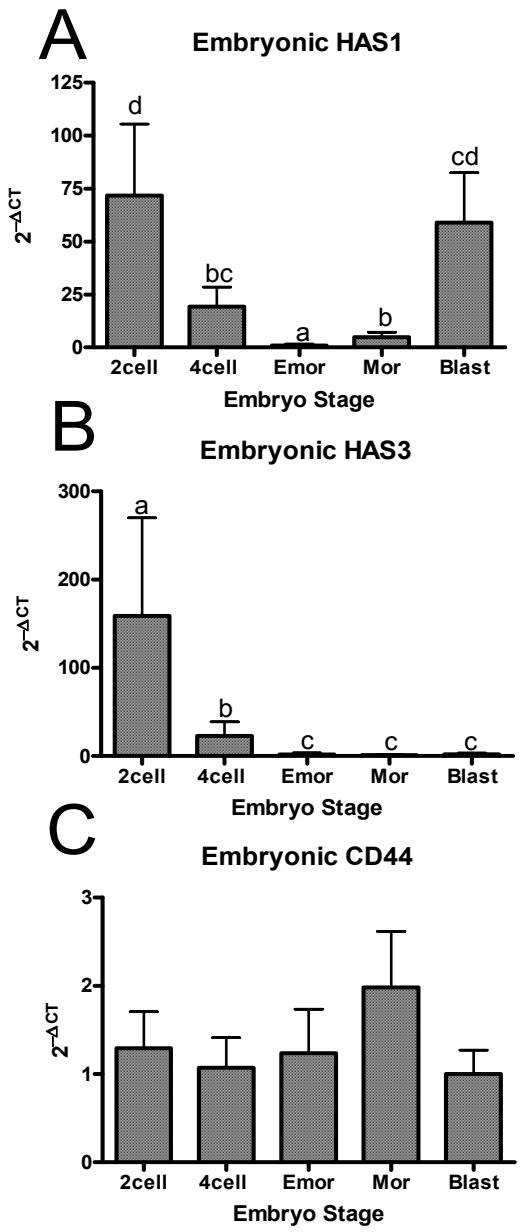

Figure 3.9: Embryonic expression profiles for HAS1, HAS3 and CD44 as determined by real time PCR for embryos classified into 2cell (n=3), 4cell (n=3), Emor (n=2), Mor (n=4) and Blast (n=4) stages. Expression data graphed as $2^{\Delta CT}$, where ΔCT is the difference between a given data point and the point of lowest expression within a gene. Different letters represent statistical significance ($P<0.05$) relative to this point. Error bars show exponential corrected standard error of the mean calculated separately for positive and negative error.

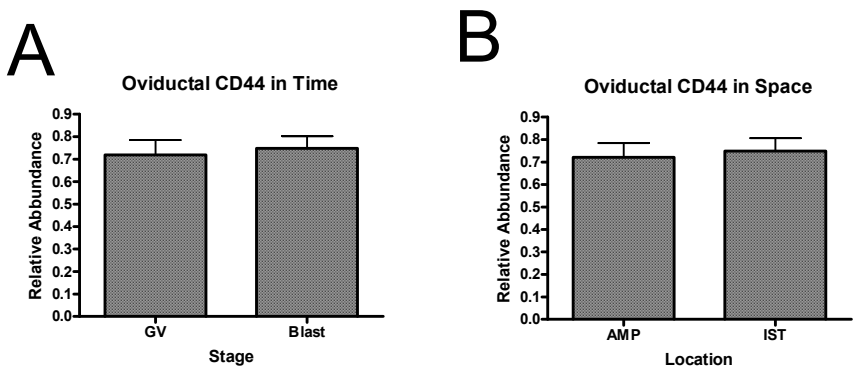

Figure 3.10: Quantification of oviductal CD44 protein by Western blot analysis. A: oviductal CD44 protein abundance at time points corresponding to the oocyte germinal vesicle stage (GV) (n=6) and embryonic Blast (n=7) stages relative to βactin. B: oviductal CD44 protein abundance in ampulla (AMP)(n=7) and isthmus (IST)(n=6) segments, relative to βactin

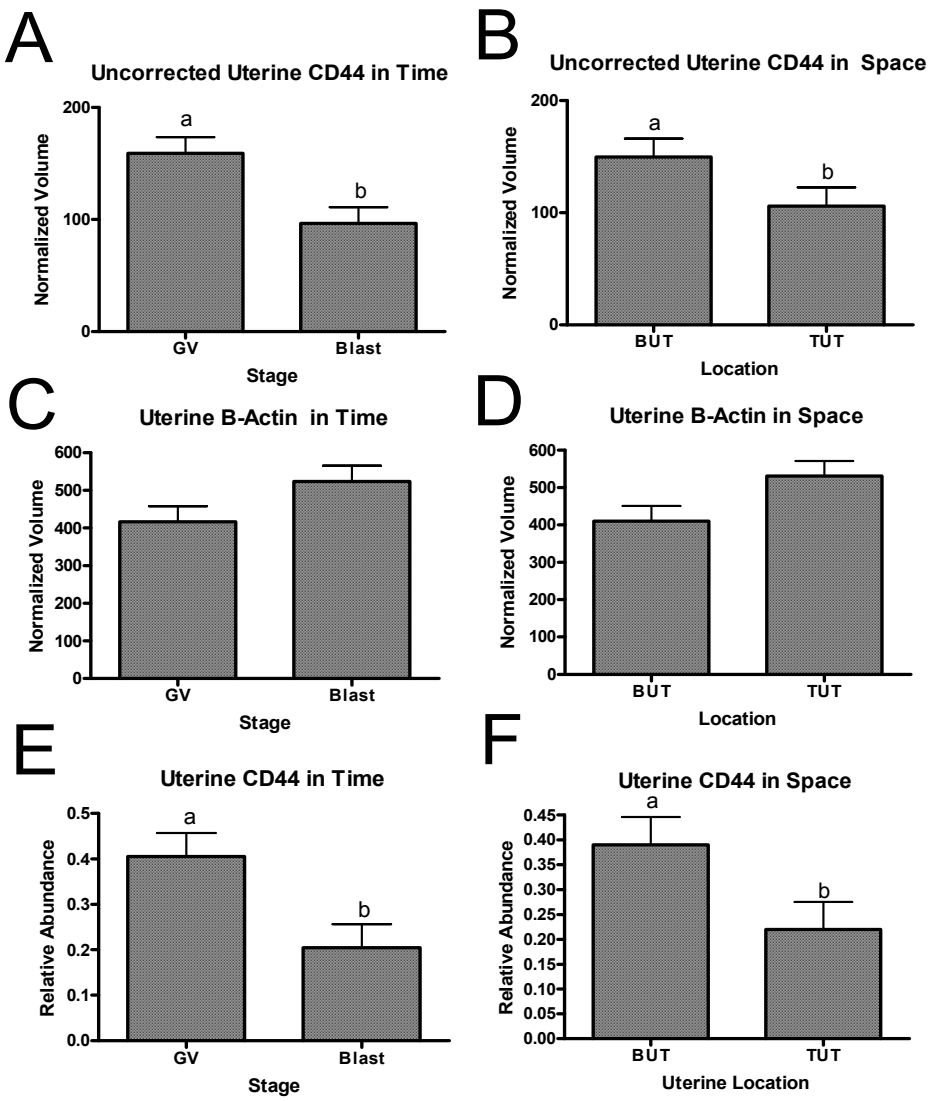

Figure 3.11: Quantification of uterine CD44 by Western blot analysis. Uncorrected normalized volume measurements for A: CD44, C: βactin and E: corrected relative abundance of CD44 at time points corresponding to the oocyte germinal vesicle (GV) (n=8) stage and embryonic blastocyst stage (Blast) (n=8). Uncorrected normalized volume measurements for B: CD44, D: βactin and F: corrected relative abundance of CD44 in segments corresponding to the top (TUT) (n=8) and bottom (BUT) (n=8) of the uterine horns. Different letters represent significant differences ($P<0.05$) and error bars show standard error of the mean.

References

Ahrens, T., Assmann, V., Fieber, C., Termeer, C.C., Herrlich, P., Hofmann, M., and Simon, J.C. (2001) CD44 is the Principal Mediator of Hyaluronic-Acid-Induced Melanoma Cell Proliferation. Nature 116(1), 93-101

Alizadeh, Z., Kageyama, S.-I., and Aoki, F. (2005) Degradation of maternal mRNA in mouse embryos: Selective degradation of specific mRNAs after fertilization. Mol Reprod Dev 72(3), 281-290

Anderson, J.E., Matteri, R.L., Abeydeera, L.R., Day, B.N., and Prather, R.S. (2001) Degradation of maternal cdc25c during the maternal to zygotic transition is dependent upon embryonic transcription. Mol Reprod Dev 60(2), 181-188

Bai, K.-J., Spicer, A.P., Mascarenhas, M.M., Yu, L., Ochoa, C.D., Garg, H.G., and Quinn, D.A. (2005) The Role of Hyaluronan Synthase 3 in Ventilator-induced Lung Injury. Am J Respir Crit Care Med 172(1), 92-98

Bains, R., Adeghe, J., and Carson, R.J. (2002) Human sperm cells express CD44. Fertil Steril 78(2), 307-312

Bains, R., Mil, D.M., Carson, R.J., and Adeghe, J. (2001) Hyaluronic Acid Increases Motility/Intracellular Ca 2+ Concentration In Human Sperm In Vitro. Syst Biol Reprod Med 47(2), 119-125

Barnes, F.L. (2000) The Effects of the Early Uterine Environment on the Subsequent Development of Embryo and Fetus. Theriogenology 53(2), 649-658

Binns, R.M., and Pabst, R. (1994) Lymphoid tissue structure and lymphocyte trafficking in the pig. Vet Immunol Immunopathol 43(1–3), 79-87

Camenisch, T.D., Spicer, A.P., Brehm-Gibson, T., Biesterfeldt, J., Augustine, M.L., Calabro, A., Kubalak, S., Klewer, S.E., and McDonald, J.A. (2000) Disruption of hyaluronan synthase-2 abrogates normal cardiac morphogenesis and hyaluronan-mediated transformation of epithelium to mesenchyme. J Clin Invest 106(3), 349-360

Chao, H., and Spicer, A.P. (2005) Natural Antisense mRNAs to Hyaluronan Synthase 2 Inhibit Hyaluronan Biosynthesis and Cell Proliferation. J Biol Chem 280(30), 27513-27522

Chen, L., Wert, S.E., Hendrix, E.M., Russell, P.T., Cannon, M., and Larsen, W.J. (1990) Hyaluronic acid synthesis and gap junction endocytosis are necessary for normal expansion of the cumulus mass. Mol Reprod Dev 26(3), 236-247

Comper, W.D., and Laurent, T.C. (1978) Physiological function of connective tissue polysaccharides. Physiol Rev 58(1), 255-315

Evans, B.R. (1999) The prospect for international regulatory interventions in embryo transfer and reproductive technologies in the next century. Theriogenology 51(1), 71-80

Fraser, J.R., Laurent, T.C., and Laurent, U.B. (1997) Hyaluronan: its nature, distribution, functions and turnover. J Intern Med 242(1), 27-33

Friedler, S., Schachter, M., Strassburger, D., Esther, K., Ron El, R., and Raziel, A. (2007) A randomized clinical trial comparing recombinant hyaluronan/recombinant albumin versus human tubal fluid for cleavage stage embryo transfer in patients with multiple IVF-embryo transfer failure. Hum Reprod 22(9), 2444-2448

Furnus, C.C., de Matos, D.G., and Martinez, A.G. (1998) Effect of hyaluronic acid on development of in vitro produced bovine embryos. Theriogenology 49(8), 1489-1499

Gardner, D.K., Rodriegez-Martinez, H., and Lane, M. (1999) Fetal development after transfer is increased by replacing protein with the glycosaminoglycan hyaluronan for mouse embryo culture and transfer. Hum Reprod 14(10), 2575-2580

Guo, N., Kanter, D., Funderburgh, M.L., Mann, M.M., Du, Y., and Funderburgh, J.L. (2007) A rapid transient increase in hyaluronan synthase-2 mRNA initiates secretion of hyaluronan by corneal keratocytes in response to transforming growth factor beta. J Biol Chem 282(17), 12475-12483

Hansen, C., Srikandakumar, A., and Downey, B.R. (1991) Presence of follicular fluid in the porcine oviduct and its contribution to the acrosome reaction. Mol Reprod Dev 30(2), 148-153

Huszar, G., Willetts, M., and Corrales, M. (1990) Hyaluronic acid (Sperm Select) improves retention of sperm motility and velocity in normospermic and oligospermic specimens. Fertil Steril 54(6), 1127-1134

Iritani, A., Sato, E., and Nishikawa, Y. (1974) Secretion Rates and Chemical Composition of Oviduct and Uterine Fluids in Sows. J Anim Sci 39(3), 582-588

Ishida, O., Tanaka, Y., Morimoto, I., Takigawa, M., and Eto, S. (1997) Chondrocytes Are Regulated by Cellular Adhesion Through CD44 and Hyaluronic Acid Pathway. J Bone Miner Res 12(10), 1657-1663

Itano, N., Atsumi, F., Sawai, T., Yamada, Y., Miyaishi, O., Senga, T., Hamaguchi, M., and Kimata, K. (2002) Abnormal accumulation of hyaluronan matrix diminishes contact inhibition of cell growth and promotes cell migration. Proc Natl Acad Sci U S A 99(6), 3609-3614

Itano, N., Sawai, T., Yoshida, M., Lenas, P., Yamada, Y., Imagawa, M., Shinomura, T., Hamaguchi, M., Yoshida, Y., Ohnuki, Y., Miyauchi, S., Spicer, A.P., McDonald, J.A., and Kimata, K. (1999) Three isoforms of mammalian hyaluronan synthases have distinct enzymatic properties. J Biol Chem 274(35), 25085-25092

Kano, K., Miyano, T., and Kato, S. (1998) Effects of glycosaminoglycans on the development of in vitro-matured and -fertilized porcine oocytes to the blastocyst stage in vitro. Biol Reprod 58(5), 1226-1232

Kikuchi, K., Kashiwazaki, N., Noguchi, J., Shimada, A., Takahashi, R., Hirabayashi, M., Shino, M., Ueda, M., and Kaneko, H. (1999) Developmental competence, after transfer to recipients, of porcine oocytes matured, fertilized, and cultured in vitro. Biol Reprod 60(2), 336-340

Kim, H.S., Lee, G.S., Hyun, S.H., Nam, D.H., Lee, S.H., Jeong, Y.W., Kim, S., Kim, J.H., Kang, S.K., Lee, B.C., and Hwang, W.S. (2005) Embryotropic effect of glycosaminoglycans and receptors in development of porcine pre-implantation embryos. Theriogenology 63(4), 1167-1180

Kimura, N., Konno, Y., Miyoshi, K., Matsumoto, H., and Sato, E. (2002) Expression of hyaluronan synthases and CD44 messenger RNAs in porcine cumulus-oocyte complexes during in vitro maturation. Biol Reprod 66(3), 707-717

Kobayashi, N., Miyoshi, S., Mikami, T., Koyama, H., Kitazawa, M., Takeoka, M., Sano, K., Amano, J., Isogai, Z., Niida, S., Oguri, K., Okayama, M., McDonald, J.A., Kimata, K., Taniguchi, S.i., and Itano, N. (2010) Hyaluronan Deficiency in Tumor Stroma Impairs Macrophage Trafficking and Tumor Neovascularization. Cancer Res 70(18), 7073-7083

Kogan, G., Soltes, L., Stern, R., and Gemeiner, P. (2007) Hyaluronic acid: a natural biopolymer with a broad range of biomedical and industrial applications. Biotechnol Lett 29(1), 17-25

Kuijk, E.W., du Puy, L., van Tol, H.T., Haagsman, H.P., Colenbrander, B., and Roelen, B.A. (2007) Validation of reference genes for quantitative RT-PCR studies in porcine oocytes and preimplantation embryos. BMC Dev Biol 7, 58

Laurent, T.C., and Fraser, J.R. (1992) Hyaluronan. FASEB J 6(7), 2397-404

Lee, C.N., and Ax, R.L. (1984) Concentrations and composition of glycosaminoglycans in the female bovine reproductive tract. J Dairy Sci 67(9), 2006-2009

Machaty, Z., Day, B.N., and Prather, R.S. (1998) Development of early porcine embryos in vitro and in vivo. Biol Reprod 59(2), 451-455

Miles, J.R., Blomberg, L.A., Krisher, R.L., Everts, R.E., Sonstegard, T.S., Van Tassell, C.P., and Zuelke, K.A. (2008) Comparative transcriptome analysis of in vivo- and in vitro-produced porcine blastocysts by small amplified RNA-serial analysis of gene expression (SAR-SAGE). Mol Reprod Dev 75(6), 976-988

Miyano, T., Hiro-oka, R.E., Kano, K., Miyake, M., Kusunoki, H., and Kato, S. (1994) Effects of hyaluronic acid on the development of 1- and 2-cell porcine embryos to the blastocyst stage in vitro. Theriogenology 41(6), 1299-1305

Miyoshi, K., Umezu, M., and Sato, E. (1999) Effect of hyaluronic acid on the development of porcine 1-cell embryos produced by a conventional or new in vitro maturation/fertilization system. Theriogenology 51(4), 777-784

Novak, S., Paradis, F., Patterson, J.L., Pasternak, J.A., Oxtoby, K., Moore, H.S., Hahn, M., Dyck, M.K., Dixon, W.T., and Foxcroft, G.R. (2012) Temporal candidate gene expression in the sow placenta and embryo during early gestation and effect of maternal Progenos supplementation on embryonic and placental development. Reprod Fertil Dev 24(4), 550-558

Paradis, F., Novak, S., Murdoch, G.K., Dyck, M.K., Dixon, W.T., and Foxcroft, G.R. (2009) Temporal regulation of BMP2, BMP6, BMP15, GDF9, BMPR1A, BMPR1B, BMPR2 and TGFBR1 mRNA expression in the oocyte, granulosa and theca cells of developing preovulatory follicles in the pig. Reproduction 138(1), 115-129

Peach, R.J., Hollenbaugh, D., Stamenkovic, I., and Aruffo, A. (1993) Identification of hyaluronic acid binding sites in the extracellular domain of CD44. J Cell Biol 122(1), 257-264

Sabeur, K., Cherr, G.N., Yudin, A.I., and Overstreet, J.W. (1998) Hyaluronic acid enhances induction of the acrosome reaction of human sperm through interaction with the PH-20 protein. Zygote 6(2), 103-111

Salustri, A., Camaioni, A., Di Giacomo, M., Fulop, C., and Hascall, V.C. (1999) Hyaluronan and proteoglycans in ovarian follicles. Hum Reprod Update 5(4), 293-301

Salustri, A., Yanagishita, M., Underhill, C.B., Laurent, T.C., and Hascall, V.C. (1992) Localization and synthesis of hyaluronic acid in the cumulus cells and mural granulosa cells of the preovulatory follicle. Dev Biol 151(2), 541-551

Sato, E., Miyamoto, H., and Koide, S.S. (1990) Glycosaminoglycans in porcine follicular fluid promoting viability of oocytes in culture. Mol Reprod Dev 26(4), 391-397

Sbracia, M., Grasso, J., Sayme, N., Stronk, J., and Huszar, G. (1997) Hyaluronic acid substantially increases the retention of motility in cryopreserved/thawed human spermatozoa. Hum Reprod 12(9), 1949-1954

Schoenfelder, M., and Einspanier, R. (2003) Expression of hyaluronan synthases and corresponding hyaluronan receptors is differentially regulated during oocyte maturation in cattle. Biol Reprod 69(1), 269-277

Simon, A., Safran, A., Revel, A., Aizenman, E., Reubinoff, B., Porat-Katz, A., Lewin, A., and Laufer, N. (2003) Hyaluronic acid can successfully replace albumin as the sole macromolecule in a human embryo transfer medium. Fertil Steril 79(6), 1434-1438

Slevin, M., Kumar, S., and Gaffney, J. (2002) Angiogenic oligosaccharides of hyaluronan induce multiple signaling pathways affecting vascular endothelial cell mitogenic and wound healing responses. J Biol Chem 277(43), 41046-41059

Spicer, A.P., and McDonald, J.A. (1998) Characterization and molecular evolution of a vertebrate hyaluronan synthase gene family. J Biol Chem 273(4), 1923-1932

Stojkovic, M., Krebs, O., Kolle, S., Prelle, K., Assmann, V., Zakhartchenko, V., Sinowatz, F., and Wolf, E. (2003) Developmental regulation of hyaluronan-binding protein (RHAMM/IHABP) expression in early bovine embryos. Biol Reprod 68(1), 60-66

Stojkovic, M., Thompson, J.G., and Tervit, H.R. (1999) Effects of hyaluronic acid supplementation on in vitro development of bovine embryos in a two-step culture system. Theriogenology 51(1), 254-254

Suchanek, E., Simunic, V., Juretic, D., and Grizelj, V. (1994) Follicular fluid contents of hyaluronic acid, follicle-stimulating hormone and steroids relative to the success of in vitro fertilization of human oocytes. Fertil Steril 62(2), 347-352

Tienthai, P., Kimura, N., Heldin, P., Sato, E., and Rodriguez-Martinez, H. (2003a) Expression of hyaluronan synthase-3 in porcine oviducal epithelium during oestrus. Reprod Fertil Dev 15(1-2), 99-105

Tienthai, P., Kjellen, L., Pertoft, H., Suzuki, K., and Rodriguez-Martinez, H. (2000) Localization and quantitation of hyaluronan and sulfated glycosaminoglycans in the tissues and intraluminal fluid of the pig oviduct. Reprod Fertil Dev 12(3-4), 173-182

Tienthai, P., Yokoo, M., Kimura, N., Heldin, P., Sato, E., and Rodriguez-Martinez, H. (2003b) Immunohistochemical localization and expression of the hyaluronan receptor CD44 in the epithelium of the pig oviduct during oestrus. Reproduction 125(1), 119-132

Turley, E.A., Austen, L., Vandeligt, K., and Clary, C. (1991) Hyaluronan and a cell-associated hyaluronan binding protein regulate the locomotion of ras-transformed cells. J Cell Biol 112(5), 1041-1047

Vallet, J.L., Miles, J.R., and Freking, B.A. (2009) Effect of fetal size on fetal placental hyaluronan and hyaluronoglucosaminidases throughout gestation in the pig. Anim Reprod Sci 118, no. 2–4 (2010): 297-309.

Valojerdi, M.R., Karimian, L., Yazdi, P.E., Gilani, M.A., Madani, T., and Baghestani, A.R. (2006) Efficacy of a human embryo transfer medium: a prospective, randomized clinical trial study. J Assist Reprod Genet 23(5), 207-212

Wallenhorst, S., and Holtz, W. (1999) Transfer of pig embryos to different uterine sites. J Anim Sci 77(9), 2327-2329

Wang, Q.T., Piotrowska, K., Ciemerych, M.A., Milenkovic, L., Scott, M.P., Davis, R.W., and Zernicka-Goetz, M. (2004) A Genome-Wide Study of Gene Activity Reveals Developmental Signaling Pathways in the Preimplantation Mouse Embryo. Dev Cell 6(1), 133-144

Weigel, P.H., Hascall, V.C., and Tammi, M. (1997) Hyaluronan synthases. J Biol Chem 272(22), 13997-4000

Yamada, Y., Itano, N., Hata, K.-i., Ueda, M., and Kimata, K. (2004) Differential Regulation by IL-1[beta] and EGF of Expression of Three Different Hyaluronan Synthases in Oral Mucosal Epithelial Cells and Fibroblasts and Dermal Fibroblasts: Quantitative Analysis Using Real-Time RT-PCR. J Investig Dermatol 122(3), 631-639

Yokoo, M., Shimizu, T., Kimura, N., Tunjung, W.A., Matsumoto, H., Abe, H., Sasada, H., Rodriguez-Martinez, H., and Sato, E. (2007) Role of the hyaluronan receptor CD44 during porcine oocyte maturation. J Reprod Dev 53(2), 263-270

Chapter 4: Proteomic Characterization of the Porcine Uterine Histotroph During the Germinal Vesicle and Blastocyst Stage of Development

Introduction

Embryonic and fetal development is a complex process which requires specific nutrients and other factors to progress. Prior to implantation the embryo must survive and develop in the aqueous environment provided by the maternal reproductive tract. This environment, termed the uterine histotroph, is a complex and dynamic mixture containing ions, carbohydrates, lipids and proteins each of which plays a unique role in early embryonic development. Perturbations in this environment have been shown to have an impact on the epigenome (Doherty *et al.* 2000), and thereby, fetal (Khosla *et al.* 2001), and post natal development (Fernandez-Gonzalez *et al.* 2004). Much of the chemical composition of uterine and oviductal histotroph has been previously characterized in swine (Iritani *et al.* 1974), including the protein content which has been shown to be regulated by both progesterone and estrogen (Knight *et al.* 1973). However, with few exceptions, the specific proteins present, their concentrations, and modifications at any given point it time during the reproductive cycle of the sow, have yet to be fully determined.

Proteomics is the study of the abundance, activity, structure or state of post-translational modification of proteins in a given system (Wright *et al.* 2012). In the past, studies have taken a candidate approach to examine the proteome of the uterine histotroph, resulting in a comprehensive understanding of the role of specific proteins such as uteroferrin (Chen *et al.* 1973; Schlosnagle *et al.* 1974) and retinol-binding protein (Adams *et al.* 1981). However, while a candidate approach to proteomics is able to provide a detailed understanding of the physiological role of a single protein, it is ill suited to the characterization of the

complete proteome of biological fluids such as the uterine histotroph. Protein profiling methodologies have been successfully applied a number of times to examine the reproductively relevant proteomic changes (Koch *et al.* 2010). Only one such study has been reported in the pig, which evaluated the histotroph proteome at days 10 and 12 of pregnancy (Kayser *et al.* 2006). In this study, 250 unique protein spots were successfully matched across gels, of which nearly 50% of them were significantly altered by day of gestation/estrus or pregnancy status, demonstrating the potentially dynamic nature of the uterine histotroph proteome. In addition, recently published work by Mullet *et al.* (2012) evaluated the proteome of the uterine histotroph in cattle at two points during the reproductive cycle using high pressure liquid chromatography (HPLC) and mass spectrometry. This study demonstrated the complexity of the uterine proteome, identifying 300 and 500 protein entities present at day 7 and 13 of the estrus cycle, respectively (Mullen *et al.* 2012). While these results suggest the histotrophic proteome is both complex and dynamic, there is currently no information regarding these factors during pre-hatching development in the pig. Although the protein requirements of the embryo are likely less complex at this stage due to the smaller and less active conceptus, it is likely that they still play a significant role.

Two dimensional sodium dodecyl sulfate polyacrylamide gel electrophoresis (2D SDS PAGE) allows for the high throughput quantification of proteomic changes within a biological fluid or tissue. When coupled to a method of protein identification such as mass spectroscopy, the technology allows for rapid characterization of a proteome and it physiological dynamics. These methodologies have been successfully applied in swine reproductive physiology to identify markers of boar fertility (Novak *et al.* 2010) and to elucidate the effect of the oocyte on cumulus cell function (Paradis *et al.* 2010). To our knowledge this is the first study utilizing high throughput technologies to evaluate the proteome of the uterine histotroph during the peri-ovulatory period in swine.

Materials and Methods

Animals and Sample Collection

All procedures were conducted in accordance within the Canadian Council on Animal Care guidelines and with the approval of the University of Alberta, Animal Care and Use Committee for Livestock (Protocol #2006-11C). Primiparous sows were allocated to trial following a 50% restriction diet during the final week of a 21 day lactation. Following weaning, animals were exposed to estrus detection twice daily and fed *ab libitum* until the end of the first standing estrus post-weaning, followed by 1.5 times maintenance feeding. Estrus detection was performed once per day for 18 days following first estrus and then twice a day to the onset of the second post-weaning estrus. Animals allocated to provide germinal vesicle (GV) stage samples (n=4) were euthanized 12 hours after the onset of standing estrus prior to first insemination. Animals allocated to provide blastocyst (Blast) stage samples were inseminated 12 hrs after the onset of standing estrus and then every 24 hours after until the end of standing estrus. The Blast animals were monitored for ovulation using transcutaneous real time ultrasound at 8 hr intervals starting at 18 days after the end of the first post weaning estrus to establish baseline measurements. Starting at the onset of estrus, animals were exposed to ultrasonography at 4 hr intervals until ovulation, which was defined as the absence of large ovarian follicles. The Blast stage animals were euthanized at 125 hrs following ovulation. Animals were stunned via captive bolt and euthanized by exsanguination and then the reproductive tracts were removed through a midline incision with the cervix being severed at the most caudal internal point. Tracts were taken to a clean dissection area, the broad ligament was removed and the uterine horn linearized. Uterine histotroph was collected using a modified internal cannula from an insemination catheter designed for post-cervical insemination in pigs (Deep Golden Pig, IMV technologies). In short, the internal catheter was removed from the larger cannula and a luer lock adapter connected via a short

length of polypropylene tubing. A small incision was made into each uterine horn immediately above the uterine bifurcation and the modified internal catheter inserted up to the utero-tubular junction. A syringe was attached and 8 ml of suction applied as the catheter was slowly pulled down the uterine horn. This process was repeated three times per uterine horn and the resulting aspirate pooled within horn. The pooled aspirates were centrifuged at 10000 X G to remove any cellular debris, measured with a positive displacement pipette and then frozen for further analysis. Each uterine horn was then split into segments corresponding to the bottom third or caudal segment of the horn (BUT) and the upper or tubal segment of horn TUT, based on the full length of each uterine horn. The segments were flushed with 20 ml modified phosphate buffered saline (mPBS) as described in Chapter 2 and the flushes examined for the presence of appropriately staged embryos. A tissue sample comprised of endometrium, myometrium and serosa was taken from the center of each of these segments using a 1 in tissue punch, and frozen in liquid nitrogen for further analysis. All samples were maintained at -80°C until processing.

2D Proteomics

Proteomic analysis was conducted using the method of 2D SDS PAGE as per the following details. Unless otherwise noted all reagents and equipment were obtained from GE Healthcare Life Sciences and base chemicals from Sigma-Aldrich. Protein samples were sub-aliquoted such that no sample was subject to more than three freeze-thaw cycles. The protein concentration in the pooled uterine histotroph was determined using the 2D Quant Kit as per the manufacturer's instructions. 100 µg of protein from each sample was diluted in rehydration solution (7.7 M urea, 2.2 M thiourea, 65mM 3-[(3-cholamidopropyl)dimethylammonio]-1-propanesulfonate) and 0.8% IPG pH 3-10 buffer(17-6000-87), 1.3% Destreak (17-6003-18) and trace bromophenol blue added. 24 cm Immobiline DryStrips with a linear pH gradient from 3-10 (#17-6002-44) were rehydrated for 18hrs in 440 µl of this solution under DryStrip

Cover fluid (17-1335-01). First dimension electrophoresis was carried out overnight on an Ettan IPG4 isoelectric focusing unit under DryStrip Cover fluid (17-1335-01). First dimension electrophoresis program consisted of 100V for 1hr, 250V for 2hrs, a gradient to 2000V over 2hrs, 1000V for 4hrs, a gradient to 4000V for 2hrs, 4000V for 4hrs, 8000V for 48000 V-hrs and then held at 100V until further processing. Strips were individually equilibrated in 10 ml SDS buffer (6M urea, 50mM Tris, 2% (w/v) SDS, 87% (v/v) Glycerol and 0.002% (w/v) bromophenol blue) with 0.1 g/ml Dithiothreitol (DTT) for 15 minutes under agitation followed by 15 minutes in SDS buffer containing 0.25 g/ml Iodoacetamide also under agitation. Equilibrated first dimension strips were then mounted onto in-house cast large format (24 x 20 x 0.5 cm) 10% (w/v) linear SDS-PAGE slab gels. A Precision Plus Protein Standard Plug (10-250kDa, Biorad) and the first dimension strips were sealed to the gel using 0.5% agarose with trace bromophenol blue. Gels were run in randomized batches of six using the Ettan DALTsix vertical gel system with 1X running buffer (250 mM glycine, 25mM Tris and 3.5mM SDS) in the lower tank and 3X buffer in the upper tank. Second dimension electrophoresis was run at a constant temperature of 2°C at 5.0 W/gel for 30 min followed by 16.0 W/gel until the bromophenol band had reached the bottom edge of the gel. Slab gels were removed from the apparatus and fixed in 10% (v/v) ethanol and 7% (v/v) glacial acetic acid for 30 min under gentle agitation. Gels were stained for 12 hrs in 200ml of SYPRO Ruby Protein Gel stain (BioRad) under gentle agitation and then destained for 30min in the previously described gel fixative. Image collection was performed on the Typhoon Trio+ with an excitation of 610 nm and emission filtering at 532 nm. Images were pre-processed using Image Quant Software and then imported into Progenesis Same Spots (Nonlinear Dynamics) at which point all gels passed the built in quality analysis. Individual images were hand seeded at more than 60 points per gel and then aligned by the software. Spot perimeters were automatically generated and then human curated, with additional alignments

made to minimize perimeter size. Composite gel images were generated and differential analysis carried out on spot volume normalized to spot intensity within a given image in Progenesis (Nonlinear Dynamics). Normalized spot volumes were exported and analysed using the MANOVA GLM model in SAS.

Protein Identification

Protein identification preparation gels were run as per the first and second dimension methods described above using 300 µg of total protein. Following the second dimension electrophoresis, slab gels were fixed in 50% methanol for 12 hrs. Gels were subsequently washed three times in distilled water under gentle agitation followed by 15 minutes in silver stain (19 mM NaOH, 47 mM $AgNO_3$ and 1.4 % v/v NH_4OH). Following washing, the gels were then treated with a developing solution (240 µM citric acid and 0.05 % v/v formaldehyde) until the first spots became visible. The gels were then treated with a stop solution (2.25 mM citric acid) and imaged using a 14 bit ImageScanner (GE) and hand-matched with composite gels from the corresponding stage. Target spots were excised by hand and stored in distilled deionized water.

Protein spots were sent for identification at the Quebec Genomics Center, Quebec, Canada, using their standard methodology and procedures. In short, in-gel pre-processing was conducted on a Mass Prep liquid handling robot (Waters) using the following method. Excised spots were reduced with 10mM DTT and alkylated with 55mM iodoacetamide prior to digestion with modified sequencing grade porcine trypsin (Promega) at 58°C for 1hr. The resulting peptides were then extracted using 1% v/v formic acid, 3% v/v acetonitrile followed by 1% v/v formic acid, 50% v/v acetonitrile. Peptides were then dried by vacuum centrifuge and re-suspended in 0.1% v/v formic acid. Peptide fragments were size separated by online reversed-phase nanoscale capillary liquid chromatography (RP-LC) using PicoFrit column (New Objective) with a linear gradient over 30 minutes, at a flow rate of 200 nL/min. Fragments where then

analyzed by electrospray mass spectrometry (ES MS/MS) using a Thermo Surveyor MS pump connected to a LTQ linear ion trap mass spectrometer (ThermoFisher), equipped with a nanoelectrospray ion source (ThermoFisher). Mass spectra were collected using a data dependent acquisition mode and Xcalibur software version 2.0.

The resulting spectra were analysed using Mascot V:2.3.0 (Matrix Science) with a fragment ion mass tolerance of 0.50 Da, parent ion tolerance of 2.0 Da and the Iodoacetamide derivative of cysteine and oxidation of methionine specified as fixed and variable modifications, respectively. Peptide sequences were aligned against the uniref_15.3_SusSerfo database, using Scaffold 3 (Proteome Software). Identities with a minimum certainty of 95% as determined by the Peptide Prophet algorithm (Searle 2010), and three or more unique peptide alignments, were accepted for each spot. Identities and uniqueness of each peptide were then manually checked against the NCBI Reference Sequence (RefSeq) protein database using the BLASTp algorithm.

Gene Expression Analysis

Uterine tissue punches from the top (TUT) and bottom (BUT) of the right uterine horn were ground to a fine powder under liquid nitrogen in a precooled mortar and pestle. Total RNA was then extracted from 150 mg of tissue in a 1 ml Trizol (Invitrogen) extraction, as per the manufacturer's protocol with the exceptions described in the previous chapter. RNA was quantified spectroscopically using a Nano Drop (Thermos) and integrity evaluated on a 1.5% w/v denaturing acrylamide gel, illuminated with SYBR safe (Life Technologies) and imaged on a Typhoon scanner (Amersham). Only samples with two clear bands corresponding to 28 and 18S were used for further analysis. Samples were DNase treated with the DNAfree kit (ABI), re-quantified and the quality assessed as above. Reverse transcription was carried out using a combination of random hexomers and oligo-dt primers and the High Capacity Reverse Transcription Kit (ABI) on 2µg RNA. Working under the assumption that all RNA

was converted to cDNA, the product was diluted to 10 ng/µl. Additional transcriptomic analysis was conducted against the large cDNA collection described in Chapter 3 representing the full temporal and spatial ranges including GV, 2-cell, 4-cell, early morula (Emor), morula (Mor) and Blast stages; as well as ampulla (AMP), ampullary-isthmic junction (AIJ) and isthmus (IST), top or posterior uterus (TUT), middle uterus (MUT) and bottom or anterior uterus (BUT) segments.

Primers were designed against 9 genes of interest, based on protein identifications and one housekeeping gene (18s) (Table 4.1). Candidate primers designed to amplify sequences of 100-150 bp were identified using primer 3 V.0.4.0 (http://frodo.wi.mit.edu/). Where chromosomal information in the Sscrofa 9.0 build was available, exon-exon junctions were identified using the Blast Like Alignment Tool (BLAT) and primers spanning these junctions were preferentially selected. No transcriptional variants were known for any of the genes of interest in swine; however, attempts were made to avoid regions of known transcript variance in humans and mice. Selected primers were analysed for homo and hetero dimers using the IDT oligo analyser with a delta G cut-off of greater than -7.55 Kcal/mol. Amplification efficiency for each primer set was assessed against a serial dilution of pooled uterine cDNA. As the SYBR green chemistry produces a fluorescent signal in response to any double stranded, DNA primer specificity was assessed initially through post-polymerase chain reaction (PCR) melting point analysis. In addition, the PCR product was analysed by gel electrophoresis on a 3% w/v agarose gel illuminated by SYBR Safe (Life Technologies) and visualized on a Typhoon scanner (Amersham). The resulting bands were excised, purified and then sequenced from both directions using the Big Dye Direct Cycle Sanger Sequencing kit (ABI). Sequence data was then generated though capillary electrophoresis on a 3700 DNA Sequencer Analyzer (ABI), and aligned against the target mRNA sequence using the SECentral local alignment tool. All primers were validated with a single melting point consistent

with that predicted for the amplicon, a single band and high quality sequence consistent with the target mRNA. Real time PCR was then conducted in duplicate using 20 ng equivalent cDNA and SYBR green intercalating dye chemistry (Kappa). Cycle thresholds (CT) were manually set in the linear portion of the amplification curve and values averaged between replicates which differed by less than 0.2 cycles.

Bioinformatics

Due to the limited gene ontology and pathway data currently available for swine, human orthologs of the sequenced proteins were identified using the Basic Logical Alignment Search Tool for proteins (BLASTp). Porcine sequences were aligned against the human reference sequence (RefSeq) database of proteins. Associated official human gene symbols for the identified orthologs were then obtained from the NCBI gene database and used for all subsequent analysis. Current human gene ontology data was obtained from the Gene Ontology Consortium (www.geneontology.org) and preliminary analysis of differentially abundant proteins was carried out using the GOTreePlus Software (Lee *et al.* 2008). Additional analysis of protein classification and pathway association was conducted using Panther Classification System (Thomas *et al.* 2003) with the Bonferroni multiple testing correction enabled.

Additional *ab initio* analysis was conducted on the porcine protein sequences as per the method described by Emanuelsson *et al.* (2007). In short, sequences were initially analysed using TargetP 1.1 (Emanuelsson *et al.* 2000) using the 'non-plant' and 'no-cutoffs' settings. Subsequent analysis was conducted using SignalP 4.0 (Petersen *et al.* 2011) and SecretomeP 2.0 (Bendtsen *et al.* 2004) using the eukaryotes and mammalian settings, respectively. Positive SignalP predictions were validated against three randomized versions of the sequence in question.

Statistics

Statistical analysis of protein abundance measured by 2D SDS PAGE was carried out using the built-in multiple analysis of variance (MANOVA) in the Progenesis software (Non-Linear Dynamics). Statistical significance in the normalized volume of identified spots was then verified using the General Linear model of SAS. Normality in real time PCR data was assessed using the univariate procedure (SAS) and homoscedasticity verified by White's General test. Data was normalized against a single endogenous control (18S) which showed no significant temporal or spatial variation in this trial. Analysis was conducted on delta CT values calculated as the difference between the CT value for each gene of interest and the endogenous control ($\Delta CT = CT_{GOI} - CT_{18S}$), in time and space using the GLM model. Final results were presented as fold changes ($2^{-\Delta\Delta CT}$) relative to the lowest expressed gene, with the standard error also adjusted above and below the mean in a similar manner.

Results

The volume fluid collected from the GV stage AND Blast stage uterine hornA was 1091 µl ± 442.48 and 798.83 µl ± 462.27, respectively. Although there appears be a numerical difference, these volumes were not significantly different (P=0.28), The protein concentration in uterine aspirates also did not differ significantly over time (P=0.82), averaging 7.36 ± 3.68 µg/µl making the average total protein collected per uterine horn just 6585.85 ± 4316.79 mg. Interestingly, the conductivity of the samples differed substantially between the GV and Blastocyst stages requiring the samples from each stage to be focused separately from one another for protein analysis. Analysis of the 2D SDS PAGE images yielded a total of 269 protein spots with definable boundary conditions in at least two gels (Figure 4.1). Estimated isoelectric points (PI) for identified spots ranged from a pH of 4.06 to 9.59, while molecular weight (MW) ranged from 25.4 to 79.1 kDa. Normalized volumes in the experimental composite gel ranged from 248 to 35,145 while the range across individual gels was 4 to 42,335. The

largest single spot in any gel or composite, based on normalized volume, was albumin. Composite gel analysis (Figure 4.1) identified 62 protein spots which showed a greater than 2-fold change over time. Of these, 28 spots were shown to have decreased abundance, while 34 showed increased abundance, between the GV and Blast stages (Table 4.2). Analysis of normalized volumes taken from individual gels shows only 16 of the 62 spots were significantly affected over time ($P<0.05$), with an additional 9 showing trends ($0.05<P<0.1$). Of the significantly altered spots, 10 decreased in abundance and 6 increased between the GV and Blast stages.

A group of 14 proteins that showed greater than a 2-fold change in protein abundance, high spot intensity (normalized volume) and were cleanly excisable from prep gels; were selected for identification by mass spectrometry. The LS MS-MS results showed evidence of keratin contamination with only two spots showing no peptide alignments to this ubiquitous protein. Despite this, all 14 spots were successfully identified with 100% probability, as determined by Scaffold 3, and had three or more unique peptide alignments (Table 4.3). Analysis of the isoelectric focusing point and molecular weight as determined by spot location and calculated from identified protein sequence showed acceptable correlation ($R^2_{PI}=0.7986$ and $R^2_{MW}=0.6963$) (Figure 4.3).

Bioinformatic analysis of the proteins identified as differentially abundant, shows the most significant families are dehydrogenases (5.97E-05) and oxidoreductases (8.92E-03). It should be noted that the genes identified in both these families are the same. Analysis of cellular location identified 13 with known intra-cellular localization and one, Protein-L-Isoaspartate (PIMT), as yet un-annotated. In addition to their intracellular localization, two proteins, carbonic anhydrase 2 (CA2) and clusterin alpha chain (CLU) are also annotated as being localized to the extracellular space (GO:115615). Two others, Ras related protein 11a (RAB11A) and pig glutathione s-transferase (GSTP1), are also

identified as localized in to the plasma membrane (GO:0005886). Analysis of the full porcine protein sequences using SignalP identified only one protein CLU with a significant signaling peptide (D=0.625) and with a cleavage site between amino acids 22 and 23, while randomized versions of this sequence failed to identify a signal peptide (Table 4.4). The D-score produced by SignalP is a weighted average of multiple predictive algorithms computed such that a value greater than 0.45 is considered to be a statistically significant indicator of a secretions signaling peptide (Peterson et al. 2011). Evaluation of the same sequences with SecretomeP would suggest that seven are secreted through alternative pathways (Table 4.4).

In terms of biological process all 14 identified proteins had multiple annotations, and all were associated with the term 'metabolic processes' (GO:008152) or one of its daughter terms. Ontology enrichment of all these proteins identified three significant terms including 'monosaccharide' (GO:0005996, P= 8.11E-06) and 'carbohydrate' (GO:0005975, P= 2.76E-05) metabolism as well as 'glycolysis' (GO:0006096, P= 2.84E-05). If only proteins which showed greater than 2-fold increase at the Blast stage were analysed the same terms were identified, while analysis of the proteins which show 2 fold decreases only enriches the term "glycolysis". Additional analysis identified two protein families that were significantly affected, oxido reductases (P= 6.41E-04) and dehydrogenases (P=2.05E-02).

From the proteins identified, eight were selected (* in Table 4.3) and their associated transcripts quantitatively assessed in the RNA extracted from uterine tissue samples taken following aspiration. All primer sets were found to have greater than 95% amplification efficiency and produced a single peak in the melting point analysis. In addition, all amplicons resolved to a single band on agarose gels and, when sequenced from both directions, matched the target sequences obtained from the NCBI database. Real time data for each gene of

interest and the endogenous control showed a normal distribution and no heteroscedasticity was detected. Data for the 18s transcript was both temporally (P=0.158) and spatially (P=0.5945) stable and it was, therefore, deemed appropriate for use as the sole housekeeping gene for the remainder of the analysis. No spatial differences were detected between the TUT and BUT segments of the uterine wall for any of the genes assayed. Three genes including phosphoglycerate dehydrogenase (3-PDGH), CA2 and RAB11A all showed significant changes (Figure 4.4). Transcript abundance for 3-PDGH and RAB11A increased by 20.16($P<0.0001$) and 1.58 ($P=0.0417$) fold respectively while CA2 abundance decreased 36.72 fold ($P<0.0001$) between the GV and Blast stages. The five remaining genes of interest including malate dehydrogenase (MDHC), aldose 1 epimerase (GALM), phosphoglycerate kinase 1 (PGK1), aldehyde dehydrogenase 9A1 (ADH9A1) and triosephosphate isomerase (TPI) showed no significant change between the GV and Blast stages.

Additional assessment at the transcriptional level was conducted for CA2 and TPI1 against the cDNA collection representing the full temporal and spatial transcriptome of the uterus and oviduct described in Chapter 4. The resulting data was normally distributed, showed homoscedasticity and the endogenous control (18s) showed no temporal ($P=0.2961$ and $P=0.6356$) or spatial ($P=0.2681$ and $P=0.884$) variation within uterine and oviductal tissue respectively. No temporo-spatial interaction was detected for either gene of interest and all subsequent analysis was conducted separately for time and space. No spatial effects were detected for either TPI or CA2 in the uterus, however a 1.49 fold ($P=0.0072$) spatial decrease in TPI was detected between the AMP and IST. Temporally, CA2 showed a 9.65 fold ($P<0.0001$) decrease from the GV to 2cell stage in the uterus followed by a further 4.27 fold ($P<0.0001$) decrease from the 2cell to Blast stages for a total 41.24 fold ($P<0.0001$) decrease from the GV to Blast stages, while TPI remained unaffected (Figure 4.5). No significant

differences in transcript abundance were detected temporally within the oviduct for either TPI of CA2.

Discussion

Total protein aspirated from each uterine horn did not change over the time course of this experiment, which would initially suggest the histotrophic proteome is relatively quiescent. In this experiment, 269 protein spots were identified in the uterine histotroph which is consistent with the results for day 10 and 12 of gestation reported by Kayser *et al.* (2006) using similar methods. It is important to note that the spots detected using 2D SDS PAGE do not necessarily represent different proteins as post translational modifications can cause a single protein to migrate to more than one location on a 2D gel. If however, the number of spots is presumed to represent unique proteins, the number identified in this experiment is ~20 % lower than that obtained at day 7 of the estrous cycle in cattle (Mullen *et al.* 2012). This difference could be the result of species or temporal variation. However, it is possible this difference also results from the limited scope of 2D SDS PAGE, which is incapable of detecting proteins larger than 250 kDa and smaller than 10 kDa, or proteins that are poorly soluble. In addition, the isoelectric gradient used in this experiment limited the detection to proteins with a PI of between 3 and 10. A much smaller proportion 10.4% (28/269) of the proteins spots detected were identified as significantly differentially abundant relative to the 47% change identified in previous studies at day 10 and 12 (Kayser *et al.* 2006). This result would suggest that the proteome of the uterine histotroph is less dynamic during early embryo development than it is during the period of maternal recognition of pregnancy.

Average total protein content in this study was only 7 mg/horn at either the GV or Blast stages which is substantially lower than that reported by Tarleton *et al.* (2003) for untreated cyclic (14mg) or pregnant (32mg) gilts at day 12 of the estrous cycle or pregnancy (Tarleton *et al.* 2003). This difference may result

from methodological inconsistency, as the previously mentioned results are based on flushes of the uterine horn, while those from the present study are based on aspirated fluid volume. However, it is likely much of this difference is the result of increased histotroph volume, or protein content later in gestation. This difference therefore further supports the hypothesis that uterine proteins play a less significant role during cleavage stage development than during maternal recognition and implantation.

Analysis of the existing human ontology information for the identified proteins shows that while all of these proteins are known to exist in the cytoplasm, some are known to inhabit either the extracellular space (CA2 and CLU), while others are known to localize to the plasma membrane (GSTP1 and RAB11A). Analysis of the porcine sequences for the canonical signaling peptide indicating translocation across the endoplasmic reticulum, transit through the Golgi apparatus and vesicle export, confirms porcine CLU as an excreted protein (Table 4.4). No signaling peptide was detected for CA2, however, it is identified by SecretomeP as an extracellular protein, suggesting it is secreted through a non-classical pathway (Table 4.4). Additionally, five sequences were identified as potential extracellular proteins including RAB11A, PIMT, G3P, LDH-H and GSTO1, none of which are currently ontology annotated to this region (Table 4.4). The lack of matching annotation may be an artifact of the false-positive-prone high-throughput methods used for this form of annotation (Emanuelsson *et al.* 2007), the limited range of tissues that have been examined in this manner, or the sequence analysis methodology itself. Interestingly, seven of the proteins identified are not classified as secreted by any of the bioinformatics methodologies applied in this experiment. This discovery of apparently non secreted proteins is potentially an artifact of the manner in which histotroph was collected from the uterine horn. Cellular debris in the histotroph aspirates was removed by centrifugation prior to freezing to prevent contamination. However, it is possible the suction applied to the aspiration apparatus resulted in lysis of

the luminal epithelium during collection releasing intercellular proteins into the histotroph. While no evidence of damage resulting from the aspiration procedure was apparent along the luminal epithelium during subsequent dissection, the proteins identified suggest some cellular lysis must have occurred. It is also important to note that the methods of *ab inito* prediction of protein secretion are based on machine learning or protein sequences known to be secreted. As a result, failure to predict a signaling peptide does not preclude the proteins potential for excretion.

The CLU protein, which is known to localize to the extracellular space, showed a highly significant decrease in abundance between the GV and Blast stages in this experiment. While the function of this protein is somewhat ambiguous, it is thought to play a role in protecting cells during apoptosis of other nearby cells possibly through detergent-like action (Bailey and Griswold 1999). Interestingly, analysis of porcine sperm, oocytes, zygotes and embryos for CLU at the transcriptomic level suggests that this particular mRNA is delivered to the zygote by the sperm (Kempisty *et al.* 2008). Given the early delivery of this transcript to the porcine embryo, it is reasonable to assume that it is required early in development and prior to the zygotic genome activation (ZGA). The CLU protein has also been identified by 2D proteomic in the secretome of cultured rat sertoli cells (Kissinger *et al.* 1982) and in human seminal plasma at levels considerably higher than serum (O'Bryan *et al.* 1990). Given its increased histotrophic abundance in the present study during the GV stage, at the onset of standing estrus in the pig, it is possible this protein is also important in maintaining a suitable environment for sperm in the female tract. As a large portion of the sperm present in the female tract will die following insemination, CLU may play a role in protecting the surviving sperm, and later the embryos, from damage. Additional analysis of the CLU protein in the porcine uterus over the course of cleavage stage development is required to better understand its role in both sperm and embryo survival.

Two isozymes belonging to the glutathione S-transferase family, GSTO-1 and GSTP-1, were identified as having greater than 2-fold increases in abundance between the GV and Blast stages in the analysis of composite gels by Progenesis. Gene ontology analysis failed to localize either protein to the extracellular space, though GSTP-1 was indicated as belonging to the plasma membrane and sequence analysis with SecretomeP did however identify GSTO-1 as a secreted protein. Two GST proteins, P1 and A1, have been identified in seminal plasma, where they are thought to play a role in protecting sperm from oxidative damage (Raijmakers *et al.* 2003). If these proteins are in fact localized to the histotroph, it is possible they play a similar role to CLU in protecting the developing embryos from stress.

Bioinformatic analysis of the identified proteins also suggests that uterine metabolism is modulated during early embryo development. Gene ontology terms for both glycolysis and carbohydrate metabolism were identified as enriched. Proteins associated with glycolysis such as G3P and TPI showed decreased abundance, while portions of the citric acid cycle such as MDH2 are up regulated. In addition key proteins like 3-PGDH, the rate limiting enzyme in serine biosynthesis, are up regulated. Cellular metabolism is extremely complicated and there is insufficient information in this current study to understand the physiological role that regulation of these enzymes might play in maintaining a normal uterine environment.

Subsequent analysis of a subset of eight identified proteins at the transcriptomic level identified only two, CA2 and 3-PDGH with significant temporal changes in expression matching the change in protein abundance (Figure 4.4). A third gene, RAB11A was shown to vary temporally between the GV and Blast stages however the abundance of this transcript increased by only 1.58 fold (P=0.0417) and in the opposite direction of protein abundance. The remaining five genes assayed showed no significant change over time. The lack

of correlation between the transcript and protein abundances measured in this experiment may suggest that some of the histotrophic proteins are imported from an outside source. This conclusion is consistent with the previous results in the rabbit, which suggested some plasma proteins are selectively released into the oviductal lumen (Feigelson and Kya 1972). It should however be noted that the relationship between transcript and corresponding protein abundance is questionable (Anderson and Seilhamer 1997; Gygi *et al.* 1999; Greenbaum *et al.* 2003; Guo *et al.* 2008). While all the studies examining the link between these two values have been conducted in steady state systems it is clear that a direct relationship likely exists for only a minority of genes. The results of the present experiment may then simply suggest the majority of changes in the uterine histotrophic proteome are post-transcriptionally regulated.

The results for two proteins which showed highly significant temporal changes, one regulated at the transcriptomic level (CA2) and one showing no transcriptomic change (TPI) were validated in the much larger temporal spatial cDNA collection described in Chapter 3 (Figure 4.5). This analysis also shows that the CA2 transcript is substantially down regulated by the 2-cell stage. If the link between transcript and protein abundance observed at the GV and Blast stages is interpolated to these intervening stages, this result would suggest that CA2 is present in at high levels in the uterine histotroph only during estrus and decreases prior to cleavage stage embryo development in the uterus. The presence of CA2 in the uterine histotroph is therefore likely associated with creating an optimal environment for sperm within the female reproductive tract. CA2 belongs to a family of metalo enzymes that interconvert carbon dioxide and bicarbonate. While human semen has been shown to contain substantial concentrations of zinc, neither sperm nor seminal plasma show appreciable quantities of CA activity (Mawson and Fischer 1953). However, in the lumen of the epididymis, an acidic pH and a low bicarbonate concentration are known to play a role in maintaining sperm quiescence (Shum *et al.* 2009). In the epididymal

lumen these conditions have been shown to be generated by CA contained within the luminal epithelium (Cohen *et al.* 1976; Caflisch and DuBose 1990). In the epididymis CA2 is found specifically in the narrow cells of the initial segment and in the epithelial cells of the remaining segments, where it is proposed to play a role in the supply of protons for export into the lumen (Kaunisto *et al.* 1995). As other peptides identified in this experiment bring into question the true localization of the detected proteins, it is unclear if the observed changes in CA2 might occur in the uterine luminal epithelium or histotroph. However, it is clear that during the initial stages of estrus in the pig, uterine CA2 levels increase under transcriptional regulation.

Conclusions

The results of this study validate the application of high throughput proteomic methodologies to the study of reproductive physiology during early embryo development. In addition, they clearly show that extreme caution should be taken in the future collection of uterine histotroph, for which there is currently no ideal method. Comparison of the results from the present study to those conducted at later stages of pregnancy suggests that proteins play a less significant role during cleavage stage development than during maternal recognition of pregnancy. Analysis of the histotrophic proteome during this time period has however, generated a number of candidate molecules which may play a role in providing an optimal environment for sperm survival in the female tract. Both CLU and CA2 are known components of the seminal plasma and were shown to increase in abundance in the histotroph of animals at the onset of standing estrus prior to insemination. Also identified in the current study is the potential increased abundance of members of the GST family at the Blast stage, which may play a role in protecting the embryo from stress. Finally, it also appears that the metabolism in the uterus is altered during the GV and Blast stages; however there is insufficient information in the present study to fully understand the dynamics of this change. Finally, dissidence between the protein

and transcriptomic results obtained in the present study suggests that elements of the histotroph are either post-transcriptionally regulated in the uterus or are imported from another source. Additional work is required to validate the localization of the identified proteins to the extracellular space, assess the effect of these proteins on sperm and embryos, and clarify their source and regulation.

Tables

Gene Target	Sequence ID	Amplicon Length		Melting Point (°C)	Sequence
ADH9A1	XM_001924860	141	For	61.20	gcaaggcgaggtttgttgta
			Rev	60.01	aggggacccatccttgtatc
CA2	XM_001927805.1	111	For	60.07	atctgatgggcaaggttctg
			Rev	60.01	aacacccaaaacagccagtc
GALM	NM_214406	123	For	59.93	gcctgtggatgaaaccctaa
			Rev	60.05	tcaaagccattgatgtggaa
MDHC	NM_213874	141	For	60.16	gatggcatggagaggaaaga
			Rev	60.14	ggcagtcaggcagttggtat
3-PGDH	NM_001123162	144	For	60.27	accacgagaaggtcatcagc
			Rev	60.76	taagagcctgggcgtttaca
PGK1	NM_001099932	128	For	60.02	gaagggaagggaaaagatgc
			Rev	60.83	cggtgagcagtaccaaaagc
RAB11A	NM_001031788	123	For	58.55	gcgacgacgagtacgactac
			Rev	59.99	caatggtgctcttgctttca
18S	NR_046261	134	For	60.12	gacaaatcgctccaccaact
			Rev	59.85	cctgcggcttaatttgactc
TPI	NM_001037151	111	For	60.40	agctgattgggcagaaagtg
			Rev	60.11	aaacgaccttctcggtgatg

Table 4.1: Details of primer sets used for real time PCR. Melting point predicted by Primer3.

Gel			Normalized Spot Volume			MANOVA[+]
Spot#	PI (pH)	MW (Da)	Blast	GV	Fold Change	P value
199	4.995	55338.95	170.55	486.26	2.85	0.0004
195	4.435	40515.37	143.92	395.66	2.75	0.0005
387	6.02	27417.24	366.39	167.80	-2.18	0.0019
17*	6.395	25583.27	1157.92	471.18	-2.46	0.0027
5*	8.96	26451.43	4359.24	797.56	-5.47	0.0039
10*	7.005	26301.17	728.65	249.24	-2.92	0.0073
77	9.035	26971.67	1959.09	372.09	-5.27	0.0135
189	9.56	40515.37	477.52	1504.15	3.15	0.0151
218	5.67	25625.69	1168.40	396.79	-2.94	0.0177
186	7.995	25939.19	818.30	256.41	-3.19	0.0219
356	4.355	56947.31	94.42	215.41	2.28	0.0279
11*	4.785	31517.79	2454.83	764.88	-3.21	0.0308
335	5.985	72243.69	490.34	1148.77	2.34	0.0319
119	6.99	32608	234.88	58.21	-4.04	0.0331
299	7.145	52946.85	605.90	1509.01	2.49	0.0362
14*	7.07	27355.1	975.67	343.66	-2.84	0.0469
8*	9.185	34048.19	445.07	1628.47	3.66	0.05
4*	6.605	25451.72	514.53	2914.10	5.66	0.051
1*	7.99	26277.85	537.78	1835.51	3.41	0.0514
210	4.65	41483.98	441.19	1318.24	2.99	0.0596
249	6.25	42853.45	1131.30	440.12	-2.57	0.066
211	4.27	29382.92	2613.50	881.39	-2.97	0.0835
416	4.365	26179.42	144.75	69.88	-2.07	0.0836
82	6.645	25923.71	423.69	2155.96	5.09	0.0894
49	6.305	26890.17	253.64	35.42	-7.16	0.0999
315	5.19	44963.51	246.49	101.86	-2.42	0.1149
2*	8.96	25481.21	444.92	2716.72	6.11	0.1184
12*	7.24	25939.19	764.10	346.33	-2.21	0.1259
13*	7.39	52829.87	3944.57	11211.98	2.84	0.1307
3*	6.415	25488.87	116.93	704.38	6.02	0.1355
124	8.88	25968.64	1196.27	454.22	-2.63	0.1441
250	7.5	38587.6	356.08	129.35	-2.75	0.1442
215	5.1	25451.29	174.07	515.38	2.96	0.1487
176	5.755	27381.69	54.35	21.78	-2.50	0.1682
41	6.68	26385.53	364.55	137.33	-2.65	0.2129
18	5.585	36052.13	736.54	317.89	-2.32	0.2259
155	8.305	52017.95	384.05	1328.07	3.46	0.2322
435	4.435	40864.1	349.60	707.42	2.02	0.2398
217	9.29	29979.71	172.77	363.25	2.10	0.2543
6	4.565	40342.5	216.66	973.81	4.49	0.2647
58	8.945	28088.37	47.40	295.34	6.23	0.267
405	8.68	46267.1	764.81	364.80	-2.10	0.2679
7*	7.27	25745.16	50.22	186.80	3.72	0.2765
156	4.065	29471.99	368.81	862.29	2.34	0.2771
370	4.815	38587.6	114.29	254.31	2.23	0.2941
42	4.135	36867.11	17.76	150.01	8.45	0.3066
161	4.56	26733.9	86.31	37.69	-2.29	0.3219
332	9.225	28746.69	401.69	943.46	2.35	0.3604
441	6.245	25850.05	269.46	539.64	2.00	0.3639
319	7.485	35549.21	83.99	201.33	2.40	0.3823

273	9.345	27229.64	210.61	80.60	-2.61	0.4114
187	5.865	26493.4	439.92	208.98	-2.11	0.4238
290	8.175	51105	416.86	1054.52	2.53	0.4412
349	6.435	26712.24	77.81	178.53	2.29	0.4493
391	6.1	72243.69	441.95	954.96	2.16	0.455
158	4.125	29745.19	155.28	436.38	2.81	0.5194
131	4.61	26662.58	952.11	244.82	-3.89	0.5347
9*	5.965	52829.87	812.71	235.16	-3.46	0.6794
222	9.13	40689.24	227.07	568.66	2.50	0.7076
401	4.64	39077.78	364.31	768.61	2.11	0.8634
159	4.43	36641.85	329.82	698.57	2.12	0.8815
409	9.505	26814.57	293.94	140.55	-2.09	0.9516

Table 4.2: Spots with greater than a 2-fold change between the GV and Blast stage. Molecular weight (M.W.) and isoelectric point (PI) values predicted by Progenesis Same Spots based on protein ladder and X axis location respectively. Normalized volumes are retrieved from composite gels at the GV and Blastocyst stages. Spots are ranked based on P value resulting from MANOVA analysis performed on individual gel normalized spot volumes using GLM model of SAS to take into account multiple hypothesis testing. *Marks spots punched for Identification by mass spectrometry.

Spot	Gene Symbol	Protein Name	Database Identifier	Aligned Spectra	Unique Peptides	Predicted		Estimated		Fold Change	Pvalue
						PI	MW(Da)	PI	MW(Da)		
1	GSTO-1	Glutathione S-transferase Omega 1	Q9N1F5	5	3	6.84	27419	7.99	26278	3.41	0.0514
2	GSTP1	Glutathione S-Transferase Pi 1	p80031	36	9	8.07	23497	8.96	25481	6.11	0.1184
3	LDH-H	L-Lactate Dehydrogenase	P00336	3	2	5.57	36481	6.415	25489	6.02	0.1355
4	MDHC*	Malate Dehydrogenase	P11708	11	6	6.16	36323	6.605	25452	5.66	0.051
5	G3P	Glyceraldehyde-3-phosphotase	P00355	9	4	8.51	35705	8.96	26451	-5.47	0.0039
7	GALM*	Aldose 1 epimerase	Q9GKX6	6	4	6.31	37816	7.27	25745	3.72	0.2765
8	PGK1*	Phosphoglycerate Kinase 1	Q7SIB7	4	3	8.02	44559	9.185	34048	3.66	0.05
9	ADH9A1*	Aldehyde dehydrogenase 9A1	NP_001038076.1	11	8	6.43	56921	5.965	52830	-3.46	0.6794
10	TPI*	Triosephosphate Isomerase	Q1PC32	177	13	5.99	21848	7.005	26301	-2.92	0.0073
11	CLU	Clusterin Alpha chain	Q29549	4	3	5.61	48696	4.785	31518	-3.21	0.0308
12	PIMT	Protein-L-Isoaspartate	P80895	4	3	6.7	24515	7.24	25939	-2.21	0.1259
13	3-PGDH*	D-3-phosphoglycerate degydrogenase	NP_001116634.1	8	6	6.44	56810	7.39	52830	2.84	0.1307
14	CA2*	Carbonic anhydrase2	XP_001927840.1	15	6	6.49	29258	7.07	27355	-2.84	0.0469
17	RAB11A*	Ras related protein Rab11a	NP_001026958.1	21	7	6.12	23907	6.395	25583	-2.46	0.0027

Table 4.3: Protein identities for 14 selected protein spots as determined by RP-LC ES MS/MS. Data on isoelectric focusing point (PI) and molecular weight (MW) as predicted by gel image analysis and estimated from porcine sequence data. Proteins marked with * were selected for further analysis at the transcriptomic level using real time PCR.

			TargetP 1.1				SignalP 4.0		SecretomeP 2.0	
Spot	ID	Symbol	mTP	SP	Other	Target‡	D-score	Signal	NN-Score	Secreted
1	Q9N1F5.2	GSTO-1	0.531	0.034	0.561	_	0.115	N	0.516	Y
2	P80031.2	GSTP1	0.317	0.088	0.607	_	0.237	N	0.338	N
3	P00336.3	LDH-H	0.058	0.144	0.903	_	0.112	N	0.606	Y
4	P11708.4	MDHC	0.128	0.531	0.356	S	0.164	N	0.386	N
5	P00355.4	G3P	0.745	0.065	0.203	M	0.068	N	0.523	Y
7	Q9GKX6.1	GALM	0.226	0.061	0.759	_	0.111	N	0.49	N
8	Q7SIB7	PGK1	0.23	0.052	0.773	_	0.099	N	0.404	N
9	NP_001038076.1	ADH9A1	0.917	0.021	0.073	M	0.414	N	0.495	N
10	Q1PC32	TPI	0.056	0.091	0.93	_	0.131	N	0.331	N
11	Q29549.1	CLU	0.024	0.937	0.126	S	0.625	Y	0.608	Y
12	P80895.3	PIMT	0.212	0.044	0.78	_	0.053	N	0.512	Y
13	NP_001116634.1	3-PGDH	0.138	0.071	0.838	_	0.148	N	0.482	N
14	XP_001927840.1	CA2	0.073	0.071	0.929	_	0.11	N	0.675	Y
17	NP_001026958.1	RAB11A	0.073	0.073	0.89	_	0.104	N	0.506	Y

Table 4.4: *Ab initio* sequence analysis results for identified proteins. mTP: TargetP mitochondrial target peptide score, SP: TargetP signal peptide score, D-score: SignalP weighted average score values greater than 0.5 considered indicative of a signaling peptide, NN-score: SeretomeP neural networking score values greater than 0.5 considered indicative of a secreted protein. ‡ Top scoring TargetP location M: mitochondrial S: signal and _: unknown target

Figures

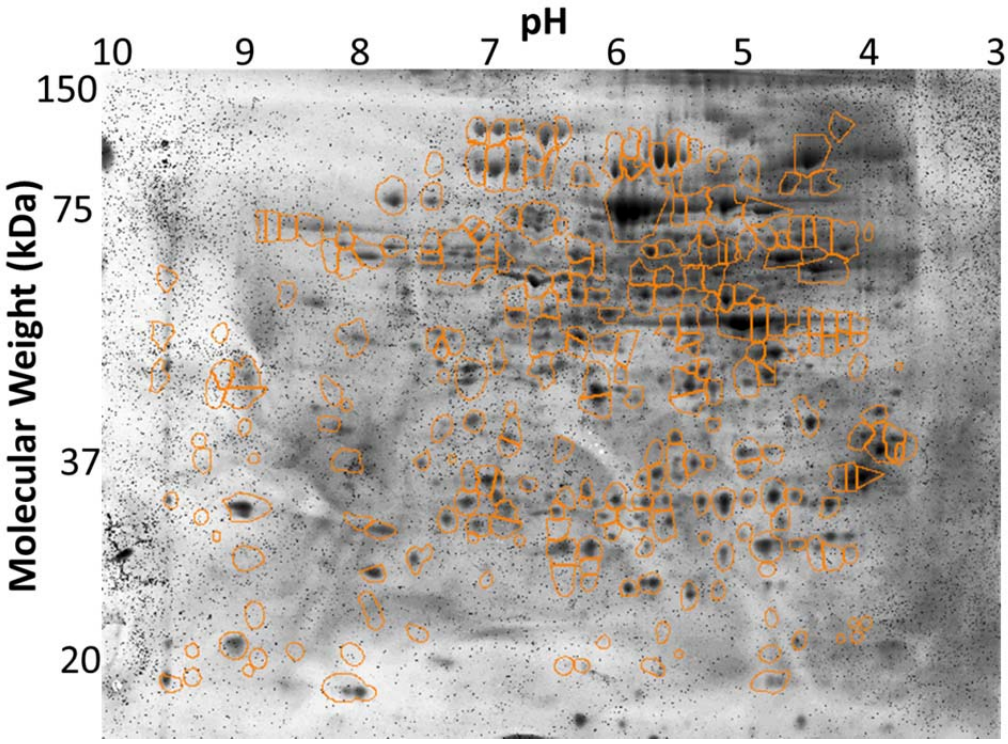

Figure 4.1: Experiment Level Composite Gel image showing all 269 identified spots. The pH and molecular weight (MW) ranges are shown on the horizontal and vertical axis, respectively.

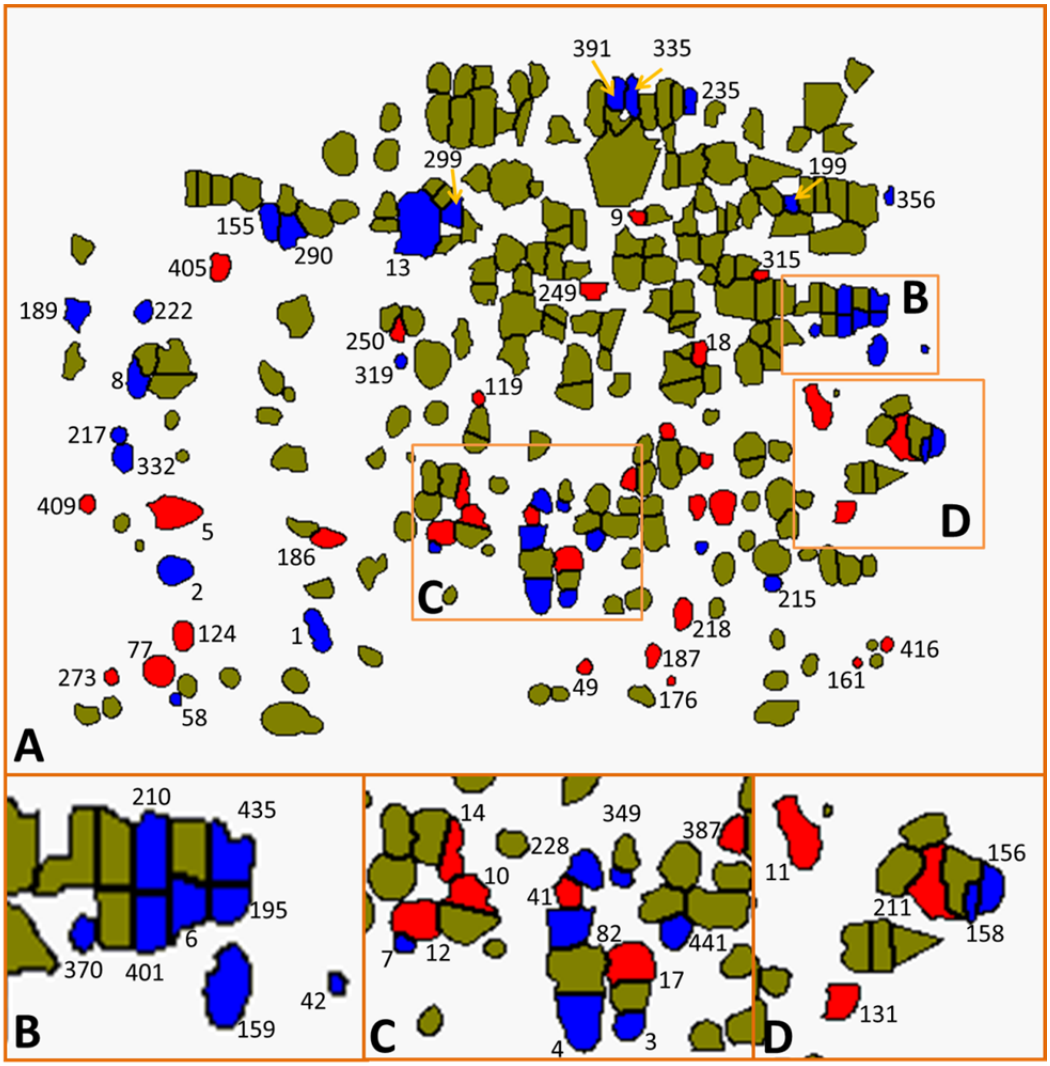

Figure 4.2: Composite Gel Analysis showing Spot ID's for the 62 proteins shown to increase (blue) and decrease (red) in abundance at the blastocyst stage relative to the GV stage.

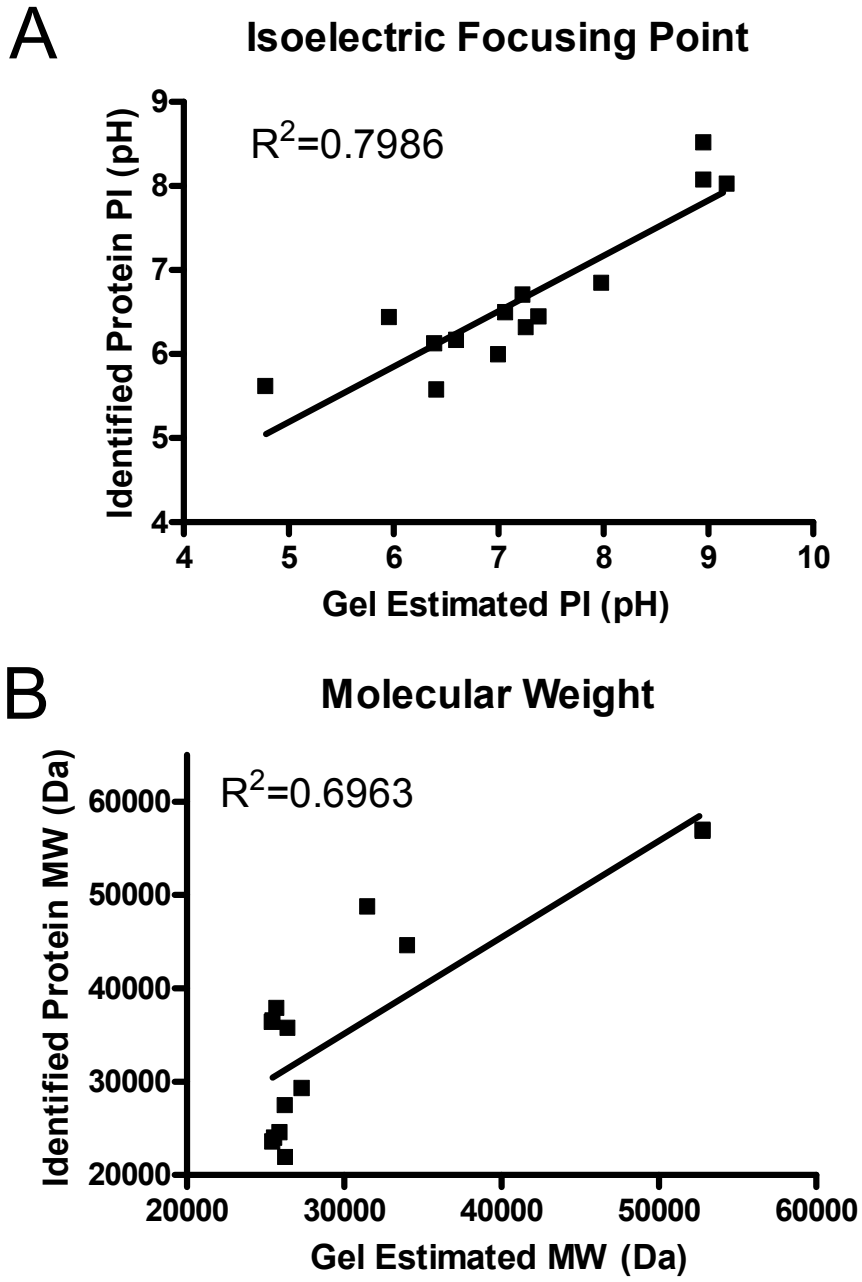

Figure 4.3: Relationship of A: Isoelectric Focusing Point (PI) and B: Molecular Weight (MW) obtained from analysis of 2D gel spot location and calculated from identified protein sequence.

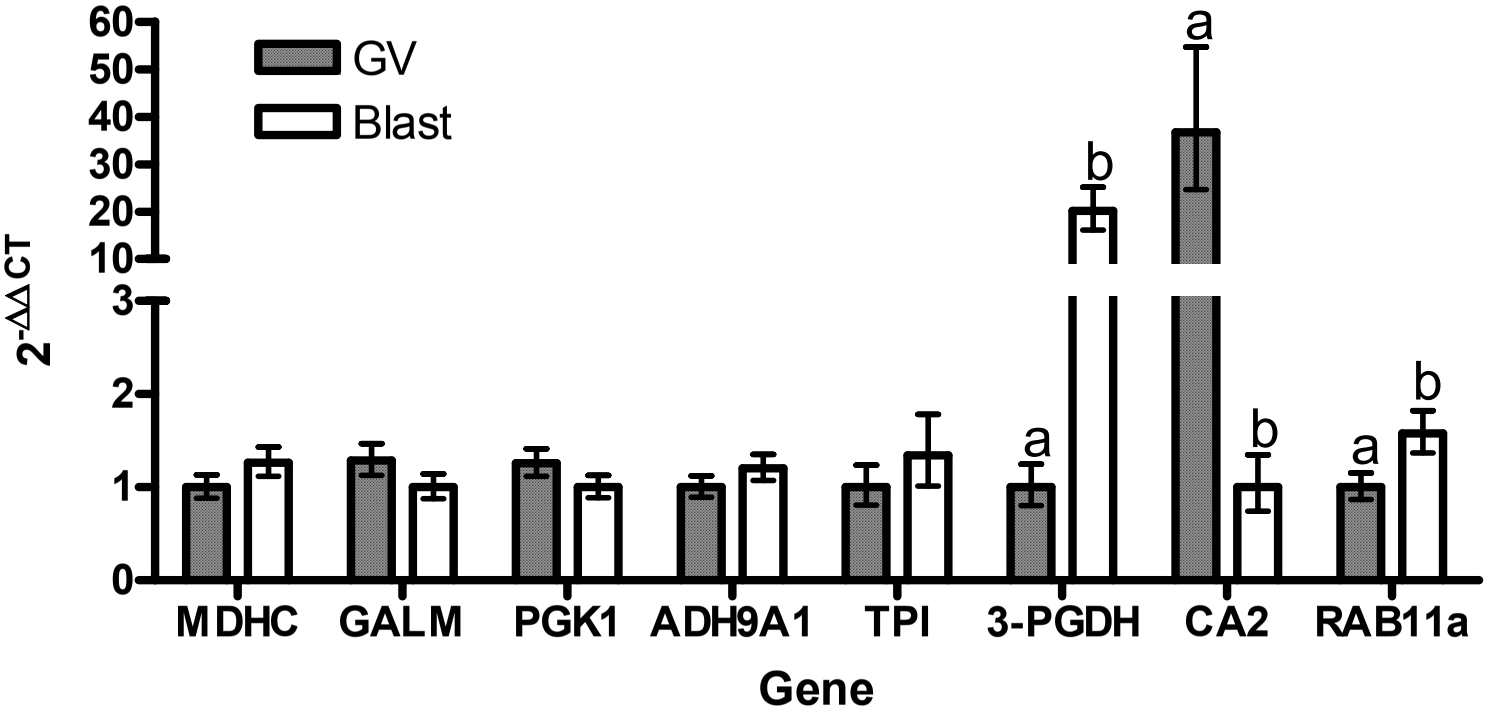

Figure 4.4: Associated transcript abundance for selected proteins as determined by real time PCR at time points corresponding to the oocyte GV stage (n=4) and the embryonic Blast stage (n=4). Data is presented as fold changes ($2^{-\Delta\Delta CT}$) relative to the point of lowest expression within a gene. Different letters represent statistical significance ($P<0.05$) within a gene. Error bars show exponentially corrected positive and negative standard error of the mean.

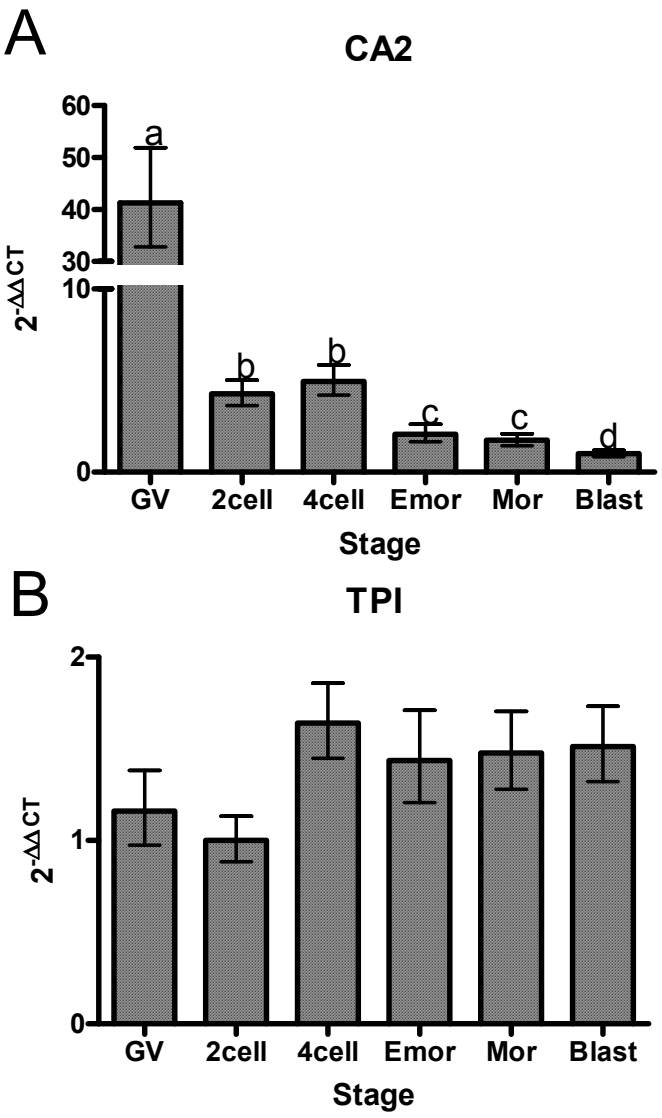

Figure 4.5: Relative expression of CA2 and TPI transcripts over the course of cleavage stage development as measured by real time PCR. Time points correspond to the oocyte GV (n=3) or embryonic 2cell (n=5), 4cell (n=4), Emor (n=2), Mor (n=3) and Blast (n=3) stages found in each animal at the time of slaughter. Data is expressed in fold changes relative to the point of lowest expression with different letters representing statistical significance ($P<0.05$) relative to this point. Error bars show exponentially corrected positive and negative standard error of the mean.

References

Adams, K.L., Bazer, F.W., and Roberts, R.M. (1981) Progesterone-induced secretion of a retinol-binding protein in the pig uterus. J Reprod Fertil 62(1), 39-47

Anderson, L., and Seilhamer, J. (1997) A comparison of selected mRNA and protein abundances in human liver. Electrophoresis 18(3-4), 533-537

Bailey, R., and Griswold, M.D. (1999) Clusterin in the male reproductive system: localization and possible function. Mol Cell Endocrinol 151(1–2), 17-23

Bendtsen, J.D., Jensen, L.J., Blom, N., von Heijne, G., and Brunak, S. (2004) Feature-based prediction of non-classical and leaderless protein secretion. Protein Eng Des Sel 17(4), 349-356

Caflisch, C.R., and DuBose, T.D. (1990) Direct evaluation of acidification by rat testis and epididymis: role of carbonic anhydrase. Am J Physiol Endocrinol Metab 258(1), E143-E150

Chen, T.T., Bazer, F.W., Cetorelli, J.J., Pollard, W.E., and Roberts, R.M. (1973) Purification and properties of a progesterone-induced basic glycoprotein from the uterine fluids of pigs. J Biol Chem 248(24), 8560-8566

Cohen, J.P., Hoffer, A.P., and Rosen, S. (1976) Carbonic Anhydrase Localization in the Epididymis and Testis of the Rat: Histochemical and Biochemical Analysis. Biol Reprod 14(3), 339-346

Doherty, A.S., Mann, M.R.W., Tremblay, K.D., Bartolomei, M.S., and Schultz, R.M. (2000) Differential Effects of Culture on Imprinted H19 Expression in the Preimplantation Mouse Embryo. Biol Reprod 62(6), 1526-1535

Emanuelsson, O., Brunak, S., von Heijne, G., and Nielsen, H. (2007) Locating proteins in the cell using TargetP, SignalP and related tools. Nat. Protocols 2(4), 953-971

Emanuelsson, O., Nielsen, H., Brunak, S., and von Heijne, G. (2000) Predicting Subcellular Localization of Proteins Based on their N-terminal Amino Acid Sequence. J Mol Biol 300(4), 1005-1016

Feigelson, M., and Kya, E. (1972) Protein Patterns of Rabbit Oviducal Fluid. Biol Reprod 6(2), 244-252

Fernandez-Gonzalez, R., Moreira, P., Bilbao, A., Jimenez, A., Perez-Crespo, M., Ramirez, M.A., Rodriguez De Fonseca, F., Pintado, B., and Gutierrez-Adan, A. (2004) Long-term effect of in vitro culture of mouse embryos with serum on mRNA expression of imprinting genes, development, and behavior. Proc Natl Acad Sci U S A 101(16), 5880-5885

Greenbaum, D., Colangelo, C., Williams, K., and Gerstein, M. (2003) Comparing protein abundance and mRNA expression levels on a genomic scale. Genome Biol 4(9), 117

Guo, Y., Xiao, P., Lei, S., Deng, F., Xiao, G.G., Liu, Y., Chen, X., Li, L., Wu, S., Chen, Y., Jiang, H., Tan, L., Xie, J., Zhu, X., Liang, S., and Deng, H. (2008) How is mRNA expression predictive for protein expression? A correlation study on human circulating monocytes. Acta Biochim Biophys Sin (Shanghai) 40(5), 426-436

Gygi, S.P., Rochon, Y., Franza, B.R., and Aebersold, R. (1999) Correlation between Protein and mRNA Abundance in Yeast. Mol Cell Biol 19(3), 1720-1730

Iritani, A., Sato, E., and Nishikawa, Y. (1974) Secretion Rates and Chemical Composition of Oviduct and Uterine Fluids in Sows. J Anim Sci 39(3), 582-588

Kaunisto, K., Parkkila, S., Parkkila, A.K., Waheed, A., Sly, W.S., and Rajaniemi, H. (1995) Expression of carbonic anhydrase isoenzymes IV and II in rat epididymal duct. Biol Reprod 52(6), 1350-1357

Kayser, J.-P.R., Kim, J.G., Cerny, R.L., and Vallet, J.L. (2006) Global characterization of porcine intrauterine proteins during early pregnancy. Reproduction 131(2), 379-388

Kempisty, B., Antosik, P., Bukowska, D., Jackowska, M., Lianeri, M., Jaśkowski, J.M., and Jagodziński, P.P. (2008) Analysis of selected transcript levels in porcine spermatozoa, oocytes, zygotes and two-cell stage embryos. Reprod Fertil Dev 20(4), 513-518

Khosla, S., Dean, W., Reik, W., and Feil, R. (2001) Culture of preimplantation embryos and its long-term effects on gene expression and phenotype. Hum Reprod Update 7(4), 419-427

Kissinger, C., Skinner, M.K., and Griswold, M.D. (1982) Analysis of Sertoli cell-secreted proteins by two-dimensional gel electrophoresis. Biol Reprod 27(1), 233-240

Knight, J.W., Bazer, F.W., and Wallace, H.D. (1973) Hormonal Regulation of Porcine Uterine Protein Secretion. J Anim Sci 36(3), 546-553

Koch, J.M., Ramadoss, J., and Magness, R.R. (2010) Proteomic Profile of Uterine Luminal Fluid from Early Pregnant Ewes. J Proteome Res 9(8), 3878-3885

Lee, B., Brown, K., Hathout, Y., and Seo, J. (2008) GOTreePlus: an interactive gene ontology browser. Bioinformatics 24(7), 1026-1028

Mullen, M.P., Elia, G., Hilliard, M., Parr, M.H., Diskin, M.G., Evans, A.C., and Crowe, M.A. (2012) Proteomic Characterization of Histotroph during the Preimplantation Phase of the Estrous Cycle in Cattle. J Proteome Res **11**(5): 3004-3018

Novak, S., Ruiz-Sanchez, A., Dixon, W.T., Foxcroft, G.R., and Dyck, M.K. (2010) Seminal Plasma Proteins as Potential Markers of Relative Fertility in Boars. J Androl 31(2), 188-200

O'Bryan, M.K., Baker, H.W., Saunders, J.R., Kirszbaum, L., Walker, I.D., Hudson, P., Liu, D.Y., Glew, M.D., d'Apice, A.J., and Murphy, B.F. (1990) Human seminal clusterin (SP-40,40). Isolation and characterization. J Clin Invest 85(5), 1477-1486

Paradis, F., Moore, H.S., Pasternak, J.A., Novak, S., Dyck, M.K., Dixon, W.T., and Foxcroft, G.R. (2010) Pig preovulatory oocytes modulate cumulus cell protein and gene expression in vitro. Mol Cell Endocrinol 320(1-2), 87-96

Petersen, T.N., Brunak, S., von Heijne, G., and Nielsen, H. (2011) SignalP 4.0: discriminating signal peptides from transmembrane regions. Nat Meth 8(10), 785-786

Raijmakers, M.T.M., Roelofs, H.M.J., Steegers, E.A.P., Steegers-Theunissen, R.é.P.M., Mulder, T.P.J., Knapen, M.F.C.M., Wong, W.Y., and Peters, W.H.M. (2003) Glutathione and glutathione S-transferases A1-1 and P1-1 in seminal plasma may play a role in protecting against oxidative damage to spermatozoa. Fertil Steril 79(1), 169-172

Schlosnagle, D.C., Bazer, F.W., Tsibris, J.C.M., and Roberts, R.M. (1974) An Iron-containing Phosphatase Induced by Progesterone in the Uterine Fluids of Pigs. J Biol Chem 249(23), 7574-7579

Searle, B.C. (2010) Scaffold: A bioinformatic tool for validating MS/MS-based proteomic studies. Proteomics 10(6), 1265-1269

Shum, W.W.C., Da Silva, N., Brown, D., and Breton, S. (2009) Regulation of luminal acidification in the male reproductive tract via cell-cell crosstalk. J Exp Biol 212(11), 1753-1761

Tarleton, B.J., Braden, T.D., Wiley, A.A., and Bartol, F.F. (2003) Estrogen-Induced Disruption of Neonatal Porcine Uterine Development Alters Adult Uterine Function. Biol Reprod 68(4), 1387-1393

Thomas, P.D., Kejariwal, A., Campbell, M.J., Mi, H., Diemer, K., Guo, N., Ladunga, I., Ulitsky-Lazareva, B., Muruganujan, A., Rabkin, S., Vandergriff, J.A., and Doremieux, O. (2003) PANTHER: a browsable database of gene products organized by biological function, using curated protein family and subfamily classification. Nucleic Acids Res 31(1), 334-341

Wright, P.C., Noirel, J., Ow, S.Y., and Fazeli, A. (2012) A review of current proteomics technologies with a survey on their widespread use in reproductive biology investigations. Theriogenology 77(4), 738-765.e52

Chapter 5: Analysis of Paired Transcriptomic Data for Extracellular Communication Networks

Introduction

Systems biology as a discipline is still developing and thus far has focused primarily on modeling systems at an intra-cellular level (Westerhoff and Palsson 2004). However, in order to understand the systems of development (Paradis *et al.* 2010), patterning (Blair 2007), differentiation (Nelson and Bissell 2006) and disease (Calorini and Bianchini 2010) in complex multicellular organisms, it is necessary to consider the signaling and communication both within and between disparate cells and tissues. Progress is being made towards system-based analysis of these higher level phenomena such as extracellular communication, and the information contained within interaction databases is rapidly evolving (Chautard *et al.* 2011). However, these interactions are often weak and transitory making them difficult to measure experimentally (Bushell *et al.* 2008). On the other hand, well developed transcriptomic methodologies such as RNASeq and microarrays have the potential to generate gene expression data with relative ease and minimal starting material. If this expression data is extrapolated to the ever growing protein-protein interaction databases, it becomes possible to infer potential extracellular communication pathways among different cells and tissues.

Tools such as STRING (Szklarczyk *et al.* 2011) and Bioverse (Chang, McDermott *et al.* 2005) have been developed for the identification and visualization of protein-protein interaction networks. However, these programs have primarily focused on internal cellular interactome analysis and, as such, are not designed to associate data from multiple expression sources. The increasing availability of raw transcriptomic data from published studies provides ready access to existing expression data on biologically-relevant interacting cells or

tissues. This existing data, combined with the ability to use gene ontology to narrow down extensive gene expression lists to factors found in the extracellular, membrane bound or receptor ligand groupings, makes secondary analysis of transcriptomic data for extracellular interactions feasible in nearly all situations.

Since many molecules participate in multiple signaling pathways, any inter-sample interaction analysis would be able to account for all potential forms of interaction or signaling (autocrine, paracrine, endocrine, juxtacrine, intracrine and extracrine) within a system for which information is available. Furthermore, as protein-protein interaction databases are constantly updated, especially with regards to extracellular interactions, it is desirable to draw on the most recent information available when exploring potential interactions. To our knowledge, no existing software is available to carry out analysis of protein-protein interactions between two paired data sets with the goal of identifying potential pathways for signaling or physical interaction both within, and between unique tissue or cell types. Here we present the Extracellular Protein Interaction Analyser 'EPIA', a novel application for identifying biologically meaningful signaling candidates from paired transcriptomic data sets. EPIA allows the user to input two genes lists which it annotates with interaction data, and then searches for matches within as well as between lists. Since these matches can be quite numerous, EPIA generates novel colour-coded three segment interaction matrices to show the database of origin for each identified interaction and to aid in the interpretation of the interaction data.

Methods

User Interface and Data Input

Gene list input is currently accepted in one of three types including RefSeq ID, GenBank gene ID and the official gene symbol. However, for reasons of stability and accuracy, it is recommended that where possible, analysis be carried out on lists of gene IDs. To date, most of the protein-protein interaction

data accessible by EPIA exists primarily in human, mouse, fly and yeast. Therefore, expressed and differentially-expressed gene lists from other species should be related to the nearest ortholog in one of these four species.

Primary Filtering and Annotation

EPIA is designed to identify extracellular interactions that make up a relatively small proportion of the existing protein-protein interaction databases so it is necessary to filter gene lists for elements capable of such interactions in order to minimize the "signal to noise" ratio of the results. EPIA contains a series of built-in and selectable filters based on gene ontology individual terms (Table 5.1). The primary filters (Table 5.2) are for the most part aggregates including genes from multiple gene ontology terms. These filters include the JAP (1-4) series, which are composites from ten terms with varying stringency generated by including genes present in an increasing number within these terms. Alternatively, users can pre-filter gene lists using any appropriate methodology prior to submission, however this limits gene list submissions to 1000 genes per tissue. Using the filtered gene lists, EPIA initially creates an up-to-date annotation file for each tissue within each analysis. This is done by automated collection of protein-protein interaction data for each list element from three curated human databases which include the Human Protein Reference Database (HPRD) (http://www.hprd.org/), Biological General Repository for Interaction Datasets (BioGRID) (http://thebiogrid.org/) and the Biomolecular Interaction Network Database (BIND) (http://bond.unleashedinformatics.com/).

Interaction Matching and Outputs

Following annotation, each gene list element is queried against all known interactants from the corresponding gene list to identify intercellular interactions. Each gene list element is then queried against all known candidates from its own gene list to identify self-interactions. Analysis with EPIA produces a set of seven tab delimited text files all of which are made available for download including: two annotation files, an inter-sample interaction file, two intra-sample

interaction files, a human readable interaction file and a file of elements found not to be involved in any interactions. To aid in the interpretation and publication of results, EPIA also produces a simple square interaction matrix or a three part matrix detailing both intra-sample and inter-sample interactions, both of which are colour-coded for the database of origin for each match (Figure 5.1).

Secondary Analysis and Backgrounds

Upon completion of the analysis, the results can be viewed and modified by applying built-in secondary gene ontology filters, which allow the user to focus the analysis further on specific types of cellular interactions. Like the primary filters these are inclusive filters (i.e. allowing only elements in the filter to be further processed) and include both individual terms and groupings of terms based on each of the three major gene ontology types (Figure 5.1). An additional built-in filter for genes previously identified as universally-expressed (Ramskold *et al.* 2009), is an exclusionary filter designed to remove interactions with genes which drastically decrease signal to noise ratio (e.g. ubiquitin). The secondary analysis options also allow the removal of internal self-interactions, defined as a gene that only interacts with itself in its tissue of origin. For complex multicellular organisms, EPIA provides a secondary analysis of each gene list against built-in background tissue and cell line expression profiles. These profiles were generated using publicly available microarray datasets found within the NCBI GEO database. The currently available background tissues are pre-annotated lists of expressed genes in human tissues based on data obtained from the NCBI GEO database. These tissues are from the "Large-scale analysis of the human transcriptome (HG-U133A)" (GDS596), expression cut offs were set at 2 standard deviations above the average expression for a 32 gene panel of tissue specific genes accumulated from existing literature for human and mouse (Kouadjo *et al.* 2007; Emig *et al.* 2011).

Discussion and Conclusions

EPIA represents a novel tool to identify potential interactions in large volumes of transcriptomic data from pairs of tissues or cell types. As it is only a first step toward systems level analysis of this type, EPIA suffers from two primary limitations. First, EPIA is not capable of estimating the statistical significance or probability of an interaction, and thus careful primary and secondary filtering using gene ontology is necessary to reduce the number of predicted interactions to a manageable number. Future work on the program will however focus on the development of statistical methods to rate interactions based on the expected number of interactions a single gene could form given information present in the databases. Such methods are likely to draw heavily on the existing statistical modeling used by the Basic Logical Alignment Search Tool (BLAST). The second limitation of EPIA, is its inability to detect interactions beyond those of a primary nature (Figure 5.2). In other words, EPIA is limited to the detection of interactions between the direct protein products of two genes, such as those between a peptide hormone and its receptor. Secondary interactions which rely on a non-protein intermediary are not detected.

As the program is heavily reliant on both gene ontology and protein-protein interaction databases, its use in non-standard model organisms will require the use of orthologous gene information. While much of this information is consistent across closely related species, the use of such information does add an additional degree of error to any interactions identified. However, in situations such as maternal embryonic cross-talk, where direct confirmation of signaling can be obtained using *in vitro* culture methods, the program represents a valuable starting point in narrowing the search for key molecules.

Tables

	GO Term ID	Go Term Name
Biological Process	GO:0007154	Cell Communication
	GO:0007165	Signal Transduction
	GO:0007267	Cell-Cell Signaling
	GO:0007565	Pregnancy
	GO:0016486	Peptide Hormone Processing
Cell Component	GO:0005265	Soluble Fraction
	GO:0005576	Extracellular Region
	GO:0005615	Extracellular Space
	GO:0005886	Plasma Membrane
	GO:0009986	Cell Surface
	GO:0031012	Extracellular Matrix
Molecular Function	GO:0001653	Peptide Receptor Activity
	GO:0004872	Receptor Activity
	GO:0005102	Receptor Binding
	GO:0005179	Hormone Activity
	GO:0017046	Peptide Hormone Binding
	GO:0024477	Peptide Binding
	GO:0042562	Hormone Binding
	GO:0043498	Cell Surface Binding
	GO:0050840	Extracellular Matrix Binding

Table 5.1: Gene ontology terms used by EPIA grouped by primary descriptor. Each term and major grouping also function as secondary filtering of EPIA output.

Filter	Filter Size (Genes)	Gene Ontology Terms
JAP1	6461	GO:0007154, GO:0005102, GO:0004872, GO:0005615, GO:0005576, GO:0031012, GO:0050840, GO:0007267, GO:0009986, GO:0043498
JAP2	2908[a]	
JAP3	1706[b]	
JAP4	752[c]	
Biological Processes	4185	GO:0007267, GO:0007154
Cell Component	2892	GO:0005615, GO:0005576, GO:0031012, GO:0009986
Molecular Function	2587	GO:0005102, GO:0004872, GO:0050840, GO:0043498
Cell-Cell Signaling	1035	GO:0007267
Receptor Binding	1073	GO:0005102
Extracellular Space	794	GO:0005615

Table 5.2: EPIA primary filter structure and identities. All filters are inclusive filters (ie. allow only gene in the list) [a] includes genes found in ≥ 2 terms [b a] includes genes found in ≥ 3 terms [c a] includes genes found in ≥ 4 terms.

Figures

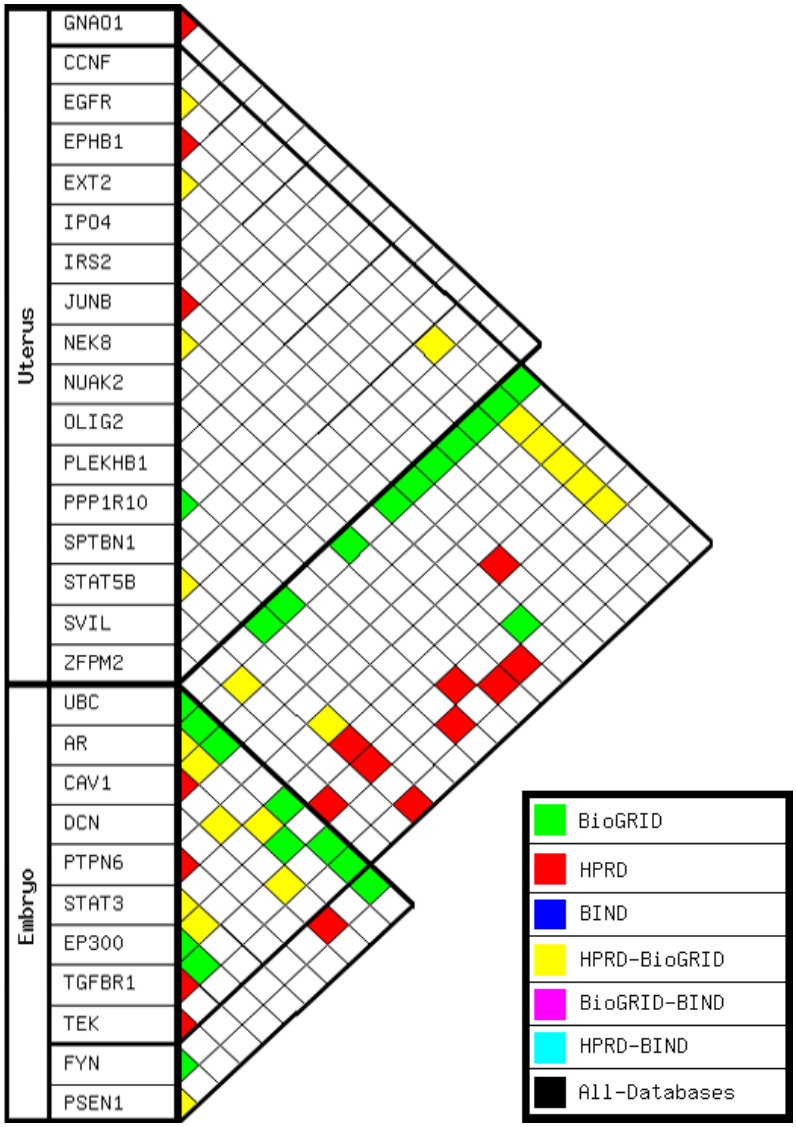

Figure 5.1: An example of EPIA's "full K-type" interaction matrix detailing the potential interactions between early stage embryos and uterus as well as within tissue interactions. Color coded squares represent matches identified in the BioGRID (green), HPRD (red) and BIND (Blue) databases.

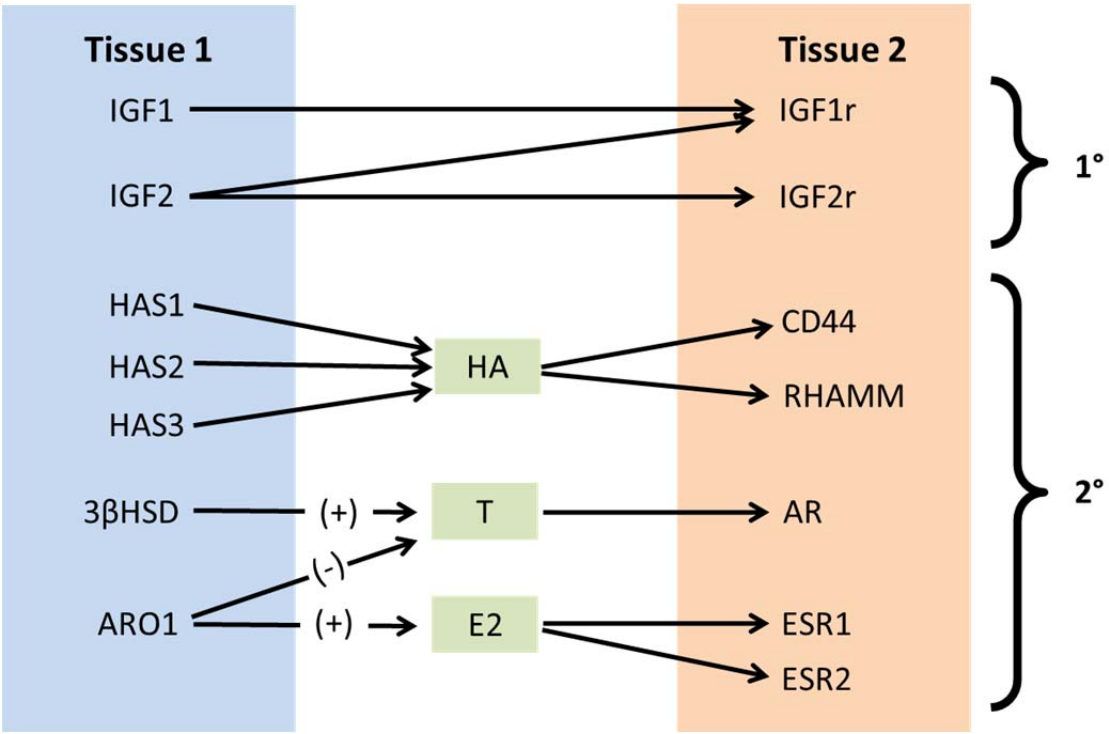

Figure 5.2: Examples of primary and secondary interactions: 1° interactions like the IGF2 system are detected while 2° interactions which include a non-protein intermediary such as HA (hyaluronic acid), T (Testosterone) or E2 (estrogen) are not detected.

References

Blair, S.S. (2007) Wing vein patterning in Drosophila and the analysis of intercellular signaling. Annu Rev Cell Dev Biol 23, 293-319

Bushell, K.M., Sollner, C., Schuster-Boeckler, B., Bateman, A., and Wright, G.J. (2008) Large-scale screening for novel low-affinity extracellular protein interactions. Genome Res 18(4), 622-630

Calorini, L., and Bianchini, F. (2010) Environmental control of invasiveness and metastatic dissemination of tumor cells: the role of tumor cell-host cell interactions. Cell Commun Signal 8, 24

Chang, A.N., McDermott, J., and Samudrala, R. (2005) An enhanced Java graph applet interface for visualizing interactomes. Bioinformatics 21(8), 1741-1742

Chautard, E., Fatoux-Ardore, M., Ballut, L., Thierry-Mieg, N., and Ricard-Blum, S. (2011) MatrixDB, the extracellular matrix interaction database. Nucleic Acids Res 39(Database issue), D235-240

Emig, D., Kacprowski, T., and Albrecht, M. (2011) Measuring and analyzing tissue specificity of human genes and protein complexes. EURASIP J Bioinform Syst Biol 2011(1), 5

Kouadjo, K.E., Nishida, Y., Cadrin-Girard, J.F., Yoshioka, M., and St-Amand, J. (2007) Housekeeping and tissue-specific genes in mouse tissues. BMC Genomics 8, 127

Nelson, C.M., and Bissell, M.J. (2006) Of extracellular matrix, scaffolds, and signaling: tissue architecture regulates development, homeostasis, and cancer. Annu Rev Cell Dev Biol 22, 287-309

Paradis, F., Moore, H.S., Pasternak, J.A., Novak, S., Dyck, M.K., Dixon, W.T., and Foxcroft, G.R. (2010) Pig preovulatory oocytes modulate cumulus cell protein and gene expression in vitro. Mol Cell Endocrinol 320(1-2), 87-96

Ramskold, D., Wang, E.T., Burge, C.B., and Sandberg, R. (2009) An abundance of ubiquitously expressed genes revealed by tissue transcriptome sequence data. PLoS Comput Biol 5(12), e1000598

Szklarczyk, D., Franceschini, A., Kuhn, M., Simonovic, M., Roth, A., Minguez, P., Doerks, T., Stark, M., Muller, J., Bork, P., Jensen, L.J., and von Mering, C. (2011) The STRING database in 2011: functional interaction networks of proteins, globally integrated and scored. Nucleic Acids Res 39(Database issue), D561-568

Westerhoff, H.V., and Palsson, B.O. (2004) The evolution of molecular biology into systems biology. Nat Biotechnol 22(10), 1249-1252

Chapter 6: Temporal and Spatial Characterization of the Uterine Transcriptome and Analysis of the Maternal Embryonic Cross-talk at the Blastocyst stage

Introduction

Both fertilization and embryonic development require specific luminal environments within the reproductive tract in order to proceed normally. The environmental requirements of gametes and early embryos are complex, involving a wide array of complex biomolecules including hormones (Strunker *et al.* 2011), amino acids (Swain *et al.* 2002), proteins (Buhi *et al.* 1990), carbohydrates (Flood and Wiebold 1988), glycosaminoglycans (Leese and Barton 1984) and lipids (Pratt 1980). In addition, the maternal immune system must be modulated to allow gametic and embryonic survival, while still preventing infection following insemination. The environment within the reproductive tract is maintained by a combination of the luminal epithelium present in both the oviduct and uterus and the endometrial glands found only in the uterus. Together these structures must not only generate the histotroph necessary to support embryonic development but also shield the gametes and embryos from the maternal immune system.

The bicornuate uterus found in swine has a small body and extremely long horns. Following oviductal to uterine transit at the 4-cell stage, approximately 48hrs after fertilization, porcine embryos will remain in the most distal portion of the uterus near the utero-tubular junction until hatching from the zona pellucida at the late blastocyst stage (Polge 1982). Previous experiments have shown that embryonic survival and development are significantly reduced when embryos are surgically transferred to more caudal regions of the uterine horns (Stein-Stefani and Holtz 1987; Wallenhorst and Holtz 1999). This would suggest that differences in the ability of the uterine

endometrium to support embryonic growth exist along the length of the uterine horn.

Historically, many aspects of the environment within the sow's reproductive tract such as the oviductal secretory proteins (OSP) and uterine lactoferrin (LF) have been shown to be regulated by maternal reproductive hormones such as estrogen and progesterone (Buhi *et al.* 1992; McMaster *et al.* 1992). Though the maternal hormones play a significant role in modulating the environment in the reproductive tract, it is well established that the porcine embryo is able to interact with this environment at day 11 of gestation in order to mediate maternal recognition of pregnancy (Bazer and Thatcher 1977). More recently however, transcriptomic profiling through suppressive subtractive hybridization (SSH) and microarray analysis have begun to show that the uterine tissue may be influenced much earlier by the presence of either gametes or embryos (Lee *et al.* 2002; Bauersachs *et al.* 2003; Georgiou *et al.* 2005; Georgiou *et al.* 2007). More specifically, microarray experiments in the pig have demonstrated a significant change in the uterine endometrial transcriptome in pregnant versus non-pregnant uterine horns at the blastocyst stage. As yet, two specific questions remain unanswered with regards to this effect. The first is how does the conceptus induce such a change in the uterine environment, when it consists of less than 150 cells and is contained within the zona pellucida? The second question is how far reaching this effect is within the large bicornuate uterine horns of the pig? In an attempt to answer these questions, a microarray experiment was designed to examine the temporal and spatial variation in the uterine endometrial transcriptome. In addition, analysis of the maternal-embryonic communication was conducted using transcriptomic data from microarray analysis of blastocyst stage embryos. While other experiments have sought to characterize the transcriptome of the uterus and its interaction with the developing embryo, to our knowledge this is the first such experiment to be

conducted during the first five days following fertilization and to take into account the potential for spatial variation.

Materials and Methods

Animals

All procedures were conducted in accordance within Canadian Council on Animal Care guidelines and with the approval of the University of Alberta, Animal Care and Use Committee for Livestock (Protocol #2006-11C). A total of 16 primiparous Landrace X Large White sows (Hypor, Regina,SK, Canada), were fed *ad libitum* up to and including first post weaning estrus followed by maintenance feeding as calculated based on post estrus body weight and back fat. Starting 18 days after first detected estrus, animals were heat checked twice daily using fence line contact with mature boars. Animals allocated to the germinal vesicle stage (GV) were slaughtered on day 1 of standing estrus. Animals allocated to the blastocyst stage (Blast) were subject to ovarian exam by transcutaneous real-time ultrasound at four hour intervals from the onset of standing estrus to ovulation. Ovarian images were examined for the presence of pre-ovulatory follicles, ovulation time, reported as the midpoint between last detection of pre-ovulatory follicles, and first detection of corpa hemoragica. Based on timing of ovulation animal euthanasia was scheduled at 125hrs post ovulation. Half of the animals at each stage were used for transcriptomic analysis using microarray and the other half used for real time PCR.

Sample collection

Following euthanasia, whole reproductive tracts were removed from sows through a midline incision and severance of the cervix at the most caudal internal point. Tracts were moved to an adjacent dissection suite where the broad ligament was removed allowing a total length measurement of each uterine horn from the uterine bifurcation to the utero-tubular junction. Each horn was then divided by ligature into three equal parts representing the

posterior (BUT), Middle (MUT) and Anterior (TUT) uterus. Each section was subsequently flushed with 20 ml of warm PBS using a blunted needle and glass flushing funnel inserted through a small incision. Embryos were isolated from each flush, imaged and staged using stereomicroscopy before flash freezing in micro-droplets. Each segment of the uterine horns were then opened longitudinally and tissue samples of the uterine wall flash frozen in liquid nitrogen. All samples were then stored at -80 °C until required for analysis.

RNA Isolation

Whole tissue sections from each uterine horn were ground to a fine powder using a mortar and pestle, under liquid nitrogen. Total RNA was extracted from 100 mg of ground tissue using Trizol (Invitrogen) with only minor modifications to manufactures instructions. In order to reduce phenol contamination RNA was initially re-suspended in 100 µl of nuclease free (nf) water (ABI) and then re-precipitated overnight with 100 µl isopropanol and 10 µl 3 M sodium acetate. After which, the RNA was pelleted at 15000 X G for 10 min, the supernatant removed and the pellet washed twice with 1 ml of ethanol and then re-suspended for a final time in a volume of 100 µl nf water. Concentration of RNA was determined by spectrophotometry and initial quality assessed based on the appearance of the 18 and 28S bands following electrophoresis on a 1.2% w/v denaturing gel containing SYBR Safe (Life Technologies). An aliquot of RNA was then DNAse treated using the DNA free kit (Ambion) with the addition of 1 µl RNAse inhibitor and then RNA concentration and quality reassessed as described above.

For real time PCR, reverse transcription using 2 µg total RNA from each sample from the right uterine horn was conducted with the High Capacity Reverse Transcription Kit (ABI) with the addition of RNAase inhibitor. Assuming complete conversion of RNA to cDNA, the resulting material was diluted to 10 ng/µl equivalent. Real Time PCR was conducted in duplicate using 20 ng cDNA (2 µl) per 20 µl reaction in 96 well plates on a 7900HT thermocycler (ABI).

Microarray

Equal quantities of total RNA from like segments of both uterine horns from two animals were pooled following the DNAse treatment described above. Final RNA cleanup was conducted using the RNeasy mini kit (Quiagen), and the final RNA quality determined using RNA 6000 nano kit and Bioanalyzer (Agilent) as per manufacturer's instructions. All RNA pools had RNA integrity numbers (RIN) greater than 9.0. First and second strand cDNA synthesis and *in vitro* transcription to produce anti-sense RNA (aRNA) with incorporated amino allyl nucleotides was conducted using the MessageAmp II kit (life technologies) with one modification to the manufacturer's protocol. The relative quantity of uridine-5'-triphosphate (UTP) to amino-allyl-UTP (aaUTP) in the *in vitro* transcription was increased from the manufacturer's recommended 1:1 ratio to a 1:3 ratio. This modification is made possible by the lack of a bulky side chain in aaUTP, and increased final signal strength. Following aRNA purification, RNA samples were sub-divided into two pools and coupled to either Cy3 or Cy5 mono-reactive dyes (Amersham Pharmacia). Excess dye was removed with the RNeasy kit (Qiagen) and dye incorporation determined on a Nano Drop spectrophotometer (Thermo Scientific).

PigOligoArrays (Garbe *et al.* 2010) were rehydrated, dried and then cross linked by exposure to 180 mJ ultra-violet light. The slides were then washed in 1% SDS solution for 5 min, rinsed in water and ethanol and then spun dry at 200 X G for 3.5 min. For each hybridization, a volume of Cy3 and Cy5 labeled RNA with incorporation equal to 160 pmol was mixed with 6 µl 20X saline sodium citrate (SSC) and 2.4 µl 2% SDS and then diluted to a total volume of 60 ul. The samples were loaded onto the microarrays under standoff cover slips and allowed to hybridize for 12 hrs at 55°C. Following hybridization, slides were washed in 2X SSC with 0.5% SDS, followed by 0.5 and 0.1X SSC and spun dry. Slides were scanned at 550 and 650 nm using a GenePix 4200AL (Molecular Devices) using automated determination of optimal photomultiplier tube voltage

(autoPMT). Feature mapping and extraction were conducted by hand on each slide using GenePix Pro 6.1 software (Molecular Devices).

Primary analysis of spot intensity files was carried out using the FlexArray V:1.6.1 (http://gqinnovationcenter.com/) interface to the Bioconductor (Gentleman *et al.* 2004) packages for R (http://www.r-project.org/). Microarray data for the uterus and embryos were analysed separately using an analysis pipeline consisting of the following steps: Background subtraction using the "Simple" method was first employed. Intra-array normalization was carried out using the print tip loess method, followed by inter-array normalization using the norm-between method. Finally, differential gene analysis was conducted for each biologically relevant temporal and spatial comparison available in the loop design (GV TUT vs GV BUT; GV BUT vs Blast BUT; Blast BUT vs Blast TUT; and Blast TUT vs GV TUT) using the Linear Models for Microarray Analysis (LiMMA) package (Smyth 2005). Thresholds for differential gene expression were set at greater than 2 fold change and significance of $P<0.05$ (Figure 6.2).

Bioinformatics

The secondary analysis of microarray data, unless otherwise specified, was carried out using human ortholog obtained from re-annotation of the PigOligoArray probes against NCBI's human RefSeq and Gene databases for the rational in Appendix A of this Thesis and by the methods described therein. Annotations were made to the Human Genome Organization Gene Nomenclature Committee (HGNC) official gene symbols. Commonality between differentially expressed gene lists generated for each temporal spatial comparison was assessed using VENNY (Oliveros 2007). Over-representation of HUGO gene families was determined using data from the HUGO database (http://www.genenames.org/) using the Fisher Exact test (Fisher 1922) as computed by R (http://www.r-project.org/).

All probes not flagged for abnormality, saturation or background and which had high quality annotations (see Appendix A) were used for Gene Ontology (GO) enrichment, using the 'background free' GOrilla algorithm described by Eden *et al.* (2009). In short, probes were ranked by fold change from smallest to largest (down-regulated) and largest to smallest (up-regulated) for each tempero-spatial comparison. Annotated gene symbols were submitted to the GOrilla server (http://cbl-gorilla.cs.technion.ac.il/) using an initial default P-value threshold of $P<0.01$ and enriching in all three primary ontology types. Piecewise regression analysis of the relationship between the resulting enrichment value and total number of known genes associated with a specific GO term was conducted on log transformed data using the non-linear regression procedure of (SAS), with initial estimates drawn from a LOESS surface regression procedure (SAS). Finally, gene lists associated with each enriched term as well as the relationship between terms were assessed using GoTreePlus (Lee *et al.* 2008) using current human gene ontology data that was obtained from the Gene Ontology Consortium (www.geneontology.org).

Potential protein-protein signalling pathways were identified using the Extra Cellular Protein Interaction Analyser (EPIA) described in Chapter 5. The PigOligoArray contains 60 negative control spots, of which 6 have been previously identified as consistently expressed at a high level in numerous experiments (Steibel *et al.* 2009). The average and standard deviation of A-values for the 54 valid negative control spots on the normalized embryo and uterine arrays was determined separately and a tissue specific expression cut off was set at 3 standard deviations above their respective means. The average A value of all remaining spots was then calculated and the expression cut off applied. Initially genes identified as either up- or down-regulated either temporally or spatially in the TUT at the Blast stage were run against the embryonic expressed gene list using the 'JAP1' primary filter and 'Biological process' secondary filter (see Figure 5.2) and the universal expression filter set to

'off'. Further analysis was conducted between the expressed gene from both tissues using the 'JAP1' Primary filter and the 'Cell-Cell Signalling' (GO:0007267) secondary filter and the 'universal expression' and 'internal self-interaction' filters set to 'on' due to the substantially larger total gene list in the uterus as well.

Gene Expression by Real Time PCR

Primer sets were designed against specific transcripts associated with ten microarray probes implicated in the hypotheses generated by microarray analysis along with three endogenous controls (Table 6.1). Transcript sequences were obtained from the NCBI RefSeq database where possible, or identified in other databases using the Basic Local Alignment Search Tool (BLAST). Primer 3 V.0.4.0 (http://frodo.wi.mit.edu/) software was used to identify primers which would amplify segments of between 100-150 bp of the target sequences. Where information was available in the Sscrofa 9.0 build, exon-exon junctions were identified using the Blast Like Alignment Tool (BLAT) and primers spanning these junctions were preferentially selected. No known transcriptional variants were identified for the genes of interest in swine, however, attempts were made to avoid regions of known transcript variance in humans. Selected primers were assessed for homo- and heterodimers using the IDT oligo analyser with a delta G cut off of greater than -7.55Kcal/mol and custom primer sequences were then produced by the company IDT.

Real time PCR was conducted against the small temporal and spatial collection of cDNA described in Chapter 4 of this Thesis. In short, this library included 4 biological replicates of uterine cDNA extracted from the TUT and BUT segments during the GV and Blast stages of embryonic development. Amplification efficiency for each primer set was assessed against a 6 point serial dilution of pooled uterine cDNA. To ensure no fluorescent signal associated with the amplification of any other double stranded sequence resulting from primer dimer or non-specific binding of the primer, post polymerase chain reaction

(PCR) melting point analysis was conducted. In addition, the PCR amplicon product was analysed by gel electrophoresis on a 3% w/v agarose gel illuminated by sybr safe (Life Technologies) and visualized on a Typhoon scanner (Amersham). The resulting bands were excised, purified and then sequenced from both directions using the Big Dye Direct Cycle Sanger Sequencing kit (ABI). Sequence data was then generated through capillary electrophoresis on a 3700 DNA Sequencer Analyzer (ABI), and aligned against the target mRNA sequence using the SECentral local alignment tool. All primers were validated with a single melting point consistent with that predicted for the amplicon and a single band and high quality sequence consistent with the target mRNA. Real time PCR was then conducted in duplicate using a 20 ng equivalent cDNA and SYBR green intercalating dye chemistry (Kappa). Cycle thresholds (CT) were manually set in the linear portion of the amplification curve and values averaged between replicates which differed by less than 0.2 cycles.

All real time PCR data was normalized against the geometric mean of CT values for three housekeeping genes including ribosomal RNA 18 S (18S), decorin (DCN) and serum response factor (SRF) determined to be the most stable by a algorithmic clone of gNORM (Vandesompele *et al.* 2002). The raw and normalized CT values were check for distribution normality and homoscedasticity prior to analysis using the Univariate procedure of SAS. Subsequent analysis was then carried out using the General Linear Model (GLM) of SAS on the normalized values ($\Delta CT = CT_{GOI} - C_{GEC}$). Data is presented in the form of $2^{-(\Delta\Delta CT)}$,where $\Delta\Delta CT$ is the difference between the mean sample ΔCT and the highest ΔCT value (lowest expression) for that gene. Standard error of the mean was independently corrected both above and below the mean for the exponential $2^{-(\Delta\Delta CT)}$.

Results

Microarray

With thresholds set at greater than a 2-fold change and $P<0.05$, microarray analysis yielded a total of 296 unique differentially expressed probes across the four temporal and spatial comparisons. Temporally, lists of 77 and 111 differentially expressed probes were detected in the TUT and BUT segments, respectively (Figure 6.2). Of the genes identified as temporally variable, a relatively equivalent number were up-regulated (68) as compared to down-regulated (79). Spatially, 127 probes were differentially expressed in uterine samples corresponding to the GV stage, while only 87 differential probes were identified at and Blast stage. Comparison of each differentially expressed probe list shows the highest degree of commonality (27 probes) occurs between the GV BUT vs Blast BUT and Blast BUT vs Blast TUT comparisons (Figure 6.3). In contrast, only 20 probes were identified as commonly differentially expressed between the comparisons of Blast TUT vs GV TUT and GV TUT vs GV BUT.

Annotation against the porcine and human RefSeq databases produced significant matches (BLAST E-value $< 1 \times 10^{-10}$) for 232 of the 296 differentially expressed probes (Table 6.2). However, while the total number of significant hits was equivalent, the number of matches against published and predicted sequences was substantially different between the porcine and human databases. When run against the porcine database only 47 probes were successfully matched to published sequences, with the remaining 186 being matched to predicted mRNA and non-coding sequences based on genomic sequence and minor transcriptional evidence (Table 6.2). Against the human database, all 232 probes were matched against published sequences, of which 8 were matched to known non-coding RNA. Furthermore, annotation against the human database yielded only 7 LOC and 7 ORF prefixed gene symbols and the remaining 218 being matched to established HUGO gene symbols (Appendix B). No single HUGO gene family was significantly enriched in the differential gene

list. However, eight members of the solute carrier family of proteins (SLC) including 25A18, 28A1, 2A4RG, 38A4, 43A3, 5A2, 5A7 and 6A1 were found in the list of temporally and spatially affected uterine genes. While 8 of the 231 currently defined SLC family members (3.46%) compared to 457 of 19,027 known genes (2.4%), differentially expressed genes is not a significant enrichment as determined by Fishers exact test (P=0.197), these genes are of particular interest with regards to changes in the uterine histotroph.

Gene ontology enrichment analysis of annotated genes using GOrilla, initially identified a total of 444 enriched terms ($P<1 \times 10^{-3}$) in the 4 temporal-spatial comparisons ranked for both up- and down-regulated genes. Piecewise regression analysis of the relationship between enrichment value calculated by GOrilla's, and the total number of known genes associated with a specific GO term (variable B), yielded a break point of 40 genes. Below this value, the enrichment scores and subsequent P-values are disproportionately affected by a low number of genes annotated to a specific term. As such, a cut off of B>40 was subsequently applied, along with a more stringent secondary P-value threshold of P<0.0001, resulting in a more manageable 90 enriched terms which can be found along with all relevant variables and statistics in Appendix C. For the primary ontology of Biological Process, regulation of response to stimulus (GO:0048583, P=1.03E-7), positive regulation of response to stimulus (GO:0048584, P=2.93E-6) and regulation of response to stress (GO:0080134, P=2.43E-5) were the top three terms identified as temporally down-regulated in the TUT samples (Table 6.3). At the same time, analysis of molecular function showed molecular (GO:0060089, P=2.25E-5) and signal (GO:004871, P=2.52E-5) transducer activity were significantly temporally up-regulated in the TUT (Table 6.3). Interestingly, these same two terms were identified as spatially down-regulated at the Blast stage (P=1.52E-5) (Table 6.3). Under the primary ontology of cellular component (GO:0005576, P=5.07E-7), extracellular region (GO:0005615, P=1.28E-6), space and region part (GO:0044421, P=1.58E-5) were

temporally down-regulated in the TUT, while the extracellular region part was found to be spatially up-regulated at the Blast stage (Table 6.3).

Of the 60 negative control probes distributed across the PigOligoArray probes identified by Steibel *et al.* (2009), 6 were found to have significantly higher expression than the remaining 54 negative control probes for both embryo (P=0.0001) and uterine (P=0.0002) arrays. As such, these probes were not included in the average signal intensity of negative control probes resulting in values of 7.022 (SD 0.754) and 5.9 (SD 1.069). Applying a limit of 3 standard deviations above the mean (9.28) to the average A values of the embryo array resulted in a total of 1470 probes being identified as expressed. Of these 1169 were successfully annotated with human gene symbols and used for analysis of the embryo uterine protein-protein interactions. When run against genes, either temporally or spatially up- and down-regulated in the Blast stage TUT, these analyses revealed a total of 14 up-regulated signals (Figure 6.4 and 6.6) and 42 down-regulated (Figure 6.5 and 6.7) inter-actions. Within the uterus only nine intra-actions were identified in all four analyses. In the embryo, a total of 67 intra-actions were identified in the genes implicated in potential inter-actions of which 38 were identified in the analysis of spatially down regulated genes. This analysis identified specific target signalling systems such as that of neurophillin 2 (NRP2) which is both temporally and spatially up-regulated in the Blast stage TUT. NRP2 is a known receptor for vascular epidermal growth factor alpha (VEGFA) which is temporally and spatially down-regulated in the uterus but expressed by the Blast stage embryo. A single uterine gene, Epidermal Growth Factor Receptor (EGFR) was identified as having 18 potential inter-actions as well as an intra-action with signal transducer and activator of transcription 5B (STAT5B) (Figure 6.7). Associated with the EGFR system, the gene tenascin C (TNC) was identified as being temporally up-regulated in both the BUT and TUT from the GV to the Blast.

Applying a signal intensity limit to the uterine microarray data resulted in 2721 expressed probes, of which 2321 were reliably annotated with human gene symbols. Comparison of this gene list with the previously mentioned 1169 'expressed' genes identified in the embryo using EPIA resulted in 31 inter-actions with 8 and 7 intra-actions, respectively (Figure 6.8). Two known signalling peptides were identified within the expressed genes analysis including low density lipoprotein receptor-related protein 2 (LRP2) and agouti signalling protein (ASIP). Each of these peptides was matched with a single peptide in the embryo and was not matched with any other uterine genes (Figure 6.8).

Real Time PCR

All primers showed greater than 95% amplification efficiency over a serial dilution of pooled uterine cDNA. In addition, all amplicons produced a single melting point, resolved to a single band on agarose gels and when sequenced from both directions matched the target sequences obtained from the NCBI database. The endogenous control genes 18S, DCN and SRF were each independently identified as stable across the temporal and spatial conditions analysed in this experiment (P=0.4596, P=0.3159 and P=0.6985 respectively). In addition, these genes were selected from a larger pool of potential housekeeping genes as the most stable group of three with their geometric mean also showing temporal spatial stability (P=0.1898).

All nine genes selected for validation by real time PCR were shown to be expressed in the uterus. Of the eight genes which belong to the SLC family identified as either temporally or spatially regulated, two were selected for validation by real time PCR. Contrary to the microarray results, analysis of solute carrier 5A2 (SLC5A2) identified no temporal or spatial variation (Figure 6.9A). In contrast, analysis of solute carrier 43A3 (SLC43A3) showed a significant 3.08 (P=0.0023) and 2.55- fold (P=0.0075) reduction from uterine samples corresponding to the GV and Blast stages, in the BUT and TUT segments, respectively (Figure 6.9B). The spatial variation suggested by the microarray

analysis for SLC43A3 was not significantly different. NRP2 showed a significant spatial variation but only during the GV stage where the BUT was 1.9-fold higher (P=0.011) than the TUT (Figure 6.10A). The VEGFA transcript was temporally regulated with a 1.8-fold increase in the TUT from the GV to Blast stages (P=0.048), however no significant difference was detected spatially (Figure 6.10B). Neither EGFR nor TNC transcripts showed significant temporal or spatial variation in this data set (Figure 6.11). However the downstream signaling protein STAT5B showed significant temporal variation with a 1.9- and 1.7- fold decrease from the GV to Blast stages in the BUT (P<0.0001) and TUT (P=0.0006) respectively. Finally of the three stably expressed genes identified by EPIA as potential signaling peptides only one, LRP2 was identified as temporally regulated, showing a 2.96 fold (P=0.0046) increase in the TUT from the GV to Blast stages. The remaining stably expressed gene, ASIP was shown to be expressed, but similar to the microarray results, showed no temporal or spatial variation.

Discussion

Based on the size of the differentially expressed gene lists the largest difference in the uterine transcriptome (127 probes) occurs spatially within the GV stage samples (Figure 6.3). In contrast, the spatial differences observed at the Blast stage uterine samples are substantially smaller (77 probes). This result would suggest that during the pre-ovulatory period the uterus is less regulated and that as embryonic development progresses the environment becomes increasingly harmonized. Temporally, variation between the GV and Blast samples was larger in the BUT segment than in the TUT segment in terms of both total and unique genes. As porcine embryos are maintained in the TUT segment of the uterus from the 4cell (48hrs post ovulation) to the hatched Blast stage (Polge 1982), such regulation would suggest the TUT segment of the uterus may make an earlier transition to a more tolerant environment for embryo development.

Gene ontology enrichment and other forms of secondary analysis of the microarray data focused primarily on the Blast stage TUT segment as this tempero-spatial condition matched with the known location of embryos for which transcriptomic data was currently available. The results of the ontology analysis suggest that functionally the TUT segment at the Blast stage temporally and spatially up-regulates signal and molecular transducer activity (Table 6.3). This increase in transducer activity would be necessary to increase the downstream cellular effect of weak signals such as those produced by the very early cleavage stage embryos in the case of maternal-embryonic cross-talk. This result is similar to that obtained in a previously published on transcriptomic analysis of the bovine endometrium during similar stages, which identified a substantial proportion of temporally and spatially regulated genes that were associated with signalling and transduction (Bauersachs *et al.* 2005). Biologically, the same tempero-spatial segment appears to temporally down-regulate its response to stimulus and stress (Table 6.3). As the uterus is known to become quiescent under the control of progesterone following ovulation (Grazzini *et al.* 1998), it is not surprising that the response stimulus is down regulated. In terms of cellular localization, ontology enrichment suggested proteins localized to the extracellular region were temporally and spatially down-regulated in the Blast TUT (Table 6.3). This particular result coincides with the findings presented in Chapter 5 of this Thesis, which suggests that the proteomic complexity of uterine histotroph is diminished relative to later stages of preimplantation development. Based on the results of the gene ontology enrichment, the majority of subsequent analysis focused primarily on the actions of the uterus with regards to maternal embryonic signalling. Also evaluated was the uterine ability to maintain an appropriate environment for cleavage stage embryo development.

The transcript for SLC5A2, which was identified by microarray as both temporally and spatially down-regulated in the Blast stage TUT, could not be validated by real time PCR and showed no significant change in either time or

space. SLC5A2 belongs to a family of genes that is involved in Na+-dependent glucose transport, and its down-regulation at the blastocyst stage would be surprising given the relative metabolism of the embryo during this period. On the other hand, the differential expression of SLC43A3 was temporally validated by real time PCR and showed significant down-regulation in the BUT and TUT segments (Figure 6.9B). SLC family 43 is made up of Na+ independent trans-membrane amino acid transporters (Ianculescu *et al.* 2009). While the favoured substrate of family members A1 and A2 are neutral amino acids, SLC43A3 remains an orphan transporter (Hediger *et al.* 2004). Human SLC43A3 has three known transcript variants whose sequences differ only in the 5' untranslated region; as such, if similar transcript variance existed in the pig, all three were measured by both the microarray probe and the real time PCR primers. The early activity of this sodium independent amino acid transporter is similar to the situation previously described in early murine embryos (Borland and Tasca 1974). The subsequent down-regulation of this Na+-independent transporter during the Blast stage may suggest that the uterus undergoes a similar change in amino acid transport.

The VEGFA ligand and one of its associated receptors, NRP2, were identified as temporally and spatially regulated in the uterus by microarray leading to the hypothesis that these factors may be involved in maternal-embryonic signalling. Analysis for potential interacting proteins identified NRP2, which was both temporally and spatially up-regulated in the Blast stage TUT, as a potential receptor for embryonic VEGF. While VEGF was identified as expressed in the Blast stage embryo, it was shown to be temporally down-regulated in both the BUT and TUT segments by microarray. While these genes play a known role in vascular development, it has also been suggested they may play a role in mediating the activity of the immune system (Stepanova *et al.* 2007). Furthermore, both of these genes have been shown to be tightly regulated in the mouse uterus by estradiol (Walter *et al.* 2010). Real time PCR analysis showed

both genes to be temporally and spatially regulated, however, the pattern of expression in the cDNA collection established in Chapter 5 varied substantially from that demonstrated by the microarray analysis. The NRP2 transcript as measured by real time PCR showed no significant temporal or spatial variation from the Blast Stage TUT and identified significant spatial variation at the GV stage (Figure 6.10A). Real time PCR analysis of VEGFA on the other hand showed a significant increase in abundance in the Blast stage TUT relative to all other tempero-spatial conditions (Figure 6.10B). The observed reversal of expression in these two transcripts may be the result of slight differences in the timing of blastocyst tissue collection between those samples used for microarray and those used to generate the cDNA library used for Real time PCR. The results of Walter *et al.* (2010) suggest that both these transcripts are acutely regulated in the uterus by estradiol, which could result in even small temporal differences producing significantly different results. In addition, the low number of animals used in both the microarray and real time PCR analysis means individual animal variation can have a substantial impact on results. Additional work will therefore be required to determine the true expression changes in these genes and their potential proteins.

In the analysis of potential interacting proteins conducted using EPIA, the gene EGFR, which was spatially down-regulated in the Blast stage TUT, had the most numerous interactions with embryonically expressed genes (Figure 6.7). EGFR is known to play a role in cell proliferation and fibroblast invasion (Kajanne *et al.* 2007), leading the hypothesis that it may play a role in regulating the maternal immune system during fertilization. In addition, this particular transcript has been identified in both its full and truncated forms in the preimplantation murine uterus (Tong *et al.* 1996). Two other genes known to be involved in the EGFR pathway, STAT5B and TNC, were also identified as differentially expressed in the microarray analysis. STAT5B, a known signal transducer and interactant of EGFR, was spatially down-regulated in a manner

similar to that of EGFR. STAT5B functions to mediate the EGFR signal from the cell membrane to the nucleus (Kegg pathway has:04012). TNC, which is known to have multiple EGF-like domains, was identified as temporally up-regulated in both the TUT and BUT segments at the Blast stage. Interestingly, the TNC protein has been previously localized to the subluminal stroma of the mouse and rat uterus, where it increases in response to progesterone (Michie and Head 1994; Noda *et al.* 2000). Analysis of transcript abundance via real time PCR failed to validate the differential expression of both EGFR and TNC. However, STAT5B was shown to be temporally down-regulated in the Blast stages BUT and TUT. Once again lack of validation may lie in the fact that a different group of animals was used in the two forms of analysis. Interestingly, previous analysis of the bovine endometrium also suggested that the EGFR system was temporally and spatially regulated particularly with the involvement of TNC (Bauersachs *et al.* 2005). As such, further work to verify the true expression pattern of these transcripts will be required.

Interacting protein analysis using the expressed gene lists extracted from the uterine and embryo array data, produced a substantial number of potential connections (Figure 6.8). From this list two genes were selected, the first of which, ASIP, was selected for its known extracellular localization and signalling function. It is important to note that none of these genes were identified as differentially expressed in the uterine microarrays. While ASIP is more commonly known for its ability to alter hair follicle pigmentation, it has also been shown to play a role in regulating lipid metabolism in adipocytes (Mynatt and Stephens 2001). Interestingly, the embryonically expressed gene melanocortin 4 receptor (MCR4) that was identified as a potential receptor for ASIP has also been implicated in the regulation of lipid metabolism (Boston and Cone 1996). Real time PCR confirmed the stable expression of ASIP in the uterus during the preimplantation period (Figure 6.12A), validating its potential role as a factor in early uterine-embryo cross-talk. If uterine derived ASIP does play a role in

regulating lipid metabolism in the Blast stage embryo it may be involved in controlling the shift toward lipids as the primary embryo energy source suggested in the Warburg effect hypothesis of Krisher and Prather (2012).

The second gene selected from the analysis of protein-protein interactions among expressed uterine and embryonic genes was the trans-membrane receptor LRP2. This particular transcript was also identified as stably expressed in the uterus by microarray, however, when assessed via real time PCR it was shown to have significantly higher expression at the Blast stage particularly in the TUT segment (Figure 6.12B). The LRP2 protein has been previously identified in the reproductive tracts of both male and female rats (Lustig 1997) and in the female appears to be primarily localized to the uterus during estrus (Wosu 1998). This particular protein is a member of the low density lipoprotein receptor family, and mediates endocytosis and degradation of specific ligands including apolipoprotein J and clusterin (CLU) (Hermo *et al.* 1999). Interestingly, CLU was identified in Chapter 5 as a histotrophic protein which was initially abundant in the GV stage uterus and decreased by greater than 3 fold by the Blast stage. Transcriptomic analysis of porcine sperm, oocytes, zygotes and embryos suggest that CLU mRNA is transported to the zygote by the sperm, further suggesting it is vital early in cleavage stage development (Kempisty *et al.* 2008). The increased expression of LRP2 at the Blast stage demonstrated by real time PCR, may explain the previous chapters findings that CLU content in the histotroph is reduced over time.

Much has been made of the dislinkage between mRNA abundance and protein abundance resulting from post transcriptional regulation, as reviewed by (Greenbaum *et al.* 2003). Previous literature suggests moderate to highly variable correlations between transcript and protein abundance (Anderson and Seilhamer 1997; Gygi *et al.* 1999; Guo *et al.* 2008). While it is true, substantial post-transcriptional regulation is likely to occur in any biological system, these

previous studies are all likely underestimating the biologically predictive value of transcriptomics for two reasons. First of all, three of these studies rely on 2D SDS PAGE to quantify protein abundance, which suffers from substantial problems with signal-to-noise ratio in particular with low quantity proteins. The most recent of these studies, also employed silver based photographic stain which, while extremely sensitive, has an extremely limited dynamic range. Second, and perhaps more importantly, all of these studies evaluate a single steady state with the exception of the most recent (Guo *et al.* 2008) that evaluated a steady state across numerous replicates. The correlation coefficients between transcript and protein in the previously mentioned experiments are drawn from many different genes and therefore more accurately represent the variability in post-transcriptional regulation between genes. Transcriptomic methodologies such as the ones employed in this study are not geared toward prediction in a steady state, but rather, evaluate the effect of an experimental condition. In particular, these methodologies evaluate the relative abundance of a gene between two points and thus predict a change in state. If the post-transcriptional regulation is assumed to remain relatively constant within a gene, a change in transcript abundance can be assumed to result in a change in the protein abundance. What is important to note however, is that while transcriptomic changes may be predictive, the relative effect of a change in abundance cannot be assumed to be constant across genes, as each has its own specific post-transcriptional and post-translational regulatory mechanisms. As high throughput methodologies are typically employed on small sample sizes, for cost reasons, there is also a substantial risk that the results will not be replicated in another sample group. This was demonstrated by the variability in the results obtained by microarray and real time PCR in this experiment. Additionally, while the databases of ontology interactions and pathways are large, they still represent only a small fraction of the potential functions for the large group of genes analysed. As a result, any conclusions drawn from such experiments must

be considered speculative and require additional experimentation to validate the quantification and biological significance.

Conclusions

To our knowledge this is the first experiment to assess the temporal and spatial variation in the uterine transcriptome over the course of cleavage stage embryo development in the pig. The results of the experiment suggest that following ovulation, the uterine environment becomes increasingly uniform along the length of the uterine horns. In addition, the top segment of the uterine horn responsible for maintaining porcine embryos following oviductal uterine transit appears to be more tightly regulated. Analysis of enriched gene ontology terms suggests that while the uterine response to stimulus is down-regulated, signal transduction activity is increased, supporting the hypothesis that maternal-embryonic communication begins earlier that previously suggested. Analysis of potential protein-protein interactions between the embryo and the uterus yielded a number of candidate communication pathways; however, temporal and spatial variation in only a small number of the genes involved could be verified by real time PCR in a similarly timed group of animals. Additional work will be required to elucidate the true expression patterns of these genes and show physiological function for their associated proteins.

Tables

Gene Target	Sequence ID	Amplicon size (bp)		Melting Point (°C)	Sequence
NRP2	XM_003360841	103	For	59	TCAAGACAGGCTCCGAAGAT
			Rev	60	GTGCAGTCCAAGTTGTGTGG
EGFR	NM_214007	147	For	60	ATCTGTAACCCGCTGTGCTC
			Rev	59	GGCATTCTCCACGAACTCTC
SLC5A2	XM_003481019	150	For	60	GTTACGCCTTCCACGAGGT
			Rev	59	GGAGCAGATGGTAGGAGTCG
STAT5B	XM_001929265	105	For	59	GTCGTGGAGCAGAGTCAGTG
			Rev	60	GGGACAGGGTCTTGACTTGA
ASIP	NM_001011647	120	For	60	GCAACTCCTCCATGAACCTG
			Rev	59	TCGAAGCCTTTTTCTTGGAA
TNC	NM_214230	124	For	60	ATTCTGGCTTGGACTGGATG
			Rev	60	GTCTCCCACGCTGAATCTGT
DCN	NM_213920	128	For	59	GGAATTGCCAGAGAAAATGC
			Rev	60	GGTTGGTGCCAAGTTCTACG
LRP2	AK393613.1	131	For	60	CAGATCAATGGCGATGAGTG
			Rev	59	CGGATACCTGGGTTGTTGTT
EEG1	BE232872	106	For	59	GCGTACTTTCCTCCTGATGC
			Rev	59	TGTCTTCCCTTCCTCTCTGG
SRF	XM_001929265	131	For	60	CCTCAACTCGCCAGACTCTC
			Rev	59	TATCCTTGGTCTCCCCACTG
VEGFA	NM_214084	150	For	59	GAGGCAAGAAAATCCCTGTG
			Rev	59	TCACATCTGCAAGTACGTTCG
18S	NR_046261	134	For	60	GACAAATCGCTCCACCAACT
			Rev	59	CCTGCGGCTTAATTTGACTC

Table 6.1: Details of primer sets used for real time PCR. Melting points predicted by Primer3.

Accession Prefix	Porcine	Human	Definition
NM_	47	224	Published mRNA sequences
NR_	0	8	Published non-coding RNA
XM_	178	0	Predicted mRNA
XR_	8	0	Predicted non-coding RNA

Table 6.2: Distribution of significant blast hits for differentially expressed genes against porcine and human RefSeq databases across NCBI accession prefix types. Threshold for significant match was established at E-value < X^{-10}.

		Blast BUT vs Blast TUT	Blast TUT vs GV TUT	GV BUT vs Blast BUT	GV TUT vs GV BUT
Biological Process	Up	axon guidance	--	regulation of neuron differentiation	cellular component movement
		taxis	--	regulation of neurogenesis	cell migration
		chemotaxis	--	regulation of nervous system development	enzyme linked receptor protein signaling pathway
	Down	regulation of purine nucleotide metabolic process	regulation of response to stimulus	axon guidance	cell-cell adhesion
		regulation of nucleotide metabolic process	positive regulation of response to stimulus	taxis	--
		lipid transport	regulation of response to stress	chemotaxis	--
Molecular Function	UP	phospholipid binding	molecular transducer activity	GTPase regulator activity	binding
		lipid binding	signal transducer activity	Rho guanyl-nucleotide exchange factor activity	actin binding
		binding		guanyl-nucleotide exchange factor activity	phospholipid binding
	Down	molecular transducer activity	endopeptidase activity	binding	Rho guanyl-nucleotide exchange factor activity
		signal transducer activity	metalloendopeptidase activity	actin binding	guanyl-nucleotide exchange factor activity
		receptor activity	--	cytoskeletal protein binding	Ras guanyl-nucleotide exchange factor activity
Cellular Component	Up	extracellular region part	--	--	synapse part
		--	--	--	cell junction
		--	--	--	--
	Down	--	extracellular region	cell junction	--
		--	extracellular space	cytoskeleton	--
		--	extracellular region part	plasma membrane	--

Table 6.3: Top three significantly enriched gene ontology terms as identified by GOrilla. Term names for up and down regulated genes in each tempero-spatial comparison within the primary ontology sections of Biological Process, Molecular Function and Cellular Component, are shown. Additional enriched terms and information regarding GO ID's, enrichment scores and P values can be found in Appendix C.

Figures

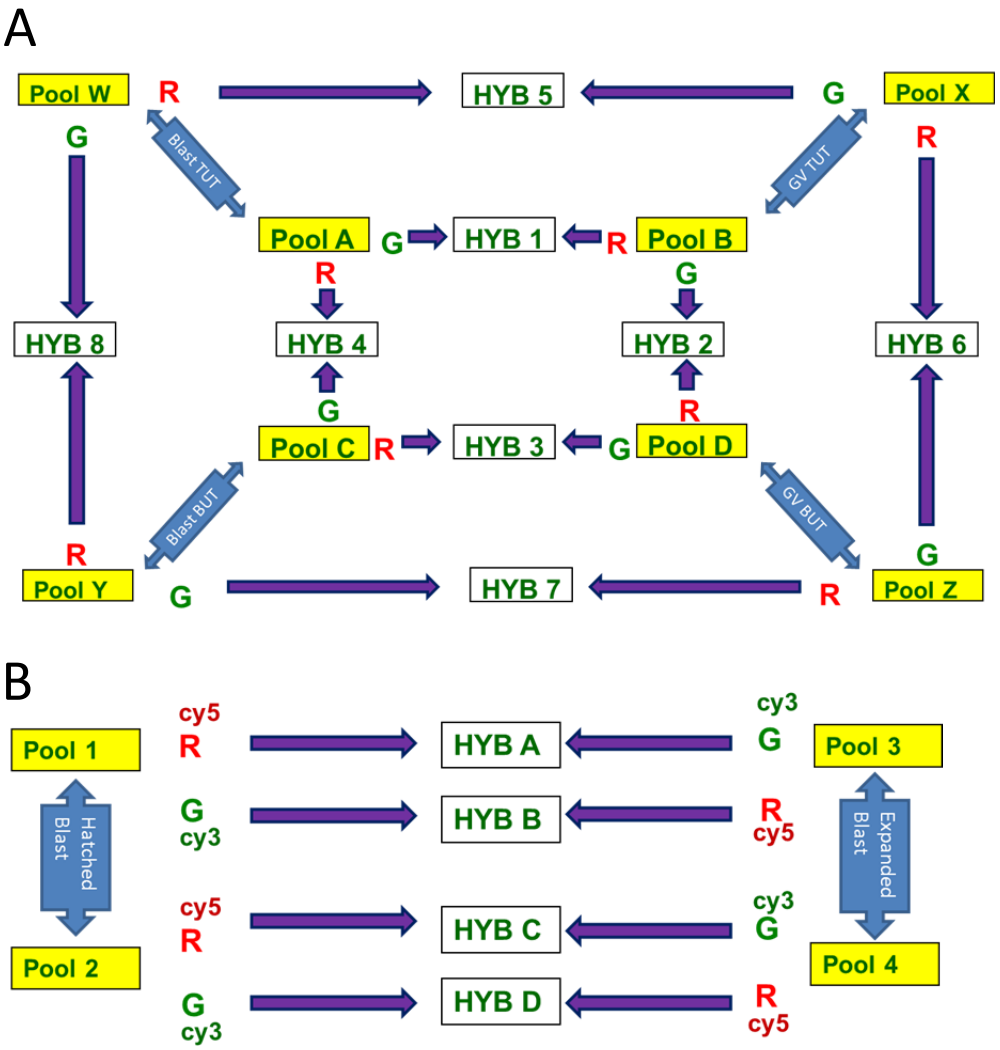

Figure 6.1: Microarray experimental design. A. Uterine microarray loop design, pool A-D and W-Z are each comprised of RNA from tissue corresponding to left and right uterine horn segments of two animals. B. Embryo microarray design, pools 1-4 are comprised of 5 embryos of a similar stage in development and from a single animal.

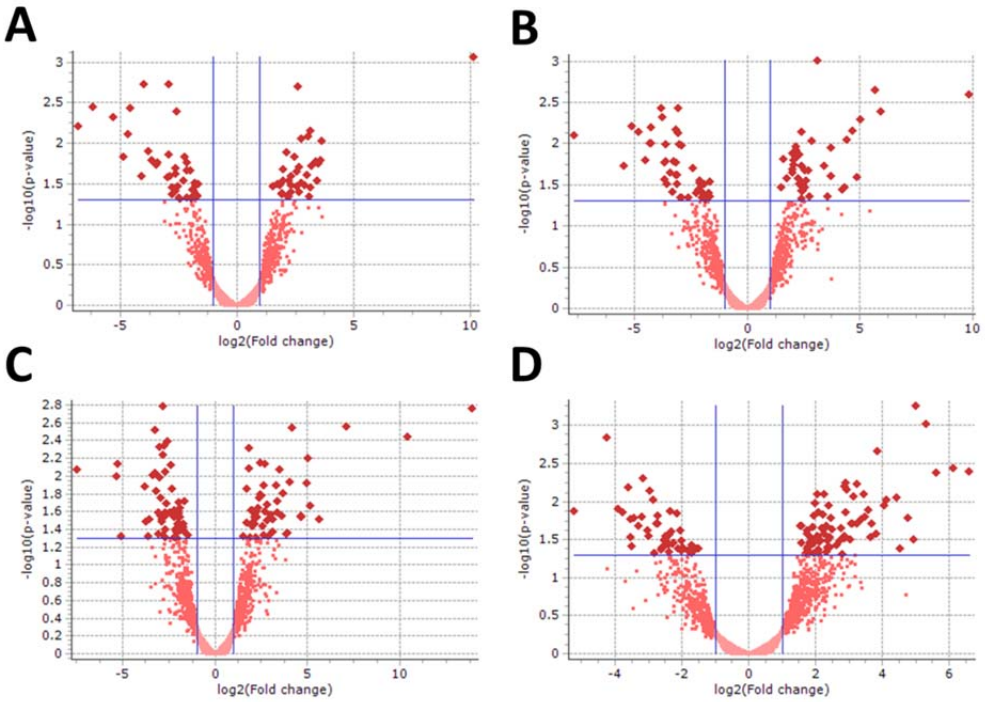

Figure 6.2: Volcano plots of differentially expressed probes for temporal and spatial comparisons A: Blast TUT vs GV TUT, B: Blast TUT vs Blast BUT, C: Blast BUT vs GV BUT and D: GV TUT vs GV BUT. Thresholds set at greater than 2-fold change and $P<0.05$ on log scales with probes above these thresholds bolded.

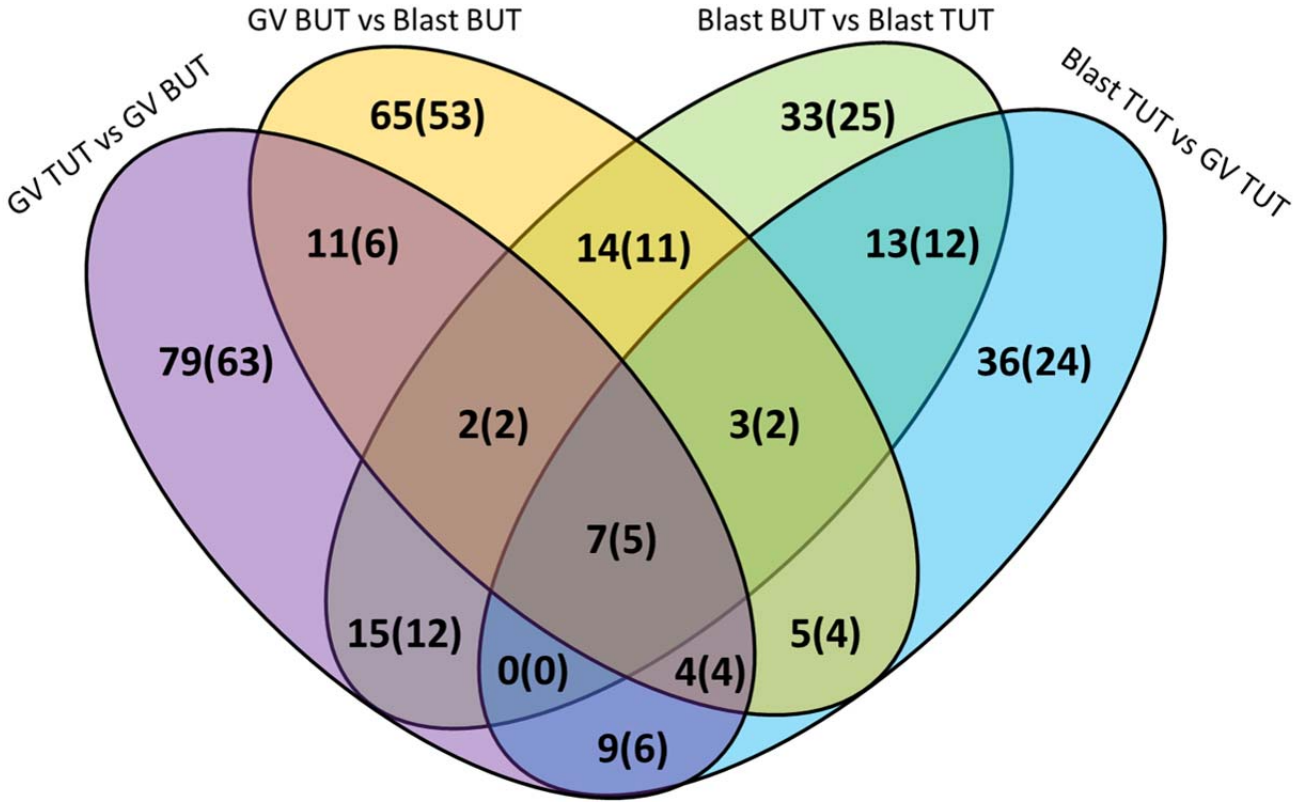

Figure 6.3: Four way Venn diagram showing commonality in probes identified as differentially expressed in each tempero-spatial comparison of the microarray data. Number of probes annotated to unique genes is shown in brackets.

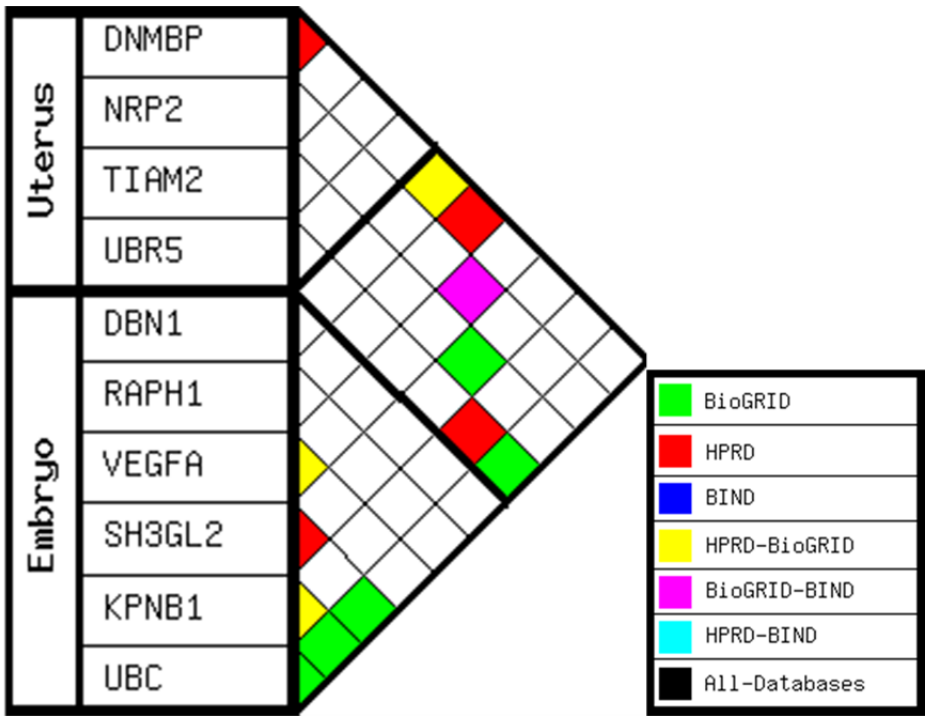

Figure 6.4: Known protein-protein interactions identified by EPIA for corresponding genes identified as temporally up-regulated in the Blast TUT relative to the GV TUT and those identified as expressed in the blastocyst stage embryo. Analysis was conducted using the 'JAP1' primary filter, 'Biological Process' secondary filter and with the universal expression filter set to 'off'.

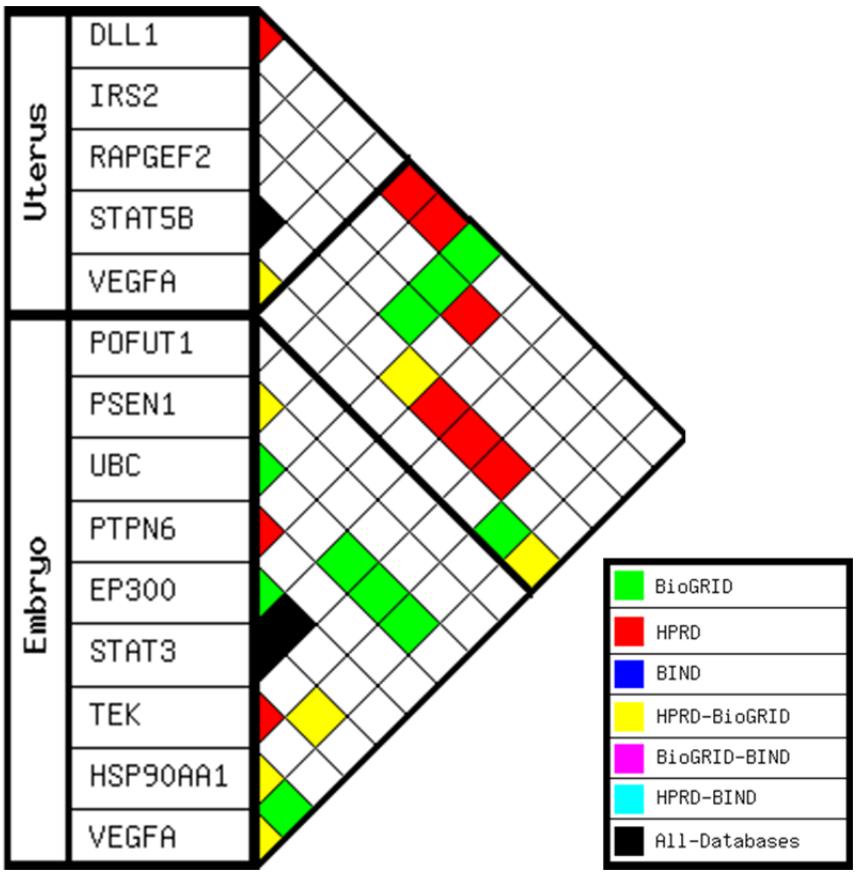

Figure 6.5: Known protein-protein interactions identified by EPIA for corresponding genes identified as temporally down-regulated in the Blast TUT relative to the GV TUT and those identified as expressed in the blastocyst stage embryo. Analysis was conducted using the 'JAP1' primary filter, 'Biological Process' secondary filter and with the universal expression filter set to 'off'.

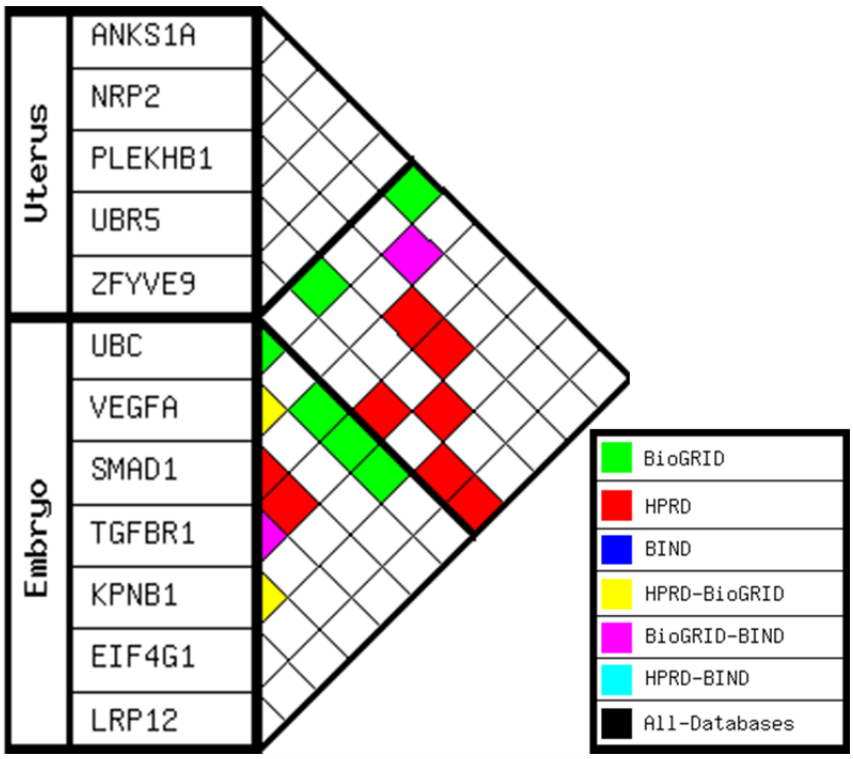

Figure 6.6: Known protein-protein interactions identified by EPIA for corresponding genes identified as spatially up-regulated in the Blast TUT relative to the GV TUT and those identified as expressed in the blastocyst stage embryo. Analysis was conducted using the 'JAP1' primary filter, 'Biological Process' secondary filter and with the universal expression filter set to 'off'.

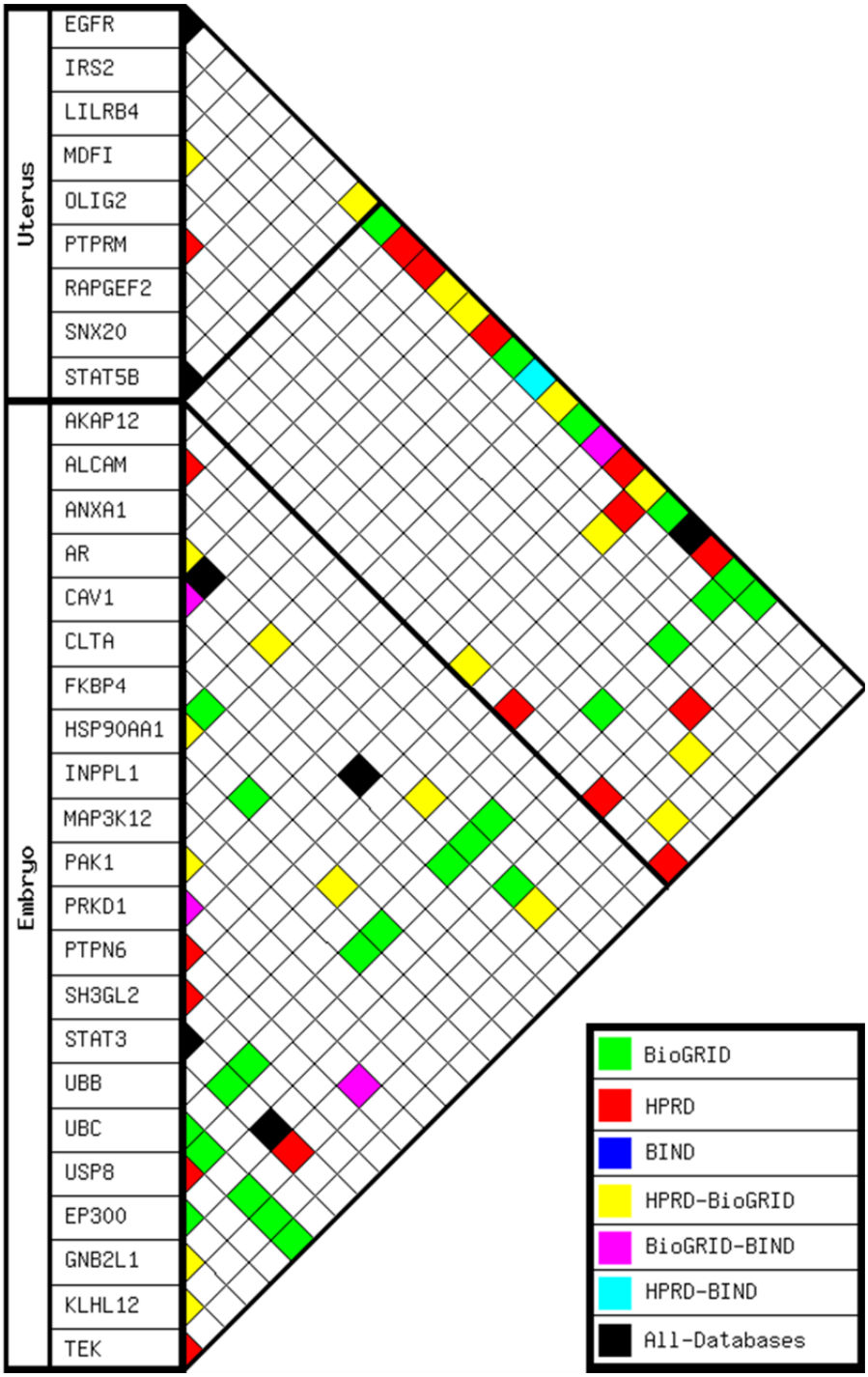

Figure 6.7: Known protein-protein interactions identified by EPIA for corresponding genes identified as spatially down-regulated in the Blast TUT relative to the GV TUT and those identified as expressed in the blastocyst stage embryo. Analysis was conducted using the 'JAP1' primary filter, 'Biological Process' secondary filter and with the universal expression filter set to 'off'.

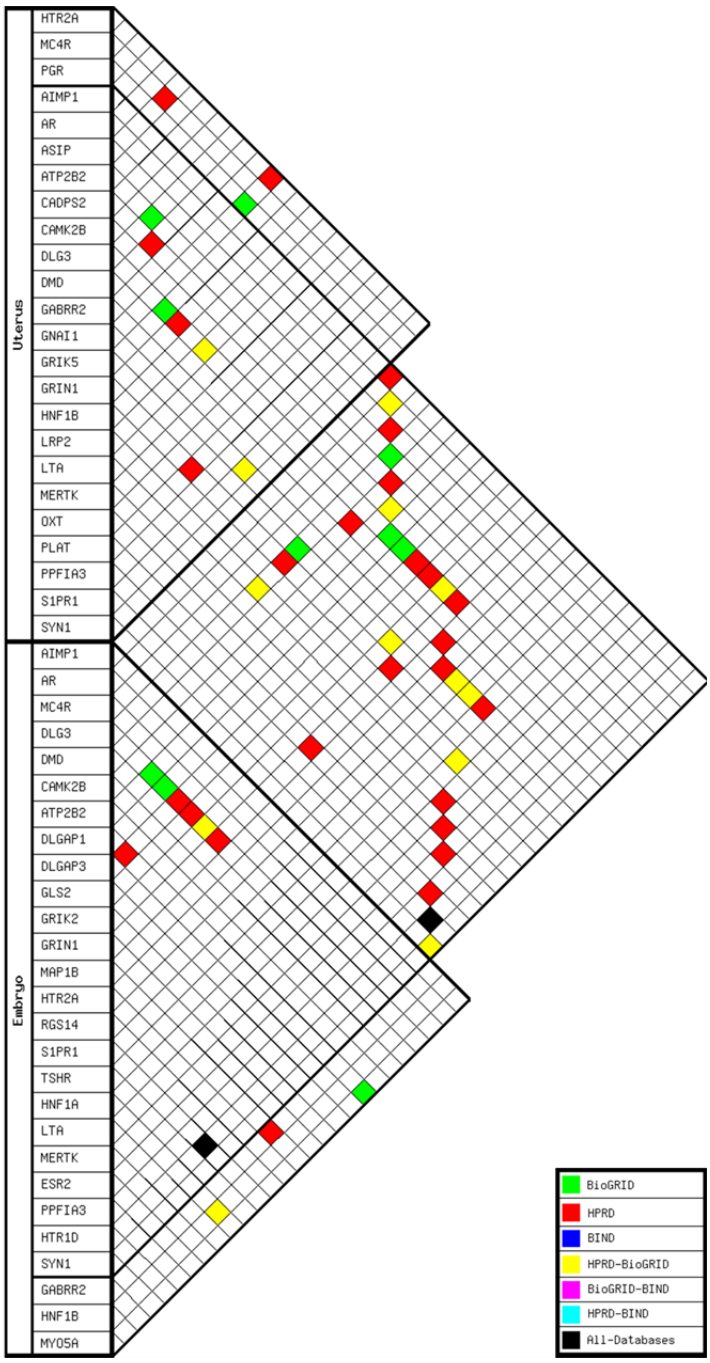

Figure 6.8: Known protein-protein interactions identified by EPIA in 'Full K-type' format for gene identified as expressed in the embryo and uterine array data. Analysis was conducted using the 'JAP1' primary filter, 'Cell-Cell Signaling' secondary filter and both the 'universal expression' and 'internal self interaction' filters set to 'On'.

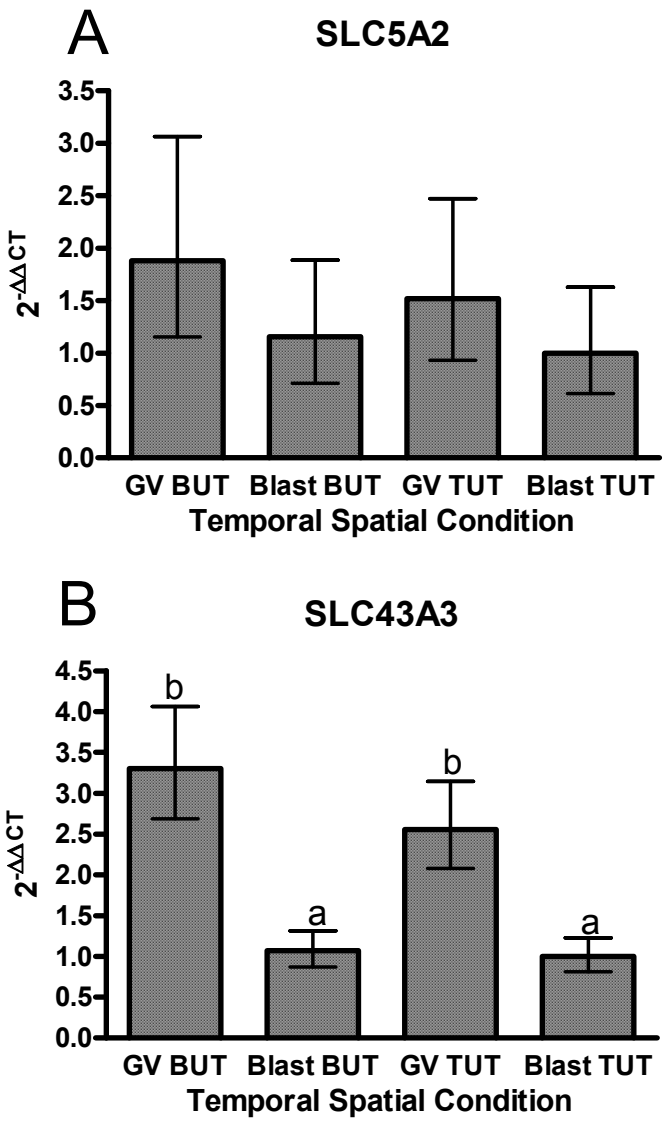

Figure 6.9: Relative expression of SLC5A2 and SLC43A3 transcripts as determined by real time PCR. Tempero-spatial conditions include GV BUT (n=4), Blast BUT (n=4), GV TUT (n=4), Blast TUT (n=4). Data is expressed in fold changes relative to the point of lowest expression with different letters representing statistical significance ($P<0.05$) relative to this point. Error bars show exponentially corrected positive and negative standard error of the mean.

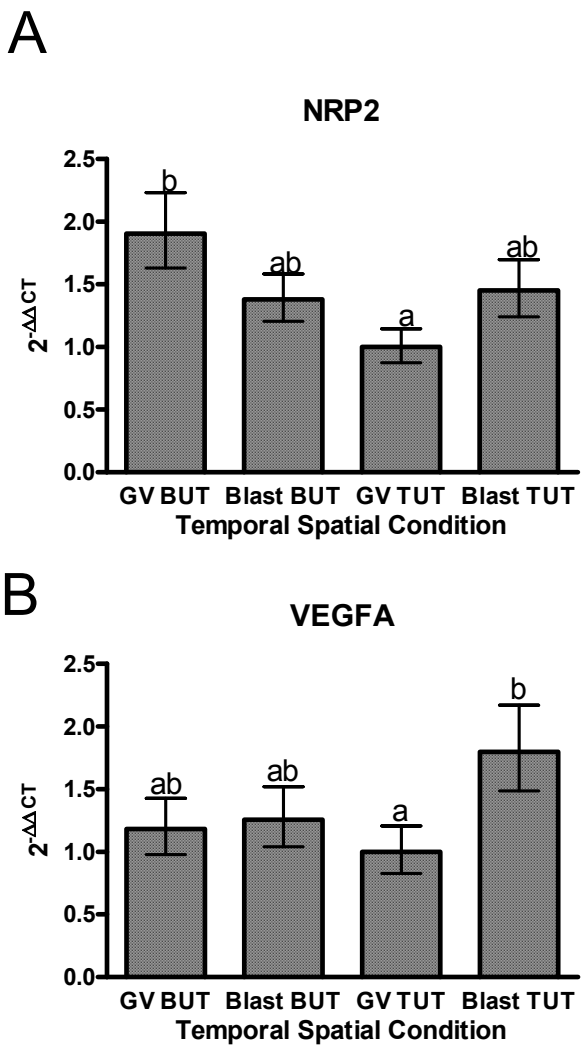

Figure 6.10: Relative expression of NRP2 and VEGFA transcripts as determined by real time PCR. Tempero-spatial conditions include GV BUT (n=4), Blast BUT (n=4), GV TUT (n=4), Blast TUT (n=4). Data is expressed in fold changes relative to the point of lowest expression with different letters representing statistical significance ($P<0.05$) relative to this point. Error bars show exponentially corrected positive and negative standard error of the mean.

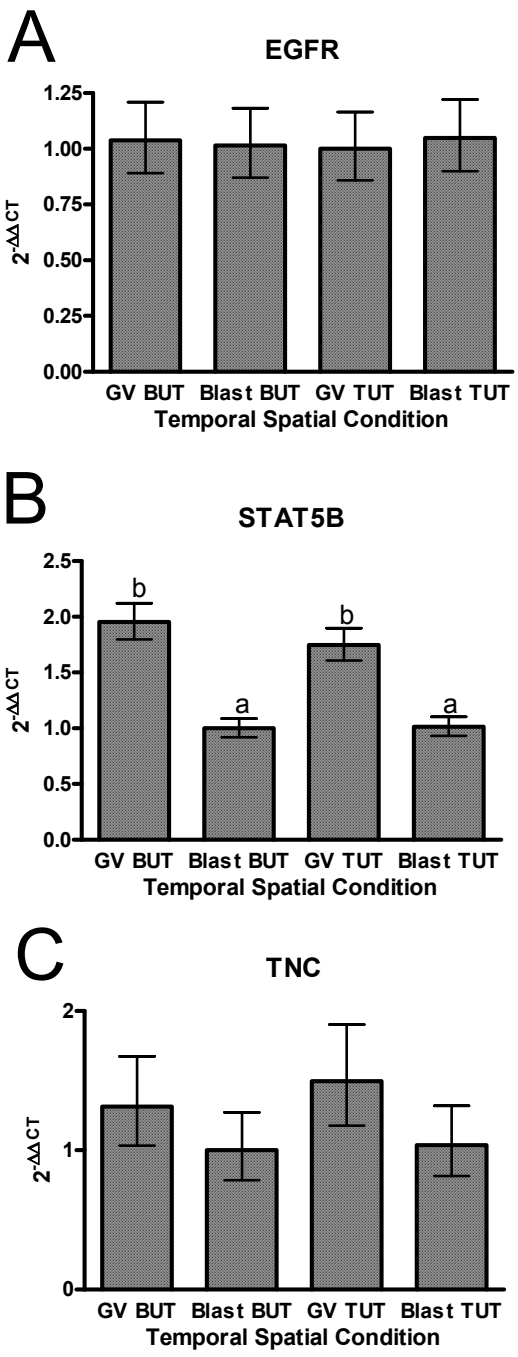

Figure 6.11: Relative expression of EGFR, STAT5B and TNC transcripts as determined by real time PCR. Tempero-spatial conditions include GV BUT (n=4), Blast BUT (n=4), GV TUT (n=4), Blast TUT (n=4). Data is expressed in fold changes relative to the point of lowest expression with different letters representing statistical significance ($P<0.05$) relative to this point. Error bars show exponentially corrected positive and negative standard error of the mean.

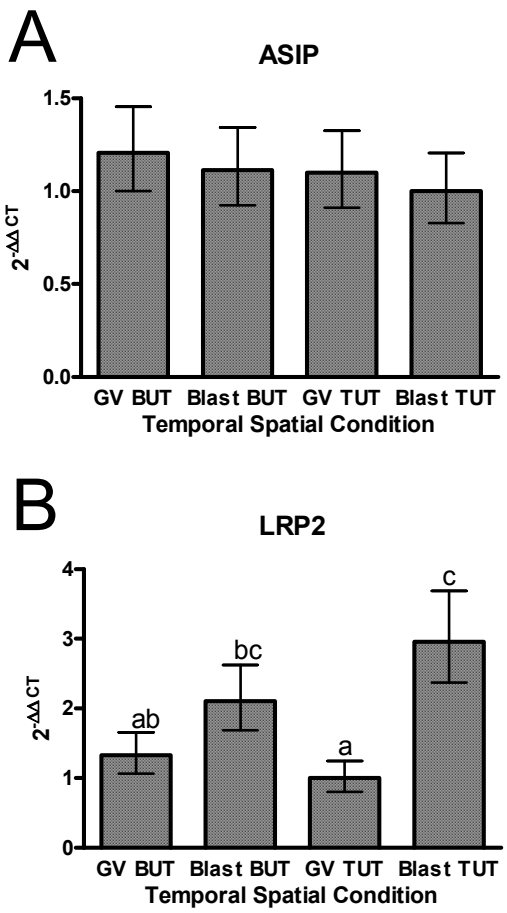

Figure 6.12: Relative expression of ASIP and LRP2 transcripts as determined by real time PCR. Tempero-spatial conditions include GV BUT (n=4), Blast BUT (n=4), GV TUT (n=4), Blast TUT (n=4). Data is expressed in fold changes relative to the point of lowest expression with different letters representing statistical significance ($P<0.05$) relative to this point. Error bars show exponentially corrected positive and negative standard error of the mean.

References

Anderson, L., and Seilhamer, J. (1997) A comparison of selected mRNA and protein abundances in human liver. Electrophoresis 18(3-4), 533-537

Bauersachs, S., Blum, H., Mallok, S., Wenigerkind, H., Rief, S., Prelle, K., and Wolf, E. (2003) Regulation of Ipsilateral and Contralateral Bovine Oviduct Epithelial Cell Function in the Postovulation Period: A Transcriptomics Approach. Biol Reprod 68(4), 1170-1177

Bauersachs, S., Ulbrich, S.E., Gross, K., Schmidt, S.E.M., Meyer, H.H.D., Einspanier, R., Wenigerkind, H., Vermehren, M., Blum, H., Sinowatz, F., and Wolf, E. (2005) Gene expression profiling of bovine endometrium during the oestrous cycle: detection of molecular pathways involved in functional changes. J Mol Endocrinol 34(3), 889-908

Bazer, F.W., and Thatcher, W.W. (1977) Theory of maternal recognition of pregnancy in swine based on estrogen controlled endocrine versus exocrine secretion of prostaglandin F2alpha by the uterine endometrium. Prostaglandins 14(2), 397-400

Borland, R.M., and Tasca, R.J. (1974) Activation of a Na+-dependent amino acid transport system in preimplantation mouse embryos. Dev Biol 36(1), 169-182

Boston, B.A., and Cone, R.D. (1996) Characterization of melanocortin receptor subtype expression in murine adipose tissues and in the 3T3-L1 cell line. Endocrinology 137(5), 2043-2050

Buhi, W.C., Alvarez, I.M., Sudhipong, V., and Dones-Smith, M.M. (1990) Identification and characterization of de novo-synthesized porcine oviductal secretory proteins. Biol Reprod 43(6), 929-938

Buhi, W.C., Ashworth, C.J., Bazer, F.W., and Alvarez, I.M. (1992) In vitro synthesis of oviductal secretory proteins by estrogen-treated ovariectomized gilts. J Exp Zool 262(4), 426-435

Eden, E., Navon, R., Steinfeld, I., Lipson, D., and Yakhini, Z. (2009) GOrilla: a tool for discovery and visualization of enriched GO terms in ranked gene lists. BMC Bioinformatics 10(1), 48

Fisher, R.A. (1922) On the Interpretation of $\chi 2$ from Contingency Tables, and the Calculation of P. J R Statistical Soc 85(1), 87-94

Flood, M.R., and Wiebold, J.L. (1988) Glucose metabolism by preimplantation pig embryos. J Reprod Fertil 84(1), 7-12

Garbe, J.R., Elsik, C.G., Antoniou, E., Reecy, J.M., Clark, K.J., Venkatraman, A., Kim, J.W., Schnabel, R.D., Michael Dickens, C., Wolfinger, R.D., Fahrenkrug, S.C., and Taylor, J.F. (2010) Development and application of bovine and porcine oligonucleotide arrays with protein-based annotation. J Biomed Biotechnol 2010, 453638

Gentleman, R.C., Carey, V.J., Bates, D.M., Bolstad, B., Dettling, M., Dudoit, S., Ellis, B., Gautier, L., Ge, Y., Gentry, J., Hornik, K., Hothorn, T., Huber, W., Iacus, S., Irizarry, R., Leisch, F., Li, C., Maechler, M., Rossini, A.J., Sawitzki, G., Smith, C., Smyth, G., Tierney, L., Yang, J.Y., and Zhang, J. (2004) Bioconductor: open software development for computational biology and bioinformatics. Genome Biol 5(10), R80

Georgiou, A.S., Snijders, A.P.L., Sostaric, E., Aflatoonian, R., Vazquez, J.L., Vazquez, J.M., Roca, J., Martinez, E.A., Wright, P.C., and Fazeli, A. (2007) Modulation of The Oviductal Environment by Gametes. J Proteome Res 6(12), 4656-4666

Georgiou, A.S., Sostaric, E., Wong, C.H., Snijders, A.P.L., Wright, P.C., Moore, H.D., and Fazeli, A. (2005) Gametes Alter the Oviductal Secretory Proteome. Mol Cell Proteomics 4(11), 1785-1796

Grazzini, E., Guillon, G., Mouillac, B., and Zingg, H.H. (1998) Inhibition of oxytocin receptor function by direct binding of progesterone. Nature 392(6675), 509-512

Greenbaum, D., Colangelo, C., Williams, K., and Gerstein, M. (2003) Comparing protein abundance and mRNA expression levels on a genomic scale. Genome Biol 4(9), 117

Guo, Y., Xiao, P., Lei, S., Deng, F., Xiao, G.G., Liu, Y., Chen, X., Li, L., Wu, S., Chen, Y., Jiang, H., Tan, L., Xie, J., Zhu, X., Liang, S., and Deng, H. (2008) How is mRNA expression predictive for protein expression? A correlation study on human circulating monocytes. Acta Biochim Biophys Sin (Shanghai) 40(5), 426-436

Gygi, S.P., Rochon, Y., Franza, B.R., and Aebersold, R. (1999) Correlation between Protein and mRNA Abundance in Yeast. Mol Cell Biol 19(3), 1720-1730

Hediger, M.A., Romero, M.F., Peng, J.B., Rolfs, A., Takanaga, H., and Bruford, E.A. (2004) The ABCs of solute carriers: physiological, pathological and therapeutic implications of human membrane transport proteinsIntroduction. Pflugers Arch 447(5), 465-468

Hermo, L., Lustig, M., Lefrancois, S., Argraves, W.S., and Morales, C.R. (1999) Expression and regulation of LRP-2/megalin in epithelial cells lining the efferent ducts and epididymis during postnatal development. Mol Reprod Dev 53(3), 282-293

Ianculescu, A.G., Giacomini, K.M., and Scanlan, T.S. (2009) Identification and Characterization of 3-Iodothyronamine Intracellular Transport. Endocrinology 150(4), 1991-1999

Kajanne, R., Miettinen, P., Mehlem, A., Leivonen, S.-K., Birrer, M., Foschi, M., Kähäri, V.-M., and Leppä, S. (2007) EGF-R regulates MMP function in fibroblasts through MAPK and AP-1 pathways. J Cell Physiol 212(2), 489-497

Kempisty, B., Antosik, P., Bukowska, D., Jackowska, M., Lianeri, M., Jaśkowski, J.M., and Jagodziński, P.P. (2008) Analysis of selected transcript levels in porcine spermatozoa, oocytes, zygotes and two-cell stage embryos. Reprod Fertil Dev 20(4), 513-518

Krisher, R.L., and Prather, R.S. (2012) A role for the Warburg effect in preimplantation embryo development: metabolic modification to support rapid cell proliferation. Mol Reprod Dev 79(5), 311-320

Lee, B., Brown, K., Hathout, Y., and Seo, J. (2008) GOTreePlus: an interactive gene ontology browser. Bioinformatics 24(7), 1026-1028

Lee, K.F., Yao, Y.Q., Kwok, K.L., Xu, J.S., and Yeung, W.S. (2002) Early developing embryos affect the gene expression patterns in the mouse oviduct. Biochem Biophys Res Commun 292(2), 564-570

Leese, H.J., and Barton, A.M. (1984) Pyruvate and glucose uptake by mouse ova and preimplantation embryos. J Reprod Fertil 72(1), 9-13

Lustig, M. (1997) Postnatal developmental localization of LRP-2 in the efferent ducts and epididymis of the male rat and the oviduct and uterus of the female rat. Thesis (McGill University)

McMaster, M.T., Teng, C.T., Dey, S.K., and Andrews, G.K. (1992) Lactoferrin in the mouse uterus: analyses of the preimplantation period and regulation by ovarian steroids. Mol Endocrinol 6(1), 101-111

Michie, H.J., and Head, J.R. (1994) Tenascin in pregnant and non-pregnant rat uterus: unique spatio-temporal expression during decidualization. Biol Reprod 50(6), 1277-1286

Mynatt, R.L., and Stephens, J.M. (2001) Agouti regulates adipocyte transcription factors. Am J Physiol Cell Physiol 280(4), C954-C961

Noda, N., Minoura, H., Nishiura, R., Toyoda, N., Imanaka-Yoshida, K., Sakakura, T., and Yoshida, T. (2000) Expression of Tenascin-C in Stromal Cells of the Murine Uterus During Early Pregnancy: Induction by Interleukin-1α, Prostaglandin E2, and Prostaglandin F2α. Biol Reprod 63(6), 1713-1720

Oliveros, J.C. (2007) VENNY: An interactive tool for comparing lists with Venn Diagrams. In '. Vol. 2007.

Polge, C. (Ed.) (1982) 'Embryo Transplantation and Preservation.' Control of Pig Reproduction (Butterworths: London)

Pratt, H.P.M. (1980) Phospholipid synthesis in the preimplantation mouse embryo. J Reprod Fertil 58(1), 237-248

Smyth, G. (2005) limma: Linear Models for Microarray Data

Bioinformatics and Computational Biology Solutions Using R and Bioconductor. In '.' (Eds. R Gentleman, VJ Carey, W Huber, RA Irizarry and S Dudoit) pp. 397-420. (Springer New York)

Steibel, J.P., Wysocki, M., Lunney, J.K., Ramos, A.M., Hu, Z.L., Rothschild, M.F., and Ernst, C.W. (2009) Assessment of the swine protein-annotated oligonucleotide microarray. Anim. Genet. 40(6), 883-893

Stein-Stefani, J., and Holtz, W. (1987) Surgical and endoscopic transfer of porcine embryos to different uterine sites. Theriogenology 27(1), 278

Stepanova, O., Krylov, A., Lioudyno, V., and Kisseleva, E. (2007) Gene expression for VEGF-A, VEGF-C, and their receptors in murine lymphocytes and macrophages. Biochemistry (Mosc). 72(11), 1194-1198

Strunker, T., Goodwin, N., Brenker, C., Kashikar, N.D., Weyand, I., Seifert, R., and Kaupp, U.B. (2011) The CatSper channel mediates progesterone-induced Ca2+ influx in human sperm. Nature 471(7338), 382-386

Swain, J., Bormann, C., Clark, S., Walters, E., Wheeler, M., and Krisher, R. (2002) Use of energy substrates by various stage preimplantation pig embryos produced in vivo and in vitro. Reproduction 123(2), 253-260

Tong, B.J., Das, S.K., Threadgill, D., Magnuson, T., and Dey, S.K. (1996) Differential expression of the full-length and truncated forms of the epidermal growth factor receptor in the preimplantation mouse uterus and blastocyst. Endocrinology 137(4), 1492-1496

Vandesompele, J., De Preter, K., Pattyn, F., Poppe, B., Van Roy, N., De Paepe, A., and Speleman, F. (2002) Accurate normalization of real-time quantitative RT-PCR data by geometric averaging of multiple internal control genes. Genome Biol 3(7), RESEARCH0034

Wallenhorst, S., and Holtz, W. (1999) Transfer of pig embryos to different uterine sites. J Anim Sci 77(9), 2327-2329

Walter, L.M., Rogers, P., and Girling, J.E. (2010) "Vascular Endothelial Growth Factor-a Isoform and (Co)Receptor Expression Are Differentially Regulated by 17beta-Oestradiol in the Ovariectomised Mouse Uterus." Reproduction 140, no. 2 (2010): 331-41.

Wosu, U.A. (1998) The distribution of the low density lipoprotein receptor related protein-2 (LRP-2) in the male and female reproductive tracts of the rat. Thesis (McGill University)

Chapter 7: General Discussion and Conclusions

Embryonic development is a highly coordinated series of events which together culminate in a complex fetus. In mammals, embryonic development can, however, be subdivided into two distinct stages separated by the implantation of the embryo. Prior to implantation the embryo must normally survive in the histotrophic environment provided by the maternal reproductive tract. In the swine industry, knowledge of the key factors in this environment is required to understand and mitigate embryonic losses in breeding females. In addition, the successful application of modern assisted reproductive technologies, which involve manipulation of the embryo, requires an understanding of this environment in order to replicate it outside the reproductive tract.

In the pig, a number of studies have evaluated the composition of the maternal environment during the early stages of the estrous cycle that would coincide with cleavage stage embryonic development (Iritani *et al.* 1974; Buhi *et al.* 1990). More recently, a number of studies have begun to use high throughput molecular methodologies to determine the effect of the cleavage stage embryo on the uterine environment (Lee *et al.* 2002; Bauersachs *et al.* 2003; Georgiou *et al.* 2005; Georgiou *et al.* 2007). However, the majority of the available information on both the uterine environment and maternal-embryonic cross-talk in the pig is centered around the time of maternal recognition and implantation (Chen *et al.* 1973; Knight *et al.* 1973; Adams *et al.* 1981; Kayser *et al.* 2006). As such, much of the literature to which the results of this Thesis are compared and contrasted has been obtained from humans and rodents which exhibit a substantially different reproductive physiology, with implantation occurring immediately after the embryo hatches from the zona pellucida at the

blastocyst stage. While we believe the work contained in this Thesis to be a substantial addition to the current understanding of reproductive physiology during early embryo development in the pig, additional work is required to fully understand this process and how it can be effectively managed or manipulated.

Many previous studies that characterized the embryonic, uterine and oviductal physiology of the pig, temporally staged animals based on the onset of standing estrus (Perry and Rowlands 1962; Polge 1982). In swine, the relationship between the onset of standing estrus and ovulation is poor (Nissen *et al.* 1997), varying by as much as 47 hours (Degenstein *et al.* 2008). In order to eliminate as much of this variation as possible, the animals used in the studies described in this Thesis were subjected to transcutaneous real time ultrasonography to accurately pinpoint the time of ovulation to within a four hour interval. What is surprising is that despite such specific temporal grouping of animals, large individual variation was still observed in nearly every measurement. Such variation brings into question the existence of a single optimal environment for embryo development. Furthermore, this variation may suggest that the uterine environment may resemble the dancing landscape model of complexity theory (Levinthal 1997), whereby many optimal formulations are likely to exist. Based on this model, the previous experiments which have focused on determining the optimal culture concentration of a particular molecule under otherwise extremely abnormal conditions are likely to have simply identified a localized peak which is physiologically irrelevant. Studies with bovine embryos have previously shown that the developmental rate of male embryos exceeds that of their female counterparts during cleavage stage development (Xu *et al.* 1992). In addition, it is understood that female porcine embryos are particularly sensitive to post-catabolism effects in the mother, which create differences in sex ratio at day 30 (Vinsky *et al.* 2006). Together these reported gender related differences would suggest that significant required variance exists between embryos. However, as the pig is a litter bearing

species, the environment of the reproductive tract would only meet the specific requirements of one embryo at the expense of another.

To evaluate the environment created within the reproductive tracts of these carefully selected animals and the embryos they contained, the experiments described in this Thesis employed the methods of molecular biology and bioinformatics. Although swine represent one of the most well studied litter bearing species behind the standard rodent models, the availability of many of the fundamental tools necessary for molecular biology such as tissue specific transcriptomic arrays are only just now becoming available (Tsoi *et al.* 2012), while others such as protein specific antibodies are still not available. The first full draft of the pig genome was not published until 2009 (Archibald, Bolund *et al.* 2010) and only became truly available and annotated in 2011, prior to which only ten chromosomes were accessible. Similarly, as discussed in Appendix A, the volume of information contained in databases of functional information such as gene ontology is still in its infancy. As a result, nearly all of the research contained in this Thesis has relied heavily on annotations and functional classification determined in humans. For this reason many of the results presented in this Thesis will require validation not only at a technical, but also at a physiological level, once full porcine genomic annotation has been made available

In order to allow for characterization of a wide array of factors, many of the experiments in this Thesis were centered around the use of transcriptomic technologies. Furthermore, these technologies were used to assess only the relative abundance of transcripts associated with protein coding genes. Previous publications have drawn into question the predictive value of transcriptomics with regards to the more functionally related protein abundance (Anderson and Seilhamer 1997; Gygi, Rochon *et al.* 1999; Guo, Xiao *et al.* 2008). While the methodological approach of these studies does not directly relate to the manner

in which transcriptomics were applied in this Thesis, the results obtained in Chapter 4 suggest that the relationship between transcript and protein abundance is limited. In addition, the recently published results from the ENCODE project suggests that the landscape of regulation at the molecular level is more complex than previously thought and involves a much wider range of transcribed elements than just the protein coding genes (Consortium 2012). It should be noted that the results obtained from microarray analysis described in Chapter 5 does include the differential expression of a number of non-coding transcripts, however, as the functional information on these elements is limited, few conclusions could be drawn from the observed changes in transcript abundance. Overall, it is important to consider the results of transcriptomic based research as starting material for functional experimentation.

Much of the transcriptomic data in this Thesis was obtained using the methods of relative quantification by reverse transcription real time PCR (Porcher *et al.* 1992). This particular methodology requires that data be normalized to an endogenous control to account for non-experimental biological and technical variation (VanGuilder *et al.* 2008). As it became increasingly apparent that no single gene was universally stable, the typical normalization came to involve the use of multiple housekeeping genes assessed iteratively through geometric averaging (Vandesompele *et al.* 2002) or model-based variance estimation (Andersen *et al.* 2004). When applied correctly these methods undoubtedly improve the accuracy of real time PCR data, however, to avoid artifacts they require the input of numerous stable housekeeping genes. Despite the fact that multiple candidate housekeeping genes were assessed in each experiment presented in this Thesis, a large stable group of housekeeping genes was only identified once in Chapter 6. Unlike the standard experimental treatment vs control paradigm for which real time PCR has been widely used, the experiments described in this Thesis were designed to characterize changes in both time and space. Similar experiments that sought to assess gene expression

over time, in particular, have also encountered great difficulty with regards to the use of canonical housekeeping genes such as ubiquitin C (UBC), cyclophilin (PPIA) and glyceraldehyde-3-phosphate dehydrogenase (GAPDH) (Vallet *et al.* 2009; Novak *et al.* 2012). This issue is further exacerbated in the ontogenetic analysis of the cleavage stage embryo, which exhibits a complex series of transcriptional changes associated with the activation of the zygotic genome (Schultz 1993; Alizadeh *et al.* 2005). Following careful analysis, it is apparent that the combination of time and space complicates the use of many existing normalization methodologies.

Chapter 3 of this Thesis sought to characterize hyaluronic acid in the reproductive tract of the pig from the onset of standing estrus to the hatching of the blastocyst. One of the key findings in this chapter is the degree of dynamic change that occurs in the sow's uterine and oviductal environments. In addition, this chapter identified high individual variation within specific time points despite the prior assignment of animals to a well-defined physiological period. Additionally, the differential gene expression patterns observed between each of the three hyaluronic acid synthases and between the oviduct and uterus suggest that there are multiple regulatory mechanisms at play. As well, the results of this experiment clearly support a role for hyaluronic acid in both fertilization and later stage cleavage development in the embryo.

Although proteinaceous macromolecules such as albumin are often added to *in vitro* culture media, they typically serve to increase viscosity and provide lubrication. However, it is likely that specific proteins released into the uterine histotroph play an active role in the physiology of the developing embryo. While the characterization of the histotrophic proteome described in Chapter 4 of this Thesis was able to identify albumin as the single most abundant protein during both periods examined, it also identified a substantial number of other protein entities. It should be noted that the complexity of the histotrophic

proteome measured at these early stages of development is reduced in comparison to those published using similar methodologies at later stages. Identification and analysis of a subset of these proteins produced two secreted proteins of interest, Clusterin (CLU) and Carbonic anhydrase 2 (CA2). These proteins have both been identified in seminal plasma and are thought to play a significant role in sperm survival and function and in this study were found to have increased abundance in the reproductive tract at the onset of standing estrus. The localization of these proteins suggests that the maternal reproductive tract may actively establish an environment conducive to sperm survival. Conversely, two members of the glutathione S-transferase family were shown to increase in abundance over the course of embryo development. As these proteins are likely associated with protecting the embryo from stress, they are ideal candidates for testing as additives to embryo culture media.

Communication between distinct entities such as the ovary, embryo and uterus are fundamental to the understanding of reproductive physiology. The accelerated identification of such interactions requires the use of a systems level approach and is heavily reliant on existing information contained within bioinformatics databases. The fifth chapter of this Thesis describes the development of a novel bioinformatics tool for the identification and visualization of potential protein-protein interactions in paired sets of transcriptomic data. While this program has proved valuable in the research presented, it will continue to add value as more complete information on the embryonic transcriptome becomes available from projects such as EmbryoGENE. In future analysis, this tool will allow for rapid identification of potential factors in the maternal-embryonic cross-talk at all stages of cleavage development. In addition, this program has broad applications to other areas of physiology, and biology, however, future development will be necessary to integrate statistical measures and allow for the detection of higher order interactions.

Finally, Chapter 6 of this Thesis examined the temporal and spatial changes in the uterine transcriptome during cleavage stage embryonic development. The results of this study identified substantial changes in genes associated with extracellular signaling. In addition, a number of potential communication pathways between the blastocyst stage embryo and the uterus were identified. Unfortunately, a combination of technological and statistical limitations combined with high individual animal variation make it difficult to draw any definite conclusions regarding the transcription of these genes. What is clear however, is that the uterus becomes increasingly regulated as embryo development progresses, suggesting increased sensitivity of the embryo to its environment in later stages of development.

Overall, the research described in this Thesis represents a significant first step into the temporal and spatial characterization of the reproductive tract during early embryonic development in swine. Figure 7.1 highlighs a group of the molecules shown to change within the uterus between the pre-ovulatory germinal vesicle stage and the embryonic blastocyst stage. A subset of these molecules, highlighted in Figure 7.2, were also found to vary spatially between the top and bottom of the uterin horns. Finaly a group of transcrips highlighted in Figure 7.3 were examined temporaly in the embryo. In addition Future studies should continue to focus on the examination of this environment with regards to embryo development, and attempt to elucidate the regulatory mechanisms involved. Such work has the potential to identify key elements required for appropriate embryonic development for both *in vitro* assisted reproductive technologies and *in vivo* reproduction.

Figures

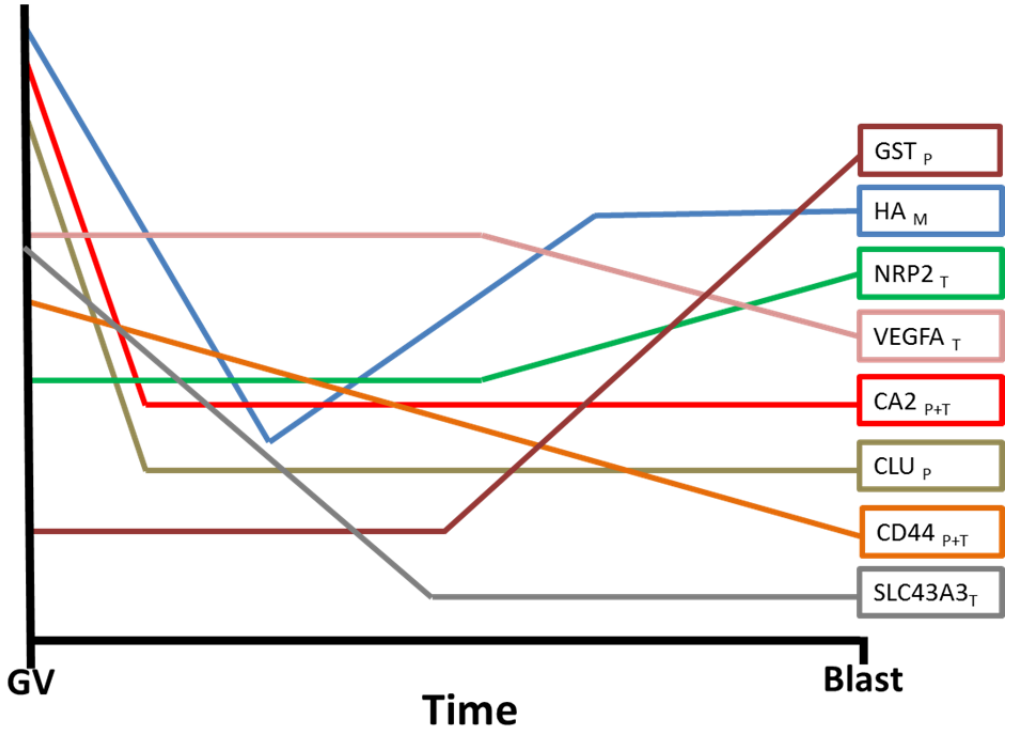

Figure 7.1: Hilights of observed temporal changes in the uterus of the pig. Subscripts refer to characterization at the T: transcriptomic, P: proteomic and M: molecular level.

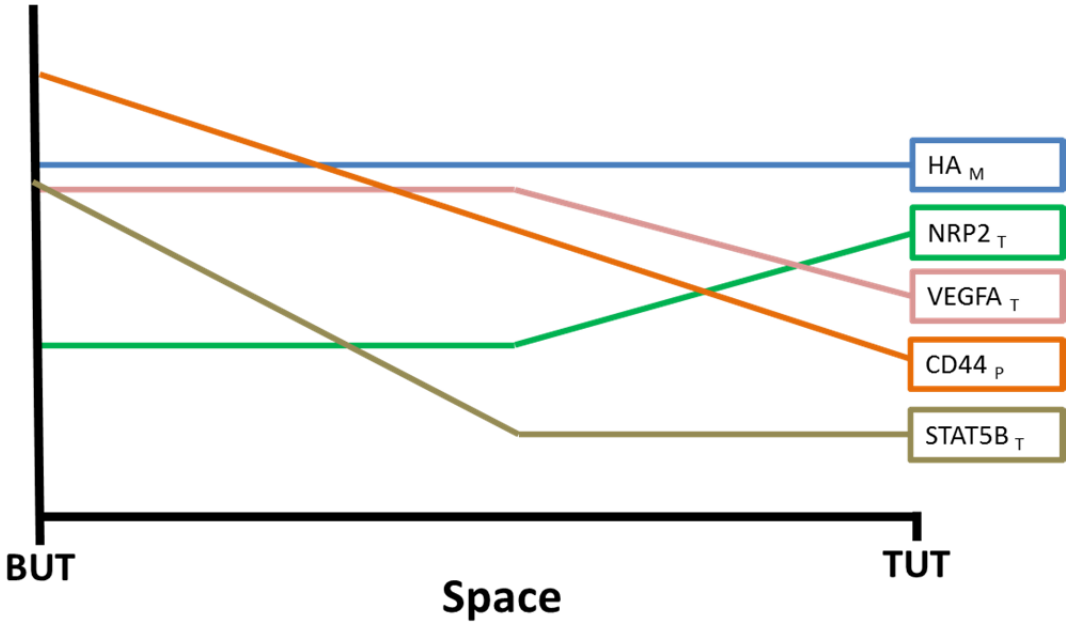

Figure 7.2: Hilights of observed spatial changes in the uterus of the pig. Subscripts refer to characterization the T: transcriptomic, P: proteomic and M: molecular level.

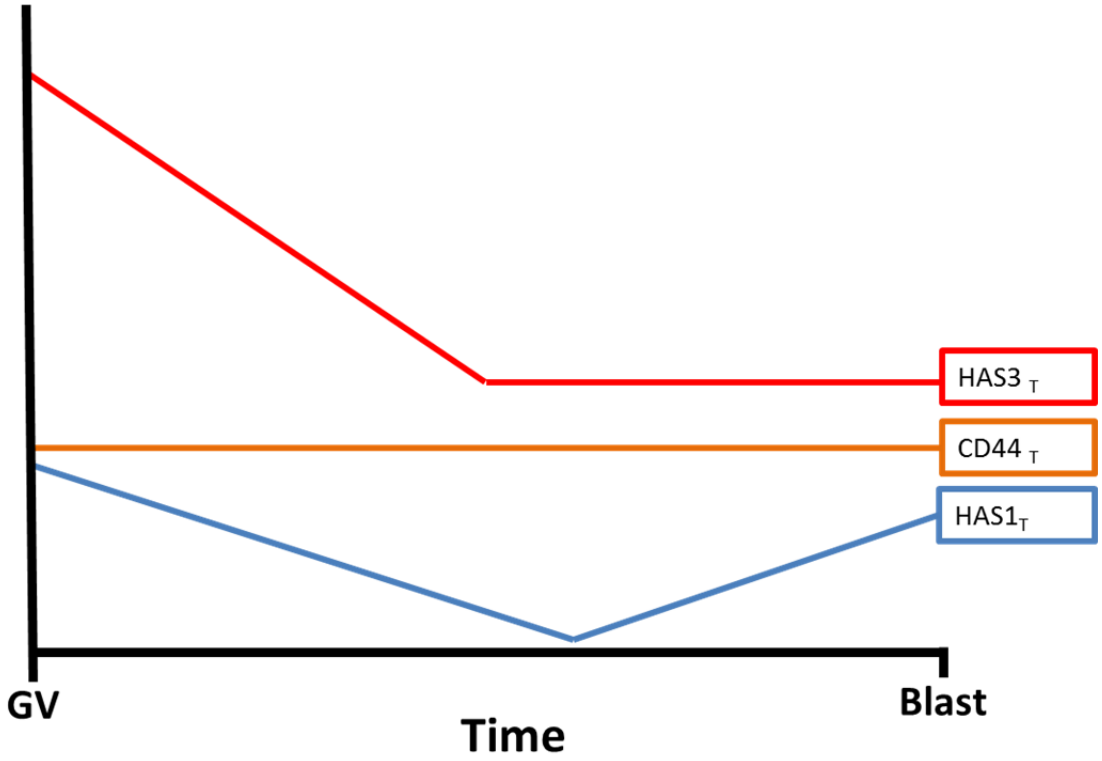

Figure 7.3: Hilights of observed temporal changes in the embryo of the pig. Subscripts refer to characterization at the T: transcriptomic, P: proteomic and M: molecular level.

References

Adams, K. L., F. W. Bazer, *et al.* (1981). "Progesterone-induced secretion of a retinol-binding protein in the pig uterus." J Reprod Fertil 62(1): 39-47.

Alizadeh, Z., S.-I. Kageyama, *et al.* (2005). "Degradation of maternal mRNA in mouse embryos: Selective degradation of specific mRNAs after fertilization." Mol Reprod Dev 72(3): 281-290.

Andersen, C. L., J. L. Jensen, *et al.* (2004). "Normalization of Real-Time Quantitative Reverse Transcription-PCR Data: A Model-Based Variance Estimation Approach to Identify Genes Suited for Normalization, Applied to Bladder and Colon Cancer Data Sets." Cancer Res 64(15): 5245-5250.

Anderson, L. and J. Seilhamer (1997). "A comparison of selected mRNA and protein abundances in human liver." Electrophoresis 18(3-4): 533-537.

Archibald, A. L., L. Bolund, *et al.* (2010). "Pig genome sequence--analysis and publication strategy." BMC Genomics 11: 438.

Bauersachs, S., H. Blum, *et al.* (2003). "Regulation of Ipsilateral and Contralateral Bovine Oviduct Epithelial Cell Function in the Postovulation Period: A Transcriptomics Approach." Biol Reprod 68(4): 1170-1177.

Buhi, W. C., I. M. Alvarez, *et al.* (1990). "Identification and characterization of de novo-synthesized porcine oviductal secretory proteins." Biol Reprod 43(6): 929-938.

Chen, T. T., F. W. Bazer, *et al.* (1973). "Purification and properties of a progesterone-induced basic glycoprotein from the uterine fluids of pigs." J Biol Chem 248(24): 8560-8566.

Consortium, E. P. (2012). "An integrated encyclopedia of DNA elements in the human genome." Nature 489(7414): 57-74.

Degenstein, K. L., R. O'Donoghue, *et al.* (2008). "Synchronization of ovulation in cyclic gilts with porcine luteinizing hormone (pLH) and its effects on reproductive function." Theriogenology 70(7): 1075-1085.

Georgiou, A. S., A. P. L. Snijders, *et al.* (2007). "Modulation of The Oviductal Environment by Gametes." J Proteome Res 6(12): 4656-4666.

Georgiou, A. S., E. Sostaric, *et al.* (2005). "Gametes Alter the Oviductal Secretory Proteome." Mol Cell Proteomics 4(11): 1785-1796.

Guo, Y., P. Xiao, *et al.* (2008). "How is mRNA expression predictive for protein expression? A correlation study on human circulating monocytes." Acta Biochim Biophys Sin (Shanghai) 40(5): 426-436.

Gygi, S. P., Y. Rochon, *et al.* (1999). "Correlation between Protein and mRNA Abundance in Yeast." Mol Cell Biol 19(3): 1720-1730.

Iritani, A., E. Sato, *et al.* (1974). "Secretion Rates and Chemical Composition of Oviduct and Uterine Fluids in Sows." J Anim Sci 39(3): 582-588.

Kayser, J.-P. R., J. G. Kim, *et al.* (2006). "Global characterization of porcine intrauterine proteins during early pregnancy." Reproduction 131(2): 379-388.

Knight, J. W., F. W. Bazer, *et al.* (1973). "Hormonal Regulation of Porcine Uterine Protein Secretion." J Anim Sci 36(3): 546-553.

Lee, K. F., Y. Q. Yao, *et al.* (2002). "Early developing embryos affect the gene expression patterns in the mouse oviduct." Biochem Biophys Res Commun 292(2): 564-570.

Levinthal, D. A. (1997). "Adaptation on Rugged Landscapes." Manag Sci 43(7): 934-950.

Nissen, A. K., N. M. Soede, *et al.* (1997). "The influence of time of insemination relative to time of ovulation on farrowing frequency and litter size in sows, as investigated by ultrasonography." Theriogenology 47(8): 1571-1582.

Novak, S., F. Paradis, *et al.* (2012). "Temporal candidate gene expression in the sow placenta and embryo during early gestation and effect of maternal Progenos supplementation on embryonic and placental development." Reprod Fertil Dev 24(4): 550-558.

Perry, J. S. and I. W. Rowlands (1962). "Early Pregnancy in the Pig." J Reprod Fertil 4(2): 175-188.

Polge, C., Ed. (1982). Embryo Transplantation and Preservation. Control of Pig Reproduction. London, Butterworths.

Porcher, C., M. C. Malinge, *et al.* (1992). "A simplified method for determination of specific DNA or RNA copy number using quantitative PCR and an automatic DNA sequencer." Biotechniques 13(1): 106-114.

Schultz, R. M. (1993). "Regulation of zygotic gene activation in the mouse." BioEssays 15(8): 531-538.

Tsoi, S., C. Zhou, *et al.* (2012). "Development of a porcine (Sus scofa) embryo-specific microarray: array annotation and validation." BMC Genomics 13(1): 370.

Vallet, J. L., J. R. Miles, *et al.* (2009). "Effect of fetal size on fetal placental hyaluronan and hyaluronoglucosaminidases throughout gestation in the pig." Anim Reprod Sci.

Vandesompele, J., K. De Preter, *et al.* (2002). "Accurate normalization of real-time quantitative RT-PCR data by geometric averaging of multiple internal control genes." Genome Biol 3(7): 0034.

VanGuilder, H. D., K. E. Vrana, *et al.* (2008). "Twenty-five years of quantitative PCR for gene expression analysis." Biotechniques 44(5): 619-626.

Vinsky, M.D., Novak, S., Dixon, W.T., Dyck, M.K., and Foxcroft, G.R. (2006) Nutritional restriction in lactating primiparous sows selectively affects female embryo survival and overall litter development. Reproduction, Fertility and Development 18(3), 347-355

Xu, K.P., Yadav, B.R., King, W.A., and Betteridge, K.J. (1992) Sex-related differences in developmental rates of bovine embryos produced and cultured in vitro. Mol Reprod Dev 31(4), 249-252

Appendix A: Re-annotation of the PigOligoArray

Introduction

Transcriptional profiling is an important tool of molecular biology that allows for the characterization of cellular response. While a number of competing technologies exist for high-throughput transcriptional profiling, microarray is not only the most applied technology to date, it's also associated with the most standardized and well developed methods for statistical analysis. This technology relies on thousands of nucleotide probes specifically designed to hybridize to a particular target sequence and arranged in a two dimensional pattern on a glass or silicon chip (Klopfleisch and Gruber 2012). While there are currently more than 10,000 array platforms logged in NCIB's GEO database, the vast majority are not only species specific but designed for humans or standard model species such as mice and rats. For livestock species, there are fewer array platforms in existence and they are often designed based on limited transcriptional information, relying heavily on expressed sequence tag (EST) databases.

The Swine Protein-Annotated Oligonucleotide Microarray (PigOligoArray) platform is a spotted long (70bp) oligonucleotide array, the first generation of which was published by Zhao *et al.* in 2005 (Zhao *et al.* 2005). Since then, the platform has undergone numerous redevelopments to reach its current form, containing 20,400 probes, of which 19,980 are targeted at expressed sequences (NCBI GEO, GPL7435). The current form of the array was designed based on clustered ESTs aligned against vertebrate proteins sequences, however, since no draft sequence of the pig genome was available at the time, genes represented in the bovine genome were preferentially selected (Garbe, Elsik *et al.* 2010). The original annotation of the array was able to assign only 26% and 44% of the probes to known pig and human cDNA sequences respectively. Failure to

annotate many of the probes was likely due to both the low volume of reported mRNA sequences and lack of a fully sequenced genome for the pig at the time when this annotation was made. In addition, the full annotation for this array was made to ensemble ID's for a total of six different species. The dynamic nature of this type of identifier makes the value in this form of annotation short lived. Furthermore, few methods of secondary analysis accept this form of identifier as an input, requiring a conversion to another form, which can be difficult as the identifiers change over time. As well, since many analysis methodologies require the use of a single species identifier or a species specific background this annotation is increasingly difficult to utilize.

As the true value in microarray data arises as a result of secondary analysis of cellular and systems level pathways and ontologies, it is necessary to associate specific array probes with such data. The potential to identify biologically meaningful information in these data sets is proportional to the amount of information available in current databases. Unfortunately, like the arrays themselves, the databases which contain information on pathways, gene ontologies and protein-protein interactions are also heavily skewed toward traditional model species (Figure A.1). In particular, the bulk of information for higher mammals is linked to human gene sequences, which are being updated at a much faster rate than other such organisms. In contrast, information on the pig is in its infancy, and the vast majority of information contained within porcine databases is computationally predicted, based on information from other species. To accumulate the most current information for the PigOligoArray probes, re-annotation was carried out against the NCBI Reference Sequence (RefSeq) and Gene databases for both pigs and humans. Probes were annotated with multiple identifiers, however the primary goal was to assign official gene symbols which are not only commonly accepted as an input type. In addition due to the efforts of the HUGO gene nomenclature committee, the official gene

symbols are maintained stable over time and universal across multiple databases.

Methods

Alignment

Prior to functional annotation of each microarray probe, it is necessary to identify the most closely matched sequence in existing databases. The Reference Sequence (RefSeq) database maintained and curated by NCBI contains non-redundant and interlinked genomic, transcript and protein sequences (Pruitt *et al.* 2007). While larger databases (nt) exist, they contain a disproportionate amount of EST information which is rarely functionally annotated. In addition, these databases are highly redundant making the identification of a single sequence match more difficult. For this reason, each probe on the PigOligoArray was individually aligned against the RefSeq database for both pig (txid: 9823) and humans (txid: 9606) using the Basic Logical Alignment Search Tool for nucleotides (BLASTn) algorithm. Due to a lack of available computing system capable of conducting the nearly 40,000 searches required in a reasonable amount of time, the NCBI web blast system was employed. To allow efficient automation a program was written in Perl, which submitted each sequence to NCBI's blast program, collected the results and parsed the relevant information from the output. The most significant alignment for each sequence within species, based on expected value (e-value), was collected and returned with the corresponding probe ID and sequence.

Annotation

The bulk of database information on protein-protein interactions, intercellular pathways and ontology are most easily accessible through official Gene Symbols (eg. VEGF, IGF2, CD44). In addition, these symbols are the most recognizable and stable references across species and over time, making them ideal for both analysis and publication. To collect this and other information on

each probes most significant BLASTn alignment to the RefSeq database a second automation script was used that accessed NCBI's RefSeq and Gene database, downloaded and then organized the information into a tab delimited format for further analysis and use. At all points an absolute reference to both probe ID and sequence were maintained to ensure annotation results were both accurate and applicable to results from the PigOligoArray.

Results

As expected, the BLAST results against the porcine RefSeq database were highly significant (Figure A.2a) with the majority (12,614) returned as perfect sequence matches (BLAST E-value=9.0^{-30}). In comparison, the BLAST results against the human RefSeq database are more widely distributed (Figure A.2b) with only a small portion of probes achieving a perfect match. For both sets of BLAST results a cut off for a significant match was established at E-value ≤ X^{-10}. Table A.1 shows both porcine and human BLAST results with significant matches broken down by ID prefixes. The vast majority of human matches were made to published mRNA(NM), published non-transcribed pseudo genes (NG) and published non-coding RNA (NR), while hits in the pig were made against computationally predicted mRNA (XM) and computationally predicted no-coding RNA (XR) sequences. In addition, BLAST returned fewer probes with no match in the human database, despite the previously mentioned distribution in e-values. Both these results are likely due to the fact that, currently, the human database contains nearly twice the number of sequence entries (65,092) as the porcine database (35,852).

Nearly half of the annotations which were made based on BLAST matches against the porcine RefSeq database return symbols beginning with the 'LOC' prefix (Figure A.3). Conversely only a small proportion of the annotations resulting from the human RefSeq database were against LOC ID's. Symbols beginning with LOC are reserved for genes with no published symbol or no

determined ortholog (NCBI 2005). Functionally this form of annotation has no value in secondary analysis of microarray data. As this type of gene symbol does not link to any known gene ontology, pathway or other information. While LOC ID's are removed when published gene symbols or orthologs are determined, the numerical portion of the ID will still correspond to the gene ID and thus this form of annotation is easily updated. Conversely, a more significant portion of the annotations made to human gene symbols (598) relative to those against swine (94) are in the format of C#ORF#. These symbols refer to open reading frames identified by their chromosomal location (C#) and the series number (ORF#). Unlike LOC ID's, many of the remaining ORF's link to functional information particularly in gene ontology databases, all be it at a minimal level. Unfortunately, these symbols are not considered stable, and are updated to a functionally descriptive form when sufficient information is available. In order to allow easy updating of these symbols as they are redefined, the numerical gene ID was also added to the annotation file.

Conclusions

Microarray analysis particularly during the secondary phase requires access to functional information on transcripts associated with each probe. Currently this information is limited to standard model organisms and humans, creating a substantial problem in the analysis of transcriptomic data in a species such as swine. Here probes were matched against both porcine and human RefSeq databases, with the latter producing a higher number of significant matches to published sequences. In addition, human sequence matches resulted in far more annotations to functionally annotated gene symbols. Therefore human ortholog annotation represents a practical temporary solution to the lack of database information currently available in non-model species such as swine and cattle. While this form of annotation is susceptible to a degree of error resulting from the cross-species BLAST search, it provides substantially more information for the secondary phase of analysis.

Tables

Match Sequence Type	Pig		Human	
	Annotations	**Non-redundant***	**Annotations**	**Non-redundant***
NM	3735	3029	15936	12351
NG	0	0	6	6
NR	14	8	740	608
XM	11897	9475	192	164
XR	575	445	85	75
Insignificant	344	320	2980	2706
No Hit	3415	0	41	0
Total	19980	13277	19980	15910

Table A.1: Comparison of best hit sequence types between Pig and Human RefSeq databases for all non-negative control probes on the PigOligoArray. Match sequence types based on RefSeq ID prefixes NM: mature mRNA transcripts, NG: mature non-transcribed pseudo genes, NR: mature non-coding transcripts, XM: computationally predicted mRNA based on current genome build, XR: computationally predicted non-coding RNA based on current genome build. *multiple probes matching the same RefSeq ID removed.

Figures

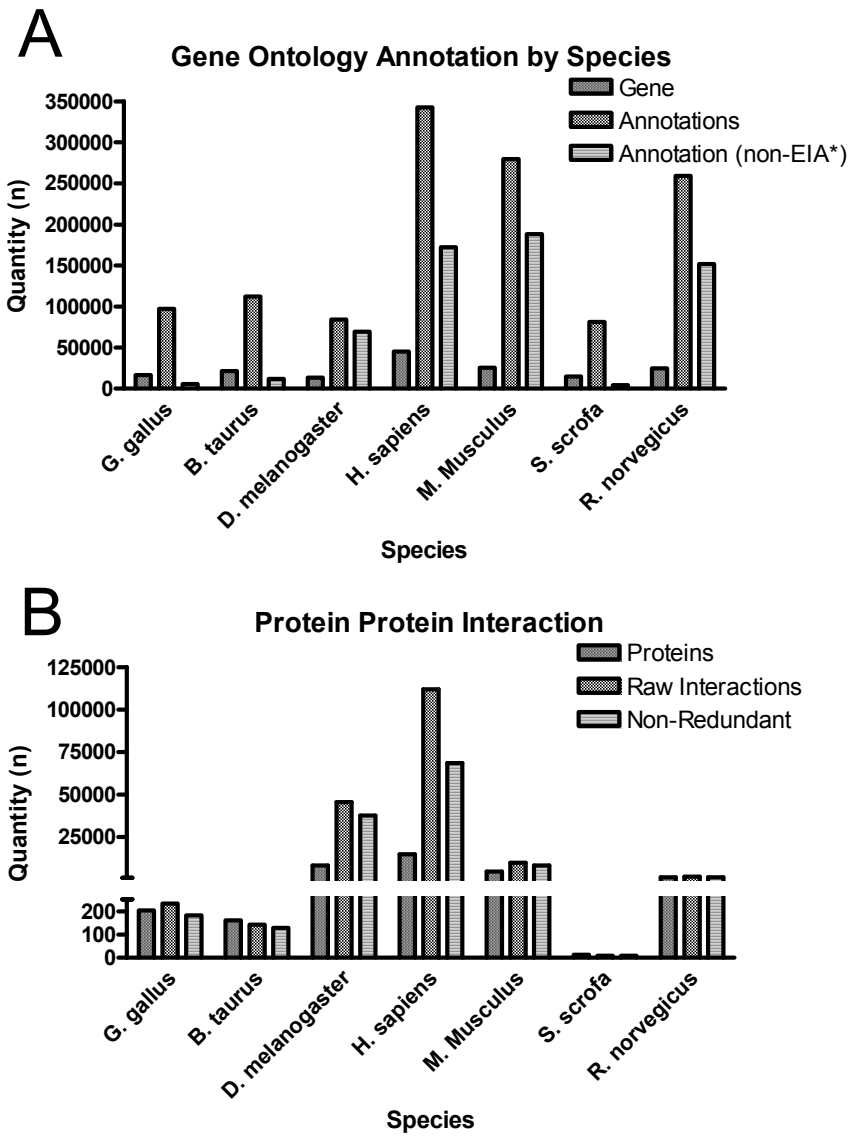

Figure A.1: Current species specific database statistics. A: Gene Ontology (GO) annotation statistics available on www.geneontology.org, as of July 2012, "Annotations" includes those which are electronically inferred (evidence code: EIA) B: Protein-Protein Interaction statistics for the BioGRID database available on www.thebiogrid.org as of July 2012. Raw interactions include each unique combination of interactors, system and publication (ie: A → B and B → A), Non-Redundant is each unique combination of interactors A and B irrespective of directionality, experimental system or publication.

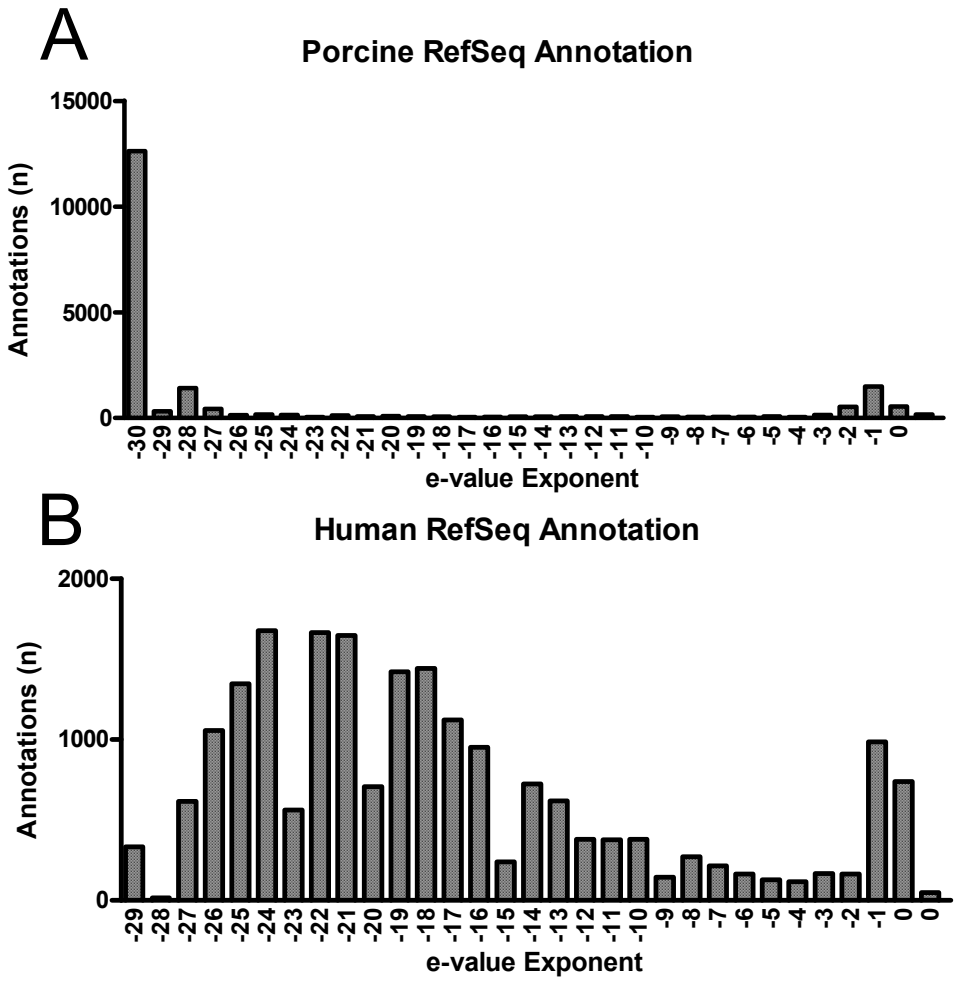

Figure A.2: Expected value distribution for probe sequence BLAST hits against Human and Pig RefSeq databases. Blast hits grouped by expected value (e-value) exponents for results against A: Porcine RefSeq and B: Human RefSeq.

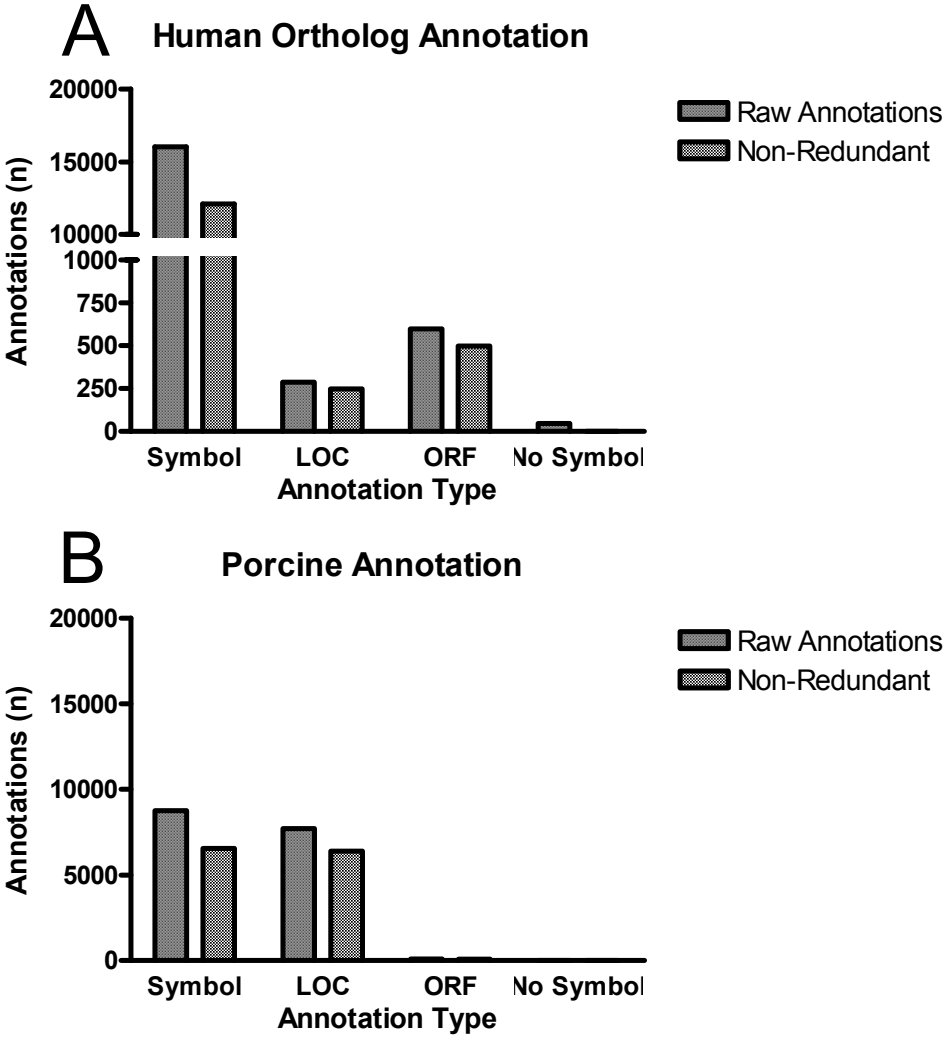

Figure A.3: Distribution of annotation types for all significant hits against A: Human and B: Porcine RefSeq Databases. Annotations are divided into Symbol (Official Gene Symbol), LOC (loci) and ORF (open reading frame).

References

Garbe, J.R., Elsik, C.G., Antoniou, E., Reecy, J.M., Clark, K.J., Venkatraman, A., Kim, J.W., Schnabel, R.D., Michael Dickens, C., Wolfinger, R.D., Fahrenkrug, S.C., and Taylor, J.F. (2010) Development and application of bovine and porcine oligonucleotide arrays with protein-based annotation. J Biomed Biotechnol 2010, 453638

Klopfleisch, R., and Gruber, A.D. (2012) Transcriptome and proteome research in veterinary science: what is possible and what questions can be asked? TSWJ 2012, 254962

NCBI (2005) Gene FAQ. In 'Gene Help.' (Ed. NCBI). (NCBI: Bethesda (MD))

Pruitt, K.D., Tatusova, T., and Maglott, D.R. (2007) NCBI reference sequences (RefSeq): a curated non-redundant sequence database of genomes, transcripts and proteins. Nucleic Acids Res 35(suppl 1), D61-D65

Zhao, S.H., Recknor, J., Lunney, J.K., Nettleton, D., Kuhar, D., Orley, S., and Tuggle, C.K. (2005) Validation of a first-generation long-oligonucleotide microarray for transcriptional profiling in the pig. Genomics 86(5), 618-25

Appendix B: Annotated Uterine Differentially Expressed Genes

		GV TUT vs GV BUT		GV BUT vs Blast BUT		Blast BUT vs Blast TUT		Blast TUT vs GV TUT	
Probe ID	**Symbol***	**Fold Change**	**P-value**	**Fold Change**	**P-value**	**Fold Change**	**P-value**	**Fold Change**	**P-value**
7204:45360_CL308Contig1:f	ABCC10	-1.62	0.248	-2.82	0.031	3.26	0.016	1.18	0.435
19604:17131_CL1Contig1:f	ACBD4	-0.51	0.886	-0.24	0.970	-1.25	0.290	2.00	0.029
8444:37222_CL6Contig1:r	ACSL1	-0.56	0.862	1.97	0.020	-0.78	0.715	-0.64	0.816
34299:30344_7422404:f	ADAMTS13	-0.25	0.951	1.99	0.040	-0.74	0.755	-1.00	0.498
NM_001001544.1	ADCYAP1	2.02	0.117	-3.64	0.028	0.95	0.565	0.67	0.747
8680:14598_CL1Contig1:r	AIFM2	2.00	0.031	-0.70	0.743	-1.09	0.427	-0.21	0.955
34008:8193_CL1Contig1:f	ANKRD58	0.79	0.719	1.54	0.079	-0.18	0.968	-2.14	0.022
7122:11056_CL1Contig1:f	ANKS1A	0.84	0.626	1.54	0.164	-2.49	0.038	0.11	0.967
31094:13917_28576534:f	AP3B1	1.72	0.048	0.70	0.823	0.14	0.989	-2.56	0.004
2966:10489_14304882:f	ARHGAP20	-1.39	0.296	3.79	0.013	-1.81	0.109	-0.59	0.777
31583:2107_49414008:f	ARHGEF38	1.28	0.231	-0.31	0.954	0.84	0.661	-1.81	0.030
30465:8634_59814994:f	ARX	-2.12	0.066	2.66	0.040	-2.71	0.021	2.17	0.045
30217:332_40428258:f	ATG14	-0.71	0.678	3.23	0.009	-1.30	0.349	-1.22	0.390
30195:3119_40407564:f	ATP13A1	0.97	0.538	-1.56	0.048	0.19	0.989	0.40	0.962
33207:3523_6944051:f	BNC2	-0.45	0.858	-0.37	0.882	2.57	0.045	-1.75	0.134
2141:8509_CL1Contig1	BPIFA1	-1.28	0.342	1.66	0.175	2.07	0.030	-2.45	0.047
2141:8509_CL1Contig1:r	BPIFA1	1.22	0.202	-0.39	0.979	0.81	0.744	-1.63	0.032
1581:15505_CL1Contig2:r	BUB1	0.63	0.793	1.39	0.224	-2.00	0.021	-0.02	0.997
TC234333:f	C14orf132	2.65	0.038	-0.94	0.552	-1.31	0.363	-0.40	0.826
33598:5401_41134262:f	C16orf72	3.14	0.009	-0.47	0.876	-2.33	0.119	-0.34	0.862
5250:20771_40435698:f	C17orf100	1.48	0.147	0.07	0.988	-2.02	0.022	0.47	0.881
30121:21662_CL1Contig1:f	C17orf105	1.84	0.045	-0.04	0.996	-1.50	0.140	-0.30	0.943
3391:12342_41142169:r	C1orf115	-1.07	0.385	1.46	0.046	0.13	0.997	-0.52	0.954
337:1082_CL1Contig1:f	C21orf2	-1.11	0.402	1.93	0.030	0.09	0.987	-0.91	0.585

Appendix B: Annotated Uterine Differentially Expressed Genes

		GV TUT vs GV BUT		GV BUT vs Blast BUT		Blast BUT vs Blast TUT		Blast TUT vs GV TUT	
Probe ID	**Symbol***	**Fold Change**	**P-value**	**Fold Change**	**P-value**	**Fold Change**	**P-value**	**Fold Change**	**P-value**
33058:43011_40404331:r	C4orf21	3.68	0.020	-3.13	0.043	2.23	0.058	-2.78	0.042
14305:31378_CL2Contig1:r	CAMK1D	-3.28	0.021	0.93	0.573	2.24	0.069	0.12	0.965
8140:27570_10874789:f	CARD11	-2.37	0.036	0.24	0.913	0.12	0.955	2.01	0.080
4882:4667_14305354:f	CBX2	2.13	0.034	-1.69	0.140	-0.29	0.966	-0.16	0.976
32072:4291_40425298:f	CCDC146	0.91	0.563	1.35	0.325	-2.57	0.034	0.31	0.874
32025:21978_CL1Contig1:r	CCDC148	-1.96	0.040	-0.13	0.975	1.05	0.471	1.04	0.473
33696:45964_CL1Contig1:r	CCDC18	1.27	0.274	-2.13	0.029	0.24	0.965	0.62	0.818
3977:2397_CL2Contig1:r	CCDC62	-2.39	0.046	0.72	0.675	0.61	0.733	1.06	0.476
32896:13559_15034448:f	CCDC63	0.78	0.662	-3.88	0.045	3.16	0.024	-0.06	0.983
7244:33352_CL1Contig1:r	CCHCR1	2.35	0.021	-1.69	0.075	-0.38	0.897	-0.28	0.931
32216:6084_CL6Contig1:r	CCNF	-0.84	0.708	1.57	0.044	-0.36	0.970	-0.38	0.966
NM_001001619.1	CCR2	0.48	0.970	0.44	0.977	-1.63	0.016	0.71	0.878
32095:5399_46176217:f	CD109	-0.72	0.730	2.71	0.009	-0.87	0.614	-1.13	0.394
7523:46145_CL4Contig1:f	CDH2	2.43	0.030	-1.73	0.126	-0.41	0.855	-0.29	0.900
7240:20773_CL1Contig2:r	CENPQ	-0.99	0.511	-0.54	0.805	-0.94	0.557	2.47	0.015
33620:45360_CL17Contig1:r	CFD	0.00	1.000	0.60	0.857	1.16	0.326	-1.76	0.033
32169:1187_10871605:f	CILP2	0.46	0.886	-2.03	0.024	0.13	0.976	1.44	0.168
15803:1539_40392287:f	CNTNAP3B	-1.71	0.048	0.56	0.880	0.00	1.000	1.14	0.328
34914:45360_CL957Contig1:r	COL5A2	2.27	0.008	-0.07	0.989	-2.18	0.011	-0.01	0.998
8239:45360_CL165Contig1:r	CPN1	-0.02	0.996	-0.91	0.574	-1.01	0.493	1.94	0.042
3358:45360_13308491:f	CRB1	2.11	0.043	0.09	0.984	-1.96	0.056	-0.23	0.954
5463:34431_2411468:f	CSF3	-1.66	0.397	5.07	0.047	-1.91	0.284	-1.50	0.410
19565:29263_CL1Contig1:r	CYB5D1	-0.22	0.949	1.92	0.041	-1.11	0.427	-0.58	0.791
14054:2011_54558552:r	CYP26B1	-0.06	0.993	-0.88	0.674	1.81	0.048	-0.88	0.625

Appendix B: Annotated Uterine Differentially Expressed Genes

		GV TUT vs GV BUT		GV BUT vs Blast BUT		Blast BUT vs Blast TUT		Blast TUT vs GV TUT	
Probe ID	**Symbol***	**Fold Change**	**P-value**	**Fold Change**	**P-value**	**Fold Change**	**P-value**	**Fold Change**	**P-value**
31221:36050_CL21Contig1:r	DHX16	-0.32	0.922	2.20	0.029	-0.19	0.985	-1.69	0.090
34207:13394_CL3Contig1:r	DICER1	1.74	0.027	-1.18	0.276	-0.47	0.941	-0.09	0.993
18418:45360_10873040:f	DLL1	3.84	0.026	2.87	0.032	0.09	0.988	-6.79	0.006
34660:5515_CL2Contig1:f	DNA2	2.49	0.017	-0.67	0.728	-1.20	0.369	-0.62	0.753
6883:35384_CL4Contig1:f	DNAH12	2.76	0.023	-0.56	0.766	-0.97	0.528	-1.22	0.385
33133:12577_CL1Contig1:r	DNAJC30	0.59	0.742	1.15	0.432	1.11	0.453	-2.84	0.026
33504:20371_CL1Contig1:f	DND1	0.90	0.591	-5.02	0.006	1.76	0.205	2.36	0.074
8249:23401_CL2Contig1:r	DNMBP	-1.69	0.037	-0.81	0.760	-0.14	0.993	2.63	0.002
31181:44376_CL11Contig1:f	DOCK10	-1.31	0.372	2.92	0.028	-0.45	0.797	-1.16	0.443
33600:32715_CL1Contig1:r	DSCR6	-1.54	0.259	3.72	0.032	-0.27	0.933	-1.91	0.105
3297:10756_CL1Contig1:f	EDEM3	2.50	0.023	-0.88	0.620	-1.99	0.053	0.38	0.916
15539:34974_34155563:f	EGFR	-1.71	0.198	-2.22	0.049	3.66	0.017	0.26	0.889
33677:7175_40412218:f	EP400	0.08	0.975	-3.51	0.008	2.15	0.113	1.28	0.362
293:4725_CL3Contig1:f	EPHB1	4.79	0.017	-5.16	0.022	0.11	0.985	0.27	0.921
33377:9590_CL1Contig1:r	EXOC3L1	-2.29	0.092	5.24	0.007	1.60	0.147	-4.56	0.004
2856:9870_CL2Contig2:f	EXT2	1.88	0.077	-2.81	0.021	-0.47	0.920	1.41	0.176
32351:2607_CL3Contig1:f	FABP7	-1.07	0.458	2.04	0.050	-0.85	0.609	-0.12	0.964
33502:15620_CL2Contig1:f	FAM132A	3.45	0.008	-0.40	0.909	-1.11	0.411	-1.95	0.057
33675:22427_CL1Contig1:f	FAM178B	0.44	0.905	0.97	0.530	-2.17	0.012	0.76	0.720
30872:2576_9019235:f	FAM53C	-1.18	0.382	2.07	0.042	-0.35	0.874	-0.54	0.796
35022:3062_13660089:f	FAM5B	-0.90	0.602	-1.51	0.389	-0.71	0.676	3.12	0.045
16601:23941_45846439:r	FAM82A1	0.31	0.886	1.60	0.208	-2.29	0.027	0.38	0.871
7109:20096_54533856:f	FKBP5	0.87	0.593	-2.67	0.025	1.29	0.392	0.52	0.771
5119:96_CL2Contig1:f	FLOT2	-0.13	0.983	-0.12	0.987	2.15	0.036	-1.89	0.047

Appendix B: Annotated Uterine Differentially Expressed Genes

		GV TUT vs GV BUT		GV BUT vs Blast BUT		Blast BUT vs Blast TUT		Blast TUT vs GV TUT	
Probe ID	**Symbol***	**Fold Change**	**P-value**	**Fold Change**	**P-value**	**Fold Change**	**P-value**	**Fold Change**	**P-value**
31526:29294_C0007736d22-7:f	FNIP2	2.02	0.188	-3.96	0.043	0.76	0.684	1.18	0.447
11255:3707_CL1Contig1:f	FRS2	1.80	0.044	-0.52	0.881	-0.73	0.756	-0.54	0.864
18944:14261_CL2Contig1:r	GABARAPL3	-2.36	0.052	-1.21	0.283	7.65	0.008	-4.08	0.026
33525:3112_CL3Contig1:r	GALNT9	2.11	0.014	0.27	0.956	-2.42	0.007	0.04	0.995
34561:38_54488312:f	GHR	1.84	0.037	-0.21	0.965	-0.68	0.779	-0.95	0.551
4541:652_CL4Contig2-B:f	GNAO1	1.08	0.433	-2.53	0.017	0.63	0.874	0.83	0.684
15189:7311_40397714:f	GPRC5B	1.74	0.042	-0.86	0.642	-0.72	0.768	-0.16	0.979
33738:14136_15034587:f	H1FNT	2.35	0.045	0.16	0.958	-2.52	0.051	0.01	0.997
TC229113:f	HARBI1	1.62	0.242	1.41	0.339	-2.43	0.046	-0.60	0.737
7354:9303_CL3Contig1:r	HIST1H1D	-0.93	0.554	-1.77	0.182	0.35	0.874	2.35	0.040
16856:7936_CL22Contig1:f	HPGD	2.37	0.040	-1.19	0.397	-2.10	0.071	0.92	0.557
33664:7936_CL25Contig1:f	HSD17B13	-0.76	0.661	3.61	0.047	-2.04	0.099	-0.81	0.629
34984:11917_CL2Contig1:f	IARS	2.78	0.022	-1.29	0.313	-0.04	0.989	-1.45	0.262
5632:24834_40409209:f	ICOS	3.10	0.019	-1.45	0.304	-1.26	0.391	-0.40	0.837
8352:11972_CL2Contig1:r	INPP5F	0.64	0.808	-2.72	0.007	1.67	0.040	0.41	0.941
20289:8402_CL1Contig1:f	INTS1	2.00	0.247	0.69	0.705	-3.59	0.043	0.90	0.617
6983:474_CL1Contig1:f	IP6K2	-3.15	0.005	0.79	0.670	1.03	0.498	1.32	0.311
7111:13367_CL1Contig1:f	IPO11	1.84	0.035	-1.31	0.209	1.18	0.275	-1.71	0.046
856:15522_CL1Contig2:r	IPO4	1.20	0.360	-2.01	0.037	-0.22	0.910	1.03	0.497
33506:2060_CL3Contig1:f	IRS2	4.46	0.009	-4.05	0.011	4.26	0.010	-4.66	0.008
32868:33560_971739:f	ISX	-0.27	0.915	-1.61	0.189	-1.73	0.155	3.61	0.016
31801:2013_34170014:f	ITIH1	-0.82	0.689	0.55	0.902	3.16	0.017	-2.89	0.014
12084:1558_49327728:f	JUNB	0.39	0.888	-2.25	0.029	1.20	0.324	0.66	0.774
34954:15855_CL5Contig1:r	KANK2	-2.75	0.019	1.23	0.366	-0.40	0.852	1.92	0.106

Appendix B: Annotated Uterine Differentially Expressed Genes

		GV TUT vs GV BUT		GV BUT vs Blast BUT		Blast BUT vs Blast TUT		Blast TUT vs GV TUT	
Probe ID	**Symbol***	**Fold Change**	**P-value**	**Fold Change**	**P-value**	**Fold Change**	**P-value**	**Fold Change**	**P-value**
TC215653:f	KCNJ5	-0.01	0.998	0.25	0.959	1.59	0.093	-1.83	0.043
31171:7792_54519777:f	KIAA0513	3.25	0.020	-0.86	0.630	0.22	0.948	-2.61	0.039
9029:6218_15038946:f	KIRREL3	-1.72	0.042	0.99	0.516	0.45	0.903	0.28	0.958
8255:29534_CL8Contig1:f	KLF13	-1.90	0.143	2.63	0.021	0.09	0.962	-0.82	0.621
7069:6050_CL3Contig1:r	KLHL31	-3.48	0.039	1.05	0.554	0.89	0.596	1.55	0.280
3491:9967_CL1Contig1:f	KMO	0.14	0.960	-4.19	0.003	3.09	0.024	0.96	0.544
32207:45360_41135259:f	KRT85	-2.15	0.014	1.48	0.080	0.73	0.733	-0.05	0.991
14278:8428_CL1Contig1:r	KSR2	1.06	0.455	0.33	0.945	-5.02	0.005	3.64	0.009
7052:19749_CL1Contig1:f	LARS2	2.87	0.031	0.10	0.961	-0.21	0.920	-2.76	0.035
30039:30042_CL3Contig1:f	LCTL	-2.23	0.035	1.95	0.057	1.74	0.089	-1.45	0.173
32562:31899_54561442:f	LILRB4	-0.76	0.845	-0.25	0.994	1.63	0.029	-0.62	0.918
32333:19962_26017984:f	LOC100505841	-3.04	0.024	2.62	0.027	0.84	0.643	-0.43	0.860
6741:12422_CL2Contig1:f	LOC100506936	6.61	0.004	-4.95	0.012	-0.16	0.977	-1.49	0.221
30150:21494_CL1Contig1:r	LOC342346	-3.78	0.014	1.10	0.457	-0.11	0.985	2.80	0.031
15620:1272_CL7Contig3:r	LOC387646	0.76	0.725	0.37	0.917	-2.57	0.021	1.44	0.181
31193:7481_CL2Contig1:r	LOC390660	3.40	0.017	-0.50	0.900	-4.24	0.036	1.34	0.382
34741:45360_40479470:f	LOC400550	-0.46	0.910	-0.34	0.940	3.04	0.004	-2.24	0.015
10027:37260_34161065:f	LOC550643	1.41	0.130	-2.47	0.007	0.85	0.673	0.20	0.977
32232:3583_34163317:r	LPPR4	-1.60	0.096	2.76	0.005	-0.73	0.768	-0.43	0.916
34837:15312_40412364:f	LYST	2.16	0.032	-0.89	0.582	-0.99	0.509	-0.28	0.918
7586:32245_3139153:f	MC2R	-2.01	0.033	1.45	0.170	-0.68	0.842	1.24	0.263
7167:37243_13659229:f	MDFI	-0.45	0.869	-0.18	0.963	1.94	0.041	-1.31	0.268
5530:12038_15031773:f	MEOX1	-2.46	0.037	-0.34	0.889	3.40	0.022	-0.61	0.748
702:15471_CL1Contig1:f	MLH3	-2.51	0.032	0.75	0.675	1.01	0.509	0.74	0.688

Appendix B: Annotated Uterine Differentially Expressed Genes

		GV TUT vs GV BUT		GV BUT vs Blast BUT		Blast BUT vs Blast TUT		Blast TUT vs GV TUT	
Probe ID	**Symbol***	**Fold Change**	**P-value**	**Fold Change**	**P-value**	**Fold Change**	**P-value**	**Fold Change**	**P-value**
16472:45360_CL311Contig1:r	MMP7	-0.08	0.987	0.64	0.797	1.29	0.250	-1.85	0.039
2954:32345_CL1Contig1:f	MS4A13	-2.04	0.084	0.87	0.648	4.78	0.007	-3.62	0.016
31437:13041_40442049:f	MSH4	1.98	0.015	-1.53	0.092	-0.80	0.710	0.35	0.955
30534:34974_CL43Contig1:f	MUSK	1.58	0.021	-1.08	0.354	-0.39	0.970	-0.11	0.996
7449:12801_11502758:f	MYLK4	0.23	0.971	-1.74	0.034	0.48	0.877	1.03	0.467
34229:12477_457338:f	MYO1D	-1.25	0.379	3.52	0.031	-2.12	0.083	-0.16	0.953
5613:6074_CL4Contig1:r	NBEAL1	1.77	0.050	-0.81	0.679	-0.78	0.700	-0.19	0.969
15563:39317_CL1Contig1:r	NBR1	-0.32	0.898	-0.84	0.630	3.76	0.005	-2.60	0.024
5114:3203_CL3Contig1:f	NEK8	3.86	0.002	3.24	0.003	-3.15	0.001	-3.95	0.002
18665:5279_7052529:f	NFATC3	1.61	0.035	-0.62	0.890	-0.47	0.949	-0.52	0.935
5220:45360_CL735Contig1:r	NLRP1	2.40	0.096	2.43	0.053	0.04	0.995	-4.87	0.015
2999:4120_CL1Contig2:f	NNMT	-2.83	0.048	2.66	0.078	0.21	0.913	-0.04	0.983
30549:2255_13306284:f	NOL4	-0.32	0.921	1.89	0.065	-2.41	0.018	0.84	0.634
7019:22586_CL1Contig2:r	NRADDP	3.08	0.020	-0.08	0.973	-1.26	0.403	-1.75	0.195
5636:44931_CL1Contig1:f	NRP2	0.29	0.964	-0.89	0.651	-2.44	0.038	3.05	0.008
6922:615_CL1Contig1:r	NT5DC2	-0.51	0.894	2.41	0.007	-0.70	0.826	-1.20	0.279
7835:31332_CL9Contig1:r	NTN1	-2.47	0.029	1.61	0.187	0.03	0.995	0.82	0.661
18603:3099_CL1Contig1:r	NUAK2	-0.77	0.808	1.63	0.019	0.05	0.999	-0.91	0.641
8432:13461_54484747:f	NUDT12	1.47	0.055	-1.82	0.008	-0.46	0.964	0.80	0.768
2899:16467_7325562:f	NUP160	-0.34	0.862	-3.12	0.079	4.28	0.010	-0.81	0.644
32242:18794_CL2Contig1:f	OLFML2B	1.02	0.496	-2.57	0.036	-0.25	0.976	1.80	0.075
33569:4591_CL1Contig1:r	OLIG2	-2.19	0.067	-2.01	0.034	3.54	0.030	0.66	0.732
33959:15812_40426838:f	PARD3B	-1.28	0.319	-0.82	0.621	-0.11	0.972	2.22	0.029
30854:42786_54539603:f	PCNX	-0.58	0.877	-0.83	0.688	-0.33	0.961	1.74	0.032

Appendix B: Annotated Uterine Differentially Expressed Genes

		GV TUT vs GV BUT		GV BUT vs Blast BUT		Blast BUT vs Blast TUT		Blast TUT vs GV TUT	
Probe ID	**Symbol***	**Fold Change**	**P-value**	**Fold Change**	**P-value**	**Fold Change**	**P-value**	**Fold Change**	**P-value**
15586:6416_CL1Contig1:f	PELI1	3.26	0.006	-1.29	0.193	-0.85	0.680	-1.11	0.413
6994:38423_CL2Contig1:f	PFKFB4	-0.28	0.891	1.96	0.228	-2.85	0.009	1.16	0.403
33370:3677_49413885:f	PHC3	-0.58	0.858	0.50	0.874	1.66	0.043	-1.58	0.067
3727:7952_CL1Contig1:r	PINK1	0.63	0.836	-0.28	0.966	1.65	0.089	-2.00	0.022
2840:10356_CL2Contig1:r	PLEKHB1	0.28	0.945	0.23	0.962	-2.07	0.018	1.56	0.110
10183:31378_CL1Contig1:r	PNCK	-3.51	0.029	1.44	0.377	0.56	0.747	1.51	0.352
31180:27971_CL2Contig1:f	PNKD	-2.04	0.024	2.59	0.004	-0.49	0.882	-0.05	0.990
7186:14899_C0007305h17-7:f	POLH	-2.09	0.042	0.63	0.752	0.35	0.889	1.11	0.423
12698:9361_CL1Contig1:r	PPAPDC2	1.00	0.550	-4.63	0.028	1.22	0.378	2.42	0.054
7262:4857_59814359:f	PPP1R10	3.58	0.013	-3.38	0.019	-3.43	0.018	3.23	0.019
33622:11131_CL1Contig1:f	PRR14L	-0.94	0.567	-2.37	0.018	1.48	0.239	1.82	0.132
34736:24600_CL1Contig1:f	PTGES2	1.57	0.021	-0.62	0.928	-1.50	0.033	0.55	0.955
1715:927_14657773:f	PTPRM	-2.27	0.036	0.98	0.521	2.23	0.040	-0.94	0.548
32430:37975_3204940:f	PTPRO	0.78	0.662	3.27	0.080	-3.74	0.025	-0.31	0.869
11964:1529_CL4Contig1:f	RAB3A	-1.51	0.041	0.29	0.988	0.55	0.944	0.67	0.887
3896:29294_40425164:f	RAPGEF2	2.20	0.065	0.39	0.933	3.57	0.017	-6.17	0.004
6927:14131_CL1Contig1:r	RBM15B	2.78	0.031	-1.75	0.059	-2.39	0.056	1.36	0.296
3456:15216_CL1Contig1:r	RGS7	-1.56	0.041	0.26	0.985	0.09	0.996	1.22	0.229
12724:209_CL15Contig1:f	RORB	0.72	0.687	-2.90	0.047	2.01	0.032	0.17	0.961
19189:42690_CL1Contig1:r	RXRA	3.04	0.032	-1.92	0.199	-1.06	0.490	-0.06	0.973
33802:18775_46181246:r	SCAI	-2.38	0.028	0.32	0.888	1.73	0.131	0.33	0.883
15725:22809_21546507:f	SCML2	-0.53	0.812	-1.98	0.073	-0.07	0.991	2.58	0.022
6952:45360_13307772:f	SEMA3F	2.45	0.040	-2.22	0.055	-0.67	0.710	0.45	0.818
8262:22427_CL2Contig1:r	SEMA4G	2.39	0.011	-0.46	0.899	-1.81	0.051	-0.12	0.982

Appendix B: Annotated Uterine Differentially Expressed Genes

		GV TUT vs GV BUT		GV BUT vs Blast BUT		Blast BUT vs Blast TUT		Blast TUT vs GV TUT	
Probe ID	**Symbol***	**Fold Change**	**P-value**	**Fold Change**	**P-value**	**Fold Change**	**P-value**	**Fold Change**	**P-value**
18104:5455_40391726:f	SGMS2	-0.47	0.899	0.99	0.513	1.38	0.184	-1.90	0.037
16801:10685_CL1Contig1:f	SHPRH	2.23	0.015	-0.60	0.806	-0.58	0.819	-1.05	0.456
33493:7422_37794949:r	SLC25A18	-2.51	0.033	2.87	0.032	-0.70	0.805	0.33	0.937
6429:23629_3169733:f	SLC28A1	1.87	0.119	-2.63	0.046	0.24	0.947	0.51	0.829
18556:2108_CL3Contig1:r	SLC2A4RG	-0.88	0.582	-0.97	0.528	-0.84	0.605	2.70	0.019
6954:7070_CL3Contig1:f	SLC38A4	-2.24	0.068	2.69	0.048	-1.25	0.342	0.81	0.646
16718:18064_9017590:f	SLC43A3	3.18	0.050	10.41	0.004	3.81	0.004	-3.42	0.017
15542:695_CL7Contig1:f	SLC5A2	0.37	0.862	-1.00	0.547	3.58	0.010	-2.95	0.026
1726:2283_CL1Contig1:r	SLC5A7	1.75	0.024	-0.72	0.808	-0.84	0.691	-0.19	0.986
TC229039:f	SLC6A1	-2.31	0.024	0.82	0.658	3.14	0.007	-1.65	0.111
9380:30721_CL21Contig1:r	SMAP2	0.36	0.984	-1.86	0.005	1.36	0.087	0.13	0.997
30155:18311_CL1Contig1:f	SMCHD1	1.88	0.029	0.17	0.979	-1.76	0.026	-0.28	0.967
1221:5833_CL1Contig2:f	SNX17	1.89	0.167	-3.39	0.026	1.37	0.353	0.12	0.951
33615:21222_14306027:f	SNX20	-0.75	0.689	-0.86	0.614	3.00	0.010	-1.39	0.260
19557:5888_CL1Contig1:r	SPAG5	-1.69	0.204	-0.94	0.548	2.91	0.045	-0.27	0.882
19633:21168_11501920:f	SPATA21	-2.37	0.053	2.20	0.049	-0.12	0.971	0.29	0.913
32526:40918_49347205:f	SPEF2	1.92	0.036	-0.94	0.557	-0.86	0.623	-0.12	0.978
30238:22417_40419800:f	SPEG	-0.26	0.928	-2.28	0.050	0.61	0.808	1.93	0.053
4910:11127_CL3Contig1:f	SPHK1	-3.60	0.006	0.97	0.530	1.87	0.127	0.76	0.654
33934:4937_CL1Contig1:r	SPHKAP	-1.10	0.415	-0.15	0.962	1.91	0.031	-0.66	0.783
33701:17740_40442168:f	SPTBN1	0.78	0.641	-3.10	0.030	1.75	0.164	0.57	0.749
300:17742_CL1Contig1:f	SRPRB	0.61	0.819	2.02	0.034	-1.10	0.368	-1.52	0.109
34019:45360_CL798Contig1:f	SRRM2	-2.58	0.040	1.50	0.115	1.56	0.208	-0.49	0.832
16736:11622_CL2Contig1:r	SSFA2	-0.06	0.993	-1.97	0.024	1.20	0.290	0.84	0.684

Appendix B: Annotated Uterine Differentially Expressed Genes

		GV TUT vs GV BUT		GV BUT vs Blast BUT		Blast BUT vs Blast TUT		Blast TUT vs GV TUT	
Probe ID	**Symbol***	**Fold Change**	**P-value**	**Fold Change**	**P-value**	**Fold Change**	**P-value**	**Fold Change**	**P-value**
8082:3029_51348509:f	STAG2	-2.03	0.205	-0.85	0.633	2.95	0.045	-0.07	0.967
5495:5785_CL1Contig2:r	STAT5B	2.88	0.028	-3.33	0.013	4.23	0.006	-3.79	0.013
34578:45360_CL871Contig1:r	SVIL	4.96	0.032	-5.66	0.031	-1.08	0.551	1.78	0.314
34333:7921_CL4Contig1:r	TCF7L2	2.10	0.047	-0.78	0.740	-1.11	0.424	-0.20	0.945
34942:21868_CL1Contig1:r	TIAM2	-4.24	0.001	2.80	0.006	-1.32	0.136	2.76	0.009
7824:26561_CL1Contig1:f	TMC5	-0.38	0.922	-0.88	0.613	-0.88	0.611	2.15	0.013
7041:44464_CL1Contig1:r	TMEM110-MUSTN	-2.94	0.007	1.96	0.035	-0.03	0.998	1.01	0.498
7042:5416_CL1Contig1:f	TMEM110-MUSTN	0.20	0.975	0.57	0.870	0.94	0.582	-1.71	0.043
NM_001001259.1	TMPRSS15	-0.37	0.890	2.69	0.026	-0.40	0.958	-1.92	0.049
335:45360_CL515Contig1:r	TMPRSS2	1.38	0.159	1.01	0.488	0.52	0.932	-2.91	0.002
12624:45360_CL225Contig1:f	TNC	0.14	0.958	-3.01	0.028	-0.62	0.764	3.49	0.018
31227:45360_40390502:f	TRIM15	0.70	0.766	2.43	0.026	-2.31	0.031	-0.83	0.671
33789:1074_CL1Contig1:f	TTC7B	1.78	0.039	-0.24	0.970	-0.87	0.615	-0.67	0.785
10026:24269_CL3Contig1:r	UBQLN3	1.05	0.461	-2.33	0.023	0.58	0.821	0.71	0.747
30651:14945_CL3Contig1:r	UBR5	-1.16	0.407	0.93	0.565	-2.12	0.013	2.34	0.026
7120:11550_CL2Contig1:f	UHRF1BP1	5.00	0.001	-2.29	0.025	-2.02	0.013	-0.69	0.811
33669:7130_11074639:f	USP45	5.64	0.004	-1.08	0.452	-2.61	0.028	-1.95	0.098
7222:32883_CL3Contig1:f	VEGFA	2.75	0.032	2.18	0.024	-1.48	0.239	-3.45	0.018
13113:14805_CL2Contig1:f	VNN2	-0.31	0.913	1.10	0.425	1.32	0.310	-2.11	0.047
32790:3740_CL2Contig2:f	VPS41	0.85	0.622	0.31	0.930	1.12	0.425	-2.28	0.029
8792:6467_CL1Contig1:f	VSTM4	2.91	0.006	-1.66	0.147	-2.32	0.014	1.06	0.452
34827:3517_CL2Contig1:r	WDHD1	2.14	0.031	-0.81	0.645	-1.39	0.237	0.05	0.986
35099:31317_10868774:f	WNT16	-2.10	0.085	-0.89	0.597	5.47	0.019	-2.47	0.099
14329:8566_13548034:f	XIRP2	2.77	0.073	-13.91	0.002	0.99	0.523	10.16	0.001

Appendix B: Annotated Uterine Differentially Expressed Genes

		GV TUT vs GV BUT		GV BUT vs Blast BUT		Blast BUT vs Blast TUT		Blast TUT vs GV TUT	
Probe ID	**Symbol***	**Fold Change**	**P-value**	**Fold Change**	**P-value**	**Fold Change**	**P-value**	**Fold Change**	**P-value**
32958:19024_40406788:f	ZBTB40	6.15	0.004	-0.34	0.891	-4.43	0.009	-1.38	0.284
30901:28983_CL2Contig1:f	ZC3H13	-1.79	0.044	0.43	0.909	0.94	0.561	0.42	0.911
31395:10306_CL1Contig1:f	ZC3H3	-5.22	0.013	7.47	0.008	3.03	0.008	-5.27	0.005
9333:4571_CL7Contig1:f	ZCCHC11	2.05	0.028	-0.69	0.761	-1.18	0.343	-0.18	0.962
3971:5502_CL2Contig1:f	ZCCHC8	-0.69	0.797	1.97	0.025	-0.48	0.929	-0.80	0.721
34365:19516_11072660:r	ZFPM2	-1.41	0.165	1.92	0.026	-0.43	0.899	-0.08	0.986
723:32575_CL13Contig1:r	ZFYVE1	1.96	0.047	-2.00	0.051	-0.07	0.984	0.11	0.978
672:32575_CL23Contig1:r	ZFYVE26	2.94	0.007	-0.48	0.893	-0.68	0.754	-1.79	0.081
9339:9367_CL1Contig1:r	ZFYVE9	0.34	0.886	3.38	0.010	-4.67	0.007	0.96	0.549
5664:4689_CL1Contig1:r	ZNF142	-0.68	0.766	-0.93	0.565	-0.41	0.924	2.02	0.021
35005:23572_54556558:f	ZNF219	2.09	0.173	-4.68	0.028	0.39	0.873	2.20	0.121
35178:45360_15036677:f	ZNF275	0.04	0.988	3.02	0.010	-2.44	0.030	-0.62	0.763
32916:3041_40411698:f	ZNF366	0.62	0.752	5.33	0.010	-5.91	0.004	-0.04	0.989
7935:45360_CL208Contig2:f	ZNF771	-3.00	0.028	-0.43	0.854	4.50	0.016	-1.07	0.485
33565:45360_CL25Contig5:f	ZNF850	2.21	0.022	-2.47	0.016	1.98	0.044	-1.73	0.074
NM_214106.1	ZPBP	-0.70	0.776	1.91	0.023	-1.20	0.296	-0.01	0.998

Table B.1: List of all annotated differentially expressed uterine genes as determined by microarray analysis. Official HUGO gene symbols as determined by annotation against the human RefSeq database. Comparisons are made across four temporal and spatial conditions including GV TUT vs GV BUT, GV BUT vs Blast BUT, Blast BUT vs Blast TUT and Blast TUT vs GV TUT.

Appendix C: Enriched Uterine Gene Ontology Terms

GO Term	Type*	Description	P-value	FDR q-value	E	B	n	b	Comparison	Direction
GO:0044421	C	extracellular region part	8.44E-05	5.12E-02	1.33	616	2658	185	BB vs BT	Up
GO:0060089	F	molecular transducer activity	1.52E-05	2.66E-02	1.29	752	3078	254	BB vs BT	Down
GO:0004871	F	signal transducer activity	1.52E-05	5.33E-02	1.29	752	3078	254	BB vs BT	Down
GO:0004872	F	receptor activity	3.27E-05	3.81E-02	1.52	666	1287	111	BB vs BT	Down
GO:0005096	F	GTPase activator activity	4.07E-05	3.56E-02	1.48	187	3830	90	BB vs BT	Down
GO:0030695	F	GTPase regulator activity	6.75E-05	4.72E-02	1.34	333	3861	147	BB vs BT	Down
GO:0005543	F	phospholipid binding	6.83E-05	3.99E-02	1.34	378	3563	154	BB vs BT	Down
GO:0038023	F	signaling receptor activity	7.68E-05	3.84E-02	1.59	522	1219	86	BB vs BT	Down
GO:0005543	F	phospholipid binding	1.00E-07	3.51E-04	2.17	378	844	59	BB vs BT	Up
GO:0008289	F	lipid binding	1.09E-06	1.90E-03	1.89	531	844	72	BB vs BT	Up
GO:0005488	F	binding	3.61E-05	4.21E-02	1.04	8277	3765	2760	BB vs BT	Up
GO:1900542	P	regulation of purine metabolic process	2.51E-05	2.56E-01	1.49	256	3112	101	BB vs BT	Down
GO:0006140	P	regulation of nucleotide metabolic process	3.17E-05	1.61E-01	1.41	258	3850	119	BB vs BT	Down
GO:0006869	P	lipid transport	6.55E-05	2.22E-01	1.9	100	2722	44	BB vs BT	Down
GO:0048870	P	cell motility	7.54E-05	1.92E-01	2.21	402	463	35	BB vs BT	Down
GO:0007411	P	axon guidance	4.09E-07	4.17E-03	1.46	254	4222	133	BB vs BT	Up
GO:0042330	P	taxis	9.32E-07	3.16E-03	1.37	366	4222	180	BB vs BT	Up
GO:0006935	P	chemotaxis	9.32E-07	4.74E-03	1.37	366	4222	180	BB vs BT	Up
GO:0050789	P	regulation of biological process	4.61E-06	1.17E-02	1.07	5578	3798	1934	BB vs BT	Up
GO:0050794	P	regulation of cellular process	8.69E-06	1.77E-02	1.07	5303	4222	2036	BB vs BT	Up
GO:0009605	P	response to external stimulus	9.29E-06	1.58E-02	1.26	709	3863	293	BB vs BT	Up
GO:0048583	P	regulation of response to stimulus	2.04E-05	2.97E-02	1.18	1522	3350	513	BB vs BT	Up
GO:0065007	P	biological regulation	5.17E-05	6.58E-02	1.06	5893	4037	2145	BB vs BT	Up
GO:0042221	P	response to chemical stimulus	8.13E-05	9.20E-02	1.14	1836	3864	687	BB vs BT	Up
GO:0002253	P	activation of immune response	9.90E-05	8.40E-02	1.46	167	3995	83	BB vs BT	Up

Appendix C: Enriched Uterine Gene Ontology Terms

GO Term	Type*	Description	P-value	FDR q-value	E	B	n	b	Comparison	Direction
GO:0005576	C	extracellular region	5.07E-07	6.16E-04	1.49	735	1764	164	BT vs GT	Down
GO:0005615	C	extracellular space	1.28E-06	7.76E-04	2.1	505	609	55	BT vs GT	Down
GO:0044421	C	extracellular region part	1.58E-05	4.79E-03	1.88	616	609	60	BT vs GT	Down
GO:0004175	F	endopeptidase activity	1.10E-06	3.85E-03	4.18	217	246	19	BT vs GT	Down
GO:0004222	F	metalloendopeptidase activity	3.13E-05	5.48E-02	6.83	63	273	10	BT vs GT	Down
GO:0060089	F	molecular transducer activity	2.52E-05	4.41E-02	1.23	752	3997	315	BT vs GT	Up
GO:0004871	F	signal transducer activity	2.52E-05	8.82E-02	1.23	752	3997	315	BT vs GT	Up
GO:0048583	P	regulation of response to stimulus	1.03E-07	1.05E-03	1.39	1522	1419	255	BT vs GT	Down
GO:0048584	P	positive regulation of response to stimulus	2.93E-06	1.49E-02	1.47	725	1686	153	BT vs GT	Down
GO:0080134	P	regulation of response to stress	2.43E-05	4.12E-02	1.64	485	1256	85	BT vs GT	Down
GO:0050670	P	regulation of lymphocyte proliferation	3.86E-05	4.37E-02	3.99	87	541	16	BT vs GT	Down
GO:0032944	P	regulation of mononuclear cell proliferation	3.86E-05	4.91E-02	3.99	87	541	16	BT vs GT	Down
GO:0002682	P	regulation of immune system process	4.24E-05	4.32E-02	1.63	540	1123	84	BT vs GT	Down
GO:0070663	P	regulation of leukocyte proliferation	4.58E-05	3.88E-02	3.38	90	733	19	BT vs GT	Down
GO:0051249	P	regulation of lymphocyte activation	5.50E-05	4.00E-02	2.69	188	557	24	BT vs GT	Down
GO:0050778	P	positive regulation of immune response	6.82E-05	4.63E-02	1.79	209	1663	53	BT vs GT	Down
GO:0030054	C	cell junction	7.74E-07	9.40E-04	1.4	513	3015	185	GB vs BB	Down
GO:0005856	C	cytoskeleton	3.99E-06	2.42E-03	1.4	521	2811	174	GB vs BB	Down
GO:0005886	C	plasma membrane	9.39E-06	3.80E-03	1.17	1951	3109	605	GB vs BB	Down
GO:0005911	C	cell-cell junction	9.11E-05	2.77E-02	1.52	208	3015	81	GB vs BB	Down
GO:0005488	F	binding	4.20E-06	1.47E-02	1.04	8277	4169	3058	GB vs BB	Down
GO:0003779	F	actin binding	1.38E-05	2.41E-02	2.08	283	896	45	GB vs BB	Down
GO:0008092	F	cytoskeletal protein binding	2.95E-05	3.45E-02	1.76	497	898	67	GB vs BB	Down
GO:0005543	F	phospholipid binding	8.43E-05	5.90E-02	1.3	378	4220	176	GB vs BB	Down
GO:0030695	F	GTPase regulator activity	1.53E-05	5.35E-02	1.63	333	1815	84	GB vs BB	Up

Appendix C: Enriched Uterine Gene Ontology Terms

GO Term	Type*	Description	P-value	FDR q-value	E	B	n	b	Comparison	Direction
GO:0005089	F	Rho guanyl-nucleotide exchange factor activity	1.56E-05	2.73E-02	2.94	63	1457	23	GB vs BB	Up
GO:0005085	F	guanyl-nucleotide exchange factor activity	2.27E-05	2.65E-02	2.11	134	1745	42	GB vs BB	Up
GO:0060589	F	nucleoside-triphosphatase regulator activity	5.81E-05	5.08E-02	1.58	344	1815	84	GB vs BB	Up
GO:0005083	F	small GTPase regulator activity	6.19E-05	4.33E-02	1.74	220	1815	59	GB vs BB	Up
GO:0007411	P	axon guidance	8.67E-08	8.82E-04	1.59	254	3287	113	GB vs BB	Down
GO:0042330	P	taxis	2.05E-06	6.95E-03	1.43	366	3312	148	GB vs BB	Down
GO:0006935	P	chemotaxis	2.05E-06	1.04E-02	1.43	366	3312	148	GB vs BB	Down
GO:0050793	P	regulation of developmental process	5.33E-06	1.36E-02	1.21	956	4217	415	GB vs BB	Down
GO:0048858	P	cell projection morphogenesis	8.08E-06	1.64E-02	3.75	136	460	20	GB vs BB	Down
GO:0032990	P	cell part morphogenesis	8.19E-06	1.39E-02	3.4	150	460	20	GB vs BB	Down
GO:0048812	P	neuron projection morphogenesis	1.57E-05	2.28E-02	4.09	106	460	17	GB vs BB	Down
GO:0007409	P	axonogenesis	2.08E-05	2.65E-02	5.14	68	437	13	GB vs BB	Down
GO:0007166	P	cell surface receptor signaling pathway	2.40E-05	2.72E-02	1.2	1337	3263	445	GB vs BB	Down
GO:0009653	P	anatomical structure morphogenesis	3.03E-05	3.08E-02	1.87	791	460	58	GB vs BB	Down
GO:0009605	P	response to external stimulus	3.05E-05	2.82E-02	1.28	709	3244	250	GB vs BB	Down
GO:0007243	P	intracellular protein kinase cascade	4.08E-05	3.47E-02	1.46	254	3261	103	GB vs BB	Down
GO:0048646	P	anatomical structure formation…	4.12E-05	3.23E-02	1.36	424	3249	159	GB vs BB	Down
GO:0050794	P	regulation of cellular process	6.95E-05	4.72E-02	1.07	5303	3268	1586	GB vs BB	Down
GO:0023051	P	regulation of signaling	7.55E-05	4.80E-02	1.16	1323	4152	541	GB vs BB	Down
GO:0045595	P	regulation of cell differentiation	7.72E-05	4.62E-02	1.22	665	4217	292	GB vs BB	Down
GO:0045664	P	regulation of neuron differentiation	5.21E-06	5.30E-02	1.98	218	1414	52	GB vs BB	Up
GO:0050767	P	regulation of neurogenesis	7.63E-06	3.89E-02	1.87	262	1414	59	GB vs BB	Up
GO:0051960	P	regulation of nervous system development	1.17E-05	3.98E-02	1.82	283	1414	62	GB vs BB	Up
GO:0006952	P	defense response	5.89E-05	8.56E-02	1.41	463	2406	134	GB vs BB	Up
GO:0009605	P	response to external stimulus	7.57E-05	8.56E-02	1.33	709	2325	187	GB vs BB	Up

Appendix C: Enriched Uterine Gene Ontology Terms

GO Term	Type*	Description	P-value	FDR q-value	E	B	n	b	Comparison	Direction
GO:0044456	C	synapse part	1.14E-06	1.38E-03	2.01	216	1515	56	GT vs GB	Up
GO:0030054	C	cell junction	2.79E-05	1.69E-02	1.51	513	1699	112	GT vs GB	Up
GO:0005089	F	Rho guanyl-nucleotide exchange factor activity	1.58E-06	5.52E-03	2.99	63	1623	26	GT vs GB	Down
GO:0005085	F	guanyl-nucleotide exchange factor activity	3.16E-06	5.53E-03	2.31	134	1556	41	GT vs GB	Down
GO:0005088	F	Ras guanyl-nucleotide exchange factor activity	3.24E-06	3.78E-03	2.73	77	1623	29	GT vs GB	Down
GO:0005543	F	phospholipid binding	1.97E-05	1.72E-02	1.6	378	1749	90	GT vs GB	Down
GO:0008289	F	lipid binding	6.20E-05	4.34E-02	1.5	531	1573	107	GT vs GB	Down
GO:0005488	F	binding	5.09E-06	1.78E-02	1.04	8277	3881	2852	GT vs GB	Up
GO:0003779	F	actin binding	8.10E-06	1.42E-02	1.47	283	3237	115	GT vs GB	Up
GO:0005543	F	phospholipid binding	1.87E-05	2.18E-02	1.4	378	3172	143	GT vs GB	Up
GO:0016337	P	cell-cell adhesion	4.18E-05	4.25E-01	4.88	195	148	12	GT vs GB	Down
GO:0006928	P	cellular component movement	5.90E-06	6.01E-02	1.27	600	4222	273	GT vs GB	Up
GO:0016477	P	cell migration	6.20E-05	3.15E-01	1.31	367	4216	172	GT vs GB	Up
GO:0007167	P	enzyme linked receptor signaling pathway	8.55E-05	1.74E-01	1.3	504	3396	190	GT vs GB	Up

Table C.1: List of all enriched gene ontology terms identified by gorilla. Types include P: Biological Process F: Molecular Function and C: Cellular Component. GOrilla vital statistics include P-value: enrichment p-value computed according to the mHG or HG model, FDR q-value: calculated as (p-value * number of GO terms) / i) for the ith term when results are ranked according to p-value, E: enrichment score = (b/n) / (B/11743) B: is the total number of genes known for the GO term, n: is the number of genes in the top of the ranked input list, B: is the number of genes associated with the GO term in the top of the ranked list. Comparisons are shortened to BB vs BT: Blast BUT vs Blast TUT, BT vs GT: Blast TUT vs GV TUT, GB vs BB: GV BUT vs Blast BUT and GT vs GB: GV TUT vs GV BUT. Directions refer to terms